ANTHER AND POLLEN DEVELOPMENT IN BARLEY

José Fernández Gómez, BSc

Thesis submitted to the University of Nottingham for the degree of Doctor of Philosophy

September 2011

Abstract.

The control of pollen viability and release is of major commercial importance in the development of crops for hybrid seed production and selective breeding. It has been shown that key transcription factors in *Arabidopsis* particularly *MALE STERILITY1* (*MS1),* are functionally conserved in rice (Li et al., 2011), therefore extending this comparative analysis and controlling fertility in temperate cereals, such as barley, is the long term goal of this project.

Although anther and pollen development of barley seems morphologically similar to Arabidopsis, the genes involved and how they are regulated are currently unknown. *Arabidopsis MS1* is a tapetum specific transcription factor which is expressed exclusively from the tetrad stage to early microspores release. Identification and accurate staging of barley anther development is essential for expression analysis and functional characterisation of genes involved in pollen development. Therefore, a complete morphological study of barley development was conducted. External characteristics have been described in parallel to anther development in order to predict anther stages by the observation of external stages phenotypic traits.

Characterization of the barley orthologue of *MS1* (*HvMS1*) has been conducted. Recently a new grass genome has been released, *Brachypodium distachyion*. This new resource has been used to aid primers design alongside the rice *OsPTC1* sequence, the orthologue of *MS1* (Li et al., 2011). Genome sequencing has indicated that the *Brachypodium* genus is more closely related to wheat and barley than it is to rice. Due to the close relationship between *Brachypodium* and barley, this new grass has been used as intermediary to identify the *OsPTC1* orthologue in barley as well as downstream *MS1* targets. A highly similar sequence to *OsPTC1* was found in *Brachypodium*, *Bradi4g31760*. This new gene, as a result of its similarities to *OsPTC1*, was considered as its putative orthologue gene in *Brachypodium*. Therefore, the most conserved areas between *OsPTC1-Bradi4g31760*

were used for primers design to successfully amplify equivalent gene in barley (*HvMS1*).

The characterization of this barley gene showed a similar expression pattern to the *MS1* putative orthologue in *Arabidopsis* of tapetum specific expression. In addition, RNAi silencing of this gene has revealed that it is essential for the normal development of pollen, with a lack of viable pollen produced in the putative *HvMS1* silenced transgenic lines.

ACKNOWLEDGEMENTS

I would like to express my most sincere gratitude to my supervisor Zoe A. Wilson for giving me the opportunity to do a PhD in her group, for her patience, motivation and endless knowledge. She has been an inspiriting mentor, giving me guidance and support throughout my PhD study and research. I am also indebted to my colleagues Dr. Caiyun Yang and Dr. Gema Vizcay-Barrena for their unlimited support and advice. I am grateful to all the members of Wilson's group who contribute to create a wonderful working environment. Also thanks to BBSRC for funding my project.

I specially would like to thank my good friends Francisco and Ester. They have been like a family for me, showing me unconditional friendship during happy and lower times. In recognition of all her patience, support and understanding through the duration of my study and when working endless hours to meet the final deadline of my PhD, I would like to thank my partner, Clementine Paro. I love you Clem, you have been the perfect companion.

Lastly, and most importantly, I wish to thank my family, my parents Jose and Maria del Valle who bore me, raised me, taught me, supported me and loved me. Also, thanks to my sister Lorena and my brothers Daniel and Jesus whom I have missed every day. Finally, I would like to commemorate my beloved grandfather Miguel and grandmother Dolores, whom passed away in my absence.

"I will prepare and one day my chance will come".

Abraham Lincoln.

Quiero dedicar esta tesis
a mi familia.

TABLE OF CONTENTS

Abbreviations.

µg/ml	microgram per millilitre
µl	microlitre
µg	microgram
µM	micromolar
bp	base pair
cDNA	complementary DNA
cm	centimetre
DEPC	diethylpyrocarbonate
dH_2O	distilled water
DNA	deoxyribonucleic acid
DNase	deoxyribonuclease
dNTP	deoxynucleoside triphosphate
dsDNA	double-stranded DNA
Fig	figure
g	gram
g/l	gram per litre
GFP	green fluorescent protein
GUS	β-glucuronidase
h	hour
Kb	kilobase pair
L	litre
mg/l	miligram per litre
min	minute
ml	millilitre
mM	milimolar
mRNA	messenger RNA
ng	nanogram
ng/µl	nanogram per microlitre
PBS	phosphate-buffered saline
PCD	programmed cell dead
RNA	ribonucleic acid
rpm	revolutions per minute
RT-PC R	reverse transcription-polymerase chain reaction
sec	second
v/v	volume to volume ratio
w/v	weight to volume radio

CHAPTER 1

1. Introduction.

1.1 Food Security.

Demand for food is increasing because of population growth, urbanisation and increasing affluence in the of the developing world. The world's population is projected to increase from 6 billion to 9 billion by 2050, including an expected doubling of the population of Africa from 1 billion to 2 billion. For the first time, more people are living in cities than in rural areas, and economic growth and increasing wealth are leading to greater demand for food, especially in Asia, and particularly for animal products in countries where diets have been traditionally vegetarian. Overall demand for food is expected to increase by 50% by 2030 and by 100% by 2050 (FAO, World Food Security, Rome 2008).

Climate and other environmental changes driven by increasing human populations and economic development pose fundamental challenges for humankind. While demand for food is rising, the area of land suitable for food production is liable to decrease (through pressures from other uses) and in any case cannot currently be increased substantially without undesirable environmental impacts that would result in the loss of wildlife habitats and biodiversity (BirdLife International 2008b), and exacerbate climate change by releasing carbon currently sequestered in forests and in soils under uncultivated land (Sutherland 2004). In some countries, there is also growing competition for the available agricultural land from biofuel production, as well as increasing use of arable crops for animal feed (FAOSTAT, 2009).

Global climate change can be expected to threaten food production and its supply, for example through changing patterns of rainfall,

increasing incidence of extreme weather and changing distribution of diseases and their vectors (Tyson, 2009). Global stocks of some staple foods have declined, and spikes in food prices (such as those seen during 2008) may become more frequent if rising demand cannot be consistently matched by supply. Environmental change will offer new opportunities (as well as threats to production), for example by extending the geographic range for some crops. Temperate regions including the UK have the potential to play a more important role in global agricultural production in the future, with the benefit of fertile soils and more moderate predicted climate chganges than some other regions that are currently major food producers. Europe could therefore potentially increase its exports of food (Tyson, 2009).

The Green Revolution of the 1960s introduced new technologies and advances in crop improvement that transformed agricultural productivity in parts of Central America and Asia, but much less successfully in Africa. However, the new "greener" revolution must reconcile increased agricultural productivity with environmental sustainability, in order to maintain food production in balance with other vital ecosystem services (The Royal Society, 2009). Compromises will however be needed to meet potentially conflicting requirements of productivity and environmental goals.

Research is also required on crops for the UK and other temperate regions, and also for the developing world, to enable the effective transfer of knowledge from model species into practical application in crops. The main target crops for the UK include wheat and other small grained cereals, oilseed rape, potatoes, horticultural and other 'minor' crops, forage crops and pasture. Key research targets include: enhancing crop productivity with optimised efficiency of resource use (water, nitrogen, other nutrients); reducing reliance on fertilisers that are; controlling fertility; raising photosynthetic efficiency through engineering C4 metabolism (Hibberd et al. 2008); introducing nitrogen fixation to cereals or other non-legume crops; enhancing resistance to pests and diseases, and research on weed control. However, to make such advances there is a requirement for improved knowledge of the

biology and genetics of these target processes. Breeding strategies should ideally anticipate future problems (e.g.; to pre-empt the emergence of new insect pests that may spread with climate change). Research is also needed to sustain effective use of herbicides, insecticides, and fungicides in the face of evolution towards resistance. In addition, research is needed especially to enhance tolerance of abiotic stresses (e.g., drought, salinity, flooding, ozone, UV, high and low extremes of temperature), especially at critical stages such as flowering, or the effects of combinations of such stresses.

Over the next 40 years, biological science-based technologies and approaches have the potential to improve food crop production in a sustainable way. Some of these technologies build on existing knowledge and technologies, while others are completely radical approaches which will require a great deal of further research. Genetic improvements to crops can occur through breeding or Genetic Manipulation (GM) to introduce a range of desirable traits (The Royal Society, 2009). Traditional plant breeding is slow, taking 10 years or more for a breeding programme. Furthermore, breeding of some crops which are not propagated by seed, such as potato and banana, is extremely difficult. GM-based methods are used widely as routine tool to understand developmental processes. GM can produce crops with improved photosynthetic efficiency or nitrogen fixation (Hibberd et al. 2008). In addition, GM can result in reduced environmental impact because they need lower fertiliser input or chemical applications for pathogen and pest control. However, the application of GM techniques in crop plants has been controversial, and is still open to debate.

New technologies in the areas of genomics and transcriptomics, particularly the advances in sequencing technologies, are providing opportunities for rapid developments in these areas. By exploiting the potential of genomics through the analysis of model plants, crops, microbes, pathogens, pests, beneficial organisms, rapid advances can be made. Effective management and sharing of genomic (and other "omic") data is becoming increasingly important, enabling data

mining, novel analyses and integration of different types of biological information, leading to improved ability to select genotypes efficiently.

Therefore, research needs to focus on applying the latest stechnological developments and knowledge to increasing crop and animal productivity globally. However, alongside this there is a need to minimise the environmental impact (including reducing greenhouse gas emissions, improving the efficient use of water, energy and other inputs), reducing losses from pests and diseases, enhancing food safety and quality for improved nutrition, and reducing waste throughout the food supply chain. Research will also be needed on issues around land tenure, food markets, supply and distribution, regulation, consumption, and affordability if the goals of increasing food production by 100% are to be met by 2050.

1.2 The role of reproduction in Global Food Security.

Control of male reproduction will facilitate breeding and the generation of high yielding hybrids varieties, which are economically important as for example, hybrids rice yield about 15-20% more than most inbred varieties (Cheng et al., 2007; Zhong et al., 2004). Grain yield is also regulated by pollen fertility, but little is known about the variation in pollen viability/development under diverse environmental or field conditions. Male sterile varieties are valuable resources that greatly facilitate the production of hybrids via cross-pollination. Work has been on-going to study the role of genes involved in pollen development, with much study focusing on the model species *Arabidopsis thaliana* and this has led to the characterization of many components of the pollen development pathway (Ma, 2005). However, there is now much interest in translating the information from such models into crops plants. One example of this is the *Arabidopsis MALE STERILITY1 (MS1)* gene (Wilson et al., 2001). *MS1* is functionally conserved in rice (Li et al., 2011), therefore, extending this knowledge into barley and other temperate crops may provide a mechanism to

understand and ultimately control fertility and then facilitate hybrid seed production.

1.3 Floral Identity.

In *Arabidopsis*, flower organs are organized into four concentric whorls (Fig.1.1; Fig.1.4) of sepals, petals, stamen and carpels, that arise sequentially from the floral meristem. The third whorl in *Arabidopsis* contains six stamens, four medial (long) and two lateral (short). Each stamen consists of an anther and a filament (Smyth et al., 1990; Goldberg et al., 1993). In the anther, two types of tissue are present, the reproductive or sporogenous tissue and the non-reproductive. Anthers are responsible for producing and releasing the pollen grains in order that pollination and fertilization can occur within the flower. The filament is a tube of vascular tissue that attaches the anther to the flower and serves as a conduit for water nutrients (Fig.1.1).

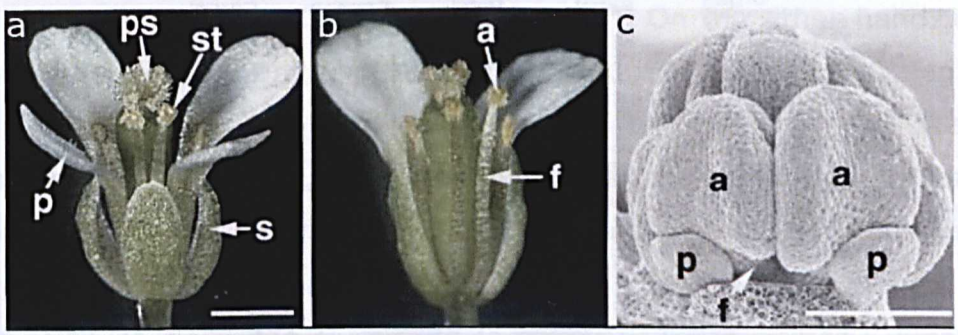

Fig.1.1 *Arabidopsis* flower. (a) An intact mature (stage 13) *Arabidopsis* flower with four types of organs, sepals (s), petals (p), stamens (st), and the pistil (ps). (b) A mature flower with one sepal and two petals removed to reveal some of the stamens, which have an anther (a) and a filament (f). A and B are of the same magnification; bar = 1.0 mm. (*c*) A scanning electron micrograph of a stage 9 flower, with its sepals removed to show the inner organs; two petal primordia (p) are round and small; two of the four long stamens can be easily seen with their anthers (a) having attained the characteristic lobed shape and the filaments (f) are still very short. Bar = 100 μm. (Ma, H., 2005).

Floral identity seems to be controlled by three classes of homeotic genes (A, B and C) with overlapping areas of activity (Fig.1.2) supported by additional transcription factors which are required to confer a full activity on the homeotic genes (*SEPALLATA (SEP)* 1/2/3/4). A function genes and *SEP1/2/3/4* specify sepal identity. A and B function plus *SEP1/2/3/4* determine petal identity. B and C plus *SEP1/2/3/4* control stamen identity. And finally, C function plus *SEP1/2/3/4* specify carpel identity. In addition, A function is indirectly involved in controlling stamen identity because it antagonizes the C function, such that in the absence of A function, stamens are formed ectopically (Ma, H., 2005).

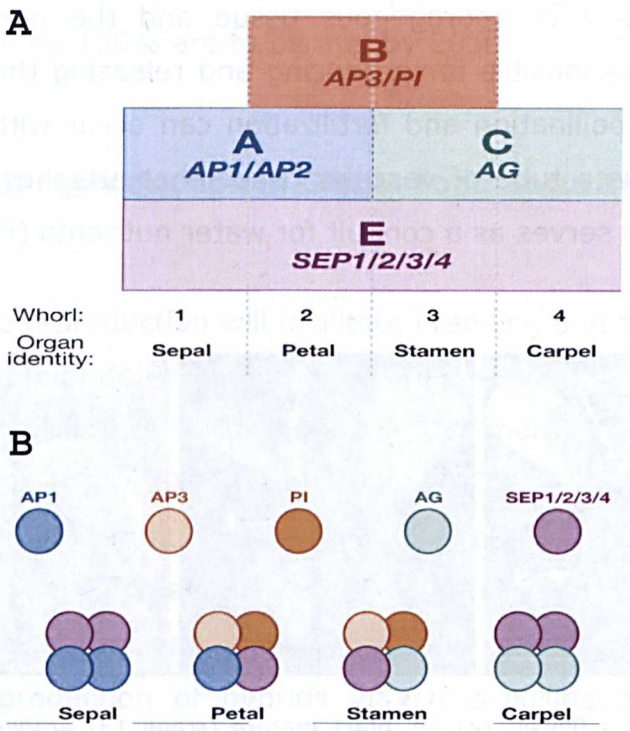

Lack of..	Results
B function	Transformation of stamens to carpels
C function	Transformation of stamens to petals
B-C function	Transformation of stamens to sepal

Fig.1.2 The ABC model. (*A*) The ABC functions are indicated as boxes with the *Arabidopsis* genes. The *SEP* genes are shown below the regions for A, B, and C functions. The normal floral organ identities corresponding to the whorls 1 through 4 are shown at the bottom. (*B*) The quartet model, with an expanded function as shown in A. ABCE MADS-domain proteins are shown as circles, with different shading as indicated at the top. Tetrameric complexes are shown for each organ identity (Ma, H., 2005).

In *Arabidopsis*, the A function requires the *APETALA1* (*AP1*) and *APETALA2* (*AP2*) genes. Stamens develop in the third whorl, where both B and C genes are expressed. The B classes of genes are *APETALA3* (*AP3*) and *PISTILLA* (*PI*), whereas the C gene is *AGAMOUS* (*AG*) (Ma, H., 2005). Molecular studies revealed that *AP1, PI* and *AG* genes are all expressed initially in regions of the floral meristem that will form stamen primordia and continue to be expressed in stamen primordia and developing stamens. The B class, C classes and SEP proteins all belong to the MADS (Ma, H., 2005) family of transcription factor, which bind a target DNA sequence (the CArG box) as homodimers or heterodimers. The dimerization of these proteins therefore explains the combinatorial action of B and C classes genes (along with SEP) in stamen (Scott et al. 2004; Honma and Goto, 2001). Mutations in any one of the B or C genes result in homeotic conversion of the third whorl organs to a different type (Fig.1.3).

Mutants lacking class A activity result in expansion of class C activity throughout the flower, for example *apetala 2 (ap2)*, produces flowers that consists of carpels in the first whorl, stamens in the second and third whorls, and carpels in the fourth whorl. On the other hand, the class B activity mutant, *pistillata (pi)* produces flowers consisting of sepals in the first and second whorls, and carpels in the third and fourth whorls. Moreover, C activity mutant, *agamous (ag)* , consists of sepals in the first whorl, petals in the second and third whorls, and reiterations of this pattern in interior whorls, consequence of expansion of class A activity and loss of floral determinacy. Finally, mutants of the four *SEPALLATA* genes (*sep1, sep2, sep3,* and *sep4*) consist of reiterating whorls of leaf-like (le) organs. Mutation of the SEP genes have a very subtle phenotypes, but in the *sep1, sep2, sep3* triple mutant, all floral organs resemble sepals, suggesting that B and C function have been abolished (Scott et al., 2004; Pelaz et al., 2000). The quadruple mutant (*sep1/2/3/4*) lacks class E activity resulting in impaired class A, B and C function and loss of floral determinacy.

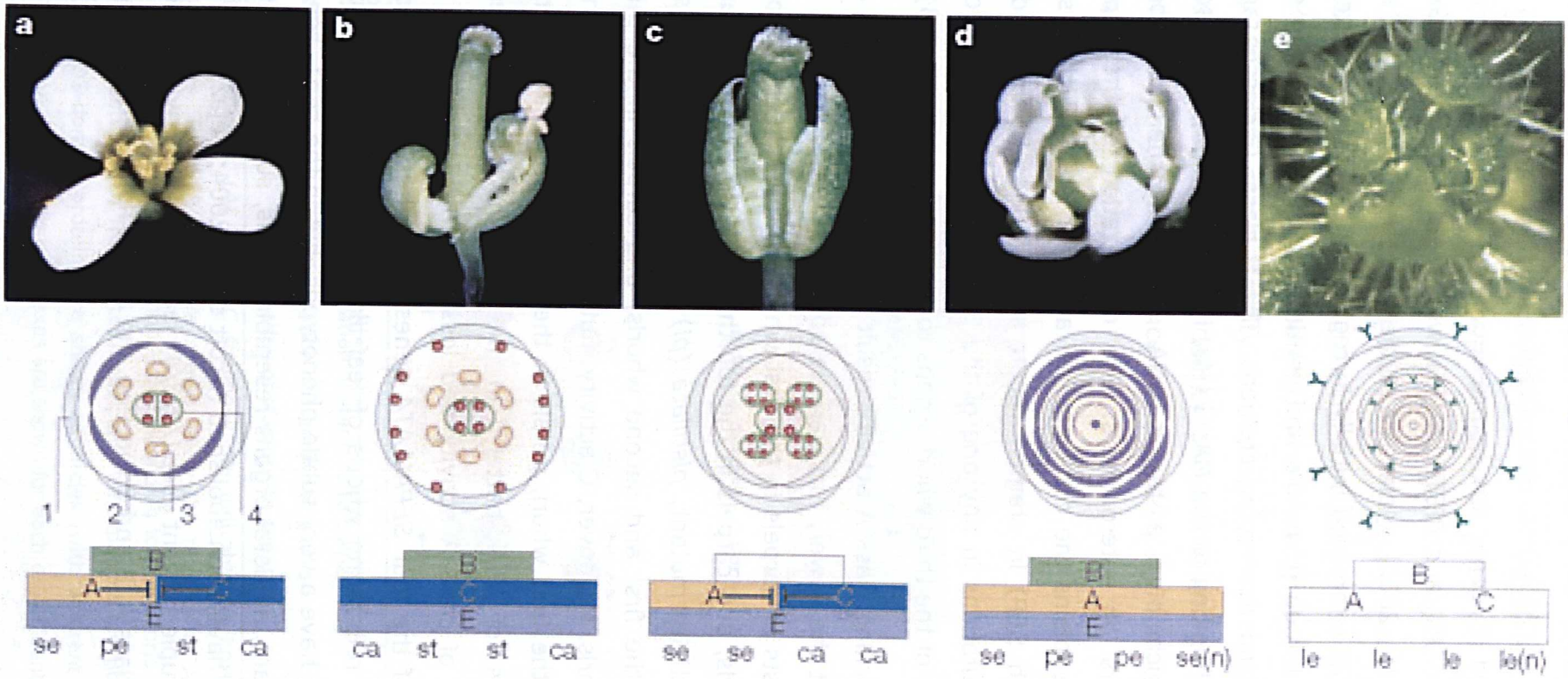
a
b
c
d
e
1
2
3
4
B
A
C
E
se
pe
st
ca
ca
st
st
ca
se
se
ca
ca
se
pe
pe
se(n)
le
le
le
le(n)

Fig.1.3 a) The wild-type *Arabidopsis thaliana* flower consists of four whorls of organs. Sepal (se) identity is conferred in the first whorl by class A activity, petal (pe) identity is conferred in the second whorl by class A and class B activity, stamen (st) identity is conferred in the third whorl by class B and class C activity and carpel (ca) identity is conferred in the fourth whorl by class C activity. Class E activity is required for the specification of each organ type. b) An *apetala2* (*ap2*) flower that consists of carpels in the first whorl, stamens in the second and third whorls, and carpels in the fourth whorl. The mutant lacks class A activity, resulting in expansion of class C activity throughout the flower. c) A *pistillata* (*pi*) flower that consists of sepals in the first and second whorls, and carpels in the third and fourth whorls. The mutant lacks class B activity. d) An *agamous* (*ag*) flower that consists of sepals in the first whorl, petals in the second and third whorls, and reiterations of this pattern in interior whorls. The mutant lacks class C activity, resulting in expansion of class A activity and loss of floral determinacy. e) A mutant flower for four *SEPALLATA* genes (*sep1 sep 2 sep3 sep4*) which consists of reiterating whorls of leaf-like (le) organs. The quadruple mutant lacks class E activity, resulting in impaired class A, B and C function and loss of floral determinacy (Krizek, et al., 2005).

After stamen specification, the B and C classes genes as well as *SEP* genes continue to be expressed during stamen development, so they could be responsible for activating many of the genes involved in stamen morphogenesis and function. Different experiments have indicated that some genes are affected by B, C or *SEP* suppression (Scott et al., 2004). Expression studies comparing *Antirrhinum* wild type and *def* mutant (lack of B function) showed 12 differentially expressed genes, including *tap1*, expressed in the tapetum and encoding a putative secreted protein, and filamentous flower1, *fil1*, expressed mainly in stamen filaments and petal bases and encoding a candidate cell wall protein (Scott et al., 2004).

1.4 Stamen development.

Stamens are the male reproductive organs of flowering plants. They consist of an anther, the site of pollen development and in most of the species a stalk-like filament, which transmits water and nutrients to the anther and position it to aid pollen dispersal (Fig.1.4). Within the anther, male sporogenous cells differentiate and undergo meiosis to produce microspores (Fig.1.5; Table.1.1). These give rise to pollen grains, whereas other cell types contribute to pollen maturation, protection or release (Scott et al, 2004).

Fig.1.4 *Arabidopsis thaliana*. s: sepal; p: petal; st: stamen; o: ovary (Picture from J. Berger, MPI for developmental Biology, Tübingen).

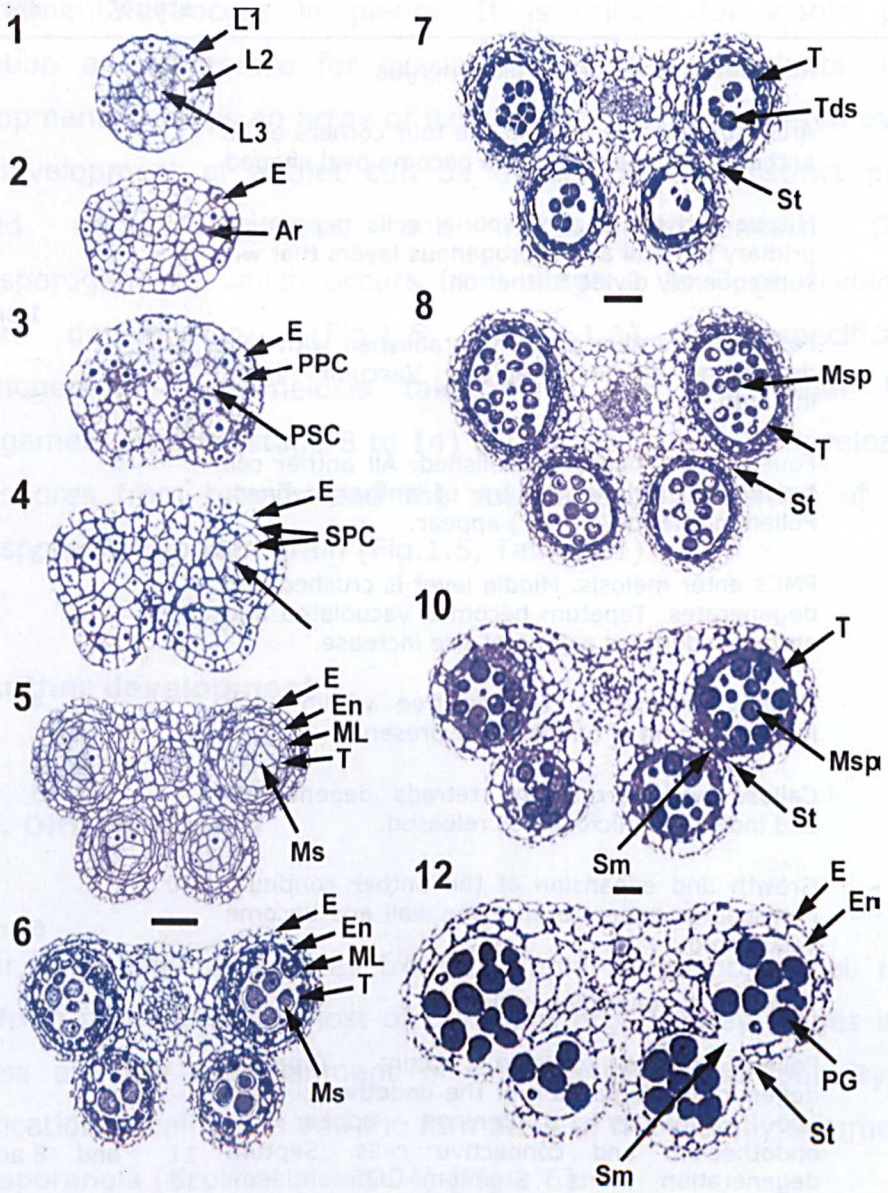

Figure.1.5 Anther cell differentiation. The stages of wild-type *Arabidopsis thaliana* anther development are shown. The numbers indicate stages. Bar = 25 μm and stages 1 to 5, 6 and 7, 8 and 10, and 12 alone have same-sized bars. Ar, archesporial; E, epidermis; En, endothecium; L1, L2, L3, Layer 1, 2, 3; ML, middle layer; Ms, microsporocytes; Msp, microspores ; PG, pollen grain; PPC, primary parietal cell; PSC, primary sporogenous cell; Sm, septum; SPC, secondary parietal cell; St, stomium; T, tapetum; Tds, tetrads. (Ma, H. 2005).

Stage	Major events and morphological changes	Flower stage[a]	Pollen stage[b]
1	Rounded stamen primordia emerges		
2	Archesporial cells arise in the four corners of he anther primordia. Primordia become oval shaped	5	
3	Mitotic activity in archesporial cells generating primary parietal and sporogenous layers that will subsequently divide further on.	7	
4	Four lobed anther pattern established with two developing stomium regions. Vascular region initiated.	8	1 and 2
5	Four defined locules established. All anther cell types present and pattern of anther defined. Pollen mother cells (PMC) appear.		
6	PMCs enter meiosis. Middle layer is crushed and degenerates. Tapetum becomes vacuolated and anther undergoes a general size increase.	9	3
7	Meiosis completed. Tetrads free within each locule. Remain of middle layer present.		4
8	Callose wall surrounding tetrads degenerates and individual microspores released.		5
9	Growth and expansion of the anther continue. Microspores generate an exine wall and become vacuolated.	10	6 and 7
10	Tapetum degeneration initiated.	11	
11	Pollen mitotic division occurs. Tapetum degenerates. Expansion of the endothecial layer and secondary thickenings appear in endothecium and connective cells. Septum degeneration starts. Stomium differentiation begins.	11 and 12	8 and 9
12	Tricellular pollen. Anthers become bilocular after breakage of septum. Stomium differentiates.		
13	Dehiscence. Breakage along stomium and pollen release.	13 and 14	10
14	Senescence of stamen. Shrinkage of cells and anther structure.	15 and 16	
15	Stamen falls off senescing flower.	17	

Table.1.1 Summary of the stages of *Arabidopsis thaliana* anther development (Sanders et al., 1999). [a] Flower development stages taken from Smyth et al. (1990) and Bowman et al. (1991) [b] Pollen development stages taken from Regan and Moffatt (1990).

Anther and pollen development represent one of the most important developmental process in plants. It is critical for viable pollen formation and therefore for sexual reproduction in plants. Pollen development involves an array of extraordinary high regulated events. The development of anther can be divided in two distinct phases termed microsporogenesis and microgametogenesis. During microsporogenesis, which occurs from stage 1 to 7 of *Arabidopsis* anther development (Fig.1.5, Table.1.1), histospecification, morphogenesis and meiosis take place. On the other hand, microgametogenesis (stage 8 to 14) is characterized by the release of microspores from tetrads and the subsequent maturation of these microspores into pollen grain (Fig.1.5, Table.1.1).

1.5 Anther development

1.5.1. Differentiation

Anther development initiates from a single Archesporial cell rather than from meristem like most of the plant organs. Key stages in this process are the establishment of an adaxial-abaxial polarity, the specification of cell types and the formation of the radially symmetrical microsporangia (Scott et al., 2004) (Fig.1.6).

The floral meristem of *Arabidopsis*, like the shoot apical meristem, is composed of three histogenic layers of cells with separate lineages: L1 (epidermis), L2 (sub epidermis) and L3 (core) (Scott et al., 2004). Stamen primordia are initiated by periclinal division in the floral meristem, usually within L2 (Jenik and Irish, 2000). The L2 gives rise to most of the cells types of the anther, including the sporogenous cells. With the growth of the anther primordium, cells of the L2 undergo a complex series of divisions leading to the formation of the four radially symmetrical microsporangia and conducting tissue that will be linked to the filament. The founder cells of the four microsporangia are single L2 archesporial cells, each of which divides

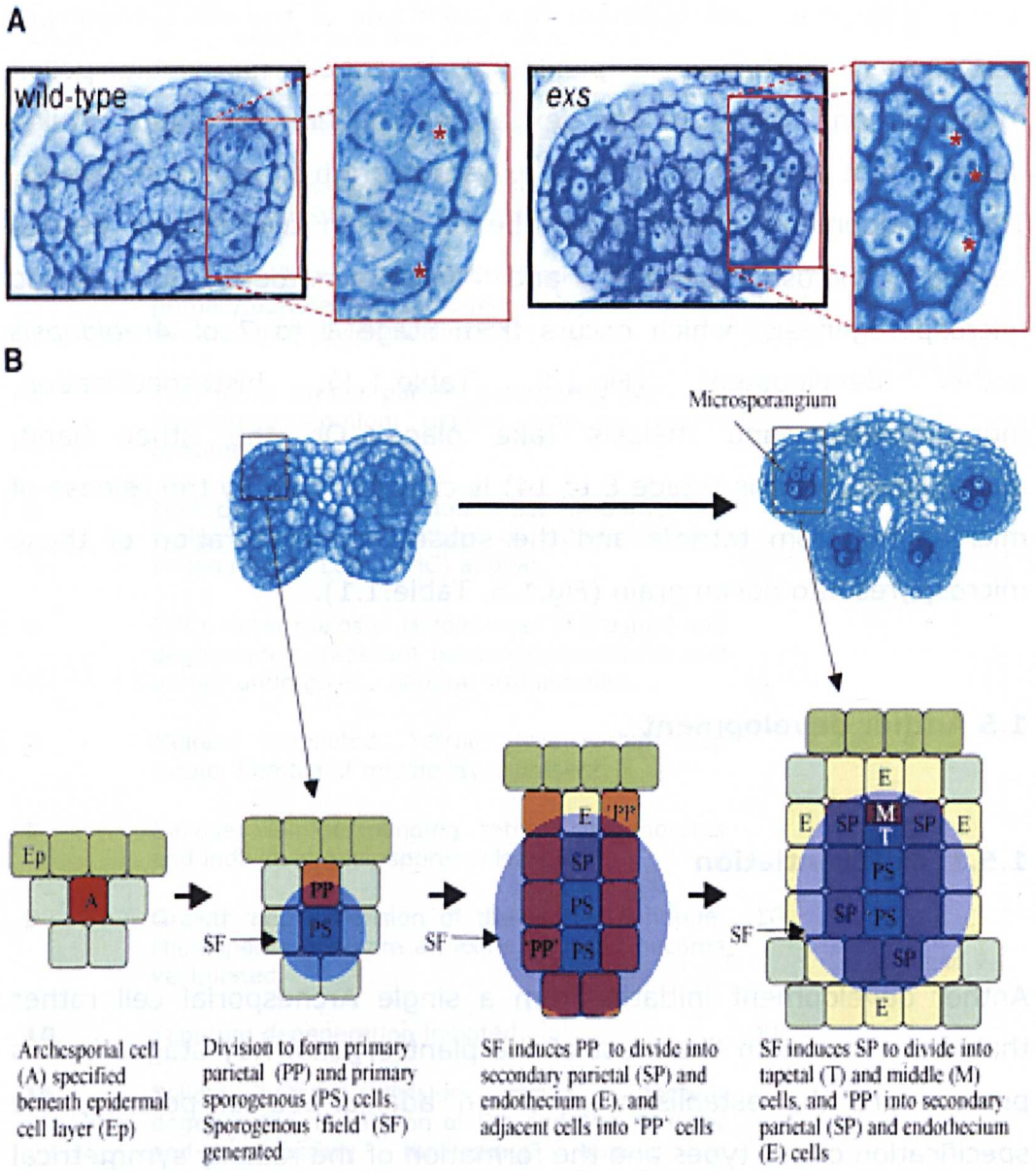

Fig.1.6 Model for the differentiation of the microsporangial cell layers in *Arabidopsis*. Scott et al (2004). A: Light micrographs of wild-type and *exs* anther primordial with archesporial cells marked by asterisks; extra archesporial cells arise in *exs* mutants (Canales et al., 2002). B: Model for the differentiation of the microsporangial in *Arabidopsis* (Scott et al., 2004).

periclinally to form a primary parietal cell (PP) subjacent to the L1 and a primary sporogenous cell (PS) facing inward (Canales et al.,2000), Fig.1.7.

The development fates of the two products of archesporial cell division in *Arabidopsis* are very different. The PS undergoes a small number of

divisions to generate the meiocytes, whereas the PP divides periclinally to form an endothecial cell subjacent to L1 and a secondary parietal cell (SP). The SPC again divides periclinally to generate a middle layer cell next to the endothecium and a tapetal cell adjacent to the sporogenous cells (Scott et al, 2004).

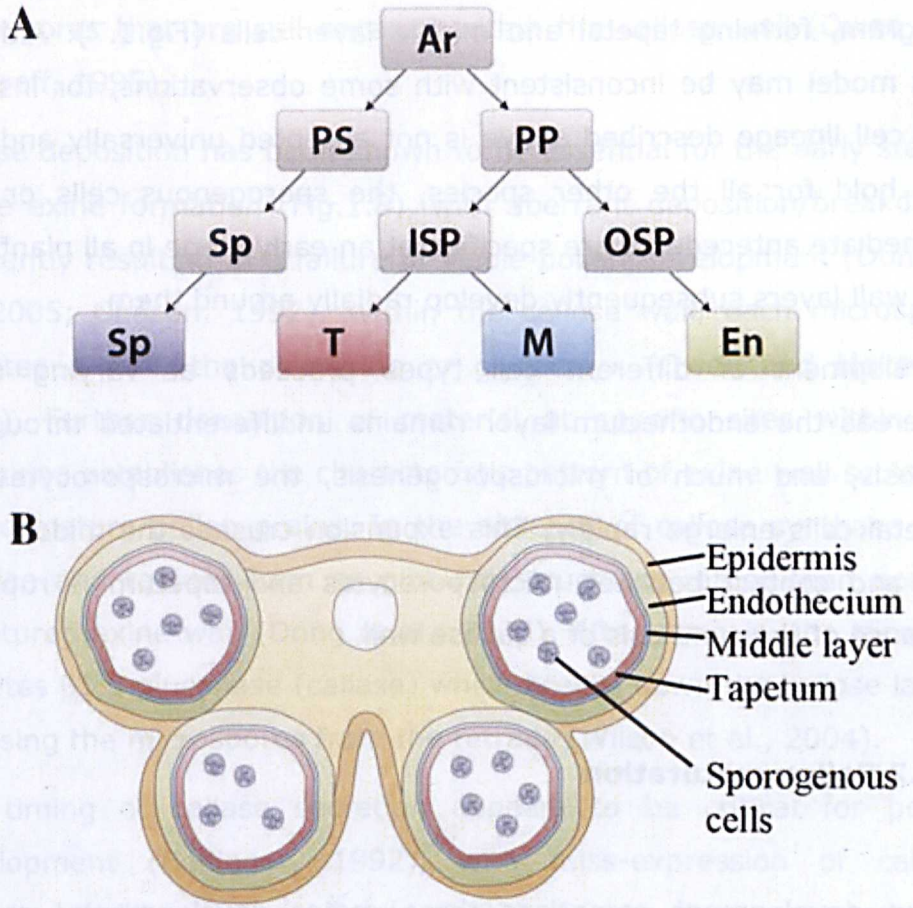

Fig.1.7 Anther structure. A) Archesporial cell division to form final anther cell layers. B) Diagram of the cell layers of the *Arabidopsis* anther Ar: Archesporial cells; PP: primary parietal cells; PS: primary sporogenous cells; Sp: sporogenous layer; ISP: inner secondary parietal layer; OSP: outer secondary parietal layer; T: tapetum; M: middle layer; En: Endothecium (Wilson et al., 2011).

Periclinal division of the single archesporial cell gives rise to a linear array of different cell types. However, to explain the radially symmetrical microsporangium a new model was developed (Scott et

al., 2004). This model confers a key organizational role on the sporogenous cells. In this scheme, the PS after its formation from the archesporial cell sets up a radial field of signals around itself (Scott et al., 2004). This field, which continues to be generated by the subsequent division products of the PS, induces periclinal division and development in adjacent cells. Thus, the PP is induced to divide to form an endothecial cell and, adjacent to the source of signals, the meristematic SP. The SP then executes the final division of the program, forming tapetal and middle layer cells (Fig.1.7). Although this model may be inconsistent with some observations, for instance the cell lineage described above is not accepted universally and does not hold for all the other species, the sporogenous cells or their immediate antecedents are specified at an early stage in all plants and the wall layers subsequently develop radially around them.

Development of different cell types proceeds at varying rates. Whereas the endothecium layer remains undifferentiated throughout meiosis, and much of microsporogenesis, the microsporocytes and tapetal cells enlarge rapidly. This expansion crushes the middle layer cell and contact between microsporocytes and tapetum is ruptured because of the synthesis of a callose wall.

1.5.2 Pollen maturation

Pollen development comprises three major developmental stages, microsporogenesis (differentiation of the sporogenous cells and meiosis), post-meiotic development of microspores and microspores mitosis (Chaudhury, 1993). Male sporogenesis occurs inside the anther locule. Before meiosis, five tissue layers have differentiated. The innermost cells, the sporocytes or pollen mother cells (PMC) are surrounded by the tapetum, the middle layer, the endothecium and the epidermis (Fig.1.5). The tapetal tissue consists of a single layer of metabolically active cells enclosing the anther locule. The tapetum surrounds the sporogenous cells and serves to nourish the developing

microspores during PMC meiosis and microspores maturation. The tapetum plays an active role in this process as it is responsible for the callose secretion, breakdown and synthesis of many pollen wall materials. Callose deposition starts before meiosis, with PMC walls accumulating callose within their walls. The callose wall becomes thicker and numerous small vacuoles are present throughout the PMC cytoplasm as they enter into meiosis. Every PMC undergoes two meiotic divisions producing a tetrad of four haploid cells called microspores that are still encased within the callose wall (Owen and Makaroff, 1995).

Callose deposition has been shown to be essential for the early stages of the exine formation (Fig.1.8), with aberrant deposition/breakdown frequently resulting in a failure of viable pollen development (Dong et al., 2005; Chasan, 1992). Within the callose wall, each microspore secretes a wall, the primexine or glycocalyx (Owen and Makaroff, 1995). Further deposition of material at specific sites within the primexine establishes the characteristic pattern of exine wall sculpting of the mature pollen grains. In the absence of callose synthase, the baculae and tectum form as globular structures rather than normal sculptured exine wall (Dong et al., 2005). After meiosis, the tapetum secretes β1,3 glucanase (callase) which breaks down the callose layer, releasing the microspores from the tetrads (Wilson et al., 2004).

The timing of callase secretion appears to be critical for pollen development (Bedinger, 1992), with miss-expression of callase causing sterility (Worral et al., 1992). It has been reported that callase activity follows a tight regulatory pattern during development. A low level of activity is present during the first meiotic division, but once the second meiotic division takes place, this rapidly increases and peaks at the time of microspore release (Steiglltz et al, 1977: Chasan, 1992: Worral et al, 1992).

The microspores then go through a process of wall deposition co-ordinated by the tapetum and also, in part, by the microspores/immature pollen grains. During normal development osmiophilic lipid bodies form in the tapetum and are exported into the

locule by exocytosis, and the acyl precursors polymerize to form the sculptured exine (Wilson et al., 2007). The tapetum in *Arabidopsis* is of the secretory type (Pacini et al., 1985) with the cells retaining their shape and position as they lose their cell walls. Only the inner tangential and radial surfaces seem to have secretory properties. Changes in the pattern of tapetal secretion are observed in the *ms1* mutant, the inner tangential membrane persists, secretion is impaired and programmed cell death fails to occur (Vizcay Barrena and Wilson, 2006). In the wild type, vesicles fuse to the radial and tangential membranes, releasing their contents into the anther locule; this fails to occur in the *ms1* mutant. Instead, they fuse to others situated in the inside of the cell, thus failing to provide crucial components of the pollen wall to maturing microspores (Vizcay Barrena and Wilson, 2006).

The tapetum has a highly regulated transient lifecycle. As pollen grain maturation occurs, the tapetal cells become increasingly vacuolated and accumulate elaioplasts and large cytoplasmic lipid bodies. Soon after the first pollen mitotic division, the tapetal cells undergo programmed cell death (PCD) (Vizcay-Barrena and Wilson, 2006) and release their contents into the anther locule. These contents are essential for pollen wall formation.

The pollen wall consists of two layers, exine and intine (Fig.1.8). The intine is the innermost (cellulose, pectin and various proteins) and is secreted by microspore. The intine is divided into two layers, the granular exintine facing the exterior and a microfibrillar endintine toward the interior. The exine, facing the exterior, comprises two layers, nexine, the innermost and the sculpted sexine that presents multiple pores and furrows. The sexine can be separated in two layers, tectum and baculae. The exine is composed mostly of sporopollenin. Sporopollenin is extremely resistant composition and it serves as a protective barrier against excess dehydratation and fungal and bacterial attack. Sporopollenin is one of the complex biopolymers that confers the exine high resistance to biological and environmental stresses (Meuter-Gerhard et al., 1999), and experimental evidence

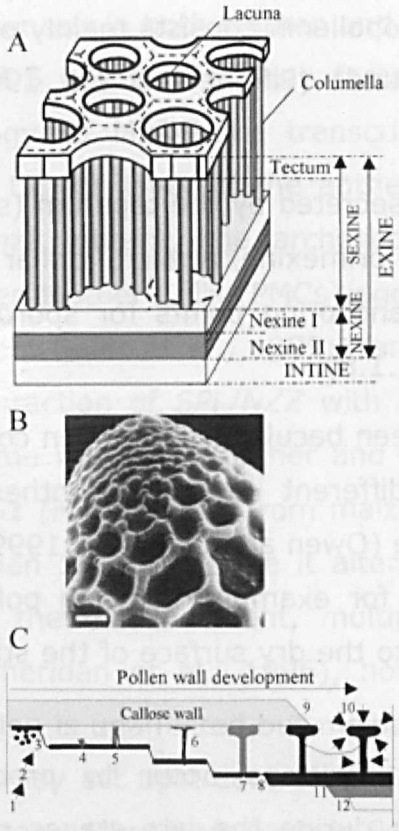

Fig.1.8 Model of pollen wall development based on *Lilium* (Scott, 2004). A) Scheme of the main architectural features of a generalized mature pollen wall. The terminology is according to Erdtman (1969). B) Scanning electron micrograph of a *Lilium* pollen wall showing a reticulate pattern formed by the fused heads of the columellae. The nexine I is visible through the lacunae. Bar = 5 µm. C) Events begin before meiosis and proceed from left to right until the mature wall is formed. 1) Transcription of "pattern" genes in the premeiotic microsporocyte nucleus. 2) Insertion of labile pattern information into the plasma membrane via endoplasmic reticulum–derived vesicles, followed by tessellation to produce a negative stencil of plates. 3) First phase of primexine synthesis over the entire microspore surface except areas destined to become apertures. 4) Conversion of primexine to a sporopollenin-receptive state through the activity of a factor(s) secreted from sites between the plates. 5) Second phase of primexine synthesis, more rapid than the first, resulting in limited primexine conversion and specification of columellae. 6) Nascent columellae are apparent as lamellated strands that lack substantial sporopollenin. 7) Consolidation of columellae by the appearance of partially polymerized (proto) sporopollenin on the receptive surfaces. 8) Final phase of primexine synthesis, during which the pattern stencil dissipates or is circumvented to produce the solid nexine I. 9) The callose wall is dissolved. 10) Wall elements are further consolidated by tapetally derived sporopollenin. 11) Nexine II is synthesized without the participation of the primexine. 12) Intine synthesis is initiated.

has proved that sporopollenin consists mainly of fatty acid derivatives and phenolic compounds (Piffanelli et al., 1998; Blackmore et al., 2007).

The sporopollenin is secreted by the tapetum (sporophytic origin) and polymerizes onto the primexine, a microfibrillar polysaccharide matrix that serves as the anchoring points for sporopollenin deposition to form the baculae (Fig.1.8).

Filling the gaps between baculae is the pollen coat (sporophytic origin) consisting of two different tapetally synthesised coat materials, pollenkit and tryphine (Owen and Makaroff, 1999). The pollen coat has numerous functions, for example, allowing pollen grains to stick to pollinator vectors or to the dry surface of the stigmas (Piffanelli et al., 1998).

Two further mitotic divisions occur to produce functional male gametes. This occurs during the late stages of pollen development (stage 11, Table.1.1) as seen in species that produce tricellular pollen. Therefore, pollen development is a post-meiotic process that produces mature pollen grains from microspores. In addition to activities within the microspores itself, sporophytic anther tissues play important roles in this process not only providing physical support but also by supplying signals and materials necessary for pollen development. Especially the tapetum, which is the innermost somatic cells layer of the anther locule and plays an essential role in pollen development.

1.5.3. Regulation of anther and pollen development

The regulation of pollen development has been studied in detail in *Arabidopsis*; this is the most widely studied plant and is being used as a model for other plant species (Fig.1.9).

One of the earliest genes required for cell division and differentiation in the anther is the *SPOROCYTELESS/ NOZZLE* (*SPL/NZZ*) gene (Schieftaler et al, 1999; Yang et al, 1999). *SPL/NZZ* is required for

the initiation of sporogenesis in both stamen and carpel and is induced by the AGAMOUS MADS box transcription factor (Ito et al., 2004). NZZ/SPL has homology to MADS-like transcription factors and is thought to act in the L2 cell layer of the anther during archesporial division. In the *spl/nzz* mutant, the archesporial initiation occurs normally, but the Pollen Mother Cells (PMCs) and the surrounding cell layers fail to form (Schieftaler et al., 1999; Yang et al., 1999). This suggests that the interaction of *SPL/NZZ* with the surrounding cells determines the outcome within the anther and ovule. The *MULTIPLE ARCHESPORIAL CELLS1 (MAC1)* gene from maize appears to function at an earlier stage than *SPL/NZZ* since it alters the specification of archesporial cells. In the *mac1* mutant, multiple archesporial cells form in the ovule (Sheridan et al., 1996), however in the anther, archesporial specification is unaffected but meiotic arrest is seen. This implies that *SPL/NZZ* may act upstream of *MAC1* in anthers (Yang et al., 1999). *AG* expression occurs from early in floral initiation until late in flower development. Early expression acts in the specification of stamen and carpel (Ito et al., 2004). *AGAMOUS* regulates stamen development at least in part by controlling the induction of *DEFECTIVE IN ANTHER DEHISCENCE1* (Ito et al., 2007b), which codes for a chloroplastic phospholipase A1, that catalyses the initial step in jasmonic acid (JA) biosynthesis. The function of *AGAMOUS* appears to be conserved in rice but has been associated with two MADS genes, *OsMADS53* and *OsMADS58* (Yamaguchi et al., 2006).

Early tapetal initiation in *Arabidopsis* is also affected by the downstream genes *EXTRA SPOROGENOUS CELLS/EXS MICROSPOROCYTES1 (EXS/EMS1)* (Canales et al 2002, Zhao et al, 2002) (Fig.1.6), *TAPETAL DETERMINANT1* (TPD1) (Yang et al., 2003) and the *EXS1/EMS1* rice orthologue *MULTIPLE SPOROCYTE1 (MSP1)* (Nonomura et al., 2003) which are required for normal anther and cell differentiation as the *msp1* mutant exhibits an increased number of male sporocytes and a lack of the tapetum. *EXS1/EMS1* appears to regulate the number of cells that divide in the L2 layer of the anther, which go to form archesporial cells, and therefore the number of

sporogenous cells initials. In the *exs1/ems1* mutant, additional meiocytes are formed, but the tapetal and middle cell layer are also missing.

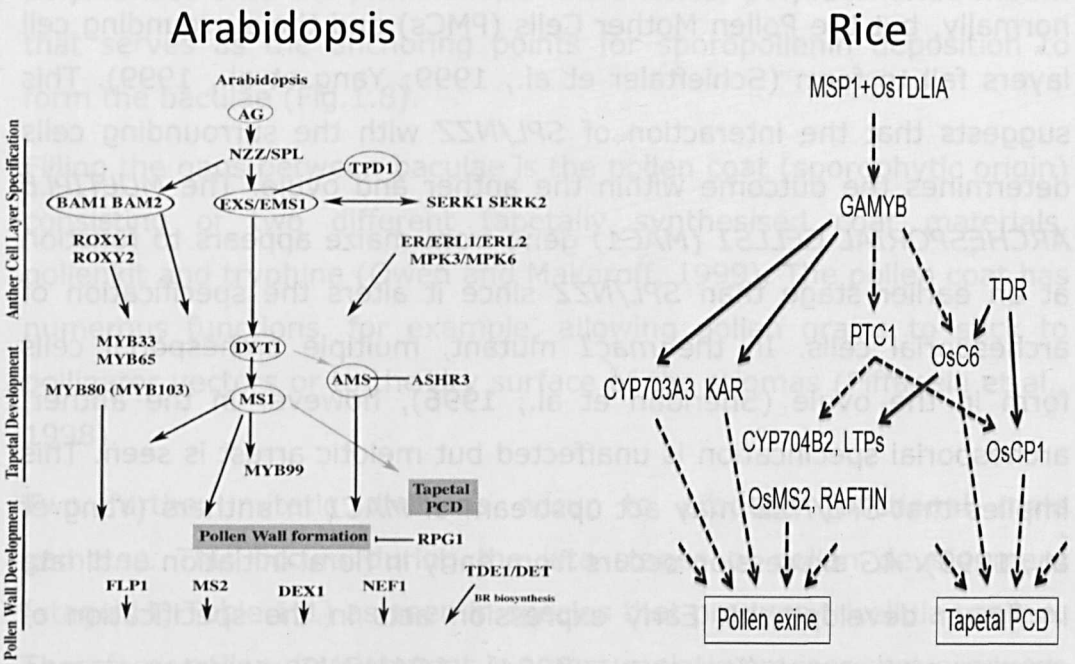

Fig.1.9 Comparisons between the regulation network for pollen development in *Arabidopsis* and rice (Wilson et al., 2009). *Arabidopsis* network has been widely studied and numerous genes have been characterized. In addition, rice has been shown to have great similarities within this regulation network. Several genes, such as *MSP1, TDR* or *PTC1* have been shown to have similar function.

The *EXS1/EMS1* gene encodes a putative serine threonine LRR (leucine rich repeat) receptor kinase (Canales et al., 2002; Zhao et al., 2002). It is thought to act by complexing with different proteins for instance TPD1 (small protein of 176 amino acids) in different tissues and therefore to restrict growth within the L2 layer of the anther or enhance growth in the embryo (Canales et al. 2002). *TPD1* is expressed predominantly within the microsporocyte and may reflect interactions between the developing sporocytes as a default pathway in the absence of *TPD1* (Yang et al., 2003). The formation of sporogenous cells in the absence of the tapetum in *tpd1* and *exs/ems1*

mutants implies that sporocytes can form, and the process of meiosis can be initiated in the absence of the tapetal cell layer. However, both mutants are male sterile with degeneration of the microsporocytes occurring during meiosis II, suggesting that the development of viable pollen requires a functional tapetum (Fig.1.10). Recently, the interaction between EMS1/EXS and TPD1 has been confirmed *in vitro* and *in vivo,* suggesting that TPD1 serves as a ligand for the EMS1 receptor kinase (Yang et al., 2005; Jia et al., 2008).

A number of leucine-rich repeat receptor-like protein kinases (LRR-RLKs) have also been shown to be important in anther cell specification. Among them, BAM1 and BAM2 (BARELY ANY MERISTEM) have been shown to act redundantly in cell fate specification in the anther, in determining the early stages defining the parietal cells that give rise to the endothecium, middle and tapetal layer. In the *bam1/bam2* double mutant, these cell layers are absent, although PMC-like cells are seen, but these subsequently degenerate, suggesting that BAM1/BAM2 act redundantly to negatively regulate sporogenous cell number by promoting differentiation of the surrounding somatic cells (Hord et al., 2006).

In addition, Somatic Embryogenesis Receptor-Like Kinase 1 (*SERK1*) and *SERK2*, also appear to have redundant functions during this early stage of tapetal initiation (Albrecht et al, 2005; Colcombet et al, 2005). When mutated, they produce a similar phenotype to that of *ems1/exs* and *tpd1* mutants in that the tapetal layer is absent, resulting in more sporogenous cells and a lack of a tapetal cell layer. Sporocyte formation occurs in these mutants, but a functional tapetum is required for completion of meiosis and production of viable pollen. Moreover, the ER-family of LRR-RLKs (*ER, ERL1* and *ERL2*) and *MPK3* and *MPK6* have both been shown to act redundantly in cell differentiation during early anther development (Hord et al., 2008). In the absence of *ER/ERL1/ERL2* expression, aberrant cell patterning occurs with increased tapetal cells, and sometimes middle layer cells numbers, suggesting that they may act in the division and regulation of signals needed for early tapetal development (Hord et al., 2008).

On the other hand, the *MPK3/MPK6* genes also affect cell division during these early stages of anther differentiation (Fig.1.9). Mutant phenotypes produced by these two families of genes are similar to that seen in the *ems1/exs, serk1, serk2* and *tpd1.* However, the *mpk3/mpk6* and *er/erl1/erl2* mutants are able to produce a tapetal layer. In addition, expression analysis has suggested that *EMS1* and *TPD1* expression is not affected in the *mpk3/+ mpk/-* mutant. This suggests that *ER/ERL1/ERL2* and *MPK3/MPK6* may act independently to the previously characterized pathway of cell differentiation in the anther (Hord et al., 2008).

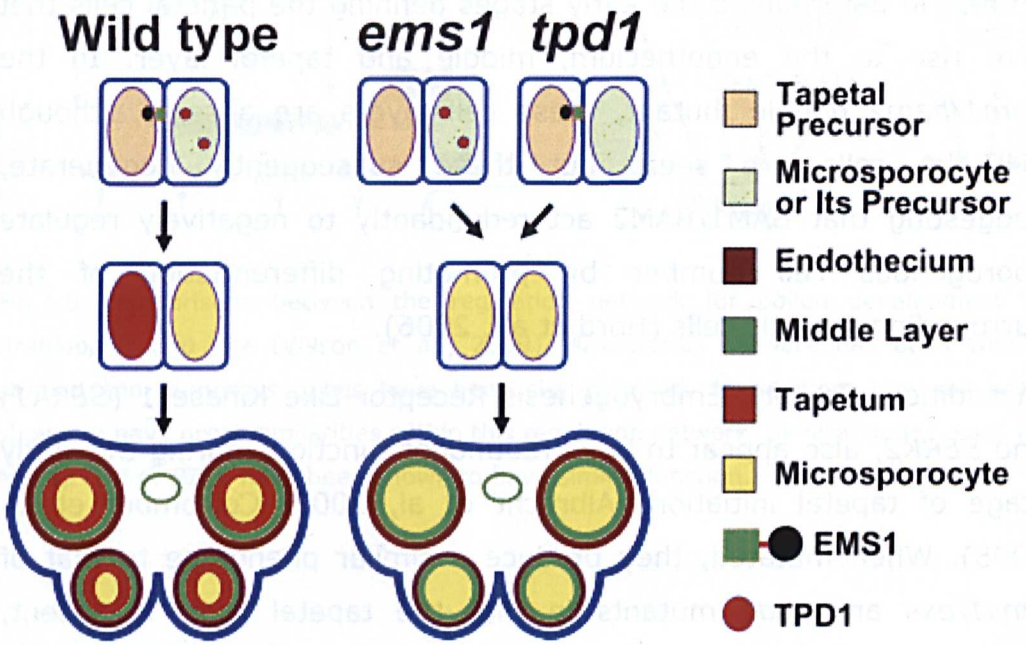

Fig.1.10 A model for EMS1-TPD1 signalling in anther cell fate determination in *Arabidopsis.* In the wild-type anther, TDP1, a small protein is secreted from microsporocytes or their precursors, which binds to EMS1 receptor kinases that are localized to tapetal precursors. EMS1-TPD1 signalling ensures specification of tapetal cell fate by activating the downstream signalling cascade. In the absence of the TPD1 ligand or EMS1 receptor in the *tpd1* or *ems1* mutant, signals directing tapetum differentiation are blocked. Consequently, tapetal precursors adopt a microsporocyte fate, resulting in the formation of excess microsporocytes. (Gengxiang et al., 2008).

MYB33 and *MYB65* also act redundantly to facilitate tapetal development around the stage of meiosis, and it has been shown that the expression of *MYB33* is regulated by miRNA. However, their effect on fertility is conditional based upon environmental conditions (Millar and Gubler, 2005). These genes, which are involved in tapetal initiation, are not affected in the *dyt1* mutant, and it has been suggested that they act by forming a complex with DYT1 (Zhang et al, 2006). *DYT1* encodes a putative a basic helix-loop-helix (bHLH) transcription factor that is predicted to act downstream of *SPL/NZZ* and *EMS1/EXS* (Fig.1.9). In the *dyt1* mutant, tapetum and meiosis initiation occurs, although tapetal development is abnormal with enlarged vacuoles and microspore degeneration, therefore, *DYT1* seems to be required for tapetal gene regulation. However, it is not sufficient for tapetal development since *DYT1* over-expression does not rescue the phenotype in the *spl/nzz*. In addition, *DYT1* has been proposed to be involved in the regulation of many tapetal genes, either directly or indirectly. These include *ABORTED MICROSPORES (AMS)* and *MALE STERILE1 (MS1)* (Zhang et al., 2006), whereas the expression of two other genes, *MYB33* and *MYB65*, which have been associated with this stage of tapetal development, remain unaffected.

The *AMS* gene encodes a putative bHLH-type transcription factor and its expression begins at a low level pre-meiotically and increases in postmeiotic flowers (Sorensen et al., 2003). It has been also shown that mutation of *AMS* results in a down regulation of gene expression commencing from meiosis. Many of these genes are associated with metabolic changes occurring in the tapetum and in the biosynthesis of pollen wall materials (Xu et al., 2010). The *ams* mutant presents premature microspore and tapetal degeneration has short stamen filament, and the tapetum becomes abnormally enlarged and vacuolated (Sorensen et al., 2003). Recently, it has been shown that the *Arabidopsis* SET-domain protein ASHR3 can interact with AMS and, when over-expressed, results in reduced male fertility. This suggests that ASHR3 may serve to target AMS to chromatin and thereby regulate stamen development (Thorstensen et al., 2008). An

orthologue of *AMS* has been described in rice (Fig.1.9). Tapetum Degeneration Retardation (*TDR*) is preferentially expressed in the tapetum and encodes a putative basic helix-loop-helix protein. TDR controls rice tapetum development and degeneration by positively regulating tapetum programmed cell death (PCD). This gene is strongly expressed in the tapetum from the meiosis stage to the young microspore stage. *tdr* plants appear normal during vegetative and floral development, but fail to produce any viable pollen, with complete male sterility. At the early tetrad stage, no significant differences are observed in the anther wall layers and microspores between the wild-type and the *tdr* mutant. The main morphological defect in the *tdr* mutant is that the tapetum seems to be abnormally expanded without degradation and the microspores collapse at the later stages. The mechanism of TDR regulating tapetum development and degradation is possibly via the positive triggering of programmed cells death (PCD) of tapetal cells during pollen development (Li et al., 2006).

MS1 is a transcription factor which shows a tightly regulated expression in the tapetum as the callose breaks down, up to the free microspore stage (Yang et al., 2007). Therefore, the pattern of *MS1* expression is highly localised both temporally and spatially (tapetal tissue in closed buds around the stage of microspores release to early microspores). *MS1* encodes a protein (672 amino acids), containing a putative Leucine Zipper (LZ) and a Plant Homeodomain (PHD) finger motif that are essential for MS1 function. Leucine zippers are found in bZIP and bHLH-ZIP transcription factors and mediate protein dimerization through a coiled-coil structure (Meshi and Iwabuchi, 1995). Thus, in MS1 the LZ may facilitate protein-protein interaction. The PHD finger domain (Cys rich; Cys-His, metal binding, T factor and transcription regulation) is a conserved motif found in histone methyltransferase, histone acetyltransferase and chromatin binding and DNA binding proteins in plants, yeast and human (Wilson et al., 2001; Ito and Shinozaki, 2002). In plants their biochemical function is unknown, however, they have been linked to chromatin modifications

in vernalization (De Lucia at al., 2008). Two roles have been suggested for MS1, on one hand, it is thought that it may function as a DNA binding transcription factor. On the other hand, it may be a non-DNA binding transcription factor and act via protein-protein interaction. Recently, the PHD-finger domain has been associated with chromatin remodelling. For example, PHD domains of the NURF and the ING2 proteins bind to trimethylated Lys-4 of the histone H3 and mediate chromatin remodelling (Li et al., 2006; Pena et al., 2006; Shi et al., 2006; Wysocka et al., 2006).

The *ms1* causes the abortion of immature pollen after the microspore release from the tetrads. In this process, the tapetum plays an important role. In normal development, soon after microspores are released from the tetrads, and before mitosis I, the tapetum cells start to degenerate by programmed cell death (PCD) (Fig.1.11). This is marked by shrinkage of the cytoplasm and subsequent separation from the cell wall. The tapetal cytoplasm becomes vacuolated as the wall degrades and multiple vesicles containing exine precursors (pollen wall component) fuse with the plasma membrane, releasing their content into the anther locule (Vizcay-Barrena and Wilson, 2006). Therefore, when tapetum cell death occurs, components for pollen wall formation are released into the locule. Mutation of *Arabidopsis MS1* has resulted in truncated transcripts that are predicted to produce a non functional protein of 199 amino acids which results in male sterility. Six *ms1* alleles have been identified, all with mutations resulting in the loss of the PHD finger motif. All the mutants show a similar phenotype of pollen degeneration soon after microspore release from tetrads. The tapetum is abnormally vacuolated and the microspores tend to stick together, suggesting an unusual composition of pollen wall material where preliminary exine development occurs but only with limited sporopollenin deposition (Ito and Shinozaki, 2002; Ariizumi et al., 2005; Vizcay-Barrena and Wilson, 2006).

PCD in wild type occurs when the tapetal cells are undergoing active synthesis and secretion of pollen wall components. A signal triggers

PCD, and the tapetum goes through cell death releasing its cell contents into anther cell locule (Paris et al., 2010). This degradation (PCD) seems to be a highly controlled process, which involves *MS1* and also a number of other genes expressed within the tapetum. Multiple alleles of the *ms1* mutant have been observed to show altered tapetal PCD. The tapetum becomes abnormally vacuolated soon after microspores are releases from the tetrad and necrotic-based breakdown rather than PCD occurs (Vizcay-Barrena and Wilson, 2006). Two different mechanisms have been proposed to explain the role of MS1 in PCD.

The first suggests that MS1 modifies the transcription of tapetal genes involved in pollen wall formation and thus initiates normal tapetal PCD to facilitate complete deposition of tapetal wall materials onto the pollen grain. Alternatively, the *MS1* gene may regulate tapetal development by directly regulating tapetal PCD. PCD is a "ready to be activated" process in the tapetal cells (Balk and Leaver, 2001; Parish et al., 2011). Normally the process of PCD is on hold until the tapetal cells have fully synthesized and secreted the required metabolites, then a signal triggers PCD and the tapetum goes through an irreversible sequence of events that leads to cell death. Caspase-like activity has been associated to PCD in plants (Solomon et al.,1999; Lam and del Pozo,2000; Hoerbertichts and Woltering, 2003); However the exact nature of these plant cysteine proteases have yet to be established. In the case of rice, a cysteine protease (OsCP1) and a protease inhibitor (OsCP6) have been shown to be direct targets of OsTDR (Li et al., 2006) and have been implicated in the process of tapetal PCD induction. During the final stages of this degeneration, the tapetum disintegrates, releasing components such as pollenkit and tryphine which will be incorporated into the pollen coat. Moreover it is also suggested that MS1 might regulate tapetal proliferation by inhibiting PCD while it is expressed (Vizcay-Barrena and Wilson, 2006).

A large number of genes are down-regulated in the *ms1* mutants, indicating the key role that MS1 plays in regulating late tapetal gene

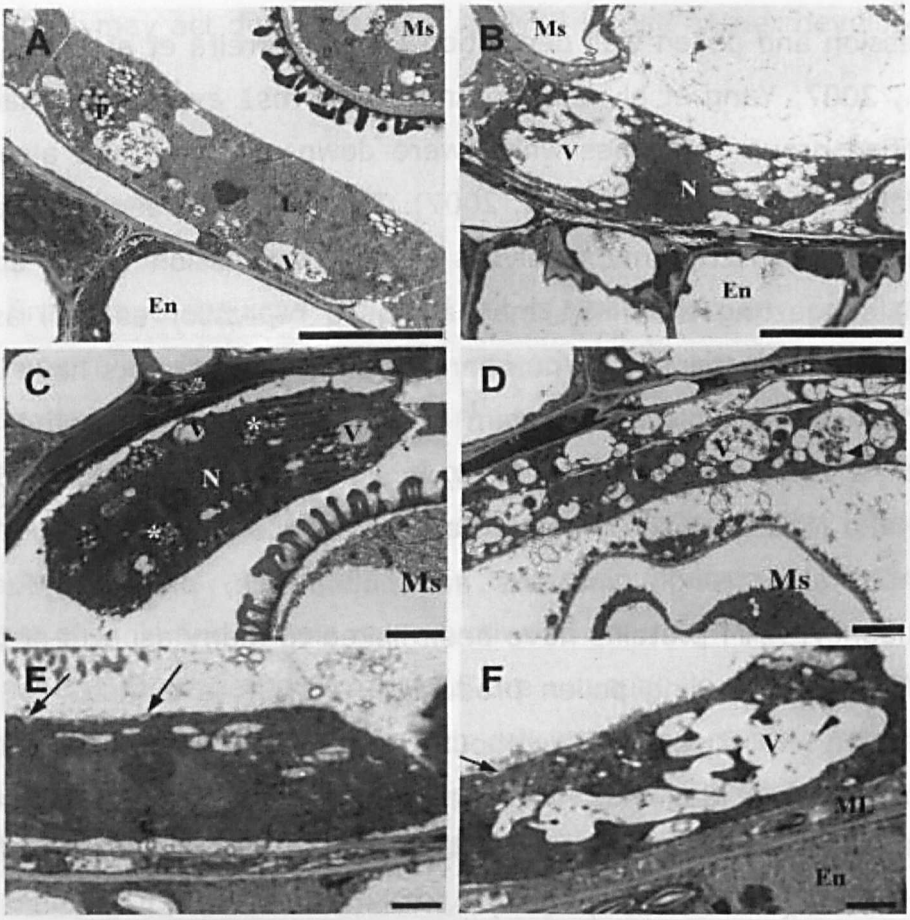

Fig.1.11 Transmission Electron Micrographs of Cross Sections through Wild-Type and *ms1* Mutant Anthers during Ring-Vacuolate Stage/Microspore Mitosis. **(A)**, **(C)**, and **(E)** The wild type. **(B)**, **(D)**, and **(F)** *ms1*. **(A)** The wild-type tapetal cells show a compact cytoplasm with some vacuoles containing fibrillar material and plastids with large inclusions. Big lipid droplets can be seen in the cytoplasm. Bar = 5 μm. **(B)** By contrast, in the mutant, the cytoplasm is filled with big vacuoles, and fewer plastids are visible. Bar = 10 μm. **(C)** and **(D)** Tapetal cells at the ring-vacuolate stage. In the wild type **(C)**, plastid inclusions (asterisks) have become more electron transparent. Some small vacuoles are present in the cytoplasm. In the mutant **(D)**, the vacuoles are increased in number and larger in size. They keep at a distance of the outer tangential membrane, and they seem to contain portions of cytoplasm and organelles, such as mitochondria (arrowhead). Bars = 2 μm. **(E)** and **(F)** Enlarged region of tapetum in the wild type and the mutant, respectively. **(E)** In the wild type, the tapetal inner membrane has degraded, while the outer membrane is still present. Plastid inclusions and vesicles containing fibrillar material (arrows) fuse to the membrane releasing material into the anther locule. **(F)** However, in the mutant, the inner membrane is still present, and larger vacuoles are present due to the fusing of the vesicles (arrow). Bars in **(E)** and **(F)** = 1 μm. Ms, microspore; En, endothecium; ML, middle cell layer; L, lipid globules; p, plastid; V, vacuole; N, nucleus (Yang et al., 2007).

expression and pollen wall deposition (Alves-Ferreira et al., 2007; Ito et al., 2007; Yang et al., 2007). Analysis of *ms1* expression changes identified groups of genes which were down-regulated and also up-regulated (Alves-Ferreira et al., 2007). This was also seen in separate Affymetrix transcriptomic analyses of *ms1* expression (Yang et al., 2007) suggesting that MS1 may act as a repressor as well as an activator of transcription. A number of transcription factors have been identified as possible downstream targets. Among these is the NAM protein (NAC domain), At1g61110, which is the most repressed in *ms1*, and MYB99 (MYB domain). However, these do not appear to be essential since single mutants are not sterile, probably due to redundancy. NAM proteins have been linked to many aspects of plant development including pollen production. MYB99 is induced by *MS1* expression (Ito et al., 2007) without the requirement for novo protein synthesis, suggesting that MYB99 may be a direct target for *MS1* and may act via At1g61110 to regulate components of sporopollenin biosynthesis (Wilson et al., 2007).

MS1 function has been shown to be conserved in monocots with the orthologue *PERSISTENT TAPETAL CELL 1 (PTC1)* recently characterized in rice (Li et al., 2011). This gene encodes a PHD finger protein, which is specially expressed in the tapetal cells and microspores. Histological analysis of the *ptc1* mutant indicated that early events in anther and anther and pollen development progressed normally until after meiosis and microspore release. In *ptc1*, as in *Arabidopsis ms1*, pollen formation is affected by the premature tapetum degeneration. Therefore, in *ptc1* anthers, at stage 13, when mature pollen grains should have formed, only cell debris of both tapetal cells and pollen grains remained. Tapetal PCD fails to occur in *ptc1* tapetum, which appears to go through over-proliferation resulting in the extrusion of cytoplasmic contents, which are constrained by the persistent plasma membrane, into the locule (Li et al., 2011). In addition, no reduction of *PTC1* expression was observed in rice *utd1* or *tdr* mutants (Jung et al., 2005; Zhang et al., 2008), while significant reduction of *PTC1* was seen in *gamyb-2* (Aya et al., 2009), suggesting

that PTC1 may act downstream of GAMYB in rice anther development (Fig.1.9).

1.6 Pollination.

The final stage required for seed set is pollination and fertilization. Angiosperm reproduction is highly selective. Female tissues are able to discriminate between pollen grains, recognizing pollen from the appropriated species while rejecting pollen from unrelated species (or from the same genetic background in self-incompatibility species). This selectivity is accompanied by tremendous diversity in the cell surface of male and female reproductive structures.

Mature angiospermas pollen grains are unusual vegetative cells that contain sperm cells, complete with cell walls and plasma membrane (Edlund et al., 2004). This arrangement is accomplished soon after meiosis, when an asymmetric mitotic division produces a large cell that engulfs its diminutive sister, the generative cell (Twell et al., 1998; Yang and Sundaresan, 2000). Subsequently, the generative cell undergoes a second mitosis to form the second sperm cell required for double fertilization; tricellular pollen complete this division before it is released from the anther, whereas bicellular pollen undergoes this division only later, within the elongation pollen tube.

Stigmas, the receptive portions of the female tissues, capture pollen and mediate tube migration into the style. Stigmas generally are classified into two groups: wet stigmas, which are covered with surface cells that often lyse to release a viscous surface secretion containing proteins, lipids, polysaccharides, and pigments; and dry stigmas, which have intact surface cells that typically protrude as papillae and are covered by a primary cell wall, a waxy cuticle, and a proteinaceous pellicle (Fig.1.12.).

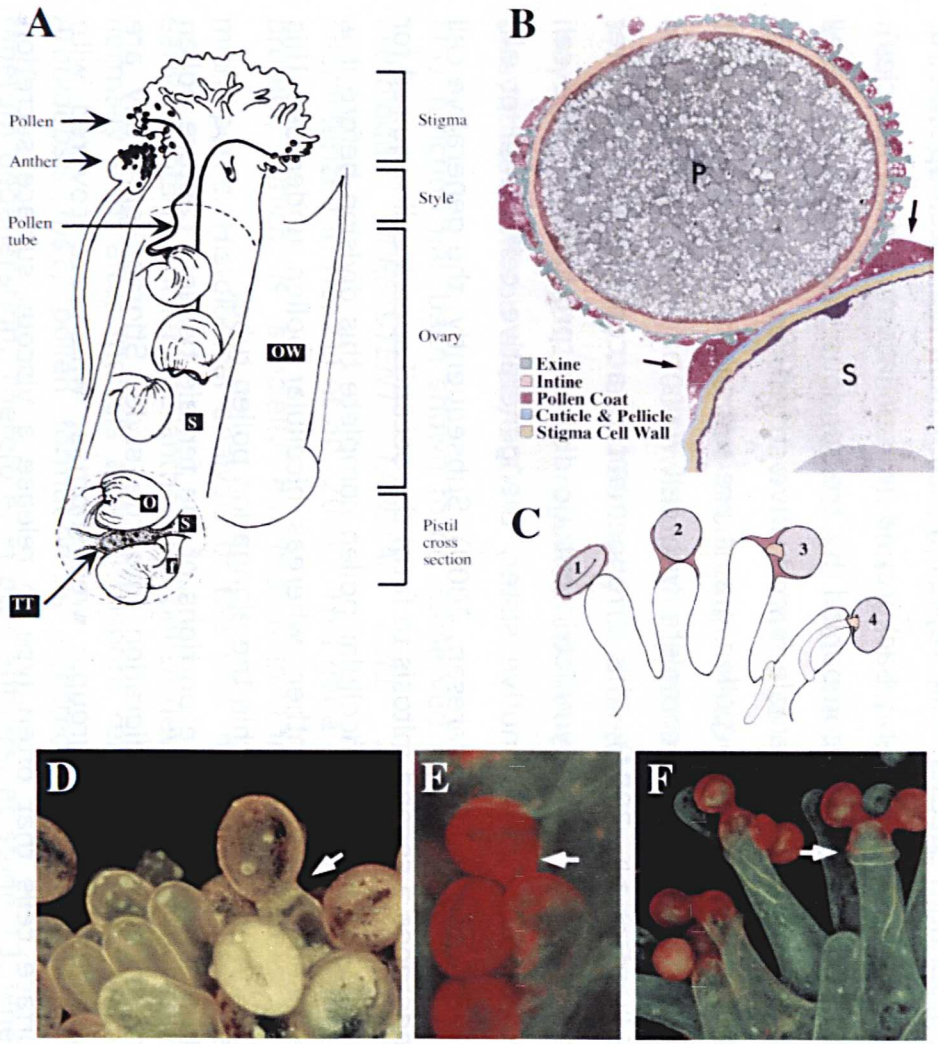
A
Pollen
Anther
Pollen tube
OW
S
O
S
I
TT
Stigma
Style
Ovary
Pistil cross section
B
P
S
Exine
Intine
Pollen Coat
Cuticle & Pellicle
Stigma Cell Wall
C
1
2
3
4
D
E
F

Fig.1.12 Pollination in *Arabidopsis*. (A) Diagram of one of the two ovary chambers after removal of the ovary wall (OW). Pollen lands on the stigma, where it hydrates, germinates, and extends a tube that enters the transmitting tract (TT). The tube emerges onto the septum (S), grows up the funiculus (f), and enters the micropyle opening of the ovule (O), where it releases sperm to fertilizes the egg and central cell. The position of the transmitting tract inside the septum is shown in the cross-section at the bottom of the pistil. (B) Transmission electron micrograph showing the point of contact between a pollen grain (P) and a stigma papillus (S), colorized to highlight the pollen coat (pink), intine (peach), exine (green), stigma cell wall (yellow), and stigma cuticle (blue). A foot of lipid-rich material (arrows) connects the two surfaces. The thin stigma pellicle that covers the cuticle is not distinct here. (C) Diagram of early events on the stigma, including adhesion (1), pollen coat "foot" formation and pollen hydration (2), pollen tube emergence from the grain (3), and pollen tube invasion of the papillae cell wall and extension toward the style (4). (D) to (F) Sequence of early events during *Arabidopsis* pollination. (D) The pollen coat has mobilized to the site of contact between the pollen and the stigma, forming a foot between the two surfaces (arrow), as visualized with the lipid dye FM1-43. (E) The pollen tube (arrow) has emerged from the grain's exine wall and projects itself into the stigma papillus, as visualized with the cell wall dye Congo red. (F) Pollen tubes (arrow) wind their way toward the style, moving between the cell walls of the papillae, where they are protected from the Congo red dye (Edlund et al., 2004).

1.6.1 Pollen adhesion to stigma: First contact.

To capture pollen grains, stigmas engage biotic and abiotic pollinators (such as insects and wind) and use rapid and strong adhesive interactions to retain pollen grains. The pollen–stigma interface can differ from species to species as a result of the wide variability in the morphology and content of stigma exudates, exine layers, and pollen coats. In *Arabidopsis,* the nature of the pollen–stigma interface has been shown to change as pollination progresses, becoming considerably stronger over time, with different types of adhesive contacts supplementing and supplanting each other (Luu et al., 1997a, 1997b; Zinkl et al., 1999). Pollen capture in *Arabidopsis* is thought to depends on biophysical and/ or chemical interactions between the stigma surface and the polymers of the pollen exine; the nature of these contacts remains unknown. After exine-mediated adhesion, mobilization of the pollen coat occurs, leading to mixing of lipids and proteins to form a "foot" of contact on the stigma surface (Fig.1.12). There is now extensive evidence that the proteins and lipids in the pollen coat, and proteins on the stigma surface, also contribute to adhesion, albeit most likely at a later stage than at the time of initial contact (Edlund et al., 2004).

As pollen tubes germinate, a final stage of adhesion begins in which the pollen tube passes through the foot into the stigma surface, tethering the emptying pollen grain to the stigma via the tube (Zinkl et al., 1999; Dickinson et al., 2000; Heizmann et al., 2000). When inappropriate pollen grains reach this stage, further access is blocked by inhibiting tube growth. This mode is common in plants with wet stigmas, in which pollen grains typically are bound and hydrated without applying species selectivity (Wheeler et al., 2001).

1.6.2 Pollen hydration: Activating metabolism.

Most pollen grains are metabolically quiescent and highly desiccated, ranging from 15 to 35% water content, when released from the anthers (Heslop-Harrison, 1979a; Buitink et al., 2000). Water immediately surrounds grains that land on a wet stigma, but those that land on dry stigmas mobilize their lipid-rich pollen coat to form an interface between the two cell surfaces. This interface converts to a histochemically distinguishable form thought to promote water flow (Elleman and Dickinson, 1986; Elleman et al., 1992). Water, nutrients, and other small molecules are transported rapidly into the grain from the stigma exudate (wet stigmas) or stigma papillae (dry stigmas) by mechanisms that remain unclear. Regardless of the mechanism of transfer, pollen hydration is often regulated, both temporally and spatially (Edlund et al., 2004).

In plants with dry stigmas, regulated pollen hydration provides an effective early barrier to incompatible pollination. This mode is active in self-incompatible crosses (Sarker et al., 1988) and in crosses between species (Lewis and Crowe, 1958; Hulskamp et al., 1995). In *Arabidopsis*, the pollen coat contains long and short-chain lipids along with a small set of proteins, including six lipases and eight Gly-rich oleosin proteins that contain a lipid binding domain (Mayfield et al., 2001; Fiebig et al., 2004). The pollen coating of *Brassica* is structured similarly and also has been shown to contain peptides involved in self-incompatibility (Doughty et al., 1993). Disrupting pollen coat lipids or pollen coat proteins in *Brassicaceae* species can delay or block pollen hydration. Hydraulic contact can be restored to these mutant grains by the addition of purified triacylglycerides (Wolters-Arts et al., 1998).

1.6.3 Pollen polarization and germination: Preparing for pollen tube growth

Hydration transforms a pollen grain from a nonpolar cell to a highly polarized cell. Whether tubes emerge on a dry stigma surface, from a grain submerged in stigma exudates, or from pollen germinated in vitro, the grain organizes its cytoplasm and cytoskeleton to support the extension of a single tube. These changes occur within minutes after hydration and include the formation of filamentous cytoskeletal structures that wrap around the nuclei, actin cytoskeleton polarization toward the site of tube emergence (Heslop-Harrison and Heslop-Harrison, 1992). There is also reorientation of the large vegetative nucleus so that it enters the extending tube before the generative cells (Lalanne and Twell, 2002), assembly of mitochondria and polysaccharide particles at the site of the elongating tube tip (Mazina et al., 2002), and selection of the pollen plasma membrane for secretory vesicle targeting and deposition of callose (b-1-3 glycan) at the site of tube emergence (Johnson and McCormick, 2001). It is not yet clear how the polarization signal is perceived and subsequently transduced to select a single point for tube emergence. Several candidate signals have been suggested, including water, lipids, and ions (Feijo et al., 1995; Lush et al., 1998; Wolters-Arts et al., 1998). Evidence for water as a polarity signal has come from *in vitro* experiments with *Nicotiana* pollen; immersing these grains in purified lipids or in stigma exudates, and providing a nearby aqueous interface, results in polarized growth toward the aqueous medium. The pollen tubes emerge from the aperture closest to the hydrophobic–aqueous interface, suggesting that the source of water provides directional cues that establish polarity, thus mimicking *in vivo* behaviour (Lush et al., 1998; Wolters-Arts et al., 1998). Not only does this example implicate water, it also suggests a role for lipids in establishing polarity.

Polarization signals ultimately trigger the recruitment of RHO OF PLANTS1 (ROP1), a GTP binding protein involved in F-actin dynamics

and the establishment of calcium gradients at the pollen tube tips (Gu et al., 2003). ROP1, with its binding partner ROP INTERACTING CRIB-CONTAINING1 protein, localizes to the tip of the growing pollen tube, where they act to focus secretory vesicle delivery (Kost et al., 1999; Li et al., 1999; Wu et al., 2001). Other proteins such as annexin, a protein believed to be involved in tip-oriented exocytosis events, exhibit calcium-dependent binding to phospholipids. This characteristic affect cytoskeletal structure, and potentially modulate voltage-dependent Ca^{2+} channels (Clark et al., 1995) suggesting that the pollen tube tip may play a role in the initial establishment of cell polarity.

Once the cell has established its internal polarity relative to an external signal, the pollen tube must breach the exine wall to emerge from the grain. Depending on the species examined, pollen tubes either grow out of the apertures or break directly through the exine wall. In rye and eucalyptus, tubes emerge strictly at the apertures, by dissolving aperture intine layers, rupturing the thin sporopollenin wall, and displacing the opercula that guard these sites (Heslop-Harrison, 1979b; Heslop-Harrison and Heslop-Harrison, 1985; Heslop-Harrison et al., 1986b).

In *Arabidopsis*, which has pollen with three distinct apertures, pollen tubes often break directly through inter-aperture exine walls precisely at the site of contact with the stigma surface (Fig.1.12). Regardless of exit site, pollen tube escape requires either (1) exine weakening by enzymatic digestion from the inside or outside of the wall, or (2) exine tearing by local gel-swelling forces or focused turgor pressure. Evidence for the former possibility comes from reports of significant exine remodelling after contact with the stigma (Gherardini and Healey, 1969; Dickinson and Lewis, 1974). Gel-swelling forces or turgor pressure also could play important roles, but because such forces radiate in all directions, they must be focused at the site of emergence. A combination of mechanisms is most likely, with the increased turgor pressure of the pollen grain contributing to the

rupture of a patch of partially degraded exine at the pollen–stigma interface.

1.6.4 Pollen tube invasion: Growing into the stigma

After crossing the exine wall, pollen tubes can only enter the style after transiting the stigma barrier. The details of this process vary considerably from species to species. In plants with open styles, the stigma is covered with an epidermis that is continuous with the style, but in species with closed stigmas, pollen tubes grow through the outer cuticle and cell wall of the stigma papillae to enter the style. Enzymes secreted by pollen have been proposed to play an important role in pollen tube invasion of the stigma surface (Green, 1894). Acid phosphatase, ribonuclease, esterase (Hiscock et al., 1994), amylase, and protease activity have been localized to the pollen intines and tubes (Knox and Heslop-Harrison, 1970).

Enzymatic penetration of the stigma surface is precisely controlled to not expose the pistil to pathogenic or inappropriate invasion. This control is likely to requires constant communication between the pollen tube and the stigma. Recently, receptor kinases have been identified as candidate mediators of communication between the pollen tube and the stigma (Edlund et al., 2004). Yeast two-hybrid experiments using the extracellular domains of these kinases yielded many candidate ligands, including cell wall–remodelling proteins and Cys-rich proteins implicated in extracellular signalling. One pollen-specific, Cys-rich protein, LATE ANTHER TOMATO52 (LAT52), interacts *in vivo* with LePRK2; LAT52 is essential for pollen hydration and germination *in vitro* and for normal tube growth *in vivo*. This finding suggests that LAT52 and LePRK2 are members of an autocrine signalling cascade that may regulate and maintain pollen tube growth (Tang et al., 2002).

On the stigma, pollen tubes germinate in an extracellular matrix (ECM) that is usually a combination of both pollen coat secretions and stigmatic exudates. In the Solanaceae, lipids (triglycerides) in the stigma exudates were shown to be essential for pollen germination oriented toward the style (Wolters-Arts et al., 1998). In this case, the cue for directional growth of the pollen tube is a physical factor, a gradient of water set up by the stigmatic lipids over an aqueous component of the exudates. In other stigma types, pollen tube guidance is required for entry into the style. The open stigma and style of lily is an example where pollen germinates over a large stigma surface, and the tube must be guided toward the central stylar canal. An abundant, secreted peptide in lily, SCA (stigma/stylar cysteine-rich adhesion) has been purified from the transmitting track and shown to be involved, with a pectic polysaccharide, in pollen tube adhesion and guidance in the style (Mollet et al., 2000; Park et al., 2000). Binding of SCA to the pectin is necessary for adhesion of pollen tubes to this specialized ECM. On the stigma, this peptide appears to act alone as a chemotropic compounds. Pollen tubes were shown to reorient their growth toward a chemical gradient of SCA *in vitro* establishing SCA as the first chemotropic peptide identified in plants (S. Kim, S.-Y. Park and E.M. Lord, unpublished results). Thus in the stigma, SCA may act alone as a chemotropic molecule, whereas in the style it acts with a pectin in haptotactic (adhesion mediated) guidance.

Entering into the ovule is the last step in fertilization process. A variety of genetic studies have revealed the importance of the ovule, and in particular, of the female gametophyte, or embryo sac in guiding a single pollen tube into the ovule opening via the micropyle where contact can occur with the embryo sac and sperm can be released (Higashiyama et al., 2001). *In vitro* assays using isolated ovules demonstrated clearly that a cue attractive to pollen tubes emanated from the ovule, and laser ablation studies on the embryo sac show definitely that the cue comes from the embryo sac synergide cells that flank the egg cell (Edlund et al., 2004). These elegant studies provide experimental support for an old hypothesis that when

the pollen tube is in the vicinity of the ovule, the secretory synergid cells, one of which will receive the pollen tube contents including the sperm cells, guide the pollen tube to the micropyle. The signal is not yet known, but heat treatment of the ovule prevents it from attracting pollen tubes. This suggests that either active secretion, a protein factor, or both are necessary for chemotropism. One intriguing aspect of this work is that pollen tubes must pass through the stigma and style in order to be capable of chemotropism in the isolated ovule assay (Higashiyama et al. 1998). When pollen is cultured in the presence of the ovules, no chemotropism to the micropyle occurs even though the generative cell has divided and produced sperm cells (Lord et al., 2002). This means that contact with the pistil, starting with the stigma and then the style, is essential in some way to prepare the pollen tube to receive the signal from the ovule. This supports the premise that a hierarchy of control points exists in pollination and that study must be done *in vivo* to decipher the complexities of these signalling pathways.

1.7 Barley

1.7.1 Introduction

In the UK, approximately 5 million hectares of agricultural land is used to grow cereals, oilseed rape, sugar beet and horticultural crops; wheat, barley and oilseed comprise approximately 80% of this.

The exact origin of barley is debatable, possibly originating in Egypt, Ethiopia, the Near East or Tibet (Hockett, 2000). However, it is fairly certain that barley was among the earliest cultivated grains, around the same time as the domestication of wheat. Barley was grown in the Middle East prior to 10,000 BC, but barley's cultivation in China and India probably occurred later. Barley was grown on the Korean Peninsula by 1500-850 BC along with millet, wheat, and legumes. Six-rowed barley did not come about until after 6000 BC. Recorded history

began on Sumerian clay tablets, which described and recommended cultural practices for raising barley around 1700 B.C. Barley was an important crop throughout the Neolithic period and the Bronze Age and continues to be an important worldwide crop up to the present time. Barley has been associated throughout its history with both the production of beer distilling and as a food and feed crop.

Nowadays, barley is a crop with worldwide distribution, and it is a preeminent plant for use in experimental genetic studies (Hockett, 2000). It is a diploid (2n=2x-14) with a small number of chromosomes, which are relatively large (6-8μm), with a genome size of 5000Mb. Barley has a high degree of self-fertilization but is easily hybridized. Several generations can be growth in one year over a wide range of environmental conditions, taking normally around three month from emergence to seed maturity. Seeds can be stored for long periods, and numerous genetic stocks are available (James Hutton Institute). Barley can be sown in either the autumn (this is known as winter barley) or in the spring. The proportion grown of each varies from year to year but is generally around 50:50. Winter barleys are higher yielding but of poorer quality and are mostly used in animal feeds whereas the spring varieties are often used for malting. The winter crop is normally harvested in July with spring sown following about a month later.

In 2011, the total utilised agricultural area in the UK remains unchanged at 17.1 million hectares. Almost 36% of this land, 5 million, is considered to be croppable (Department for Environment Food and Rural Affairs, DEFRA). The total UK crop production was over 21.8 millions tonnes, from which barley totalised 5.6 million tonnes, second after wheat (15.4 million tonnes) and ahead of oil seed rape (2.8 million tonnes). Barley is a grass with a swollen grain that is similar to wheat that can be ground to produce flour suitable for the production of bread. However unlike wheat, barley has always been particularly important in the production of beers and ales. Barley is grown for many purposes, but the majority of all barley is used for

animal feed, human consumption, or malting. High protein barleys are generally valued for food and feeding, and starchy barley for malting.

1.7.2 Anther and pollen development in barley.

Anther and pollen development in *Arabidopsis* and rice appears to be highly conserved (Fig.1.9) and seems to follow a similar pattern in barley and is highly conserved. This suggests that this developmental process may be highly conserved between dicots and monocots. As shown in fig.1.9, a cascade of rice orthologues genes have been characterized which act in similar way than these in *Arabidopsis* (Jung et al., 2005; Li et al., 2006; Li et al., 2011).

To date, no genes involved in anther and pollen development in barley have been characterized to date. Moreover, the complete barley genome is not yet available, therefore, BLAST analysis against barley databases depend on EST sequences, which may or may not contain the targeted gene sequences. Therefore, searching for orthologues barley genes involved in anther and pollen development may currently require a different approach.

Brachypodium distachyon has recently emerged as an attractive experimental model for the study of small-grain temperate cereals and related grasses (Draper et al., 2001). The agronomical important grasses tend to be physically large, and to have relatively long life cycles and large, complex genomes, characteristics that are inconvenient and expensive for research purpose. *Brachypodium*, however, possesses many of the characteristics required of a tractable experimental model, such as a short life cycle, small plant size, resilient and easy cultivation. Moreover, it has one of the smallest genomes of any grass (300Mb), a factor that has led to it being chosen as a candidate for genome sequencing.

Sequencing of *Brachypodium distachyon* inbred line Bd21 has been completed by the US Department of Energy Joint Genome Institute as part of its 'Community Sequencing Program' (International

Brachypodium initiative, 2010). This small grass species is a model system for structural and functional genomics research on temperate grasses, including small grain crops such as wheat and barley, emerging bioenergy crops, and forage and turf grasses. The whole genome shotgun sequence assembly has been integrated with BAC-based physical maps and genetic linkage maps to produce a high quality final sequence assembly with 99.6% of the sequence contained in five scaffolds, each representing one of the chromosomes of *Brachypodium*.

Genome sequencing projects have shown that the *Brachypodium* genus is more closely related to wheat, barley and forage grasses that it is to rice (Fig.1.13) (Opanowicz et al., 2008). Therefore, due to the variability of the genome and close evolutionary relationship, *Brachypodium distachyon* provides an essential tool for barley gene characterization. Related rice genes of interest, for instance *OsPTC1, OsTDR* and *OsUTD1* (*AtMS1, AtAMS* and *AtDYT1*) may be first compared against the *Brachypodium distachyon* database. These comparative analysis may provide significant similarities, which can be use to characterize the equivalent genes in barley.

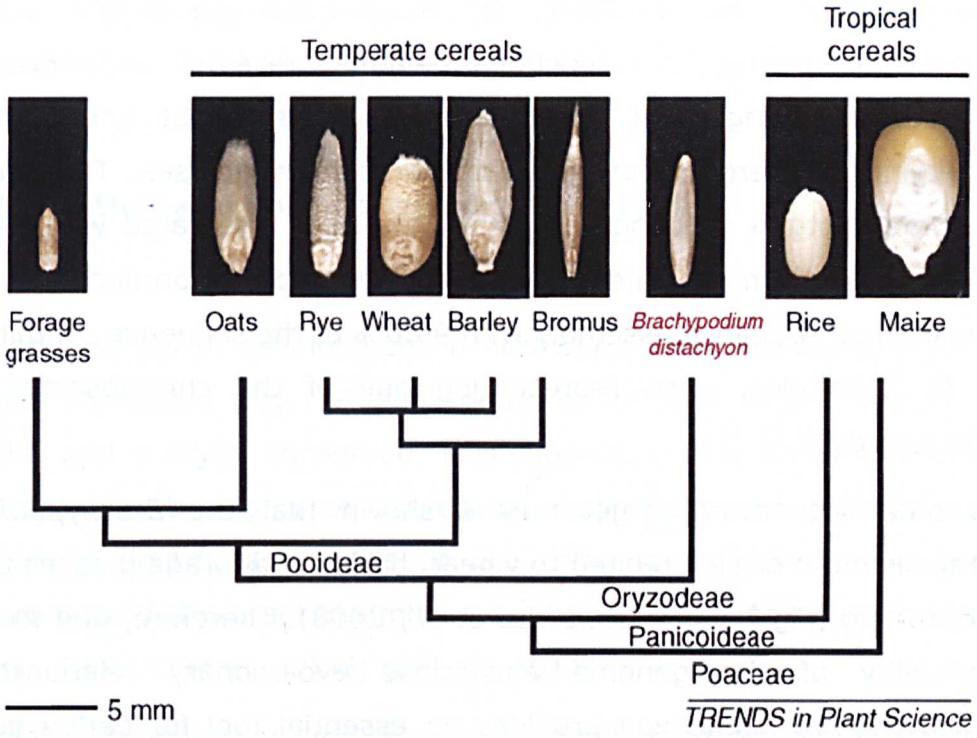

Figure.1.13 Phylogenetic relationships between *Brachypodium* and the small grain cereals. The Pooideae subfamily includes forage grasses, *Brachypodium* and many economically important small grain cereals adapted to cool or dry climates, such as wheat (*Triticum aestivum*), rye (*Secale cereale*), barley (*Hordeum vulgare*) and oats (*Avena sativa*). Rice (*Oryza sativa*) and maize (*Zea mays*) belong to distinct subfamilies and have many adaptations for tropical climate (Opanowicz et al., 2008).

1.8 Objectives.

The aims of this project were to find and characterize the *MS1* orthologue in barley and identify other genes involved in barley anther and pollen development.

1. A detailed morphological analysis of barley development was conducted in order to facilitate anther developmental analysis and *HvMS1* characterization (Chapter 3).
2. Barley *Agrobacterium*-mediated transformation was conducted in order to gain knowledge of this technique and characterize HvMS1 function by RNAi silencing of this gene (Chapter 4).

3. Putative male sterile mutants from SCRI produced by EMS mutagenesis were phenotyped in the attempt to find male sterile plants resembling some of the phenotypes described for *Arabidopsis* and rice male sterile mutants (Chapter 5).
4. *HvMS1* amplification and characterization was conducted. RT-PCR as well as RNA *in situ* hybridization were carried out to establish the *HvMS1* expression pattern (Chapter 6).
5. *HVMS1* RNAi silencing was conducted to observe if *hvms1* showed a similar phenotype to that observed in *Arabidopsis* and rice. Finally, *Arabidopsis ms1* complementation was attempted by *HvMS1* expression in this mutant background (Chapter 7).

CHAPTER 2.

2. Materials and Methods.

2.1 Plant growth.

Arabidopsis ecotype *Ler* obtained from Nottingham *Arabidopsis* Stock Center (NASC) was used as wild type for transformation and crossing (unless otherwise stated). Growth conditions consisted of a 22h photoperiod under 111 µmol s-1 m-2 warm white fluorescent light at 75% rh and 22±2ºC. Plants were grown in 13 cm plastic pots filled with Levington M3 compost (Scotts Company, UK). Intercepts 5 GR (21 g in 75 L; Scotts Company, UK) was added and mixed thoroughly before sowing seeds. Cross-pollination in plants was avoided using transparent plastic sleeves (Zwapak, Netherlands) which isolated each pot from its neighbours. Plants were watered until at least 90% of the siliques had dried completely and then the plants were allowed to dry slowly on dry benches for maximum viable seed production. Seeds were harvested after the whole plants had dried out and were stored in moisture-porous paper bags in a dry atmosphere at room temperature.

Two double rowed spring barley varieties were used, Optic and Golden Promise (Seeds provided by the University of Nottingham). Both were grown in a growth room under controlled conditions of 15ºC/12 ºC and 16 hours photoperiod, 80% relative humidity, and with light levels of 500 µmol/m2/s at the mature plants canopy level provided by metal halide lamps (HQI) supplemented with tungsten bulbs. Seeds were first sown in 36 well pots using John Innes Nº 3 compost. After 2-3 weeks (Zadok stage 11-12: One shoot with 1 or 2 unfolded leaves), plants were transferred to a 5 litres pots using Levington C2 compost (4 plants each).

2.2 DNA extraction.

Plant genomic DNA was extracted from different tissues using Sigma DNA extraction kit, following the protocol supplied by the manufacturer. DNA quality and quantity were determined using a NanoDrop ND-1000 fluorospectrometer (NanoDrop Technologies, USA). DNA samples were stored at -20°C.

2.3 PCR.

PCR conditions depended on the downstream application of products and the specific primers used. Two main enzymes were used: 1) Taq polymerase: PCR experimental reaction (20 µl) comprised of the following reagents: 0.2 µl Taq Polymerase enzyme (5 u/µl, New England Biolabs, USA), 2 µl 10x Standard Taq Reaction Buffer (for 1x working solution, 10nM Tris-HCL, 50mM KCL, 1.5 mM MgCl2, pH 8.3 at 25°C, New England Biolabs, USA), 0.5 µl of each primer (10 µM), 0.5 µl dNTP (2.5mM), 0.5 µl DNA template (~100 ng/µl) and molecular grade distilled water to make up 20 µl. 2) Phusion: (Phusion High-Fidelity DNA Polymerase, New England BioLabs). Phusion enzyme offers extreme performance for all PCR applications at different conditions and it was used for most of the reactions performed (Table.2.1.). For 10 µl reaction: : 0.15 µl Phusion Polymerase enzyme (5 u/µl, New England Biolabs, USA), 5 µl 10x HF/GC Buffer, 0.5 µl of each primer (10 µM),), 0.5 µl dNTP (2.5mM), 0.5 µl DMSO, 0.5 µl DNA template (~100 ng/µl) and molecular grade distilled water to make up 10 µl.

In addition, Red-Taq (Sigma) was used for genotyping barley transgenic plants. Red Taq reactions consisted of: 5 µl Red-Taq mix, 0.3 µl each primer (10µM) and 5µl of distilled water. Reaction conditions are showed in Table.2.1.

PCR type	Reaction conditions
Phusion (NEB)High-Fidelity DNA Polymerase **	Cycle: 98°C 30 sec; 30x(98°C 30s, Tm *°C 30s, 72°C 30-60 s); 72°C 6 min.
Taq polymerase***	Cycle: 94°C 3 min; 30x(94°C 30s, * °C 30s, 72°C 30-60 s); 72°C 6 min

Table.2.1. PCR reaction conditions.

*Tm depended on the primers, normally primers are designed to have a Tm between 59 to 65°C.

**For this enzyme two different buffers could be used. The utilization of either of these buffers depended on the length of the template or its composition. For instance, HF is recommended for high fidelity amplification, whereas GC is preferred for long templates or templates with a complex secondary structure.

***Red Taq needed the same reaction conditions as other standard Taq polymerases.

Electrophoresis was carried out after PCR to check the size and /or amount of the products. PCR products were run on agarose gels (Bioline, USA, ranging from 0.8%-2.0% (w:v) depending on DNA size) at 80-120 V with DNA loading buffer (Bioline, USA) in 0.5x TBE (Appendix) and visualized by ethidium bromide (5 µl (0.5mg/ml) in 100 ml gel,) using a HyperLadder I-V (Bioline, USA) marker.

2.4 Sequencing.

Sequencing reactions were performed using 100-200 ng template DNA and BigDye Terminator v1.1 Cycle Sequencing Kit (Applied Biosynthesis, USA) following the manufacturer's instruction (Table.2.2). Samples were run on an ABI 3130 analyzer (Genomics Facility, Queen's Medical Centre, University of Nottingham) and analysed MacVector software (MacVector, Inc, USA.

Big dye Reaction
Cycle: 96°C 1 min 30 sec; 28 x(96°C 30s, * °C 20s, 60°C 4 min); 28°C 1 min
H_2O: ; Buffer: 2 µl; Primer (10 µM): 0.5 µl; PCR product:** ; Big dye (ABI): 0.8 µl**
*** : Temperature <60°C, but was generally the Tm used for the PCR reaction.**
****: A clear single PCR product was needed, or gel purified of the PCR product was carried out. Volume (usually 3-4 µl) depended on the PCR product concentration (100-200 ngr). The total volume reaction was made to 10µl using dH_2O.**

Table.2.2. Sequencing reaction using Big dye terminator mix.

2.5 Plasmid extraction.

Plasmid DNA was extracted from 10 ml *Escherichia coli* (DH5alpha) overnight culture in LB medium (Appendix.1) with the appropriated antibiotic selection agents by using QIAprep Spin Miniprep Kit (Qiagen Kit) following the protocol supplied by manufacturer.

2.6 DNA purification from gel.

PCR products were isolated from agarose gels DNA extraction by membrane electrodialysis (Gobel et al., 1987).

DNA products were cut out off the gel (minimising the size of gel and UV exposure). Gel pieces did not exceed three PCR lanes and the number of gel pieces loaded in the membrane was less than four.

Dialysis membrane (Sigma D9777) was prepared by boiling and stored submerged in 0.5x TBE buffer at 4°C. The membrane was cut to size depending of the sample to be loaded. Firstly, the membrane was

washed with TBE buffer inside and outside (Appendix.1). Then, one of the ends was clipped and 2 ml of TBE buffer poured into the membrane. The gel pieces were introduced and excess buffer and air removed. The gel pieces were placed on one side of the membrane, the other side closed using a new clip. The dialysis membrane was then placed into an electrophoresis tank (100 volts for one hour) orientated so that the membrane was in line with the electrodes. After one hour, the electric field was inverted 30 seconds and DNA checked under a UV lamp. At this point the DNA had moved to the opposite site from the gel pieces. Using a 1 ml pipette, the buffer was mixed with the DNA floating within the membrane and transferred to a 1.5 ml microfuge tube. Butanol concentration was conducted by adding an equal volume of butanol to the sample, shaking briefly and centrifuging for 3 min (12.000 x g). The sample supernatant was then discarded and an equivalent amount of fresh butanol added. This was repeated until the volume of DNA was 50-60 µl. The DNA was then precipitated : 0.5 vol of sodium acetate 3M and 10 vol of 100% Ethanol were added and stored at -20°C for 30 min or overnight; Samples were centrifuged (15 min at 12.000 rpm), washed in 200 µl 70% (v:v) ethanol, centrifuged again (15 min, 12.000 rpm) and air dried 30 mins. Samples were resuspended in 20-50 µl distilled water depending on the expected concentration.

2.7 Primer design

Primers were designed using Primer3 software (http://frodo.wi.mit.edu/primer3). Conditions were specific for individual products. Primers were routinely between 20-21 nucleotides. Each pair of primers was tested using MacVector software and BLAST analysis to confirm their specificity.

2.8 PCR purification.

PCR products were purified using the PCR purification kit (Qiagen, UK) following the protocols supplied by the manufacturer. To obtain highly concentrated PCR product, samples were precipitated by adding 1/10 volumes of sodium acetate (NaAc, 3M, pH 5.2) and 3 volumes of 100% ethanol, pelleted by centrifugation (4°C, 13,000 rpm for 15 min), washed twice with 70% (v:v) ethanol and resuspended in 20-50 µl of dH2O.

2.9 Cloning.

Topoisomerase based cloning technology allows ligation of DNA with compatible ends. PCR products were amplified using Taq polymerase or Phusion (Section.2.3). Purified products were cloned using pCR4-TOPO/pCR8/GW/TOPO or pCR-BluntII-TOPO using the protocol supplied by the manufacturer (Invitrogen, USA). This was then transformed into competent *E.coli* cells (DH5α). 2 to 4 µl from the TOPO cloning reaction were mixed into a 1.5 ml vial of one Shot Chemically Competent *E.coli*. After 30 min of incubation on ice, the cells were heat shocked at 42°C for 1 min and 30 seconds, then, immediately, transferred to ice and 250 µl of S.O.C (Appendix.1) was added. The sample was incubated for 1 hour at 37°C, then 75 µl spread onto LB (Appendix.1) + Kanamycin plates (50 µg/ml Kanamycin). Colonies were screened using vector specific sequences (M13F/M13R) flanking the cloning sites (Table.2.3.) to amplify the target fragment plus part of the vector sequence between the two primers (~170bp).

pCR8GW combines TOPO cloning and Gateway technologies, therefore, fragments inserted into this vector can easily be transferred to a destination vector by LR . reaction. This vector confers Spectinomycin resistance.

Primer	Sequence (5'-3')	Tm°C
M13F	TGTAAAACGACGGCCAG	55
M13R	CAGGAAACAGCTATGAC	

Table.2.3 Cloning vector primers.

2.10 RNA extraction.

RNA was extracted from plant tissues to test expression levels of gene of interest in different lines and different developmental stages. RNA extraction was conducted using the QIAGEN, RNeasy Mini Kit following the manufacturer's protocol. RNA (60 µl) samples were eluted from the RNeasy column and DNase treated to eliminate DNA contamination (1 µl RNase inhibitor (40 u/µl, Promega, USA), 5 µl RQ1 (RNA-Qualified) RNase-free DNase (1 u/µl, Promega, USA), RQ1 10 µl reaction Buffer (Promega, USA), and 24 µl dH2O) to make to 100 µl, incubated at 37°C for 45 min-2 hours. RNA in the 100 µl reaction was subsequently purified using the RNeasy Plant Mini Kit. RNA quality and quantity were tested on a NanoDrop fluorospectrometer. RNA samples were stored at -80°C until required.

2.11 Expression analysis.

RT (reverse transcription)-PCR was performed to determine gene expression in plants.

2.11.1 cDNA synthesis.

cDNA was synthesized from total RNA by adding the following components to a nuclease free microcentrifuge tubes: 1-5 µg RNA, 1

µl of Oligo dt (0.5 µg/µl, Invitrogen, USA), 1 µl of dNTP (10mM, Bioline, USA)) and dH2O to a total volume of 13 µl. The mixture was mixed and incubated at 65°C for 5 mins. Reaction was placed on ice directly from incubation for one minute. Then 1 µl of dTT, 1 µl of RNAse out, 4 µl of 5x buffer and 1 µl of Superscript III (2200 u/µl, Invitrogen, USA) were added and incubated at 55°C for 1 h. After incubation, the reaction was heated to 72°C for 15 mins to inactivate the SuperscriptIII.

2.11.2 α-Tubulin amplification and normalization.

The house-keeping α-Tubulin transcript were amplified from freshly synthesised cDNA templates (no more than 22 cycles; primers α-TubF and α-TubR, primer sequence in section.6.2.4.2) to determine the initial quantity of the cDNA templates. Comparisons between the extent of amplification and band intensity were used to confirm that initial levels of RNA/cDNA were equivalent between samples and that cDNA synthesis had been successful.

2.12 *Agrobacterium* electrocompetent cells.

Agrobacterium electrocompetent cells, AGL1, were prepared as follow:

- *Agrobacterium* was streaked out on LB plate with selection antibiotics (Rifampicilin 50 mg/l, and Carbenicillin 150 mg/l) and allowed to grow for 1-3 days at 28°C.

- Several colonies were placed in 20 ml of LB medium + selection and grew overnight at 28°C with shaking (200 rpm).

- 10 ml of the overnight culture were transferred into 100 ml LB media in a large flask (improves aeration).

- Culture were grown at 28°C until OD600 is 1-1.5 (~4 hours) and then transferred into 50 ml falcon tubes and placed on ice for 20 minutes.

- Falcon tubes containing the cell culture were centrifuged at 4°C for 15 min at 4000g. The medium was poured off and the pellet was gently resuspended in 50 ml of cold dH_2O.

- This solution was then centrifuged at 4°C for 15 minutes at 4000g.

- Steps 8-9 were repeated four more times.

- The supernatant was then poured off and the pellet resuspended in 5 ml of 10% sterile cold glycerol.

- The glycerol-cell mix was centrifuged and the supernatant poured off. The pellet was resuspended in a total volume of 400 µl of 10% glycerol (resuspension was in 2 ml of 10% glycerol per 500 ml of original culture at step 4-5).

- The 400 µl glycerol-cell mix was divided into 40 µl aliquots in pre-chilled (-80°C) 0.5 ml Eppendorf in liquid nitrogen and stored at -80°C.

2.13 LR reaction.

The Gateway® Technology is a universal cloning method that takes advantage of the site-specific recombination properties of bacteriophage lambda (1) to provide a rapid and highly efficient way to move DNA sequences into multiple vector systems (Fig.2.1).

The following components were added to a 1.5 ml microcentrifuge tube at room temperature and mixed:

- pCR8GW Entry clone (50 ng) 1-7 µl

- Destination vector (100 ng/µl) 1 µl

- TE buffer, pH 8.0 to 8 µl

The LR Clonase™ II enzyme was thawed on ice and mixed for about 2 minutes, then vortexed briefly twice (2 seconds each time).

- To each sample (Step 1, above), 1.2 µl of LR Clonase™ II enzyme mix was added to the reaction, mixed by vortexing and centrifuged briefly (15 sec, 10000rpm). LR Clonase™ II enzyme mix was returned immediately to -20°C or -80°C storage.

- The reaction was incubated at 25°C overnight.

- After incubation, 1 µl of the Proteinase K solution was added to each sample to terminate the reaction. Samples were vortexed briefly and incubated at 37°C for 10 minutes.

- 4-6 µl of reaction was used to transform DH5α competent cells and proceed as explained in section.2.7.

- DH5α were plated on LB containing the antibiotic specified by the expression vector. Selected colonies containing the expected expression vector and the gene of interest were also plated on LB + Spec (100 mg/l). Colonies that grew on these 2 different plates were rejected as they were suspected of containing the entry and the expression vector within.

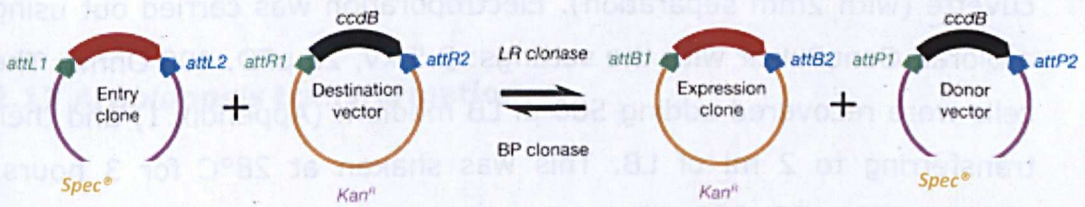

Fig.2.1 Recombination reaction between an entry clone (containing attL) and a destination vector (containing attR), mediated by a host of recombination proteins to generate an expression clone.

2.14 Restriction enzyme digestion.

Restriction enzyme digestion was carried out in 15 µl volume by adding 0.2 µl of the required enzyme, 200 ng of plasmid DNA, 1.5 µl enzyme specific buffer, 1 µl of BSA (diluted 1/100). Incubation was carried out following the instruction supplied by the manufacturer for each enzyme (New England BioLabs, UK). Double digestion was conducted according to the enzyme supplier specification. In addition, if double digestion was not possible due to buffer incompatibility, sequential digestion was conducted. Once the first digestion was performed, the enzyme was inactivated and product precipitated with ethanol. The pellet was then digested using the second buffer.

2.15 *Agrobacterium* electroporation.

Each electroporation was set up by adding 1 µl of the construct carrying the gene of interest (100 ng/µl) and 1 µl of pSoup (only when the pGreen construct was used) (100ng/µl) to 40 µl of electro-competent *Agrobacterium tumefaciens* AGL1 or C58 cells on ice. The cells and DNA were gently mixed, and then transferred to a pre-chilled cuvette (with 2mm separation). Electroporation was carried out using a Biorad GenePulser with the settings: 2.5 kv, 25 µFD, 400 Ohms. The cells were recovered adding 500 µl LB medium (Appendix.1) and then transferring to 2 ml of LB. This was shaken at 28°C for 3 hours; Aliquots (50, 100, 200 µl) were plated onto the LB plates containing the required antibiotic. These plates were incubated at 28°C up to 48h.

2.16 Overhanging.

PCR products amplified by Phusion enzyme need to be overhang in order to be cloned into the TOPO vector PCR8GW, as Phusion

amplification produces blunt PCR products. Before adding the overhangs it was important to remove all the proofreading DNA Polymerase (Pfu) by purifying the PCR product carefully (e.g. with a commercial PCR purification kit or phenol extraction and DNA precipitation); since the proofreading activity of DNA Polymerase will degrade the A overhangs, creating blunt ends again. The over-hanged PCR product was cloned into a PCR-Topo cloning vector.

Taq DNA polymerase reaction mix for a typical 20 - 50 µl reaction was prepared as follow:

	Final Concentration	**Vol (µl)**
Purified PCR product	0.15 to 1.5 pmol	Varies*
dATP (10 mM)	0.2 mM	1
PCR Buffer with Mg (10x)	1x (1.5 mM MgCl2)	5
Taq DNA Polymerase (5 U/µl)	1U	0.2
ddH_2O		to 50 µl

Table.2.4 Overhang reaction.

2.17 *Arabidopsis* transformation.

Agrobacterium tumefaciens competent cells (C58 strain) were transformed with plasmid DNA by 2.2kV electroporation (MicroPulser, BioiRad), and screened on solid LB, medium with selective antibiotics for the plasmid. Rifampicin (30 µg/ml) was added for C58 selection.

Positive colonies were PCR screened and propagated firstly in 5 ml then in 100-200 ml LB medium with antibiotic at 28°C for 3-4 days, or until an OD600 of 0.7-1.0 was reached (Spectrophotometer from Cecil, UK). The cells were pelleted by centrifugation at 3500xg for 10

min and then re-suspended in 5% (w:v) fresh sucrose (Fisher scientific, UK) aqueous solution to OD600=0.8. Silwet L-77 (0.02% v:v, Michigan State University, USA) was added to the suspension just prior to dipping. Plants with numerous buds and few siliques present were used for floral dipping (Clough and Bent 1998). After dipping, plants were placed in the bag and the bag closed. Plants were tilted under the benches, away from light for three days. After the three days, plants were placed back on the bench and the bags were opened. Seeds were subsequently screened on MS medium (Appendix.1) with selective antibiotics. Genotyping for confirmation of the T-DNA insertion or plant genotype background was performed by using the Extract-N-Amp Plant PCR Kit (Sigma) with the desired primers.

2.18 Standard inoculums preparation for *Agrobacterium*-mediated transformation of barley embryos.

A single *Agrobacterium* colony carrying the construct plus the gene of interest was used to inoculate 10 ml of MG/L (Appendix.1) medium containing the required antibiotic for the construct as well as the *Agrobacterium* strain (Kan 50 µg/ml; Rif 50 µg/ml). The inoculum was left to grow for minimum 40-48 hours in a shaker at 28°C. Glycerol stock was prepared as follow: To prepare aliquots of 400µl of the standard inoculums, 100µl of 80% aqueous glycerol was mixed with 300µl of the *Agrobacterium* inoculums in a 2 ml cryo-Eppenforf. The mix was inverted several time and placed in liquid nitrogen, then storaged at -80°C. *Agrobacterium* inoculum for inoculation was prepared overnight by adding one of the standard inoculums prepared above to 10 ml of liquid MG/L medium without any antibiotics. This was incubated in a shaker at 180 rpm at 28°C for 17-20 h. The full-strength *Agrobacterium* culture was ready then for embryo inoculation.

2.19 X-Gal reaction.

Histochemical analysis of *gus* gene expression was performed based in the method of Jefferson (1987). Tissues were incubated for 48 h at 37°C in 100 mM sodium phosphate (pH 7.0) containing 0.1% (v/v) Triton X-100 and 1 mM Xgluc (5-bromo-4chloro-3-indolyl-β-glucuronic acid; Melford, Ipswich, UK). The reaction was terminated by transferring the callus into 100% ethanol facilitating visualization of GUS activity.

2.20 Alexander staining.

Alexander's stain (Alexander, 1969) is a reliable and rapid way to score pollen viability and requires only a light microscope (Johnson-Brousseau and McCormick, 2004). The stain contains malachite green, which stains the cellulose in pollen walls and acid fuchsin, which stains the pollen protoplasm. Aborted pollen grains lack protoplasm and thus fail to stain with acid fuchsin. Procedure:

1 – Flowers were collected that contained mature non-dehisced anthers, just before anthesis.

2 - The anthers were removed from the flowers and placed into a droplet of stain on a slide and shake gently to release the pollen grains into the solution.

4 - The empty anthers were discarded and the pollen suspension covered with a cover slip.

5 - Grains that are viable stained dark blue or purple and grains that are dead will stain pale turquoise blue under a light microscope.

CHAPTER 3.

3. Morphological classification of Barley

3.1 Introduction

Plants are not static organisms, and, as they grow, they pass through a series of different growth stages, beginning with germination, the development of leaves, a stem elongation stage, preceded in some plants such as cereals, with a tillering stage, through to a flowering and fruiting, prior to senescence and death. Although these phenological stages are continuous and gradual, it is possible to recognise, with a fair degree of precision, at which stage an individual plant or crop is at on a particular date. Despite this, many scientists in these days of fast throughput molecular biology research that depends on a detailed and precise knowledge of gene sequences and positions still describe their experimental plants by their age, rather than their growth stage (Simmons *et al.*, 2006; Ninkovic & Ahman, 2009).

Anther and pollen development represents one of the most important developmental processes in plants, which is essential for plant reproduction. The regulatory network of these processes has been described in the dicot model *Arabidopsis* and seems to be conserved in higher plants, including monocots such as rice (Wilson & Zhang, 2009). Although no barley genes involved in anther and pollen development have been described to date, it is likely that the regulation of this process may be conserved as seen in rice.

Morphological characterization of anther development in barley is essential to identify the key stages of pollen formation and enable molecular characterization of its regulation. For instance, *AtMS1* expression pattern is an example of localised temporal and spatial expression, tapetal tissue in closed buds around the stage of microspores release to early microspores (Wilson et al., 2001).

Therefore, the identification of these stages in barley is critical to easily select material for stage characterization and also for genetic and molecular analysis. Barley floret development occurs mainly within the pseudostem shoot (a false stem composed of concentric rolled or folded blades and sheaths that surround the growing point). This makes the observation of floret development and the access to the floret particularly difficult without dissecting the plant.

Over the last decade, considerable advances have been made in understanding of cereal crop growth and yield. A combination of physiological measurement with detailed monitoring of plant development has led to the formulation of simulation models which can be used to predict plant development and crop phenology with some degree of accuracy from a relatively simple set of environmental data, principally temperature and day length (Fischer et al., 1984). Descriptions of development of the main stem apex from the mature embryo to the maximum number of primordia stage (barley) (Tottman, 1987), alongside the plant external development abound in literature (Hay, 1986; Kirby, 1993; Arduini et al., 2010). Moreover, detailed studies have been carried out on the factors that affect grain production such as temperature, photoperiod or vernalization (Miralles et al., 2000; Arinsnabarreta et al., 2008).

Therefore, a morphological study was conducted with the aim of establishing a direct relationship between developmental staging of plant development, following a scale based on the Zadok code (Zadok et al., 1974) specially modified for barley, and the sequence of events occurring inside the anther. To achieve this, several parameters were measured. First of all, barley external development stages, based on Zadok's code (Fig.3.1; Appendix.4), were studied in detail. This was in order to establish constant key stages, which are easy to recognise, that allows accurate and repeatable data collection. In addition, the pseudostem and internode growing pattern, as well as the spike size and the events occurring inside the anther throughout the plant development were studied. This relationship allowed a more accurate staging for efficient collection of material based on visual observation

of external characteristics. The characterization of these developmental events in the barley anther is crucial to understand the regulation of this process which can lead to future crop improvement.

3.1.1 External development in barley.

Several staging systems have been proposed to describe development in barley. Some of them characterize plant growth through external plant appearance, without requiring dissection of the shoot apex (Large, 1954; Zadok, 1974; Haun, 1973), while others describe the morphological changes that occur within the apical meristem (Kirby and Appleyard, 1986). Staging based on external features (Fig.3.1) gives a non-destructive identification of growth stages but does not provide information about the sequence and timing of changes at the shoot apex. However, this non-destructive characterization is needed as a guide to identify events taking place inside the shoot apex that are not visible without dissection.

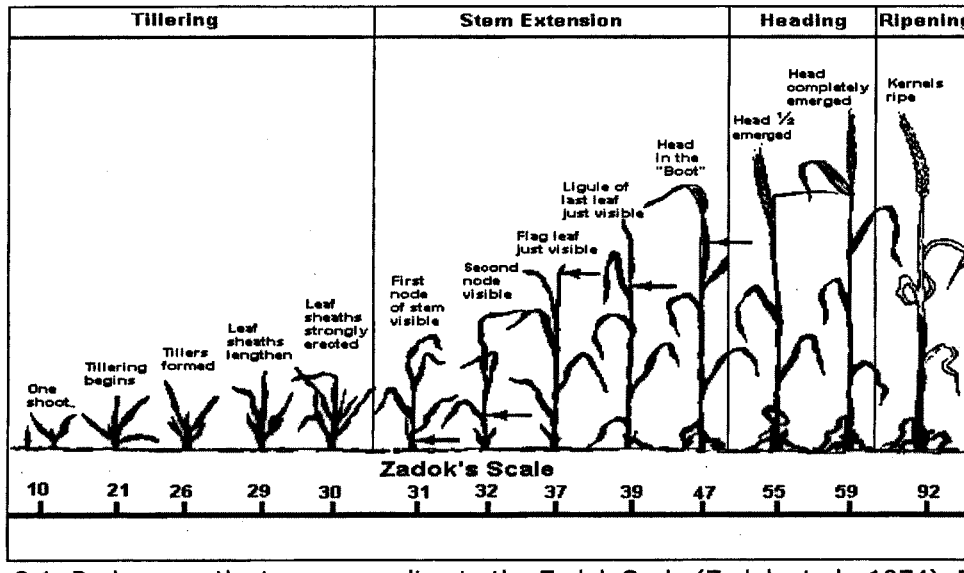

Fig.3.1. Barley growth stages according to the Zadok Scale (Zadok et al., 1974). From stage 10 to 30, the barley plant is characterised by the leaf and tiller emergence. From stage 30, the barley plant adopts an upright appearance, starting the elongation stage that will lead to heading stage and then to ripening. (www.omafra.gov.on.ca).

The Zadok system is becoming the most universally accepted staging approach. It is applicable to any small grain, and the stages are easy to identify in the field. The Zadok system uses a two-digit code, from 0.0 to 9.9. The first digit, from 0 to 9, refers to the principal stage of development, beginning with germination and ending with kernel ripening (Table.3.1; Appendix.4). The second digit (also between 0 and 9) subdivides each principal growth stage; a second digit value of 5 usually indicates the midpoint of that stage (Appendix.4).

Main stage	Description	Sub stage	Main stage	Description	Sub stage
0	Germination	0.0-0.9	5	Heading	5.0-5.9
1	MS leaf production	1.0-1.9	6	Anthesis	6.0-6.9
2	Tiller production	2.0-2.9	7	Grain milk stage	7.0-7.9
3	Stem elongation	3.0-3.9	8	Grain dough stage	8.0-8.9
4	Booting	4.0-4.9	9	Ripening	9.0-9.9

Table.3.1. Zadok growth stages. Zadok decimal code is divided into ten main stages which are also divided into a further ten sub-stages (Appendix.4).

The Zadok code is a useful tool to classify barley external development and to establish "key stages" that can be used in future comparison to internal apex development. Although the stages overlap, they are sufficiently distinct to establish a chronological sequence of events that allows an easy identification by external observation. Zadok code is not a sequential scale where one stage finishes and the next starts, rather different stages overlap throughout

plant development. Therefore the different stages must be carefully identified.

Germination is the first stage described by Zadok code, starting at dry seed, 0.0, and finishing at 0.9 when the leaf is just at the coleoptile tip (Appendix.4).

The next stage is seedling growth or leaf production stage (Appendix.4). During this stage, the leaves start emerging one by one to a maximum number of nine (depending on the phenotype and growing conditions). The sub-stages within this seedling stage are identified by the number of the main stage, 1 (Table.3.1), followed by the number of leaves that are unfolded at the time of observation at the main shoot (Appendix.4). This stage lasts well into the next stages as leaf emergence occurs sequentially alongside pseudostem elongation.

The Tiller production stage starts parallel to stem seedling stage (Appendix.4). First tillers appear when approximately three leaves are unfolded on the main stem. This means that a double staging for the main stem is required, the first one to describe the number of leaves unfolded on the main stem, and the second to describe the tiller's emergence. Tiller formation phase ends when 9 or more tillers have emerged (depending on the variety).

The elongation stage marks one of the phases of greatest changes in barley development (Fig.3.1). During this stage, the barley plants adopt an upright appearance and the pseudostem starts elongating. Throughout this phase, the plant carries on generating new leaves and tillers. Elongation begins when the first internode is visible and the apex is already 1 cm above the ground, Zadok stage 30. Generally, barley stems will possess several internodes increasing in length from the base of the plant to the top. Prior to this stage, the nodes are all formed but are so close together that they are not readily distinguishable to the naked eye (Tottman, 1987). As elongation begins, the first node is swollen and appears above the soil surface. Above the nodes, linked by the rachis, the head starts to elongate and

is pushed upwards by the internode elongation. The first node is counted when the internode below exceeds 1 cm, whereas subsequent nodes are counted when the internode below them exceeds 2 cm (Tottman, 1987). The elongation phase lasts until the last flag leaf is completely emerged and its ligule is visible (stage 39). This stage coincides with the beginning of the last flag sheath extension, booting stage (40 to 49).

Throughout this period, the last flag sheath carries on extending until the boot starts becoming visibly swollen, stage 43. Booting becomes more and more obvious at stages 45 and 47, turning to stage 49 when the first awns are visible. Furthers stages until anthesis are marked by the head emergence (Stage 50, Appendix.4) moment at which, the head emerges and anthesis occurs, leading to the last stages of this developmental scale (Table.3.1; Apendix.3.1).

3.1.2 Internal development.

3.1.2.1 Leaf and spikelet initiation.

Development in barley can be divided into three major phases: vegetative, reproductive and grain filling phase (Slafer et al., 2002). The vegetative phase from sowing to floral initiation is characterized by leaf and tiller initiation (Fig.3.2). The reproductive phase starts with the onset of the spikelet differentiation in the apex (Fig.3.3.c) and finishes with the pollination of the ovary within the spikelets bearing fertile florets, normally coinciding with heading (Fig.3.3.g). The grain filling phase is the last developmental phase, subsequent to pollination. During this phase, the grain endosperm develops a variable number of cells and then dry matter is accumulated to determine the final grain weight. Moreover, in the meantime, the embryo develops the initial vegetative primordia (roots and leaves) to be able to produce a successful seedling in the next generation (Slafer et al., 2002).

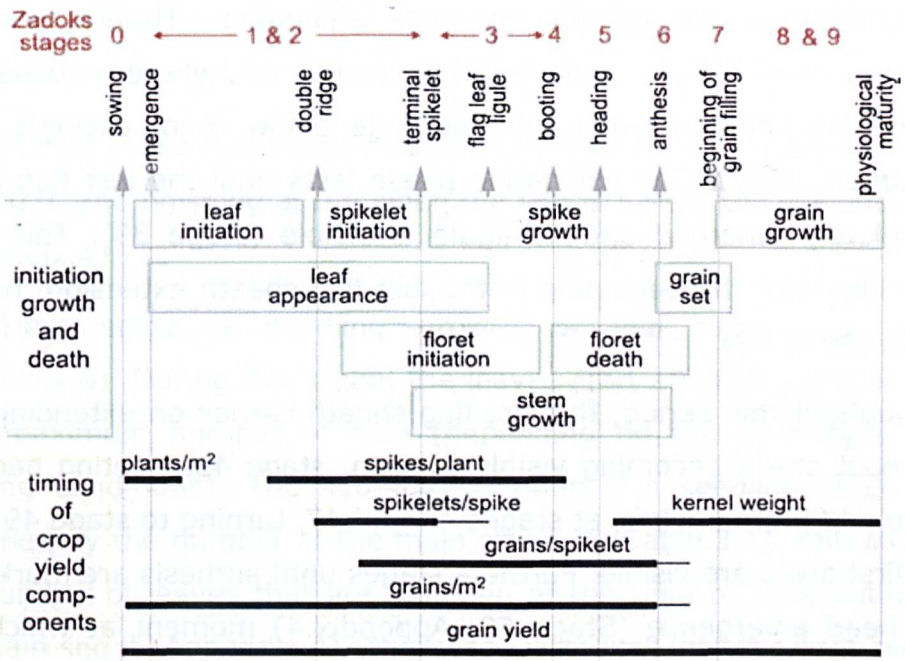

Fig.3.2 Schematic diagram of barley development. The vegetative phase from sowing to floral initiation is characterized by leaf and tiller initiation (two first main stages in Zadok code). The reproductive phase starts with the onset of spikelet differentiation in the apex and finishes with the pollination of the ovary within the spikelets bearing fertile florets, normally coinciding with heading. During the "spike" part of the reproductive phase, spikelets are initiated until a maximum number of spikelet primordia are reached. Later on, during the last part of this phase, spikelet and stem grow rapidly and some tillers and spikelets die, making the number of fertile floret concomitantly determined. The grain filling is the last developmental phase before pollination, during which the grain endosperm develops a variable number of cells and then the dry matter is accumulated to determine the final grain weight. It is during these last stages when the embryo develops the initial vegetative primordia to be able to produce a successful seedling in the next generation. http://www.fao.org/docrep/006/x8234e/ x8234e05.htm.

In barley, as in most Gramineae species, the apex produces leaf and spikelet primordia in chronological order (Arduini et al., 2010), so that all leaf primordia have been formed when the first spikelet primordia is initiated (Fig.3.2). The mature barley embryo contains the primordia of the first three to four leaves of the future main shoot (Kirby and Appleyard, 1986). From germination to seedling emergence, the apex initiates from one to three new leaf primordia (Fig.3.3.a-b). Therefore,

at seedling emergence, the shoot apex has five to seven leaf primordia (Slaffer et al., 2002).

During the vegetative phase, the apical meristem produces single ridges that will grow up into leaves (Fig.3.4 (1)), having initially a conical shape (dome) of about 0.2 mm in length that later elongates. The maximum number of leaves in the main shoot is determined by the time of cessation of leaf initiation, and start of the spikelet initiation, at which point, the apex changes from vegetative to reproductive stage, Zadok stage 15-19 (Fig.3.2 and 3.4 (1-5)).

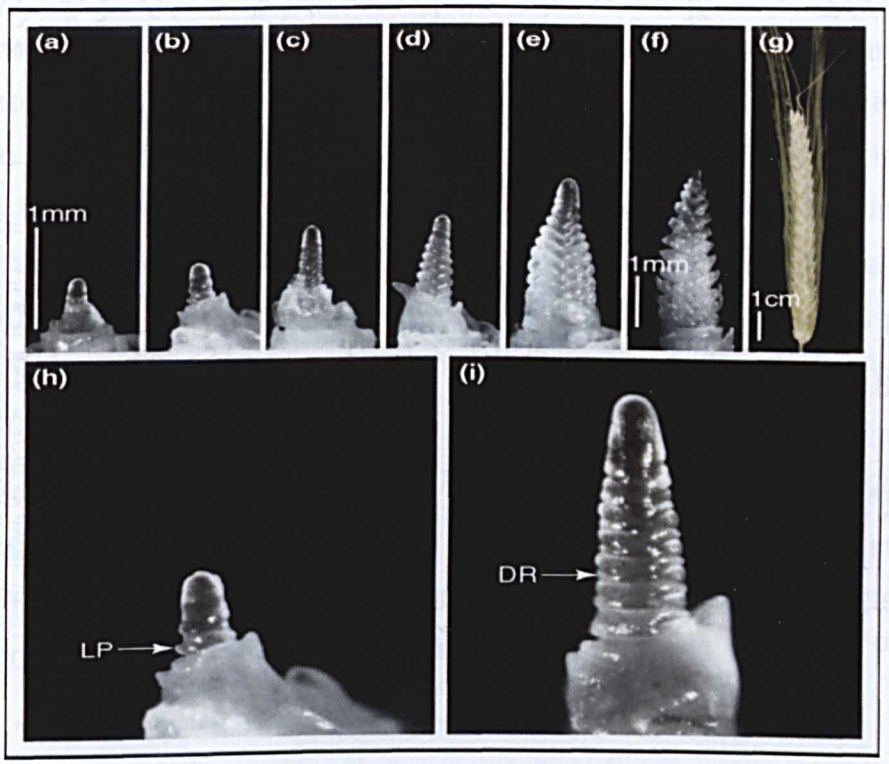

Fig.3.3 Phases of cereal shoot apex development. The shoot apex of barley develops vegetatively and produces leaf primordia (a,b) until inflorescence initiation occurs (c). At this point, floral primordia appear above the leaf primordia, giving rise to distinctive double ridges (Fig.3.4) along the side of the shoot apex. The floral primordia then differentiate into the floral organs that give rise to the florets (d–g). Anthesis occurs around the time of head emergence (g). Higher magnification images show the morphological differences between a vegetative shoot apex (h) and a reproductive shoot apex (i). The leaf primordia (LP) and double ridges (DR) are indicated by arrows (Trevaskis et al., 2007).

During the early part of the reproductive phase, spikelets are initiated until the terminal spikelet is reached (Fig.3.2). Later on, during the last part of this phase, the spikes and stem grow rapidly and some tillers and spikelets die, with the number of fertile florets being concomitantly determined (Fig.3.2).

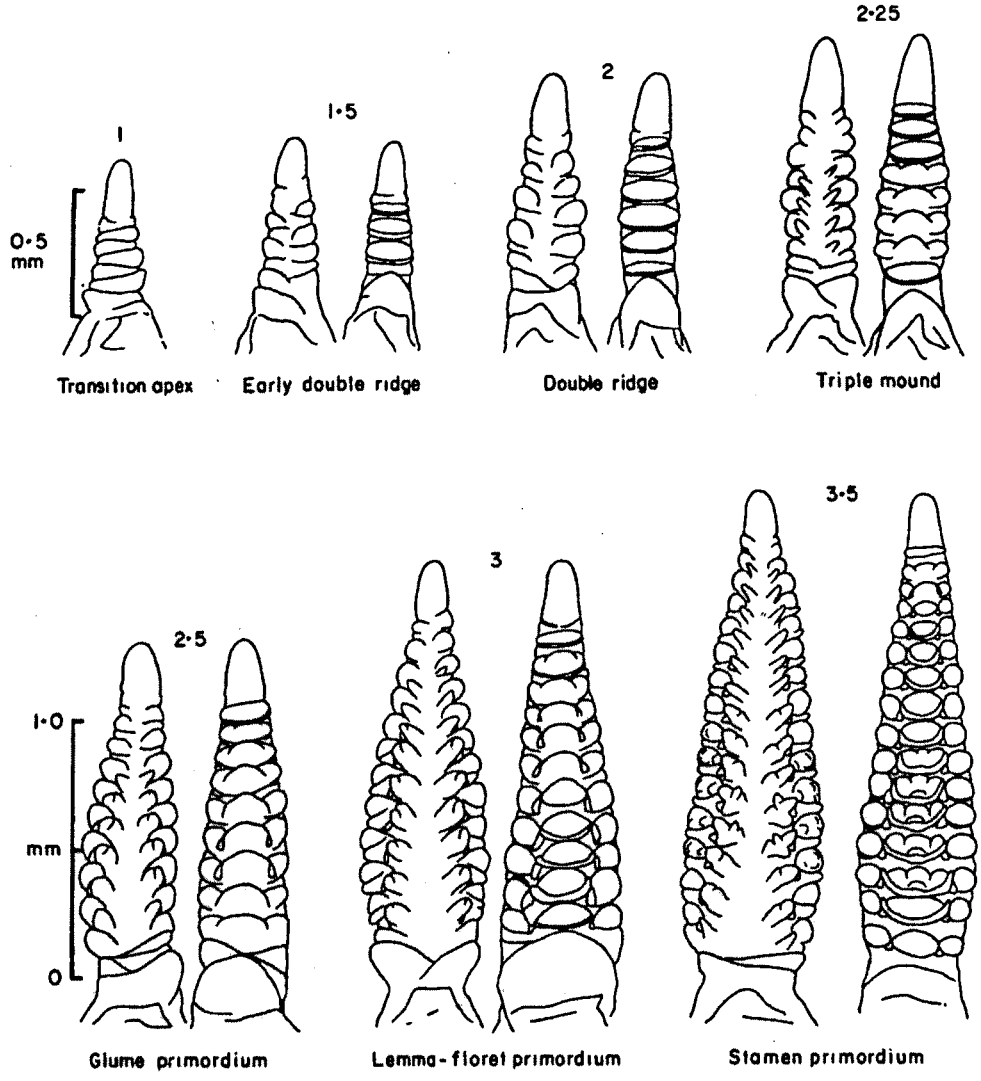

Fig.3.4 Morphogenesis of spike initial (Waddington and Cartwright, 1982).

Usually, the first visual evidence of the change from the vegetative to the reproductive stage in the apex is the appearance of a double ridge (Fig.3.4 (2) and Fig.3.3 (h-i)). The lower ridge corresponds to a leaf primordium (Fig.3.3 (h)) that does not develop further, and the upper ridge to a spikelet primordium. The apex at this moment is over 0.5

mm long; this stage is usually referred to as the beginning of floral initiation, although about half of the total number of spikelet primordia have already been formed; Zadok stage 23-25 (Fig.3.2)

The following important apical stage is known as the triple mound stage (Fig.3.4 (2-25)) because the spikelet primordium has differentiated into three protuberances that constitute the central and lateral spikelet. The subsequent stages are characterized by the appearance in sequence of the glume, lemma and stamen on the median spikelet (Fig.3.4 (2-5; 3)). The spikelet initiation ceases when awns primordia are evident on the most advanced spikelets (Zadok stage 25-27). A number of later initiated primordia at the tip of the shot apex do not progress to produce mature florets.

Coincidentally with the cessation of the spikelet initiation and the formation of the maximum number of spikelet primordia, at the base of the spike, the young collar encircles the developing rachis and forms the first nodes (Bonnets, 1966). At this stage, which coincides with the beginning of the stem elongation (Zadok stage 30), the spike is about 3 mm long and still at or below the soil level. From this point, the apex starts growing rapidly in parallel to the elongation of the pseudostem.

The duration of the different developmental phases varies widely, depending on the geographic area (e.g.; different latitudes), time of sowing and cultivar, in response to the interplay of the genetic and environmental factors controlling developmental rates.

3.1.2.2 Leaf emergence.

At the time the tip of the first initiated leaf appears, between 5 and 7 leaves have been initiated. Single leaves appear at each node of the stem, and these are borne alternately on opposite sides of the stem. Each leaf consists of a sheath, ligule, auricle and blade (Fig.3.5). The leaf sheath encloses the stem and is split to the base on the side opposite the blade and the two edges overlap. The auricle consists of

two claw-like appendages that clasp the culm at the juncture of the leaf sheath and blade. The ligule is an appendage that extends upward along the culm at the auricle.

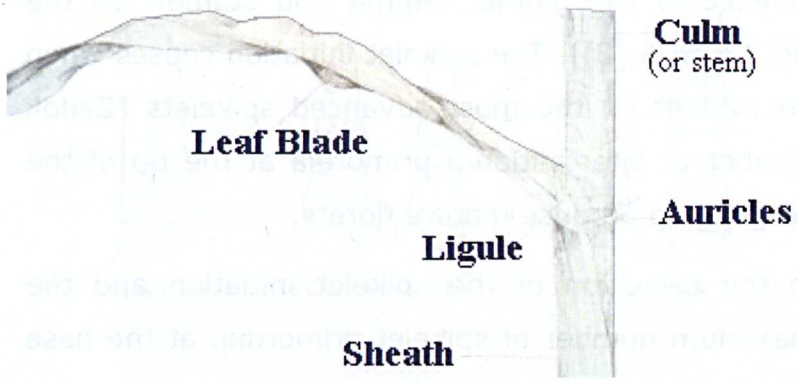

Fig.3.5 Junction of blade and leaf sheath.

The final leaf number is a critical determinant of the duration of the whole cycle to heading, as all the initiated leaf primordia must appear before the last internode elongates and the spikes emerge from the sheath of the last leaf (last flag). Therefore, time to heading strongly depends on the number of leaves initiated in the main shoot and the rate of leaf appearance (Slafer et al., 2002). The number of leaves that appear after leaf initiation is greater when the timing of floral initiation is delayed. Consequently, the longer the period from seedling emergence to floral initiation, due to the lack of satisfactory photoperiod or vernalization requirement, the higher the number of leaf primordia that has to appear after the floral initiation (Hay amd Kirby, 1991).

The duration of leaf emergence is also important for maximum grain yield. The maximum leaf area is usually reached at the onset of the

heading stage, and then declines during grain growth when the demand is great for photosynthate. As the lower leaves die, the upper leaf blades, leaf sheaths, and heads become very important as photosynthetic sources for grain filling (Anderson et al., 2002).

3.1.2.3 Tillering.

Tillering is one of the most important developmental events for barley, since it has a decisive influence on yield potential. A characteristic pattern has been observed for barley under field conditions. Tiller number increases rapidly during the first few weeks after seedling emergence, reaching a maximum shortly after floral initiation. It then diminishes rapidly before spike emergence, and finally stabilizes until harvest. Furthermore, the growth of many developing tillers may be suppressed after tiller emergence. Tiller mortality often begins after floral initiation in the main shoot, as developing tillers compete with limited success for available assimilates against developing spikelets and florets on the main stem (Miralles and Slafer, 1999).

The proportion of tillers that senesce without contributing to grain yield varies with the cultivar and environment. Barley shows pronounced differences between cultivars for maximum tiller production and tiller mortality. In general, two rowed barley shows higher tillering than six-rowed cultivars, and the winter forms generally produce more tillers than the spring ones. Long day length, high temperatures, and higher plants tend to diminish tillering, while high light intensity, water and nitrogen availability promote the formation and growth of secondary tillers. Competition among the shoots for nutrients, light and water seems to be one of the principal causes of tiller mortality in barley. Thus, tillers that have at least three fully emerged leaves or are over one-third the height of the main stem at jointing are those which are most likely survive

3.1.2.4 Flower development and morphology.

At the double ridge stage, the upper ridge grows fastest and gives rise to the floral primordium, while the lower ridge appears to give rise to the rachis internode, which is the extension of the stem that is the supporting axis of the spike. By a process of differential growth and folding a series of ridges and papillae form, which differentiate into glume initials, followed by the lemma. The palea develops later. Then, three papillae appear and grow into stamens. The pistils develop as a dome between the stamen initials; the styles with their stigmatic hairs form later. In time, the rachilla appears on the axis side of the palea, and lodicules form at the flower base. The palea and lemma grow up and eventually enclose the floral parts, although for some time the stamens protrude. Therefore, each spikelet consists of one ovary and its stigmas, three stamens and two lodicules packed between the palea and the overlapping lemma. The rachilla is between the rachis and the palea (Fig.3.6).

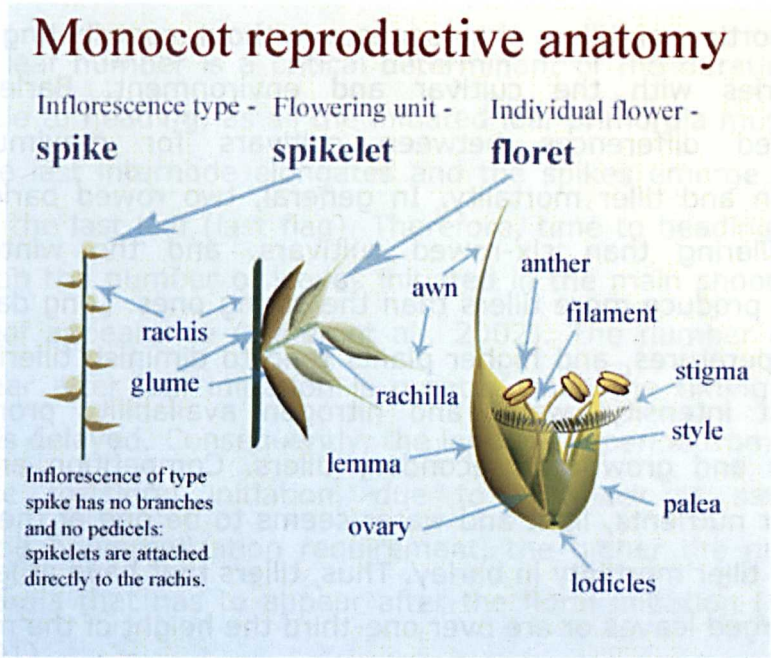

Fig.3.6 Monocot reproductive anatomy. In monocots, the inflorescence type is the spike, while the flower unit is known as the spikelet. The individual flower is called a floret. The spike has no branches and no pedicels. Spikelets are attached directly to the rachis (www.geochembio.com).

The pollen and ovules in each floret mature together. The course of flowering differs slightly between open and closed flowering varieties. It usually begins in the florets around the middle of the spike and spreads upward and downward, taking 2-4 days to complete. Most of the pollen is shed within the spikelet, therefore, self-pollination is usual in barley, but not inevitable. Sometimes, pollination occurs while the head is in the boot, but usually, it occurs during emergence.

3.1.2.5 Anther and pollen development in barley.

Anther and pollen development in barley has been well characterized (Murray et al., 2003). Sections of barley anthers show a similar development to *Arabidopsis* (Fig.3.7). Although small differences in pollen mother cells arrangement during meiosis and tetrad stage have been observed. Table.3.2 describes in detail the most important events occurring during development in barley.

First, the stamen differentiates into a four-lobed anther. The chamber of the anther lobes are separated first. Within each lobe, a multicellular archesporial develops. These cells divide into an outer layer of parietal cells and an inner region of sporogenous cells (Fig.3.7). The outer part the anther consists of an epidermis, the endothecium, a middle layer and the tapetum (Fig.3.7 (3)). The sporogenous cells divide to form the pollen mother cells which undergo meiosis at stage 3 to 4, ending in tetrad formation and the microspores release at stage 5 (Fig.3.7). During these stages, the tapetal layer is prominent. Stage 6 and 7 represents major events, not only for pollen, but also for the anthers. Microspores become vacuolated and the tapetum starts degenerating. At stage 8, bicellular pollen is observed within the vacuolated pollen (generative and vegetative nucleus) and the tapetum has almost completely disappeared. The generative nucleus will divide again to produce the two male gametes. Finally, at stage 9, the pollen starts accumulating starch and will be released when starch accumulation concludes.

Before dehiscence, the walls between the spaces in adjacent lobes give way. Anthesis is through longitudinal slits that appears in the anther lateral wall.

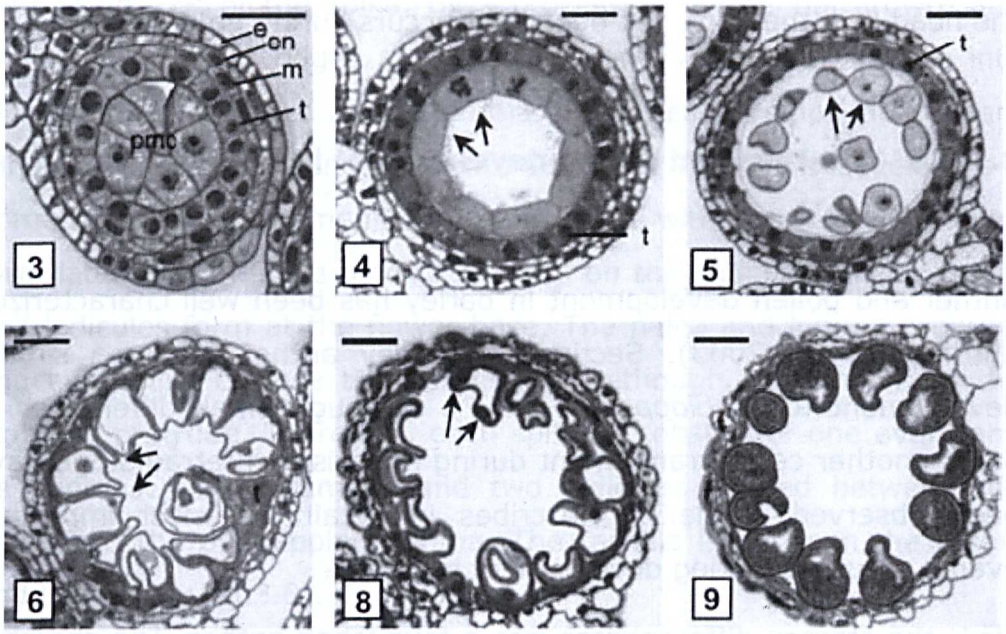

Figure.3.7 Stages of development in barley anthers ,stages 3–9. Stage 3: locule consisting of an epidermis (e), endothecium (en), middle layer (m) and tapetum (t). Pollen mother cells (pmc) are in the centre of each locule. Stage 4: pollen mother cells (arrows) undergoing meiosis are in prophase I. The tapetal layer (t) is prominent. Stage 5: microspores, irregular in shape (arrows) immediately after release from the tetrad. The prominent tapetal layer (t) is starting to degenerate. Stage 6: uninucleate, vacuolated microspores (arrows), tapetal layer degenerating (t). Stage 8: bicellular, vacuolated pollen grains showing the generative and vegetative nuclei (arrows). Partially collapsed pollen grains are typical during stages 6–8, and is thought to be due to fixation. Stage 9: starch accumulation in the pollen grains, tapetal layer has degenerated (Murray et al, 2003).

The main stages of pollen development occur within the anther from the five leaf stage and the following five days (Zadok stage 15-17), these are described in Fig.3.8 (Abiko et al., 2005). Archesporial cells are observed inside the anther at the beginning of stage 15. This

takes place while the apex is still under the ground and the elongation stage has not been reached. Parallel to the apex upright movement, events continue inside the anthers. The primary parietal cells appear on the second day after the 5 leaf stage and in the following days will develop to form the endothecium, the middle layer and the tapetum. At the same time, the primary sporogenous cells, derived from the archesporial cells will form the secondary sporogenous cells within the next day and finally will become the pollen mother cells between the third and the fourth day after the 5 leaf stage (Fig.3.8).

Stage	Developmental stage
1.	Archesporial initials present: beginning of the four lobe condition.
2.	Primary sporogenous cell/s surrounded by a three-layered wall.
3.	Four outer cell layers (epidermis, endothecium, middle layer and tapetum) present. Secondary sporogenous cells present.
4.	Tapetum prominent, pollen mother cells undergo meiosis.
5.	Non-vacuolate microspores newly released from tetrad. Middle layer compressed.
6.	Vacuolate microspores (1.8mm anther). Tapetum degenerating.
7.	Vacuolate microspores (2.3mm anther).
8.	Bicellular vacuolated pollen.
9.	Pollen grains accumulating starch.
10.	Pollen grains completely starch filled.
11.	Dehiscence.

Table.3.2 Anther and pollen developmental stages in barley (Murray et al,2003).

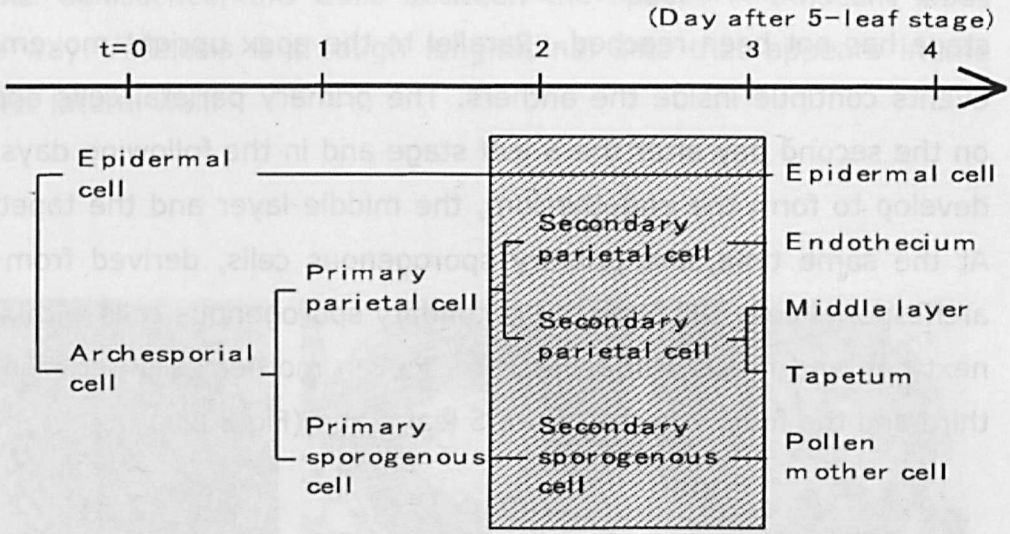

Fig.3.8 Barley anther development. The figure represents the anther development in barley from the 5 leaf stage (Zadok stage 15-17) to 4 days after. At T=0, archesporial cells are present. One day after archesporial cells divide in primary parietal cells and primary sporogenous cells. The former is the origin of the secondary parietal cells within the second and third day which will form the endothecium, the middle layer and the tapetum by the third day. The later, is the origin of the parietal sporogenous cells which are the precursors of the pollen mother cells three days after the 5-leaf stage. The timing represented here is subject to growing conditions and phenotype (Abiko et al., 2005).

This clear succession of events has not been accompanied by a parallel external study that can relate these stages to easily recognizable and constant vegetative growth external features. As mentioned previously, developmental variability, due to growing conditions or phenotype, make it difficult to establish such classification methods. Therefore, detailed analysis of barley development was conducted using a specific barley variety, Optic (One of the most common varieties in the UK malting industry), as well as constant growing conditions to provide key external markers to enable accurate selection of specific anther and pollen stages.

3.2 Materials and methods.

3.2.1 Growing conditions.

Double rowed spring barley supplied by the SCRI (*Hordeum vulgare*, optic variety) was grown in a growth room under controlled conditions (Section.2.1). Plants were grown until stages 30-31 were detected; material was collected from this point until anthesis occurred (Section.3.2.2).

3.2.2 Material collection and classification.

Barley morphological development was studied in detail from the onset of the elongation stage to anthesis in order to gain a better knowledge of barley external development and its relation with spike and anther/pollen development.

The Zadok stages were used for external staging of the plant and further material collection (Table.3.3). From stage 30 to 55, three different main Zadok stages take place, elongation, booting and heading (Appendix.4). Throughout these three main stages, thirty different tillers were studied. Constant parameters were recorded every three days, pseudostem size (from the base of the pseudostem to the last auricle visible), number of nodes identifiable, internode elongation and any change recorded, such as last flag appearance and elongation. These parameters were all accompanied by a description of the Zadok stage at the moment of data collection based on Table.3.3 (Appendix.4). The material used for data collection was restricted to the oldest tillers, i.e. tillers that were already within the elongation stage when the main shoot had finished its elongation phase. Therefore, shoots appearing from this point, or still at stages previous to elongation were not used. The main shoot was also not used due to its rapid growth rate compared to that of the other tillers.

This made comparative growth rate analysing between the main shoot and tillers impossible.

Zadok Stage	External characteristic
30	First node still under the ground.
31	First node detectable
32	Second node detectable
33	Third node detectable
34	Forth node detectable
35	Fifth node detectable
36	Sixth node detectable

Zadok stage	External characteristic
37	Flag leaf just visible but still rolled
39	Flag leaf ligule visible
43	Boot just visibly swollen
45	Boot swollen
49	First aws visible
53	¼ spike emerged
55	½ spike emerged

Table.3.3 Zadok developmental stages for cereals (Appendix.4). Stages shown go from the start of the elongation stage (30) to head emergence, and the moment at which anthesis occurs (Appendix.4). Key and easily recognisable Zadok stages were selected as reference for sample collection and developmental study.

In addition, and in parallel to the external study, spikes were collected and measured in order to establish a relationship between external stages (Table.3.3) and the spike size. A minimum of 20-50 shoots per stage were split open, from elongation stage 30 to 55, and spikes size measured (from the base of the first floret to the tip of the top one). The shoots used were also the oldest as specified above. In addition, the floral development stage of each floret within a particular spike size was determined following the scale of Waddington et al. (1983) (Table.3.4); this is mostly based on pistil development from stage W1 (Transition apex) to stage W10 (styles curved and stigmatic branches spread wide, pollen grains on well-developed stigmatic hairs). The florets analysed were those in the central positions of the spike. Moreover, and in parallel to spike sizing, floret and anther external

development was recorded. This data collection aimed to establish a constant development pattern of the reproductive organs in relation to the spike size, which related to plant external development.

Stage	Pistil Description
1	Transition apex
1.5	Early double ridge stage
2	Double ridge stage
2.25	Triple mound present
2.5	Glumen primordium present
3	Lemma-floret primordium present
3.5	Stamen primordium present
4	Pistil primordium present
4.5	Carpel primordium present
5	Carpel extending round three sides of ovule
5.5	Stylar canal closing

Stage	Pistil Description
6	Stylar canal remaining as a narrow opening
6.5	Styles prominent
7	Styles elongation
7.5	Stigmatic branches just differentiating
8	Stigmatic branches elongating
8.5	Hairs on ovary wall just differentiating
8.75	Stigmatic branches and hairs on ovary wall and elongating
9	Stigmatic branches and hairs on ovary wall and elongating
9.25	Styles and stigmatic branches erect
9.5	Styles and stigmatic branches spreading
10	Pollination

Table.3.4 Scale of pistil morphogenesis in barley (Waddington et al., 1983).

Moreover, florets collected from the above mentioned spikes (at different spike sizes and stages), were resin fixed in order to study the anther and pollen development from stage 30 to stage 55 (Table.3.3) Different spikes were selected depending on their sizes in intervals of 0.5-1 cm length; 2-3 florets were always collected from the middle zone of the spike. For each sample a detailed description of the barley external appearance was recorded.

3.2.3 Histological analysis of anther development.

To visualize anthers and pollen development, barley panicles were resin fixed. Plant florets were collected from Zadok elongation stage to anthesis. Spike size was essential for selecting the material. Spikes were collected every 0.5-1 cm, starting at 0.5 cm long (Spike Elongation stage), identifying the Zadok stage at collection. Individual florets were used, however, when spikes were too small, the whole spike was fixed (spike < 1cm). Selected material was immediately placed in 4% (v:v) fresh prepared paraformaldehyde (Appendix.1) solution and kept on ice. Following this, and to prevent air bubbles within the samples, vacuum infiltration was performed for 30 min. The fixative was then changed and vials placed overnight in a cold room (4°C; rotating). After 24 hours, the tissues were washed twice (30 min each) with 1xPBS (Appendix.1). Fixed panicles were immediately dehydrated by treatment with increasing concentration of ethyl alcohol, 30,50,70,90 and 100% (v:v), one hour each except at 100% where samples were left for two hours (samples could be left at 70% (v:v) ethanol at 4°C for long period before carrying on to the 90% ethanol (v:v) if needed. Pre-infiltration of the tissue was carried out using a mixture of Ethanol/resin (100 ml of Technovit 7100 resin + 1 g of Hardener I, solution A) at increasing proportion of resin, 2:1, 1:1, 1:2 for 1 hour, finishing with 100% resin. After leaving the tissue overnight in 100% resin (4°C), material was placed into a capsule and solution A was replaced by solution B (375 µl of solution A + 25 µl of hardener II). This was conducted as quickly as possible since solution B polymerises immediately in contact with air. Then, after 24 hours, the capsule was removed using a blade and sample was placed onto a mould orientated to the top. Then, it was fixed using the fast and the cold-curing Technovit resins (Technovit 3040). After 24 hours, samples were ready for serial sectioning with a microtome (Model: 5040; Bright Instrument Company, Huntingdon, UK).

The block was firmly attached to the balancing head and then the blade. The block was cut and slices were placed in clean water in order

to expand the slices. Expanded sections were then recovered from the water using a plastic cover-slip. After drying them using a warm plate (20-25ºC), sections were stained using Toluidine blue (0.05%)/DAPI (4',6' diamino-2-phenylindole-2HC) (DAPI was used only at the latest stages in order to stain the nucleus) (0.05% w:v). A drop of Toluidine blue/DAPI was placed on each tissue slice and then left for 30 seconds. Toluidine blue/DAPI was washed out, placing the cover-slip on the plate for drying. Dried samples were observed under the microscope in order to confirm that the expected tissue area and its orientation were correct. After 24 hours on the warm plate a drop of DePex (BHD, Pool, England) was placed on each slide and then covered with a coverslip. After 24 hours, the samples were ready for observation.

3.3 Results.

3.3.1 External morphological scale.

Barley development was studied in detail from stage 30 to 55 in order to establish constant and easily recognizable stages that could be used in future studies and material collection. The Zadok scale was used as a basic model for stages identification. However, after a detailed study, some of the stages were substituted by new and easily identifiable stages adapted to barley (Optic).

Pseudostem and internode elongation, in relation to external development stages, is shown in Fig.3.9. Pseudostem elongation showed clear differences in size depending on external development stages. Elongation was rapid during the first stages, growing from 15±2.61 cm to 44±5.17 cm from stage 31 to 35-37; however, from 37 to 49 the pseudostem elongated only a further 10 cm, until the point at which the plant reached almost its maximum height. The pattern of pseudostem growth was driven by the internode elongation; the first and the fifth internode elongated less than the second, third and fourth which showed a similar size beyond stages 35-37. Internodes elongation was studied for the first five nodes; elongation occurred only when the previous internode had elongated 2 or more cm, and never before, facilitating the identification of the different nodes, and the classification of the plant following the Zadok's system at these early stages during the elongation phase (Table.3.1). However, although, the relationship between the external stages and the pseudostem elongation was clear, this elongation was not used for developmental staging prediction. Pseudostem size variation was on occasions high as internode elongation did not progress uniformly within the different plants. Thus, tillers showing great differences in size were found to be at the same developmental stages according to the number of node detected.

Developmental stages from the onset of the elongation phase to stage 34 were clearly defined by the appearance of nodes and their elongation as described by the Zadok system (Table.3.3; Fig.3.9). These stages, from 31 to 34, followed consecutively without overlapping, and were easily recognisable (Fig.3.10). In addition, stage 37 was observed normally after stage 34 as the fifth and sixth nodes did not have time to elongate before the last flag emerged. This figure shows a representation of these stages and how they were recognised *in vivo* based on results from Fig.3.9.

Characterization of barley growth stages beyond stage 37 proved to be confusing using the Zadok system. Some stages overlapped, making it difficult to establish continuous samples collection points. For instance, using Zadok's code, stage 37 is followed by stage 39 (stage at which point the flag leaf ligule is visible); however, plants normally reached booting stage without showing this ligule. In addition, at booting stages (Appendix.4), first awns, which were proposed as being visible at stage 49, occurred as early stages as 41-43 (Appendix.4), when booting was still not obvious. This method was therefore extremely complicated and a sequential staging method was needed.

Fig.3.11 shows the last flag extension scale (LFE), which was created as an alternative to Zadok stages 39 to 53 (Table.3.5). Each of these four new stages was identified by a combination of new features based on developmental observations, such as last flag sheath elongation and the spike position within the pseudostem (Table.3.5).

1) LFE1: last flag sheath elongates 0.5-5 cm. The tip of the inflorescence is palpable (with fingertips) above the leaf blade base of the second leaf below the flag leaf.

2) LFE2: last flag sheath elongates 5-10 cm and is slightly swollen. The tip of the inflorescence has grown into the flag leaf sheath, remaining the rest within the previous sheath.

3) LFE3: last flag sheath elongates >10 cm and boot visibly swollen, spike in between the previous to the last flag sheath.

4) LFE4: Spike within the last flag sheath and about to emerge, or showing some spikelets (Fig.3.11).

Stage	Characteristics
31	One node detectable.
32	Two nodes detectable.
33	Three nodes detectable.
34	Four nodes detectable.
35	Fifth node detectable. This stage was normally absent as last flag emerged completely before the fifth node was detectable. Only when present, was this stage used for staging purposes. Stage 36 was never observed before stage 37 appears.
37	Last flag completely emerged, still rolled. This stage followed stage 34 when 35 and 36 were not present.
LFE1	Flag leaf has emerged completely and is unrolling, ligule may be visible and flag leaf sheath extended between 0.5 to 5 cm.
LFE2	Last flag sheath extended 5-10 cm. Boot swelling became obvious. At these stages, awns may be visible. Stag. Spike was still inside the sheath before last, as rachis did not start elongating
LFE3	Flag leaf opening and awns clearly visible. Last flag sheath extended over 10 cm. Rachis started elongation, moving the spike in between the previous to the last flag sheath.
LFE4	Spike has completed its upward movement and was entirely localised within the last flag sheath. Heading is imminent.

Table.3.5. Barley external development stages including the new last flag extension scale (LFE), created to describe the last developmental stages in substitution of Zadok stages from 39 to 53. These stages were used for sample collection in further experiment.

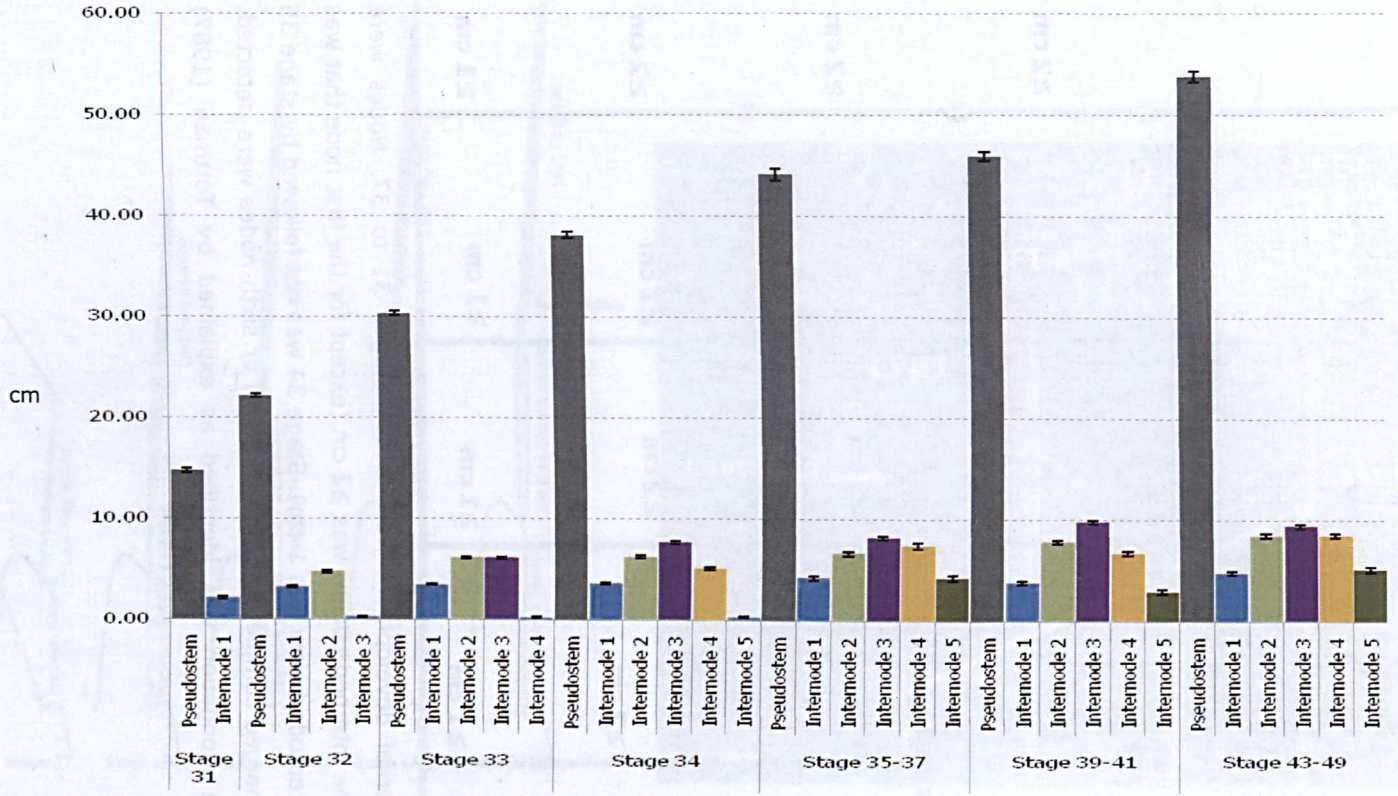

Fig.3.9 Pseudostem and internodes elongation during the barley development from stage 31 to 49. Grey column represents the pseudostem elongation (cm) from the base to the last ligule visible. The smaller columns show the internodes elongation average at each stage. Pseudostems elongation was linked to the internode elongation. Clear differences in growing pattern were observed within the different internodes. Internodes 2, 3 and 4 elongated longer than the first or the fifth internodes, maintaining this differences at least until stage 43-49.

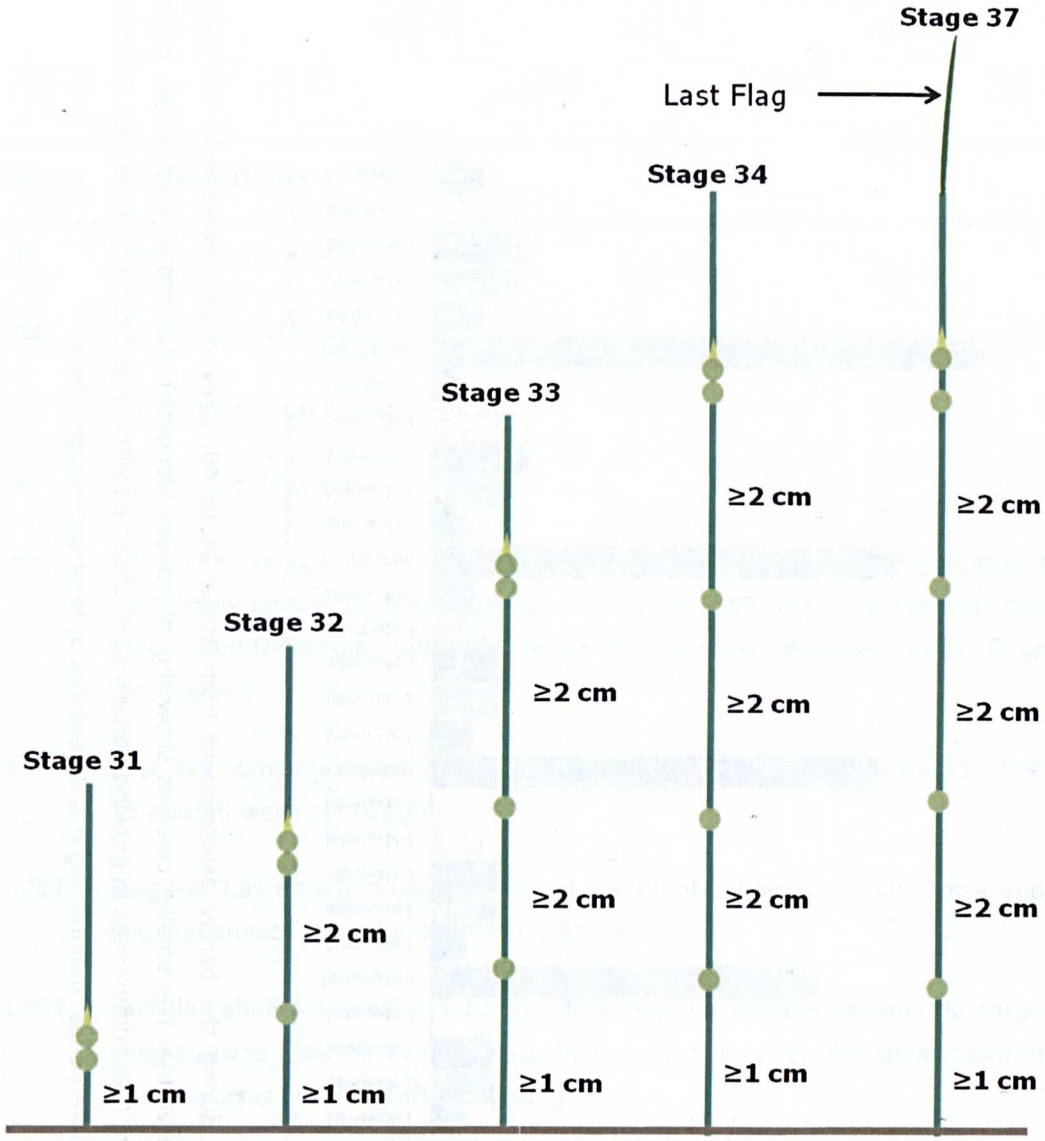

Fig.3.10 Barley external development from Zadok stages 31 to 37. Nodes were counted only when the internode below was ≥2 cm (except for the first node that was counted when the internode below was 1 cm). Stage 34 was not followed by stage 35 or 36 as last flag emerged completely before the fifth or sixth nodes were detected. Node and internode elongation was identified as explained by Tottman (1987) (Section.3.1.1).

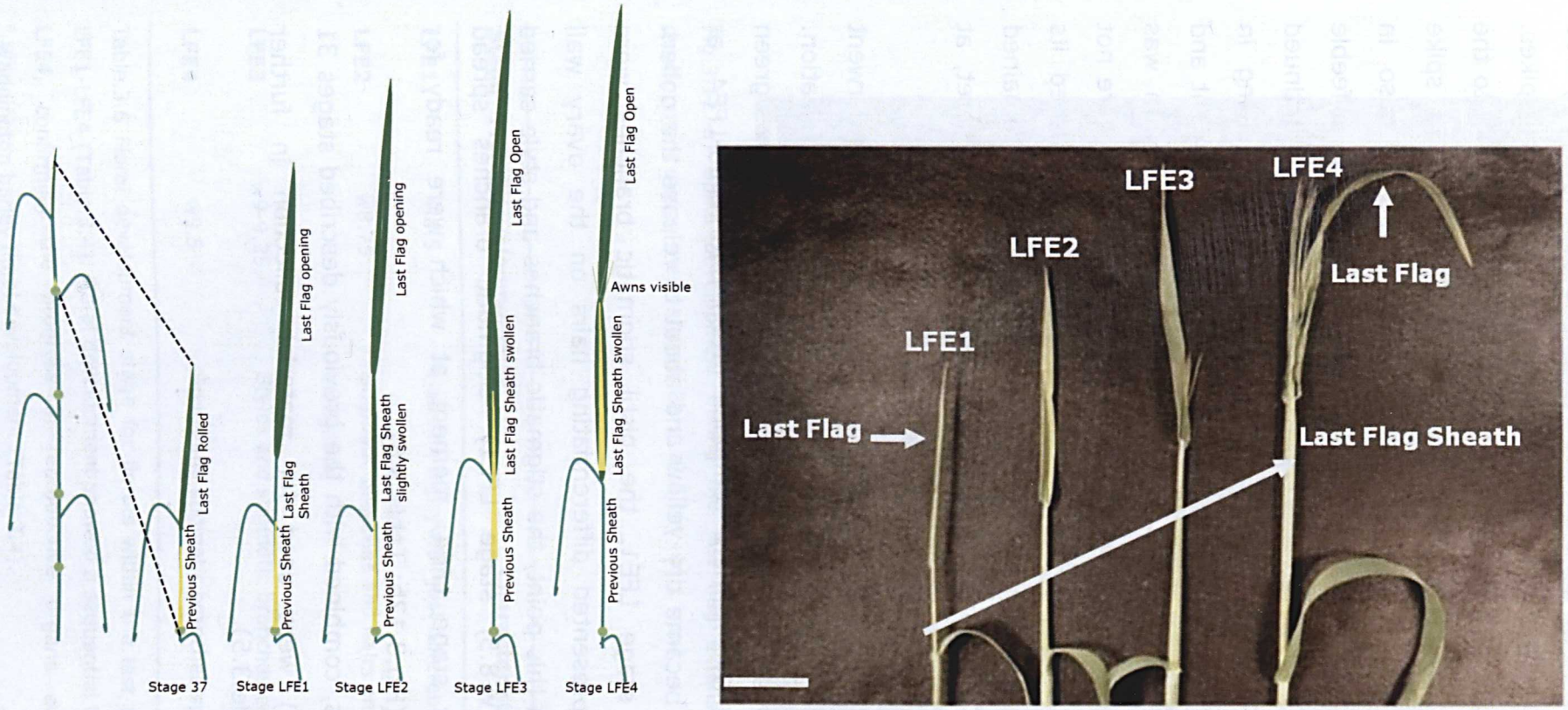

Fig.3.11 Last flag extension scale (LFE). These stages substituted Zadok stages from 39 to 53 (Table.3.5). These stages were defined by the last flag sheath elongation and the spike upward movement that ended with the spike emergence. Left picture shows a detailed description of the stages. Elongation of the last flag sheath was accompanied by the upward movement of the spike (Yellow head) that ended when the spike was completely established within the last flag sheath (LFE4). Right picture: *In vivo* appearance of the stages described in the left picture. Bar= 4 cm.

To confirm that the succession of new stages shown in Fig.3.11 maintain a direct relationship to other organ development, spikes, florets, anthers and pistil development were studied in parallel to the last flag extension stages (Table.3.5). From stage LFE1 to LFE4, spike appearance changed significantly, not only in size, but also in structure (Fig.3.12a). At stage LFE1, the spike showed a feeble appearance, and was unable to stand upright. Spikes continued growing during the subsequent developmental stages, gaining in resistance. At stage LFE3, spike and awns presented an upright and compact conformation (Fig.3.12a). Increase in spike strength was accompanied by the floret final changes (Fig.3.13). Florets were not completely closed at stage 37, as the lema had not finished its development, thus, the green anthers were visible. Anthers remained visible until lema development was completed, closing the floret, at stages LFE2 to LFE3 (Fig.3.13).

Parallel to spike and floret development, anthers and pistils underwent significant changes that finished with anthesis and fertilization. Anther colour changes are represented in Fig.3.12b. This shows green anthers at stage 37. Anthers remained green until LFE3-LFE4, at which point they became dry-yellow and about to release the pollen. In addition, at stage LFE1, the pistil stigmatic branches were elongating and presented differentiating hairs on the ovary wall (Fig.3.12b). From this point, the stigmatic branches and style carried on elongating (w.8.5, stage LFE1). Stigmatic branches spread approximately at stage LFE4, moment at which were ready for pollination, w.10 (Fig.3.12b; Table.3.6).

These new stages, combined with the previously described stages 31 to 37 (Fig.3.10) were used for material collection in further experiments (Table.3.5).

Fig.3.12 a) Spike development during the last flag extension stages. b) Pistil development during these stages. Bars: a) 2 cm b) 1 mm.

Stage	Floral development[a]	Characteristics
LFE1	w8.5	Hairs on ovary wall just differentiating
LFE2	w8.75	Stigmatic branches and hairs on ovary wall elongating
LFE3	w9-9.25	Styles and stigmatic branches erect
LFE4	w9.5	Styles and stigmatic branches spreading

Table.3.6 Floral development stage for florets within the last flag extension stages LFE1-LFE4 (Table.3.4). Floral development showed a sequential increase from LFE1 to LFE4, confirming the progress in reproductive organs during these stages. [a] Waddington barley floral development (Table.3.4).

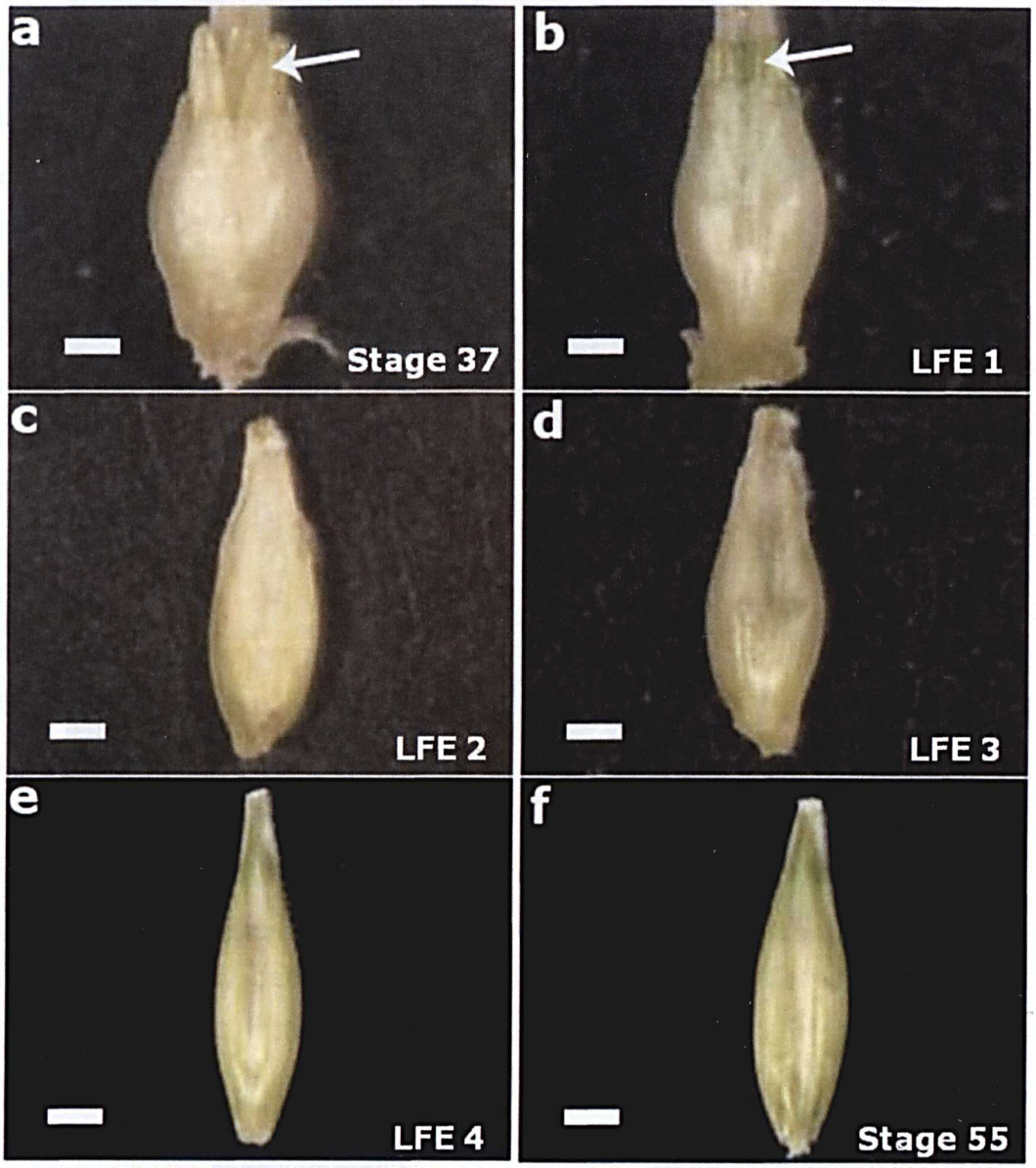

Fig.3.13 Morphological development of barley florets from stage 37 and throughout the last flag extension stages. a) Stage 37: floret is not completely closed; the lemma has not grown enough to cover the anthers completely (arrow). b) Stage LFE1: The anthers are still visible, but almost covered by the growing lemma (arrow). c) Stage LFE2: Anthers completely enclosed. d-f) From this point, florets (d-f) carry on growing and tissues become harder. d) Stage LFE3. e) Stage LFE4. f) Stage 55. Bars: 2 mm.

3.3.2 Spike size prediction.

During the stem elongation phase, the spike started a fast growing period that commenced around stage 32 and lasted until approximately stage LFE3 (Fig.3.14). Spike elongation runs parallel to the pseudostem elongation phase that starts not long before the spike elongation (Stages 30-31). Spike sizes measured at different stages of barley external development (Table.3.7) confirmed a low spike growing pattern from stage 30 to 32 (0.5±0.18 cm to 1.17±0.50 cm) changing to a faster growth between stages 32 to LFE2, where spikes grew from 2.46±0.97 cm at stages 33 to 9.38±1.27 at stage LFE2 (Table.3.7), although the greatest growth point was between LFE1 and LFE2. Finally from stages LFE2 to LFE3, the variation in spike size was very small, confirming a reduced spike growing rate until it reach its maximum size (Fig.3.14).

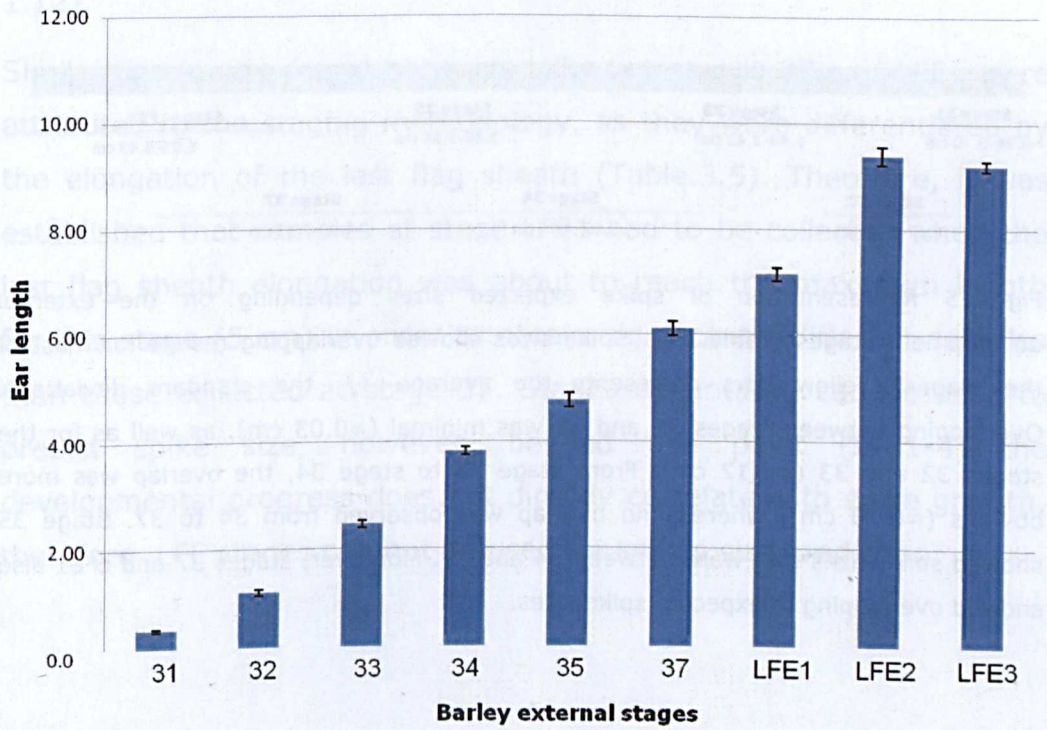

Fig.3.14 Expected spike sizes in relation to different barley external stages (Table.3.7.). Spikes showed a constant growing pattern from stage 31 to LFE1-2, where spikes reached their maximum size (LFE2-3).

The alignment of the expected spike sizes depending on the external development stages, 31 to LFE1, represented in Fig.3.15, showed that the expected spike sizes overlapped from one stage to the other, making it difficult to accurately predict their sizes.

Stage	Spike size (cm)
31	0.52±0.18
32	1.17±0.54
33	2.46±0.97
34	3.83±1.16
3	4.77±0.89

Stage	Spike size (cm)
37	6.11±1.12
LFE1	7.14±1.29
LFE2	9.38±1.27
LFE3	9.19±0.77
LFE4	----

Table.3.7 Spike size expected values depending on external stages (Table.3.3) (based upon 20-30 spikes analysed per plant).

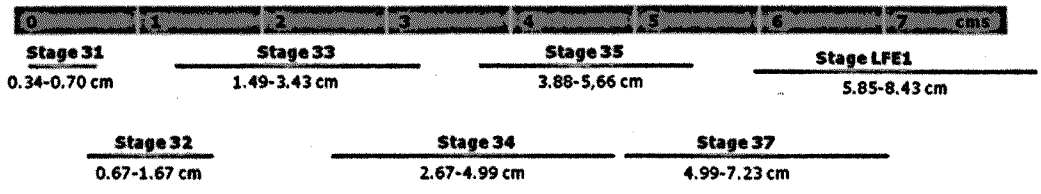

Fig.3.15 Representation of spike expected sizes depending on the external development stages (Table.3.7). Spike sizes showed overlapping results for most of the stages (Yellow bars represents the average +/- the standard deviation). Overlapping between stages 31 and 32 was minimal (≈0.03 cm), as well as for the stages 32 and 33 (≈0.12 cm). From stage 33 to stage 34, the overlap was more obvious (≈0.70 cm), whereas no overlap was observed from 34 to 37. Stage 35 showed spike sizes that were between 34 and 37. Moreover, stages 37 and LFE1 also showed overlapping in expected spike sizes.

To reduce the overlapping observed at certain stages and gain more accuracy in spike size prediction, sub-stages were introduced. Between the stages 33 to 34 and 34 to 37, sub-stages 33.5 and 34.5

were included respectively (Fig.3.16). Sub-stage 33.5 was constant and easily recognizable after stage 33 due to the elongation of the fourth internode (Fig.3.16). However, stage 35 was not always detectable. Although the fifth node was frequently seen at stage 34, the fifth intenode rarely elongated before the emergence of the last flag. Thus, stage 35 was rarely achieved before the emergence of the last flag leaf (stage 37). Sub-stage 34.5 was only detected when the fifth internode extended, but did not reach the 2 cm required to be defined as stage 35 (section.3.3.1). Therefore, only when stage 35 was observed, were spike sizes at this stage considered as the sub-stage between 34 and 37 (34.5, Fig.3.16; Table.3.8) thus facilitating a more accurate spike size prediction between 34 and 37. Table.3.8 shows the stage 33 to 37, including the two sub-stages and the expected spike sizes observed. Results show that spike sizes varied when collected at stages 33 (1.69+/-0.53) or 33.5 (3.14+/-0.72). In addition, sub-stage 34.5 (4.77+/-0.889) also allowed a more accurate spike size prediction between stage 34 (3.90+/-1.15) and 37 (6.11+/-1.12).

Similarities in size found between spikes at stages 37 and LFE1 were attributed to the staging methodology, as they were differentiated by the elongation of the last flag sheath (Table.3.5). Therefore, it was established that samples at stage LFE1 had to be collected when the last flag sheath elongation was about to reach the maximum length for this stage (5 cm) in order to obtain significantly different samples than those collected at stage 37. Stages up until 37 can be used to predict spike size, however, beyond this point (LFE1-4) the developmental progress does not directly correlate with spike growth, therefore, LFE stages can not be used for spikes size prediction.

Stage	Spike size	
	Main stage	Sub-stage
Stage 33	1.69±0.53	3.14±0.72
Stage 34	3.90±1.15	4.77±0.89
Stage 35	4.77±0.89	------
Stage 37	6.11±1.12	------

Table.3.8 Spike sizes expected for the stages and sub-stages.

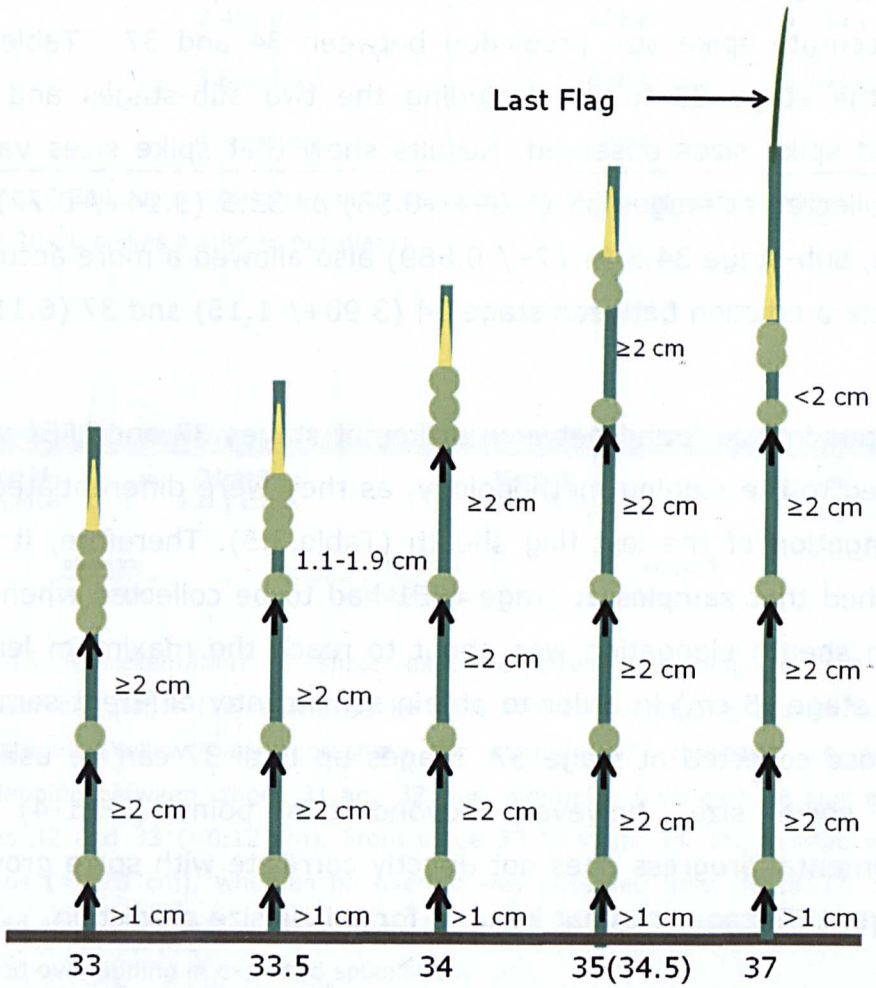

Fig.3.16 Barley external development from stage 33 to 37 including sub-stages 33.5 and 35 (34.5). Sub-stages were recognized when the internode above a given stage was elongating from 1.1 to 1.9 cm. In the case of 34.5, stage 35 was taken as the sub-stage between 34 and 37, therefore, when the fifth internode had elongated 2 or more cm, the sub-stage 34.5 was identified.

Therefore, spike size prediction was restricted to stages 31 to 37 including the two sub-stages (Fig.3.17), and comprised sizes from 0.52±0.18 to 6.11±1.12 cm. Fig.3.17 shows the final stages and sub-stages used for spike size prediction and the probability of finding the expected spike size. Vertical columns represent the probability of finding specific spike sizes within any stage. Spike sizes followed a clear pattern where bigger spikes were found as stages got closer to stage 37. For instance, the probability of finding spikes between 0-2 cm was higher in stages 31 to 33, however, spikes 0-1 cm were more likely in stages 31-32, whereas in stages 32-33, spikes of 1-2 cm was more likely. Moreover, spikes between 2-4 cm were observed more often in stages 33.5 to 34, and spikes of 4-6 cm in stages 34-37. Accuracy was gained by introducing sub-stages that helped provide a higher degree of differentiation between the closely related stages. In sub-stage 33.5 spikes collection of 2-4 cm, more likely than 3-4 cm. Spikes 3-5 cm were found between stages 33 to 35, however, spikes of 3-4 cm and 4-5 cm were more likely between 33.5-34 and 34-35 respectively. Finally, in stage 37, the last stage used for spikes size prediction, spikes 5-7 cm were found, and although some spikes 4-5 cm long were observed, these were more likely at previous stages.

From stage LFE1, spike size showed fewer differences in size (Fig3.14), therefore, spike size was not considered as a developmental feature for predicting further developmental staging. Last flag extension stages (LFE1 to LFE4) showed sufficiently differentiation (Section.3.3.1) to be used as subsequent staging points and were considered the continuation of Zadok stages 31 to 37. Only the first stage, LFE1 showed problems in differentiation from the previous stage, 37, therefore, this stage was considered as a transition stage between the Zadok scale 31-37 and LFE1-4 (Table.3.5).

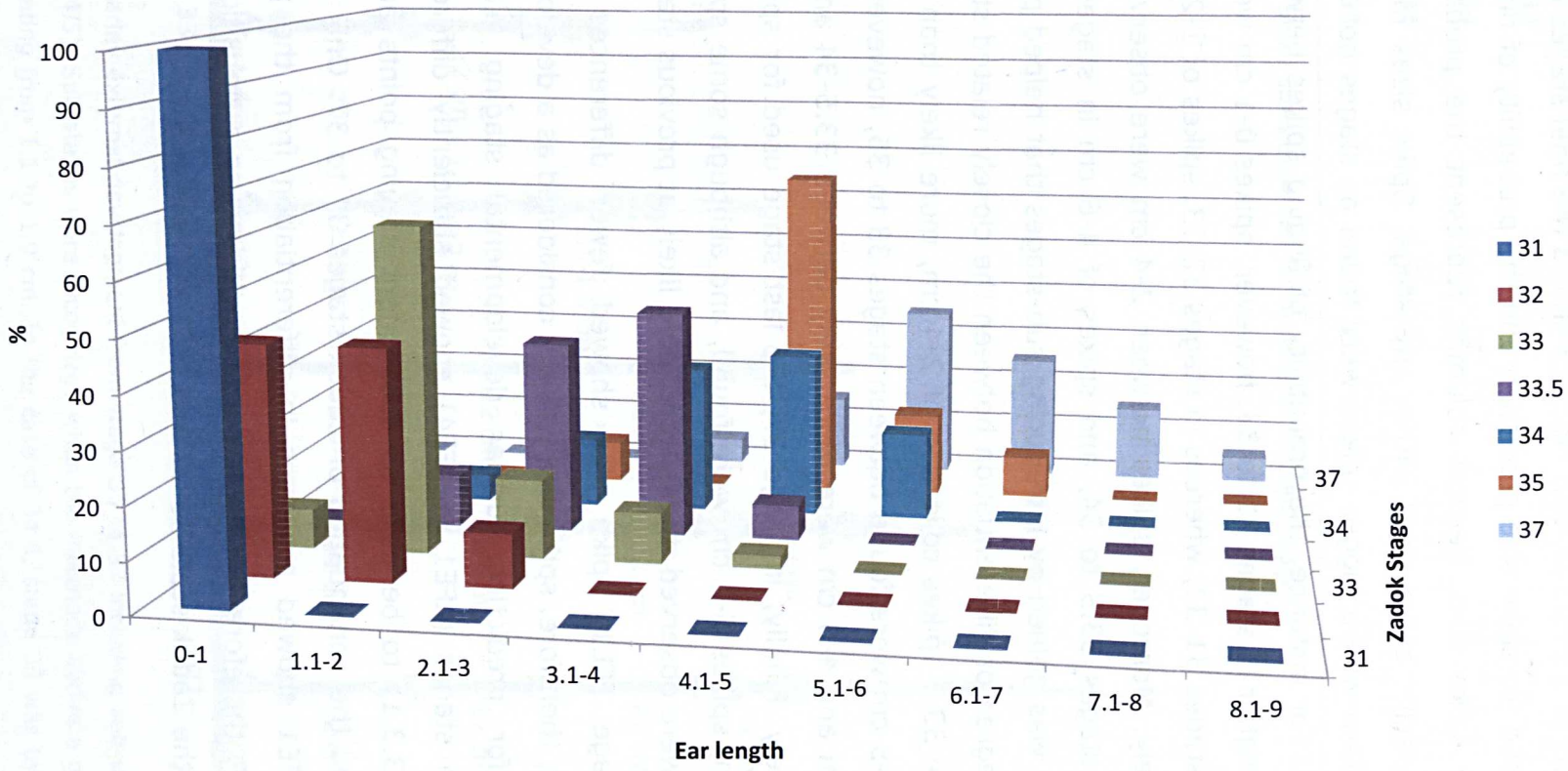

Fig.3.17 3-D Histogram representing the spike size prediction depending on barley external development from stages 31 to 37, including the sub-stages 33.5 and 35 (34.5). Vertical columns show the probability of finding and specific spike size within any stage.

3.3.3 Staging of barley anther and pollen development.

The ultimate target of this morphological study has been the prediction of anther and pollen development events throughout external observation of the barley plant development. The relationship between external staging and the spike sizes has been observed at specific point during barley development (Section.3.3.2). Staging points were established in order to study the changes taking place within the anthers alongside the spike size and the final stages of barley development. From stage 31 to 37, spike samples were collected at different sizes, in intervals of ±1 cm (Table.3.9), whereas, from stage LFE1, last flag extension (LFE) stages (Table.3.5) were used for floret collection and resin sectioning analysis.

Fig.3.18 shows a series of transverse resin sections through barley anthers from different spike sizes and stages (Table.3.9). Table.3.9 describes in detail the differences found and the events occurring in the anther during these spike and the LFE stages. From spike 0.6 cm to stage LFE4, anther and pollen development can be correlated, in relation to spike size (0.6 to 5.7 cm, Stages 31-37; Table.3.9), and also to the last flag extension stages (LFE1 to LFE4; Table.3.9). Sections shown in Fig.3.18 are representative examples of these samples (florets collected for sectioning were from the middle region of the spikes).

These sections indicated a developmental progression of anther and pollen development correlated with the observed spike size changes and the four LFE stages. Samples from spikes 0.6 cm showed sporogenous cells and three anther layers (Fig.3.18a; Table.3.9). Four cell layers were seen when the spikes were 1.7 cm (Fig.3.18b). Spikes of 2.8 cm showed entry of PCM into meiosis and by 3.5 cm microspore release occurred. Spikes 4.9 cm had released microspores and the middle layer was undergoing crushing (Fig.3.18e). Tapetum degeneration was evident in spikes of 5.7 cm, at which stage, microspores become vacuolated (Fig.3.18f). From stage LFE1, anthers

and pollen development entered in the last stages before anthesis (Fig3.18g). Tapetum degeneration finished and microspores entered in two mitosis cycles (MI: LFE1-2 and MII: LFE3) that conclude at stage LFE4 with tri-nucleated pollen and anthesis was taking place (Table.3.9; Fig3.18g-l). The developmental progression observed through these latest stages was reinforced by the stomium development. Stomium area increased in size as anthers got closer to dehiscence (Fig.3.19). In addition, the stomium became thinner closer to dehiscence, finally breaking and releasing the pollen at stage LFE4.

Spike Size/Stage	Anther and Pollen development stage
Spike 0.6 cm	Primary sporogenous cells. Three layers surrounding the anther locule.
Spike 1.7 cm	Secondary sporogenous cells to Pollen Mother Cells (PMC). Four layers surrounding the anther locule, epidermis, endothecium, middle layer and tapetum.
Spike 2.8 cm	PMC enter in meiosis. Tapetum layer is prominent.
Spike 3.5 cm	Miscrospore release from the tetrad occurred. Tapetum vacuolated.
Spike 4.9 cm	Microspores release. Middle layer is undergoing crushing. The prominent tapetum layer is starting to degenerate.
Spike 5.7 cm	Microspores become vacuolated. Tapetum degenerating.
Stage LFE1	Mitosis I occurs through these stages. Tapetum degenerating, but still present.
Stage LFE2	
Stage LFE3	Binuclear pollen. Mitosis II occurs.
Stage LFE4	Trinuclear pollen. Septum breakage.

Table.3.9 Anther and pollen development description corresponding to samples collected at different spike sizes and the last flag extension stages (Fig.3.18).

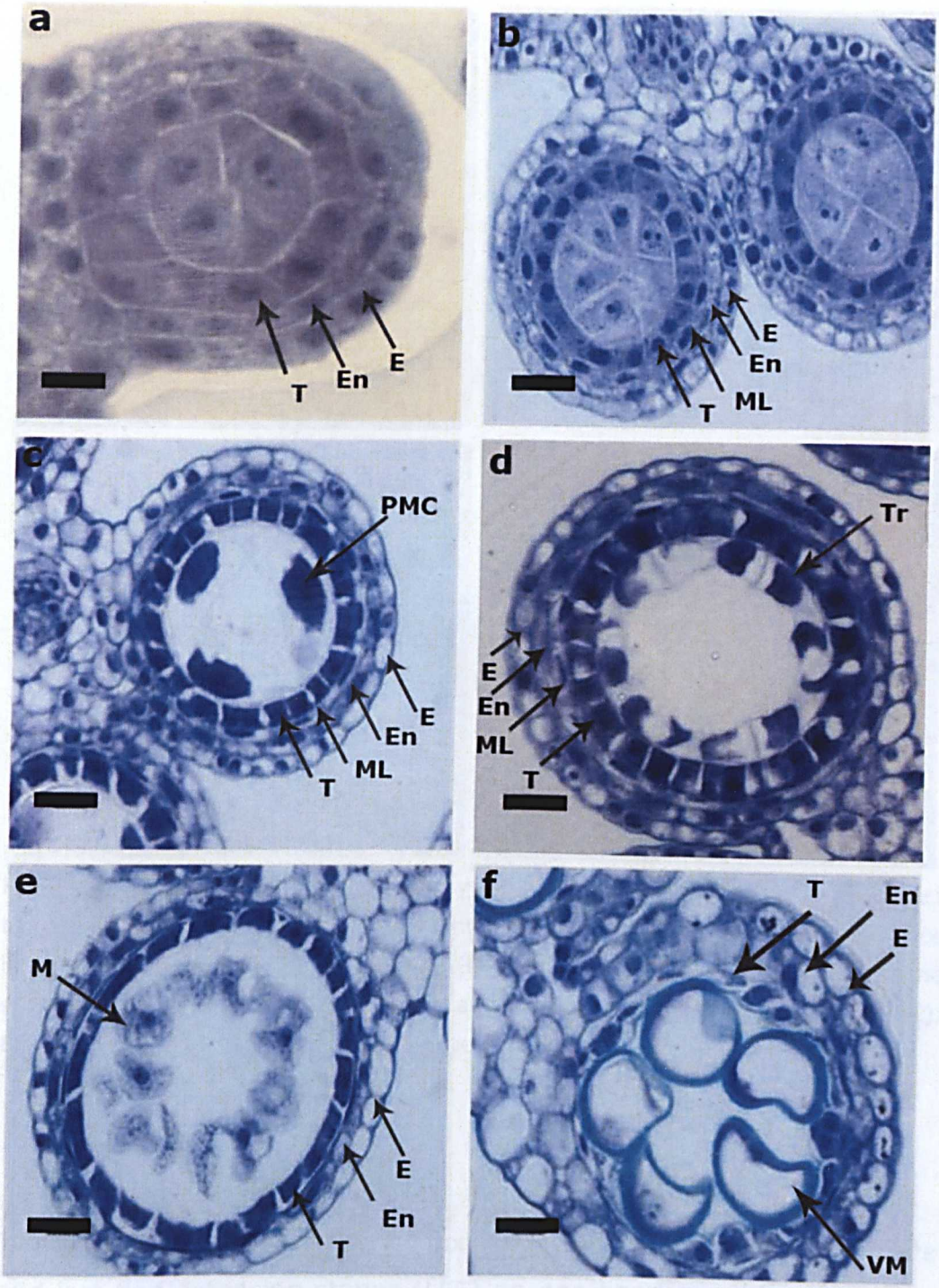

Fig.3.18 Transverse sections (Toluidine blue stained) through barley anthers from spike size 0.6- 5.7 cm (a-f). a) Primary sporogenous cells (0.6 cm). Three layers surrounding the anther locule. b) Secondary sporogenous cells to Pollen Mother Cells (1.7 cm). Four layers surrounding the anther. c) PMC enter in meiosis (2.8 cm). Tapetum layer is prominent. d) Miscrospore release from the tetrad occurred (3.5 cm). Tapetum is becoming vacuolated. e) Free microspores (4.9 cm). Middle layer is undergoing crushing. The prominent Tapetum layer is starting to degenerate. f) Microspores become vacuolated (5.7 cm). Tapetum degenerating. Bars: 40 µm.

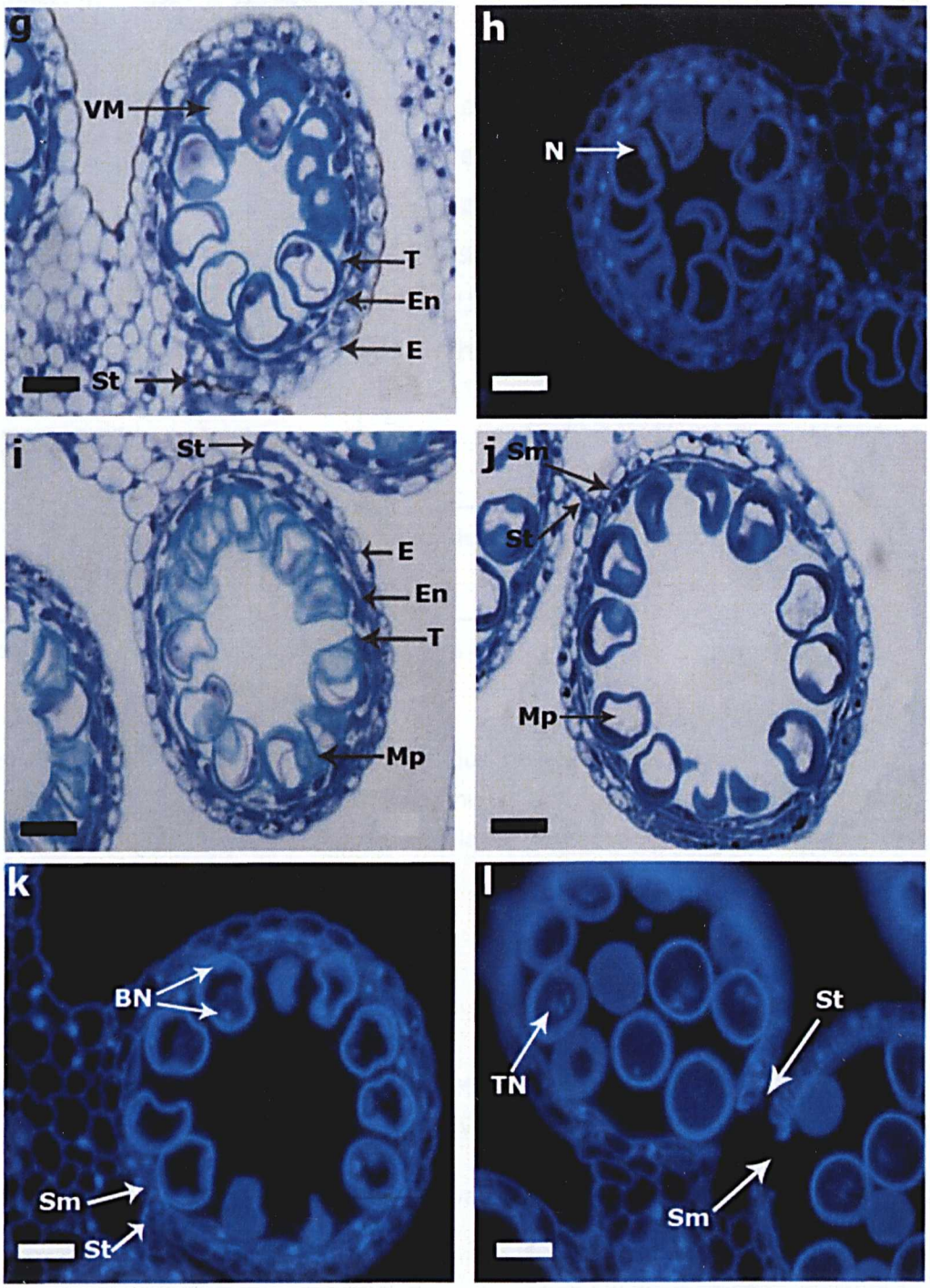

Fig.3.18 continued. Transverse section through barley anthers from last flag extension stages, LFE1-4 (g-l). g-i) Mitosis I occurs through these stages. Tapetum is degenerating, but still present. j-k) Binuclear pollen. Mitosis II occurs. l) Trinuclear pollen. Septum breakage. E, epidermis; En, endothecium ; ML, middle layer; T, tapetum; VM, vacuolated microspores; Sm, septum; St, stomium ; N, nucleus; M, microspores; BN, binuclear cells; TN, trinuclear cells; PMC, pollen mother cells; Tr, tetrads. Bars= 40um. (toluidine blue: g, i and j; DAPI: h, k and l).

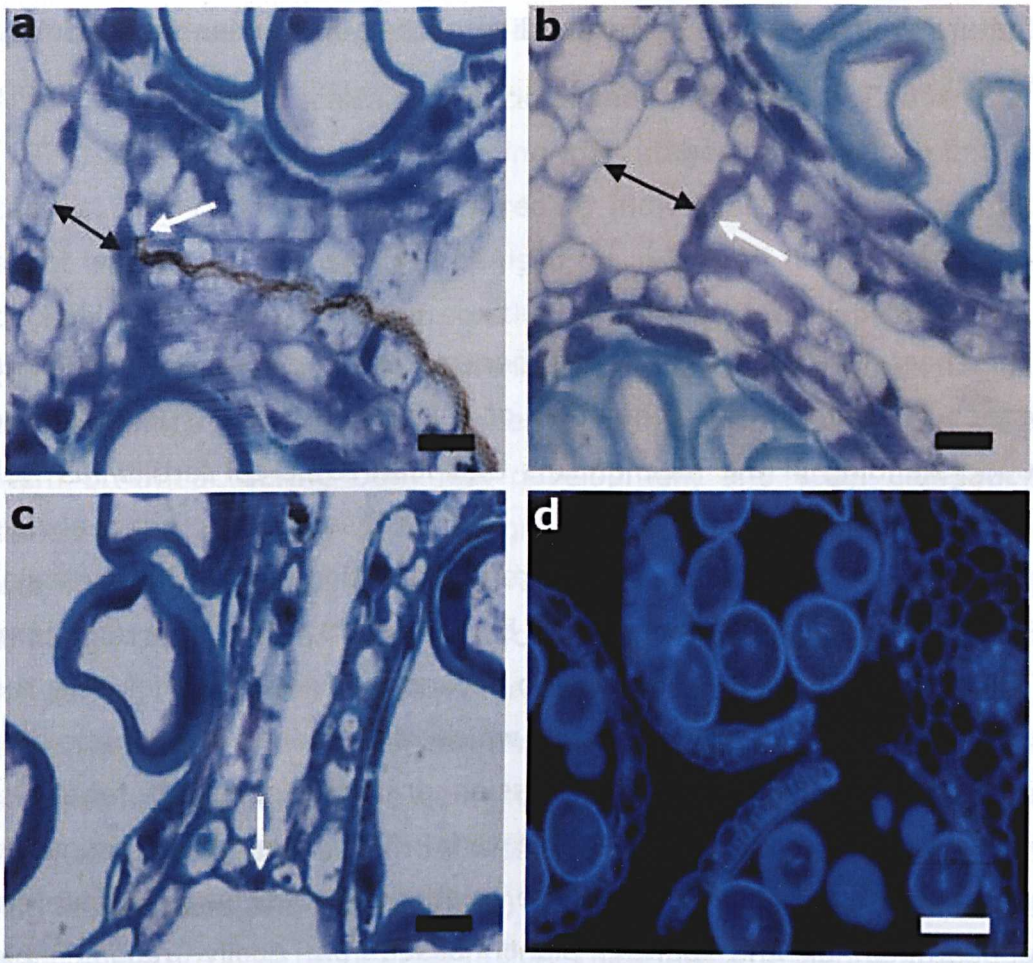

Fig.3.19 Transverse section through barley anthers at last flag extension stages, LFE1 to LFE4. Closer view of the stomium intercellular space revealed that this space increased in size closer to dehiscence (black arrows, a and b). In addition, the stomium became thinner before breaking and releasing the pollen (white arrows, a-c). Bars: a-c= 10um; d= 30um. (toluidine blue: a, b and c; DAPI: d).

The correlation between barley external development and spike size and last flag extension stages (LFE) on one hand, combined with the relationship between spike size/LFE stages and anther and pollen development on the other, confirms the ability to predict anther and pollen development by observations of external development. In addition, the four latest developmental stages introduced provided greater clarification of Zadok description of barley external development. The ability to predict spike size and developmental

stage indicate that this approach provides a reliable key vegetative feature which predicts corresponding anther and pollen development stages.

3.4 Discussion.

The characterization of barley anther and pollen development and the genes involved in the regulation of this process are crucial for the understanding of the mechanisms that lead to cereal fertility as well as hybrid seeds production. This characterisation has been always restricted by the difficulties of material collection due to the particular inflorescence development that in barley occurs within a pseudostem. This makes it extremely difficult to accurately select material from the pollen and anther development, which is essential for genetic and molecular studies such as expression or tissue specificity analysis, without wasting valuable plant material. Therefore, an investigation was undertaken to determine the relationship between the external appearance of the barley plant, based on easily recognisable developmental staging, and the events occurring within the anther.

In order to be able to establish a relationship between external plant development and the pollen regulation network, a clear external morphological staging is needed. There have been various proposals to divide the life cycle of cereal plants into periods and stages. Landes and Porter (1989) identified two principal ways to describe cereal development: one based on the 'exterior' morphology (visible to the naked eye without dissection) and the other based on the 'interior' morphology of the shoot apical meristem. Internal scales have greater potential for precision. However, 'interior morphology'- based methods such as these have the disadvantage of requiring dissection and microscopy, which are time-consuming and destructive. Furthermore, for most purposes, external classification is sufficient, and if the characteristics used for identification are chosen so that classification

can be visual, or tactile (using fingertips), the classification of tillers is both less time-consuming and non-destructive.

Among the external scales, the decimal code proposed by Zadok et al. (1974) is very useful for recording the stages of development of cereals. The code originally referred to individual plants, or a main shoot with tillers, but can also be used for individual tillers. Beside the decimal code approach, an interesting system was developed by Haun (1973). This involves a numerical expression of morphological development, based on the number of leaves produced on the main stem of wheat during both leaf development and stem elongation periods. This scale has a high degree of precision for describing the leaf-insertion rate during the leaf development period. Furthermore, although the scale was developed for wheat, it can be used as a guide for early management decisions for crops of perennial forage grasses, especially grazing management (Frank, 1996). However, during the stem-elongation period, the Haun scale can be difficult to use if leaves start to senesce and become difficult to count. For stages above the flag leaf, Landes and Porter (1989) stated that the descriptions in the Haun scale are of little general utility. Therefore, the Zadok scale has become the most widely used system for developmental staging in cereals, with or without various modifications. For instance, Tottman and Broad (1987) redefined some descriptive phases of cereals such as wheat, barley and oat plants based on the Zadok scale. In addition, Lancashire et al. (1991) presented a universal development scale (also called the BBCH scale), designed to suit most agricultural crops and weeds, largely based on the Zadok decimal code for cereals. Developmentally similar morphological stages of different crops are given the same codes. The aim was to present a general framework within which more specific scales for individual crops could be constructed. To define this general code, Lancashire et al. (1991) made some modifications to the Zadok scale; the major ones were for late maturity stages.

Examples of this staging adaptation can also be seen in the recent literature. Gustavsson et al. (2011) adapted the universal decimal

code for grasses to the perennial forage grasses based upon the Lancashire (1991) modifications, introducing changes that facilitated the identification of constant stages; this staging scale was then applicable for important managerial decisions. Significant similarities were found between the Gustavsson decimal code and the scale presented in Table.3.5 modified for the barley spring cultivar Optic. However, whereas the current barley scale maintained the stages 31 to 37 as explained in the original Zadok code, Gustavsson ignored 37 due to the difficulties in identifying this stage in the perennial forage grasses. He continued to count each new node appearance regardless of flag leaf development, until 8 nodes, or stage 38. In this current analysis of barley development, stage 37 was considered a transition stage between the nodes staging period (stages 31-37) and the new stages defined in Table.3.5 (LFE) that describe the last stages before anthesis. LFE staging in barley is very similar to the scale presented by Gustavsson (2011) for the stages following stage 38. However, whereas Gustavsson used the position of the spike within the pseudostem and some characteristics from the original decimal scale, the LFE scale is based upon the spike position and the elongation of the last flag sheath (Table3.5; Fig.3.11). From stage LFE1 to LFE4, spikes move progressively upwards from the previous sheath, towards the last flag sheath (Fig.3.12; Section.3.3.1). Barley last flag extension stages (LFE1-4), as a continuation of the previous stages (31-37), were validated by analysis of the spike appearance as well as the anther and the pistil development score (Fig.3.12) (Waddington et al., 1986). These analyses showed that last flag extension stages and their characteristics, were related to the spike formation and reproductive organs development (Fig.3.12-13; Table.3.5), making these stages key collection points for further experiments.

The direct relationship between stem growth and the development of the spike has been widely suggested (Kitchen and Rasmussen, 1983; Kirby et al., 1988). Kirby (1988) showed a relationship between thermal time in combination to the wheat external stages, before last flag appearance to anthesis, and the spike size, showing the increase

of the spike size along with the successive internodes elongation. However, the relationship between external stages and spike size was vague, and not very precise. In addition, the duration of the stem elongation was also related to the number of fertile florets and therefore to the reproductive organs development; stating that longer stem elongation periods produced a higher number of fertile flowers (Miralles et al., 2000). Moreover, three important events in crop development: the achievement of the maximum number of primordia (Barley and rye; Fig.3.2) on the main shoot (Kirby and Appleyard, 1984a), the beginning of the upward movement of the main stem apex (stem internode extension), and the rapid decline in number of leaving tillers, appear to be closed linked (Baker and Gallagher, 1983). The first and second points were further confirmed by Arduini et al. (2010). Arduini et al. (2010) showed that the stage of maximum primordia (leaf and spikelet primordia have been all initiated) coincides with the starting of the elongation stage (Zadok stages 30-31) for three different barley varieties, independently of the sowing date. Therefore, the synchrony observed in barley to reach the stage of maximum primordial (Zadok stage 30, Fig.3.2), the moment at which spike growth is due to commence, correlating with the pseudostem elongation, suggests that under controlled conditions (photoperiod and temperature) spike growth can be predicted with a high degree of accuracy.

The spike size prediction shown in section.3.3.2 was conducted under controlled conditions in order to avoid significant variations in plants growth conditions (Section.3.2.1). These results show a clear relationship between spike size and external stages (Fig.3.17; Table.3.7-8). Furthermore, the spike growth pattern (Fig.3.14) confirmed that spike elongation occurs in parallel to stem elongation (Reynolds et al, 2009; Kirby et al., 1988), showing the same sinusoidal shape shown by Reynolds et al. (2009) (Fig.3.20). Investigation conducted to relate pseudostem/internode growth rates and spike size did not show a clear relationship (Fig.3.9). This was due

to the high variability observed in internode elongation between two tillers at the same external stage.

Spike growth lasted until stage approximately LFE2 (Fig.3.14), from this point no significant changes were observed in relation to the spike size, and therefore, no developmental features could be attributed to spike size changes. Due to these circumstances, the spike size prediction scale was restricted to stages identified by the node and internodes elongation, including stage 37 and the sub-stages 33.5 and 34.5 that helped to gain accuracy in spike size prediction. This prediction, although not 100% accurate, was sufficient to provide a key to enable the collection of the expected spike size by simple external observation (Fig.3.17).

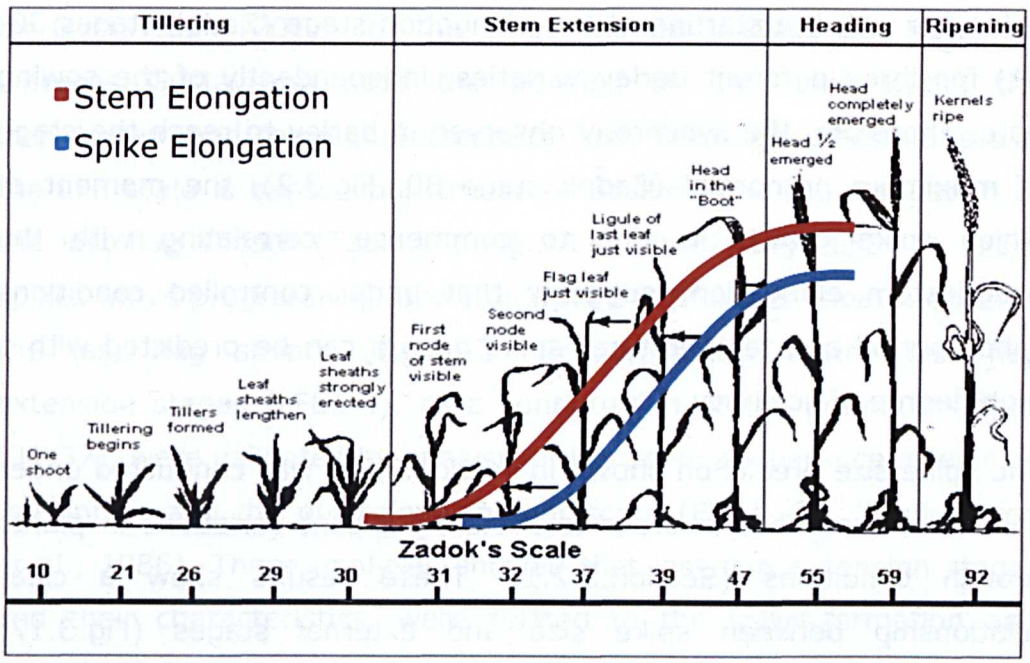

Fig.3.20 Representation of the stem and spike elongation. Stem and spike showed a parallel elongation phase that started early in the Zadok elongation stage and finished at booting stages (Reynolds et al., 2009).

The anther sectioning analysis (Section.3.3.3) confirmed the relationship between spike size and the events occurring within the anthers (anthers analysed were restricted to florets collected from the middle region of the spikes). This relationship, therefore, allowed the prediction of anther and pollen development stages based upon spike size that can be determined by the external appearance of the plant. Moreover, last flag extension stages were also confirmed as valid for predicting the anther and pollen development as a clear sequence of stages were observed in samples LFE1 to LFE4. The transition from spike size prediction stages (31-37) and the last flag extension stage, LFE1-LFE4 (Table.3.5), was observed in between 37 and LFE1, where both anther samples showed vacuolated pollen and the start of tapetal degeneration (Fig3.18f-g), these stages can therefore be considered as a transition point between stages 31-37 and LFE1-4 (Table.3.7).

Therefore, the prediction of anther and pollen development has been facilitated by the method described in this chapter. This approach allows the accurate staging of reproductive tissues based upon vegetative growth characteristics. Thus, permitting a high degree of accuracy in sample collection, which is critical for genetic, molecular and microscopy analysis such as gene characterization, expression analysis or tissue expression specificity. In addition, the combination of spike size prediction and the last flag extension stages was critical for an accurate continued staging scale.

CHAPTER 4.

4. Barley transformation.

4.1 Introduction.

Over the past century, improvement of cereals has been mostly achieved by conventional breeding. However, due to the ever-growing world population, limited availability of water, increasingly exhausted fossil energy resources, and the changing climatic conditions, new technologies are urgently required to cope with future challenges. Since the mid 1990s, genetic engineering of cereals has provided a novel field of opportunities for faster and more directed modifications or introductions of agronomical useful traits. While the first successful genetic transformation events in cereals species were based on direct gene transfer, which was associated with a number of disadvantages such as the detection of gene expression by *Agrobacterium* attached to inoculated tissues and not from the plantlets regenerated from them (Potrykus et al., 1990). Potrykus et al (1990) concluded that there was no unequivocal evidence for stable transformation of monocotyledons with *Agrobacterium.* Appropriate evidence for such transformation would be a demonstration of random integration of transgenes into chromosomes in a number of independent transformants, with Mendelian segregation of transgenes in the progeny. The pioneering study of Hiei et al. (1994) on *Agrobacterium*-mediated transformation of rice represents a milestone in cereal *Agrobacterium* mediated transformation. They presented evidence based on molecular and genetic studies of a large number of transgenic rice plants and the analysis of T-DNA junctions in rice. This study (Hie et al., 1994) and that of Chan *et al.* (1993) have clearly demonstrated the stable integration of foreign DNA in rice chromosomes mediated by *Agrobacterium tumefaciens,* as well as the

Mendelian transmission of the DNA to the progeny. They also showed that co-cultivation of callus, derived from scutella, with *A. tumefaciens* can produce rice transformants with efficiency similar to that of transformation in dicotyledons. Ishida et al. (1996) published the first protocol for the generation of transgenic maize, which also relied on *Agrobacterium*. In the following year, similar protocols for all the major cereal crops including barley (Tingay et al., 1997) and wheat (Cheng et al., 1997) were published.

The first fertile transgenic barley plants were produced by particle bombardment of immature embryos (Wan et al., 1994). This was followed by reports of *Agrobacterium*-mediated transformation of barley immature embryos. In some recent reports of *Agrobacterium*-mediated barley transformation, efficiencies of 5.4% were reported by Lange et al., 2007, while Shrawat et al (2007) obtained frequencies ranging from 2.6 up to 6.7%. Matthews et al., (2001) described barley transformation frequencies in the range of 2-12% and Murray et al (2004), obtained average efficiencies between 4.4-9.2%. A more recent report describes a transformation efficiency of 21.7%, averaged across two experiments starting with a total of 600 immature embryos (Hensel et al., 2008). However, this last report has been very difficult to reproduce in others laboratories (Harwood et al., 2008).

The cereals have generally proven more difficult to transform than dicot species. A prerequisite for efficient transformation, using either biolistic or *Agrobacterium* for gene delivery, is the ability to regenerate fertile plants efficiently from tissue culture (Kerry et al., 2001). It has been shown that plant transformation efficiencies have the potential to be as high as 40% if all the callus lines, produced by particle bombardment, regenerated into independently transformed plants (Harwood et al., 2002). However, there are many factors affecting cereal transformation efficiency (Appendix 15). Most commonly, these factors are media composition, *Agrobacterium* inoculation procedure and strain, selective agents, or explant type and size. For instance, factors such as pre-culture of immature embryos, co-cultivation period

and temperature, pH of the medium, sonication and vacuum infiltration were studied by Shrawat et al., 2007. This study determined that the increase in the pre-culture length from 1 to 3 days resulted in a significant decrease in the number of explants showing GUS and GFP expression and therefore in transgenic plants. No GUS expression was detected in 5-day pre-cultured immature embryos. Co-cultivation duration for 2–3 days was considered preferable for transformation, with 3 days co-cultivation in the dark at 25ºC the most efficient, as at 25ºC plant cell appeared more susceptible to infection and T-DNA insertion into immature embryos of barley. In addition, lower pH (5.2-5.8) during the co-cultivation stage and the use of sonication and vacuum infiltration have shown an increase in the number of transgenic plants; sometimes when vacuum infiltration was conducted for 15 minutes, the frequency of plants showing GFP expression increased from 28% to 52.8% (Shrawat et al., 2007). Moreover, Hensel et al., 2008, examined embryo treatment, addition of acetoseryngone and L-cysteine and *Agrobacterium* strain on the frequency of transformation. The anti-oxidative property of L-cysteine attenuated tissue necrosis and cell death upon inoculation of immature embryos with *Agrobacteria* (800 mg/L-1). Besides a markedly reduced browning of the embryo's surface, this treatment resulted in a more than threefold increased frequency of transgenic plant formation.

A further substantial improvement was achieved by the use of 500 µM acetosyringone in the co-cultivation medium (Hensel et al., 2008). The application of this substance, which is well known to trigger the transformation activity of *Agrobacterium tumefaciens*, did eventually lead to a transformation efficiency of 86.7%. In addition, the benefits of including increased levels of copper in culture media, was first noticed by Murashige et al., (1962). Improved plant regeneration in using increased levels of copper has also been reported (Dahleen et al., 1995 and Joshi et al., 2007). Optimal copper levels vary between cultivars (Dahleen, 1995) and also the timing of copper addition is critical. Copper (5µM) addition to callus induction and transition

medium proved to be highly beneficial for callus formation which not only grew faster, but then appeared more embryogenic (Harwood et al., 2008). In addition, the same study revealed that an average of 53 shoots per embryo were obtained when copper was added, which was twice the number of shoots than generated by non-copper treated embryos.

The composition of the media used, both for callus initiation and shoot regeneration, had a significant impact on the success of embryo culture in all cereals species where this has been investigated. Most studies have utilized basal MS media (Murashige and Skoog, 1962) with or without supplements, but other basal media types have also been tested including N6 (Chu et al., 1975), B5 (Gamborg and Wetter, 1975), CC (Potrykus et al., 1979), Blaydes-B (Blaydes, 1966), Kao's media (Kao, 1977), SH (Shenk and Hildebrandt, 1972) and Norstog media (Norstog, 1973). Studies that have compared media types generally found MS media to yield the most embryogenic cultures and the greatest subsequent plant regeneration (Hanzel et al., 1985; Luhrs and Lorz, 1987; Bregitzer, 1992).

Other components have also been tested. Sucrose and maltose have been compared as a carbon source in media for barley embryogenesis. Rates of somatic embryogenesis were higher on media containing maltose compared to sucrose, however this study was not extended to shoot regeneration (Walmsley et al., 1995). King and Kasha (1994) found that the media containing 6% (w/v) maltose yielded the most barley somatic embryos, while few were formed on the standard 3% (w/v) sucrose. In addition, the role of growth regulators in cereal tissue culture proved to be essential. In general, auxins, usually 2,4-dichlorophenoxyacetic acid (2,4-D) in the range of 1-3 mg/l (4-14μM), are essential for the establishment of embryogenic callus from cereal embryos, while shoot regeneration from this callus is most successful on media either devoid or containing very low levels of 2,4-D (Bhaskaran and Smith, 1990). 2,4-D, dicamba and picloran were compared as auxin sources for barley embryo culture (Castillo et al., 1998). Dicamba was the preferred auxin source, picloran the poorest,

both for callus formation and plant regeneration. Moreover, the addition of cytokinins (BAP, 0.001mg/l) has been reported to promote germination and development of somatic embryos (Sharma et al., 2005).

The effects of minor components in the culture media have also being investigated in a number of cereal species. Coconut milk (5-10%) and casein hydrosylate (0.01-0.5%) were tested in the culture of immature rye embryos, but neither was found to have any effect (Lu et al., 1984). In barley culture, the addition of amino acids suppressed callus development, but supplementing the medium with casein hydrosylate (1g/l) increased the amount of embryogenic callus (Lührs and Lörz, 1987). Thiamine (1mg/l) and myo-insitol (0.25g/l) were also beneficial in callus embryogenesis (Lührs and Lörz, 1987).

The efficiency of barley transformation also relies on the *Agrobacterium* strain or the binary vector used. Protocols for cereal transformation generally rely on the use of hypervirulent *Agrobacterium* strain such as EHA101 and EHA105 in maize (Hood et al., 1986), AGL-0 and AGL-1 in barley and wheat (Tingay et al., 1997; Hensel et al., 2008; Matthews et al., 2001; Wu et al., 2003; Harwood et al., 2008), as well as hyper-virulent derivatives of LBA4404 in maize, barley and wheat (Kumlehn et al., 2006; Hensel et al., 2008; Coronado et al., 2005; Khanna et al., 2003). In addition, particular attention is needed to the binary vectors used for cereals transformation. Many binary vectors that had been developed for dicots species are not suitable for cereals, mainly due to inappropriate promoters and selectable marker genes (Himmelbach et al., 2007). Moreover, an exceedingly high stability of the plasmids in *Agrobacterium* appears to be vital so as to provide an adequate proportion of transformation competent bacteria throughout co-cultivation, in which there are no selective conditions in terms of the bacteria resistance mediated by the binary vector (Himmelbach et al., 2007).

In addition, the development of a standard protocol for cereal tissue transformation has been elusive, mainly due to large amounts of

variation observed in regeneration capacity due to genotype, even within species. Cultivar differences in rates of somatic embryogenesis and plant regeneration were observed among four rye cultivars cultured from young leaves (Linacero and Vazquez, 1986). Moreover, Bebeli et al (1988) cultured five sister lines of rye from immature embryos, and found significant differences between the lines in their ability to form callus and to regenerate shoots from callus. Genotype has also being found to affect both callus formation and plant regeneration from immature embryos in the other cereal species, in particular the economically important cereals such as wheat (Sears and Deckard, 1982; Machii et al., 1998), barley (Hanzel et al., 1985; Castillo et al., 1998; Baillie et al., 1993b), oats (Gana et al., 1995) and triticale (Sharma et al., 1980). To date, Golden Promise has been well-known for its high tissue culture ability, and hence this genotype has been widely used in barley tissue transformation (Wan and Lemaux, 1994; Tingay *et al.*, 1997; Holme *et al.*, 2006; Kumlehn *et al.*, 2006).

A new transformation-regeneration protocol was used here based upon Harwood et al., (2008). This protocol combines regeneration with a very simple transformation procedure that does not require any special embryo treatment to develop a robust straightforward and highly efficient method. This method has previously yielded large numbers of independently transformed barley plants with average transformation efficiency of 25% (Harwood et al., 2008). Two different experiments were conducted; the first one was to test the regeneration capacity and timescale of non-inoculated immature after tissue culture. The second experiment was conducted to test the transformation efficiency as well as testing different aspects within the protocol, such as regeneration of inoculated immature embryos, or the capability to the callus regenerate after inoculation.

4.2 Materials and methods.

4.2.1 Plant growth.

Donor plants of the spring barley cultivar, Golden Promise (University of Nottingham), were grown for these experiments under controlled environment conditions (Section.2.1). Spraying these plants was not permitted, therefore, the growing condition were maintained as clean as possible in a growth room exclusively used for this experiment.

4.2.2 Culture media preparation.

Three different basic plant tissue culture media, based on Harwood et al (2008), were used during the regeneration process: Callus induction, transition and regeneration media (Appendix.5).

4.2.3 Immature embryo isolation.

Barley, Golden promise variety, was grown as specified in section.4.2.1 until anthesis had occurred and grains were filling. The immature seeds were removed from the spike when the immature embryos were 1.5-2 mm in diameter (Fig.4.1). At this stage, spikes were already fully emerged and the endosperm of the immature seeds was still soft and quite liquid in appearance. Floury endosperm meant that the embryo was too old. Immature seeds were collected and had their awns broken off without damaging the seed coat. Sterilization was carried out by washing in 70% (v/v) ethanol for 30 seconds followed by three washes in sterile distilled water. Afterwards, seeds were washed in 50% (v/v) sodium hypochlorite solution for five minutes. Finally, seeds were rinsed with sterile distilled water four times, and then used for immature embryo isolation. The immature

embryos were exposed using fine forceps and the embryonic axis removed in order to avoid the growth of roots or shoots. After isolation, the embryos were placed on Callus Induction plates scutellum side up. From here, embryos were kept for 24 hours in the dark at 22-23ºC to induce callus formation. After this, embryos were either transferred to new Callus Induction plates without antibiotic for regeneration experiments (Section.4.24), or inoculated with *Agrobacterium* carrying a specifically designed construct for barley transformation experiment (Section.4.2.5).

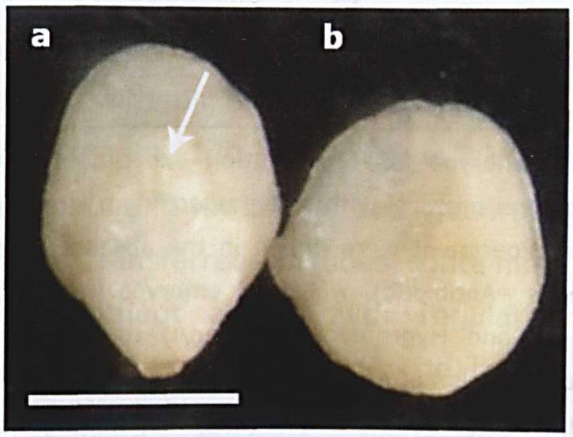

Fig.4.1 Immature Embryos, 1.5-2 mm diameter.

a) Immature embryo with embryonic axis intact (arrow).

b) Immature embryo with axis removed.

Scale bar 1.5 mm.

4.2.4 Regeneration protocol.

The barley regeneration protocol was carried out using immature embryos extracted from the barley cultivar Golden Promise (Section.4.2.3) according to Harwood et al (2008). This protocol was followed step by step including pre-culture and co-culture step, however initially no *Agrobacterium* inoculation was performed and

therefore no antibiotic was added to the media. The duration of barley regeneration from immature embryos to mature seeds was studied. Two experiments were set up, 091109 and 101109ER (Table.4.1). In addition, the Hygromycin selection was tested using two groups of embryos that went through the regeneration protocol (Hygromycin, 50 mg/l, and Timentin, 160 mg/l) to determine their efficiency of selection.

Experiment	Callus - Antibiotic	Callus + Antibiotic
091109ER	12	10
101109ER	12	10

Table.4.1 Immature embryos for regeneration experiment. These embryos went through the regeneration protocol with no *Agrobacterium* inoculation (Section.4.2.4). Twelve embryo per experiment were grown in the absence of antibiotic during the different steps (Callus –Antibiotic), whilst 10 embryos were grown with antibiotics (Timentin, 160 mg/l, and Hygromycin, 50 mg/l) to confirm antibiotic selection efficiency against regeneration of non transformed embryos (Callus +Antibiotic).

Immature embryos collected from immature seeds for the regeneration experiment were plated scutellum side up on Callus Induction agar without antibiotics and incubated overnight in the dark at 23-24°C. After 24 hours, embryos were gently removed and transferred to a fresh Callus Induction (Appendix.5) plates removing any excess of agar, scutellum side down. Plates were sealed with micropore surgical tape and incubated at 23-24°C for 3 days in the dark (Co-cultivation stage). After the co-cultivation stage, the embryos were transferred to fresh Callus Induction plates without antibiotics to start the Selection stage. These embryos were kept at 23-24°C in the dark. The Selection stage lasted for six weeks (Selection 1, 2 and 3, two weeks each), changing the embryo-derived

callus to fresh callus induction media without antibiotic every two weeks. After six weeks in the Selection stage, embryo derived callus were transferred to Transition medium without antibiotics (Appendix.5). Individual calli were divided into pieces containing individual embryogenic callus (Hiei et al., 2008). Callus pieces, generated from the same main embryo derived callus were kept together and labelled in order to track their origin. At this stage it was necessary to reduce the number of callus per plate since these grew rapidly. Plates were kept under low light conditions (75 $\mu mol/m^2s$) at 22-24 °C. In order to achieve this, plates were covered with a thin sheet of white paper. During the two weeks on Transition medium callus produced green areas and small shoots.

Finally, after two weeks in Transition, callus were transferred to Regeneration plates without antibiotics (Appendix.5). Petri dishes were placed under full light (140 $\mu mol/m^2s$) at 22-24 °C. At this stage, callus generated shoots and roots. Plantlets generating shoots 2-3 cm long and roots were transferred to tubes containing 12 ml of Callus Induction medium without any growth regulators (Dicamba) or antibiotics (Appendix.5). Plants reaching the top of the tube were transferred to soil (Levington C2). Plants were handled very gently to avoid damaging the root system and all tissue culture medium was washed from the roots prior to transfer to soil. For these experiments, plants were grown in a glasshouse with a 16/8 hours photoperiod and a temperature of 20-23°C. Once in soil, plants were covered with small plastics bags with holes at the top as individual propagators for a few days to maintain humidity until the plants were well established in soil. Bags were opened after 1-2 weeks, however plants often remained inside the bag for another week. After opening the bag, plants remained in the same pot until an upright appearance was observed, at this stage, plants were transferred to 5 litre pots (Levington C2). The regeneration efficiency was defined as the number of independent plants obtained in relation to the number of immature embryos used.

4.2.5 Transformation efficiency.

Various experiments were carried out to study the plant regeneration frequency after *Agrobacterium* mediated transformation (Table.4.2). Immature embryos were extracted from barley plants (Section.4.2.3), Golden Promise, grown as explained in section.4.2.1. Moreover, the efficiency of transformation/regeneration and the formation of escapes were studied. The transformation and regeneration protocol developed by Wendy Harwood (John Innes Centre) was used, this time antibiotics the antibiotic (Hygromycin, 50 mg/l, and Timentin, 160 mg/l) were added to all of the culture media from Selection 1 (Section.4.2.4; Apendixe.4.1). 100-120 embryos were inoculated per experiment using constructs that contain Hygromycin as the selectable marker (Section.4.2.5.1; Table.4.2).

The efficiency of plant transformation was calculated based upon Harwood's protocol specification (Harwood et al., 2009). This protocol defines the efficiency as the number of independent transformed plants as a percentage of the original number of immature embryos treated. Therefore, plants were considered as individual transformation event independently of their embryo-derived callus origin.

Moreover, immature embryo *Agrobacterium*-mediated transformation efficiency was checked using the AGL1 + PBI121-GUS expression vector (kindly provided by Dr. Caiyun Yang). This vector contains the *NPTII* gene under the control of the NOS promoter and a *GUS* gene under the control of the CaMV35S promoter (Appendix.6). Embryos were inoculated as described in section.4.2.5.2. After 3 weeks growing in the correspondent selection media, Callus Induction medium (Appendix.5), containing 50 mg/l of Kanamycin and 160 mg/l of Timentin in the dark, at 23-24ºC, the callus derived immature embryos were tested for GUS expression (Section.2.19).

Experiment	pBract207::HvMS1-3 Silencing	pBract214:: AtMY26 Overexpression	pBract214:: HvMS1 Overexpression
200410IET	100		
070510IET	115		
060710IET		100	
010710IET	120		
170910IET	120		
021210IET			120

Table.4.2. Transformation experiments. 100-120 barley immature embryos were inoculated with *Agrobacterium* AGL1 containing three different constructs designed in section.4.2.5.1. These three construct contained Hygromycin as selective marker.

4.2.5.1 Constructs for barley transformation.

Constructs used for this experiment were prepared for *HvMS1* characterization as described in Section.7.2; AGL1:pBract207:: HvMS1-3 silencing and AGL1::pBract214::AtMS1/HvMS1Overexp all carry the Hygromycin as a selection marker (Table.6.2). *Agrobacterium* electroporation and immature embryo inoculation was carried out as described in Sections 2.15 and 4.2.5.2 respectively.

4.2.5.2 Inoculation of immature embryos and regeneration.

Agrobacterium inoculation was conducted on barley immature embryos extracted (Section.4.2.3) and plated onto callus induction plates (Section.4.2.4). After 24 hours on this plate, embryos were inoculated by placing a drop of *Agrobacterium* suspension, containing the appropriated vector (Section.2.18) onto each of the immature

embryos, making sure that all the embryos were covered by the *Agrobacterium* suspension. The plate was then tilted to allow any excess *Agrobacterium* suspension to run off. Immature embryos were then gently removed and transferred to fresh Callus Induction plates removing any excess of agar (no antibiotic was used at these stages), scutellum side down. Plates were sealed with micropore surgical tape and incubated at 23-24°C for 3 days in the dark (Co-cultivation). After co-cultivation, the embryos were transferred to fresh Callus Induction plates containing Hygromycin (50 mg/l) as selective agent and Timentin (160 mg/l) to remove *Agrobacterium* from the cultures, starting the Selection stage. Any excess of agar as well as *Agrobacterium* contamination was removed to avoid *Agrobacterium* overgrowth and embryo damage. Embryos overwhelmed by the *Agrobacterium* growing were rejected for further stages (Fig.4.2). From this point, these embryos went through the regeneration protocol as detailed in section.4.2.4, this time including Hygromycin (50 mg/l) as selective agent and Timentin (160 mg/l) until the regenerated plantlets were transferred to soil.

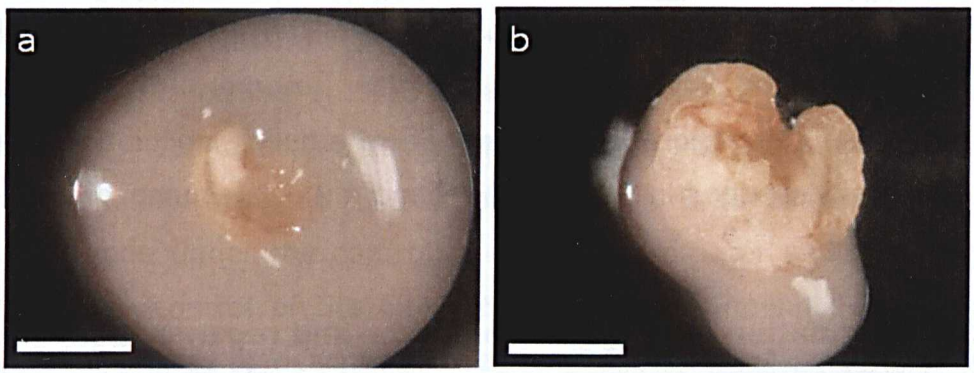

Fig.4.2 *Agrobacterium* inoculated embryos. During the three days of co-culture, the *Agrobacterium* grew, sometimes covering the immature embryos (a) Embryos completely covered by the *Agrobacterium* were discarded. This contamination was more likely to occur when immature embryos were smaller than 1.5-2 cm. b) Example of viable inoculated embryo which was subsequently used for regeneration of transgenic plants. Bars= 1.5 mm.

4.2.5.3 PCR analysis.

Leaf samples were used for DNA extraction (Section.2.9) and testing of transgenic lines. The constructs used for the transformation experiment (Section.4.2.5.1) contain the Hpt gene (Conferring Hygromycin resistance) under the control of CaMV35S promoter. Hygromycin primers were used to confirm the transformation efficiency (Table.4.3) by PCR using Red-Taq (Section.2.3).

Primer	Primers (5´...3´)	Size	Tm
HygromycinF	TACACAGCCATCGGTCCAGA		
HygromycinR	TAGGAGGGCGTGGATATGT	900 bp	61°C

Table.4.3. Hygromycin primers designed to genotype barley plants transformed by pBract constructs.

4.3 Results.

4.3.1 Regeneration experiment.

Handling the embryos proved to be critical for regeneration success, as damaged embryos did not regenerate, or showed a lower level of regeneration. Moreover, identification of the exact stage when embryos could be collected was also conducted (1.5-2 cm). Checking one seed per spike before collection was sufficient to know the approximate size of the embryos along the whole spike. In addition, seed disinfection, as explained in section.4.2.3, was highly efficient. However, excessive sterilisation caused damage to the embryos and loss of regeneration efficiency.

Fig.4.3 shows the different stages needed for plant regeneration from non-inoculated immature embryos. The duration of this process is shown in Fig.4.4. Stages from Pre-culture to the end of Transition stage were constant, taking in total 8 weeks and 4 days. Callus generation was observed 2-3 days after embryos were plated on Callus Induction medium (Selection stage; Fig.4.5). Non-inoculated control callus growing on medium with or without antibiotic did not show any difference in term of callus formation for the first stages, however, different growing patterns were observed from Selection 2 onwards. Non-inoculated control callus growing on Callus Induction medium with antibiotic (Table.4.1) was smaller with a loose or granular appearance that makes them fragile and difficult to handle. Non-inoculated control callus growing without antibiotics grew much bigger and was compact (Fig.4.5).

At transition stage, callus showing green areas (Fig.4.3d, arrow) within the first two weeks were transferred to regeneration medium, where green areas started to regenerate shoots and roots. From the beginning of regeneration stage to the plantlet transference to soil, the duration varied between 4-8 weeks. After being transferred to soil, it took 10-13 weeks for the regenerated plants to produce mature

seeds. Therefore, the total time from immature embryo to mature seed was 24-26 weeks.

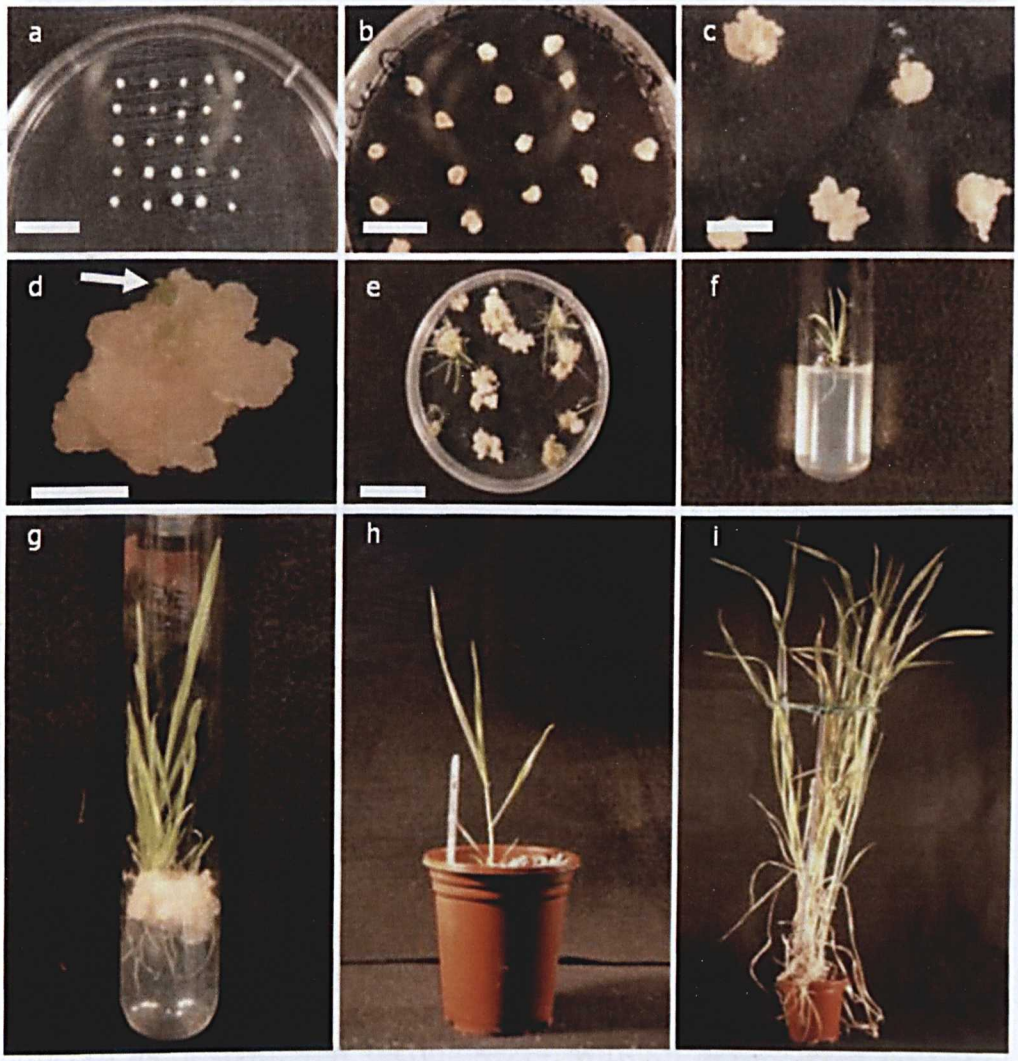

Fig.4.3. Barley regeneration from immature embryos. The regeneration process followed was described in section.4.2.4 and figure.4.4. a) Immature embryos; b) Selection1; c) Selection 3; d) Transition; e) Regeneration; f-g) Shoots and roots regenerated in Callus Induction without dicamba (Appendix.5); h-i) Plants growing in soil. Bars: a, b, d= 10mm; c, e= 20mm.

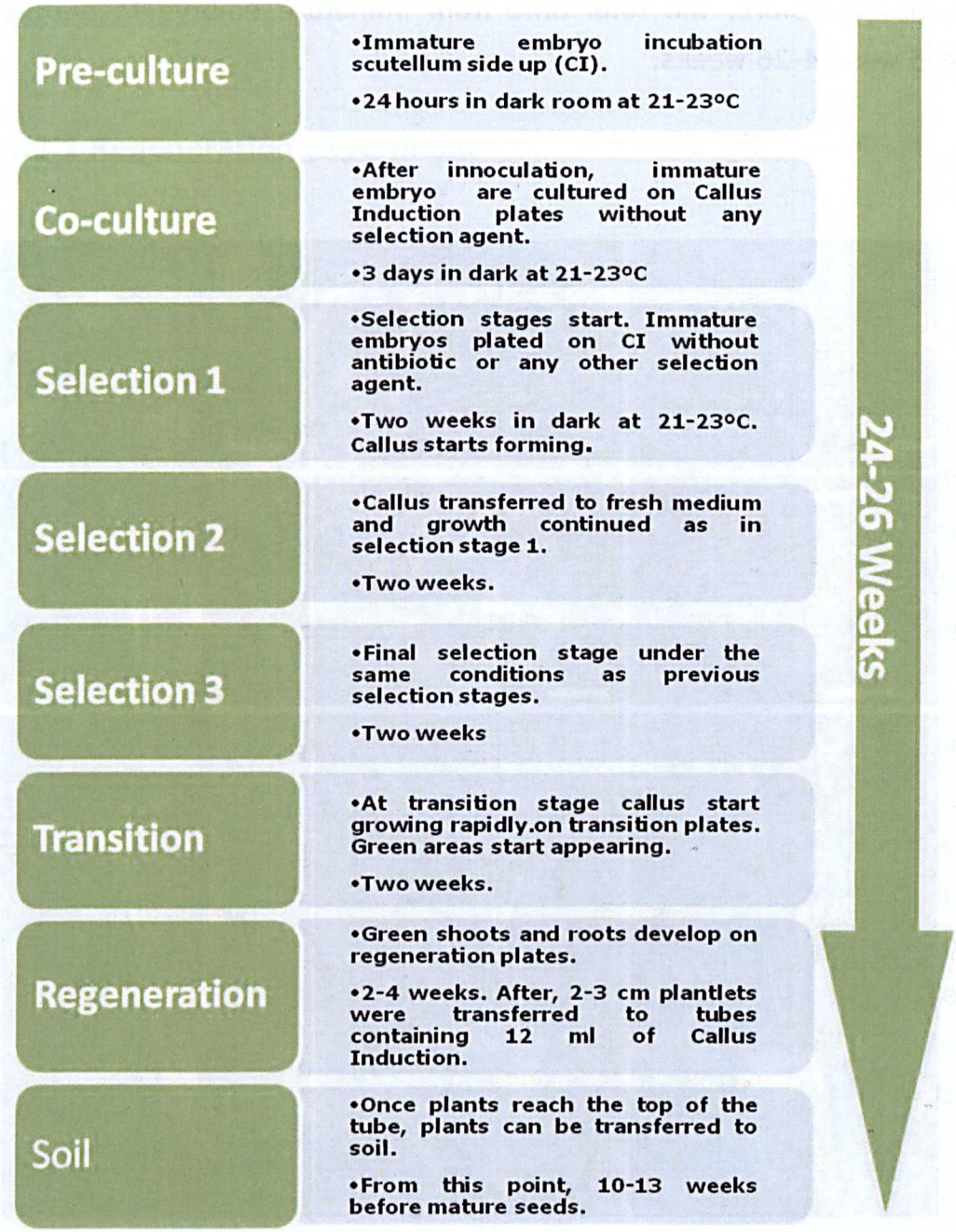

Fig.4.4 Barley regeneration protocol from immature embryos. From pre-culture to the end of transition stage takes 8 weeks and 4 days. From the end of the transition, callus development time varies but 2-4 weeks were needed for most to generate shoots for transfer to glass tubes (Section.4.2.2). Plantlets took around 2-4 weeks to reach the top of the tubes, at which stage plants were transferred to soil. From this point, it took 10-13 weeks for mature seeds to form. In total, the process took 22-26 weeks from immature embryos to plants.

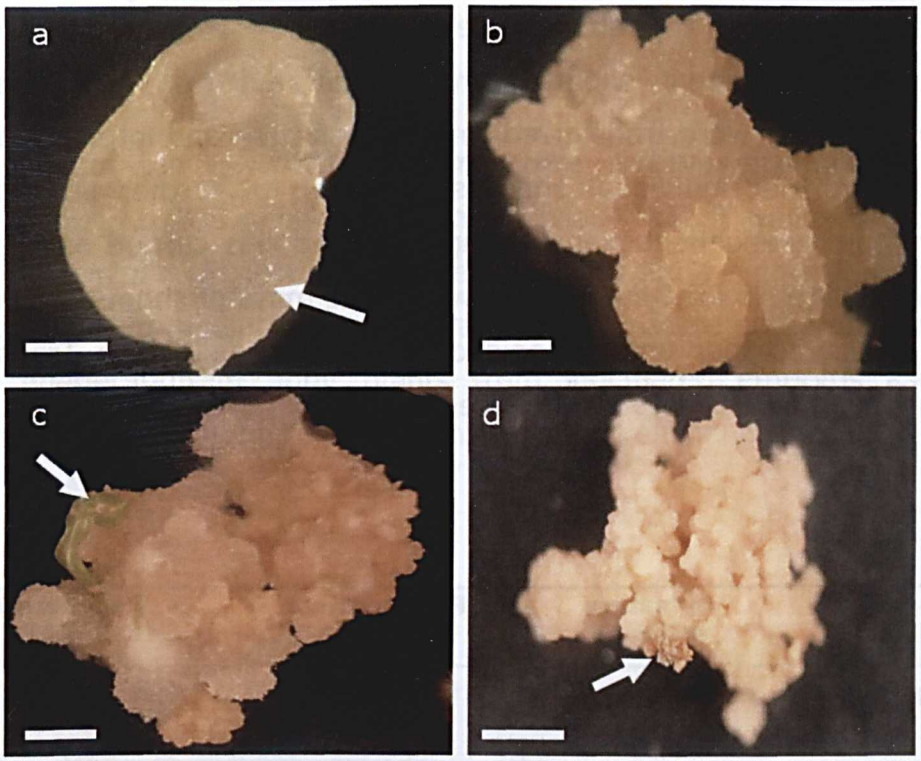

Fig.4.5. Callus formation. a) Callus formation observed 2-3 days after being plated on the Callus Induction plate without antibiotics (arrow). b) Embryo derived callus at Selection 2 stage (No antibiotic), callus size has almost doubled. c) Embryo derived callus at Transition stage without antibiotic showing green shoots (arrow). d) Non-inoculated embryo derived callus at transition growing in presence of Hygromycin. Necrotic areas have appeared (arrow). Bars: a= 1mm; b, c and d= 3mm.

Two experiments were conducted to study the number of plants regenerated per immature embryo. The regeneration protocol was conducted as described in section.4.2.4, without antibiotic selection at any stage. At the end of Selection 3, callus were divided into 2-3 smaller pieces, keeping the callus derived pieces properly labelled to recognise their origin. At transition, most of the callus generated green areas and several embryogenic callus could be identified within each callus-derived piece. At regeneration, every derived callus piece regenerated one or more green shoots, however this number was not consistent or predictable. Table.4.4 shows the results obtained for the two regeneration experiments using 12 individual immature embryos per experiment (Table.4.1). Thirteen and 10 regenerative callus pieces

were obtained at the end of the regeneration stage, respectively. Multiple independent shoots were regenerated from each callus. However, they were transferred to the glass tube and later on to soil without further individual shoot separation. No further attempt to count the independent plants being produced was carried out due to the difficulties in identifying them within the mass of shoots produced. This indicates that embryogenic callus separation at the Transition stage failed to separate each of these potential regenerative units.

	Immature embryos	Regenerative embryos	Regenerative callus pieces
091109IER	12	7	13
101109IER	12	7	10

Table.4.4. Plant regeneration experiment. Twelve immature embryos were used per experiment. Only seven embryo derived callus regenerated green shoots per experiment. After callus division at transition, 13 and 10 regenerative callus pieces were obtained which generated adult plants.

A separate attempt to overcome the problem of embryogenic callus separation was conducted using two embryo derived callus originated on the same conditions as those from the experiments in Table.4.4. Five and six independent plants per each embryo were obtained. A triple separation protocol was performed. Callus were separated at the end of Selection 3 into smaller pieces. No further separation was attempted until clearly identifiable shoots were observed at the Regeneration stage. These independent shoots were then cut and separated and plated again on the same plate to allow regeneration new roots. These individual shoots were transferred to glass tubes (Section.4.2.4) where further shoot separation was conducted when necessary before transferring the individual plantlets to soil.

4.3.2 Transformation results.

Five out of ten of the barley immature embryos inoculated with AGL1::pBI121-GUS showed GUS expression after 3 weeks on callus induction media (Fig.4.6). These results indicated a high frequency of *Agrobacterium* mediated transformation of immature embryos, leaving the regeneration of adult plants from inoculated embryos as the limiting factor to higher overall transformation efficiencies.

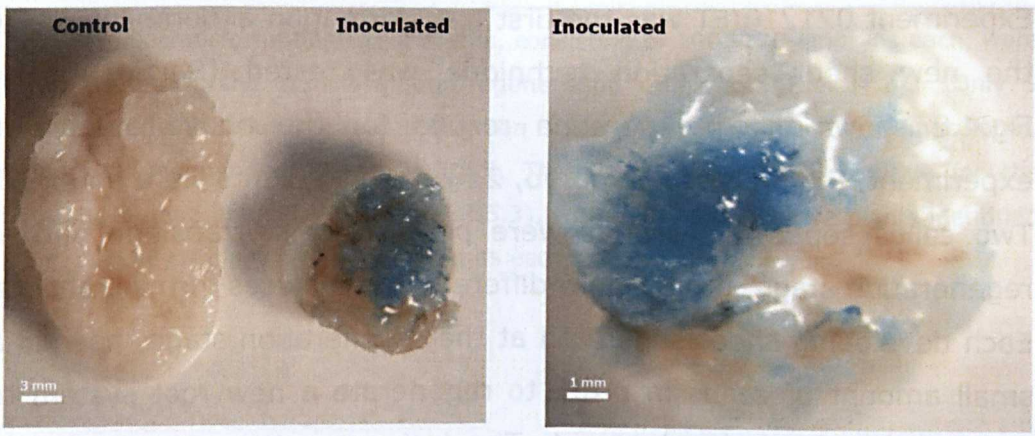

Fig.4.6 Embryo showing GUS expression. Gus expression was observed on embryo derived callus inoculated with AGL1 + PBI121-GUS expression vector. Five out of ten embryos inoculated expressed GUS after 3 weeks on callus induction. The control did not show expression.

The capacity for regeneration of numerous independent shoots by a single non-inoculated immature embryo was high (Section.4.3.1). Table.4.5 shows the results for the transformation/regeneration experiments, where several hundreds of immature embryos were inoculated with *Agrobacterium* carrying 4 different constructs (Table.4.2). A total of 9 embryos regenerated viable shoots out of 675 embryos inoculated with different constructs (Table.4.5). From these 9 embryos, 68 independent shoots were identified, giving a 10 % of efficiency of independent plants from the total number of embryos

used (Section.4.2.5). In addition, these 68 shoots were PCR analysed to confirm the presence of the Hygromycin gene (Fig.4.7) using DNA extracted from leaves (Section.2.2). Sixty-four individual plants contained the Hygromycin gene (94%), confirming the high Hygromycin efficiency of transformation as only 4 out of the 68 individual plants were negative for the Hygromycin gene, and were considered as escapes. Although these results showed a high transformation efficiency and also a reduced number of escapes, the total number of independent plants could have been higher if a better embryogenic callus separation could have been conducted during the Transition stages.

Experiment 021210IET was the first transformation experiment where the new shoot separation technique was tested (Section.4.3.1). Fig.4.8 shows the regeneration results for the above mentioned experiment. From a single embryo, 21 individual plants were obtained. Two callus separation rounds were performed, at transition and at regeneration stage, producing 5 different callus pieces forming shoots. Each developing shoot separated at the regeneration stage, needed a small amount of callus in order to regenerate a new root system to support the shoot development. The last separation was conducted once the plantlets were growing within the tube. They were left to grow for 2-3 weeks, until the most developed shoot reached the top of the tube and a well root system was developed. Once plantlets reached the top of the tubes the independent shoots were further separated and reintroduced into fresh tubes. These separated shoots were left to grow until the root system was ready for transferring to soil (Section.4.2.4).

Experiment	Immature Embryos	Regenerative Callus	Independent Shoot	Hyg (+)	Hyg(-)
200410IET	100	2	27	25	2
070510IET	115	1	7	7	0
060710IET	100	3	9	7	2
010710IET	120	1	3	3	0
170910IET	120	1	1	1	0
021210IET	120	1	21	21	0
	675	9	68	64	4

Table.4.5 Six transformation experiments, consisting of 100 -120 embryos each, were set up to study the transformation/regeneration efficiency (Table.4.2). Only 9 embryos derived callus regenerated green shoots out of 600 embryos inoculated, forming 68 independent plants in total. These plants were PCR positive for the Hygromycin gene presence (Section.4.2.5.3), with overall 64 positive plants identified (Fig.4.7). Only 4 plants were identified as escapes. Hyg: Hygromycin.

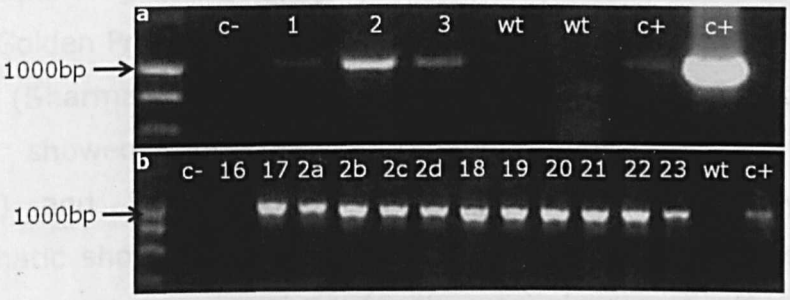

Fig.4.7 PCR to confirm transformation using HygromycinF/R primers (Table.4.3). a) Samples 1 to 3 were extracted from transgenic line 200410IET (Table.4.5). c+: Positive control using the expression vectors that contained the Hygromycin gene. c-: negative water control. Wt: Two wild type DNA samples were used as control. These three samples (1-3) were positive for the Hygromycin gene. b) Samples 16 to 23 were extracted from transgenic line 200410IET (Table.4.5). c+, c- and wt were the same as a. Only sample 16 was negative for the Hygromycin gene, and was considered an escape.

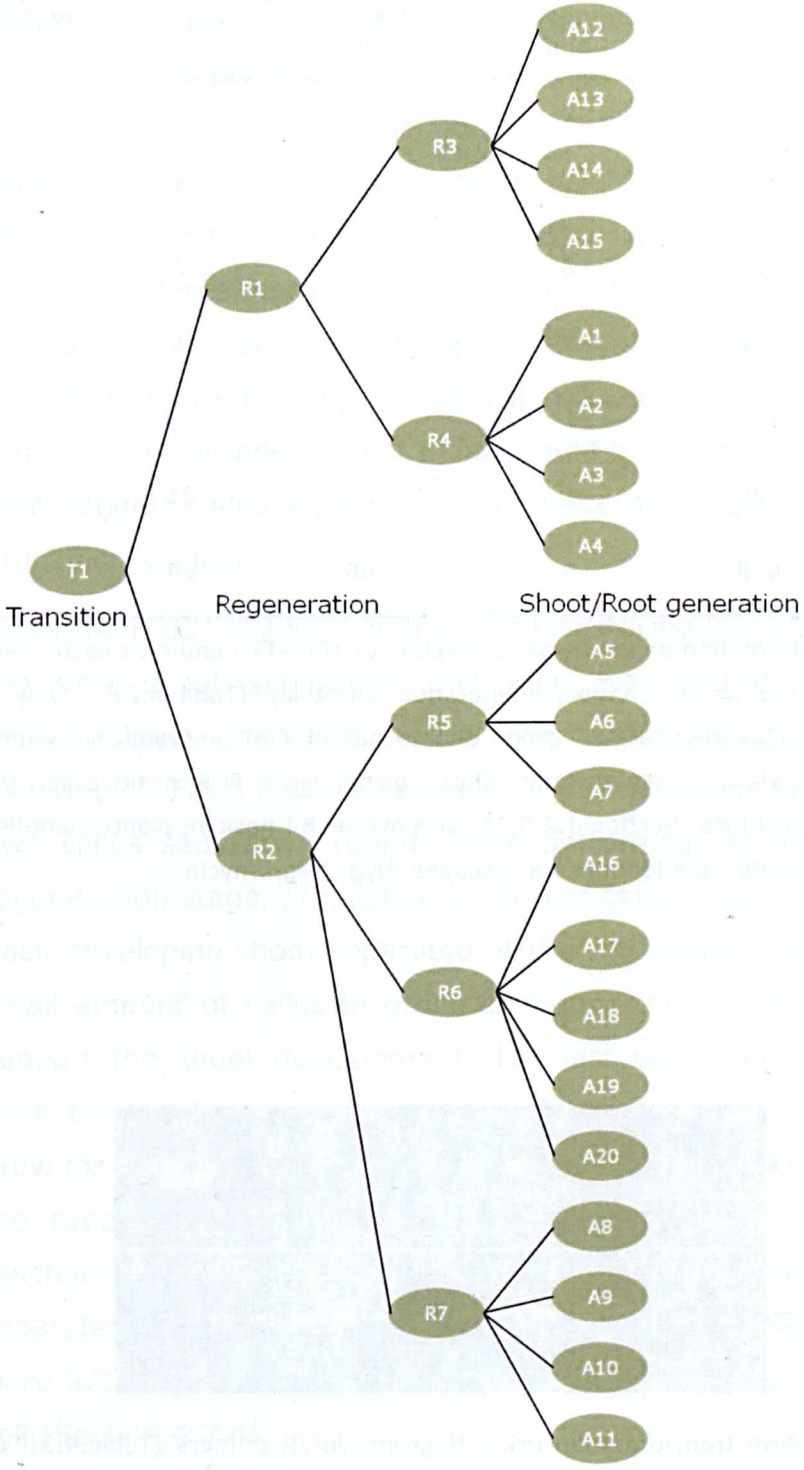

Fig.4.8. Regeneration efficiency of individual plants for experiment 021210IET (Table.4.2). Twenty individual plantlets (A1-A20) were obtained from a single embryo derived callus after three different rounds of division at different stages (Section.4.3.1).

4.4 Discussion.

Barley *Agrobacterium*-mediated transformation efficiency has encountered problems in terms of a low frequency of regeneration of adult plants from inoculated material (Harwood et al., 2002; Kerry et al., 2001). However, the improvement of culture media, the utilization of more responsive starting tissue (Caligari et al., 1987; Bregitzer et al., 1998), selective agent or *Agrobacterium* strain have increased not only the transformation efficiency, but also the frequency of regeneration of adult plants (Dahleen et al., 1995; Harwood et al., 2008).

Experiments leading to study the regeneration capacity of immature embryos as well as the *Agrobacterium*-mediated transformation/ regeneration efficiency of these embryos were conducted following Harwood's protocol (2008). Regeneration experiments in barley as well as in other cereals have previously been conducted using different starting tissue. For instance, mature seeds (Sharma et al., 2005) and meristematic shoots segments (Sharma et al., 2004) have been used with considerable success, although great variability of responses was found depending on genotype. Mature embryos from the spring cultivar Golden Promise showed higher plant regeneration per embryo, 5.8±1.0 (Sharma et al., 2005), whilst Golden Promise and Bowina varieties showed higher shoot regeneration, 33.4 (out of 454 explants) and 34.1 (out of 348 explants) respectively, when meristematic shoot segments were used. Using immature embryos, plant regeneration on a given media was also most efficient from Golden Promise (Dahleen et al., 2002).

Tissue culture and plant regeneration experiments of non inoculated embryos, 091109 and 101109IER (twelve immature embryos each), showed satisfactory results as 14 out of 24 immature embryo regenerated one or more plants, obtaining a total of 13 and 10 plants respectively (Table.4.4). These results showed the high efficiency of this protocol in plant regeneration from immature embryos. However,

separation of independent plants was not very efficient. Harwood's protocol (2008) reported the callus separation at the end of Selection 3 into smaller pieces containing independent embryogenic callus, as an essential step to improve the regeneration of individual plants. This separation protocol failed as the independent embryogenic calli were not satisfactorily separated. Therefore, the smaller callus pieces regenerated multiple plants all growing in a very close area, reducing the capacity to calculate the number of independent plants generated. Therefore, although only 13 and 10 plants were reported per experiment, it is thought that a more efficient separation method could have increased the overall regeneration frequency of individual plants.

In addition to the results already discussed, the newly developed method for accurate independent plant separation described in Section.4.3.1 was very successful and solved the problem of close embryogenic callus regeneration (Section.4.3.1). Twelve independent plants, all of them growing in separated pots, were obtained from two independent immature embryos. This triple separation protocol proved essential for high efficiency in separating and regenerating independent plants. Separation at the end of Selection 3 enhanced the production of more embryogenic callus at the Transition stage, due to the presence of copper sulphate at this stage (Joshi et al., 2007; Harwood et al., 2008), increasing the likelihood of obtaining a higher shoot regeneration. The two further shoots separation steps also increased the number of plantlets growing independently, facilitating further analysis.

The time required for the regeneration of adult plants starting from non-inoculated barley immature embryos was approximately 23-26 weeks. The first 10-11 weeks, from immature embryo collection to the formation of plantlets was similar for every barley embryo derived callus. From regeneration stage to plantlets transferred to soil, plantlets demonstrated a more variable growth, although most of the plants were ready to be transferred to soil after 4-8 weeks. The reasons why different plantlets needed longer periods to grow are

unknown; however it may be due to initial immature embryo size or condition that causes different responses to the regeneration media (Kerry et al., 2001). Kerry et al (2001) reported that not only embryo size but age plays an important role in callus formation in rye, which will also influence plant regeneration. After being transferred to soil, adult plants regeneration was observed within 10-13 weeks, however this may vary depending on the growth conditions or seasonal effects (Sharma et al., 2005). The duration of this regeneration protocol is very similar to other regeneration attempts conducted using mature embryos or meristematic shoots segments excised from germinated mature embryos as starting tissue (Sharma et al., 2005; Sharma et al., 2004). These two studies reported duration of 13-17 and 11-13 weeks respectively before plants could be transferred to soil.

Agrobacterium-mediated transformation efficiency of barley proved to be highly efficient as showed in section.4.3.2. GUS expression was observed in five out of ten embryos inoculated after only three weeks. Harwood et al (2002) reported immature embryo transformation efficiency up to 40% by bombardment. This shows the clear potential of high transformation efficiencies if regeneration of inoculated embryos were improved. Barley transformation (Harwood et al., 2008) have already reached transformation/regeneration efficiencies up to 25%, improving previous protocols that acieved lower efficiencies ranging between 5.4 (Lange et al., 2007) or 2.6-6.7% (Shrawat et al., 2007). This high efficiency has been possible due to an improvement in not one, but several aspects of the transformation protocol. Beside factors such as the plant genotype and the tissue used, medium has been widely studied (Section.4.1). However, none of these protocols has ever reached efficiencies as high as that obtained by Harwood's protocol (25%; Harwood et al., 2008). One of the main factors for this improvement has been the vector used. The selection of the right vector is crucial for an efficient transfer of the T-DNA into the plant, and their subsequent selection. Binary vectors used for the generation of transgenic cereal species are typically cumbersome due to their large size and the rather limited number of useful restriction sites.

Most promoters available to date are derived from dicotyledonous plants. Unfortunately, such promoters are typically dysfunctional in cereal species. Thus, the expression of transgenes in cereals has been largely driven by ubiquitous promoters such as the ones from the maize ubiquitin 1 (Christensen et al., 1992; Oldach et al., 2001). The pBRACT vectors have been designed for crop transformation, and specifically for expression studies in wheat, barley and Brassica. Transformation of immature embryos with pBract216, 215 and 216 (Hygromycin marker under the 35Spromoter and firefly luciferase under the Ub1promoter; Harwood et al., 2008) has shown high efficiencies, 21.5, 27.3 and 25.4% respectively, confirming that this vector family is highly successful for barley transformation. In addition, these vectors showed a low transgene insertion ratio, with almost 50% the transformed plants carrying only one copy, while 20% were observed to carry 2 copies.

Agrobacterium strains other than AGL1, such as LBA4404, harbouring either pUGB7 or pYF133 transformation vectors, also proved efficient in delivering T-DNA into barley cells under a range of *in vitro* conditions (Shrawat et al., 2006). However, a higher frequency of transformation was observed when immature embryos were co-cultivated with LBA4404 harbouring binary vector pYF133. In addition, compared with Hygromycin, the effect of Bialaphos selection was markedly less efficient *in vitro* (Kumlehn et al., 2006), indicating the clear advantage of using vectors carrying Hygromycin resistance. Analysis conducted on several media indicated that Bialaphos resistant plants were obtained with an average of 5.6% transformation efficiency, compared to 6.7% for Hygromycin resistant plants (Shrawat et al., 2006). In addition, a series of modular binary plasmids for stable *Agrobacterium*-mediated transformation of cereals such as barley and wheat have been developed, pIPKb (Himmelbach et al., 2007). The modular configuration of these vectors permit convenient introduction of coding sequences for over-expression or knock-down experiment. Various promoter sequences have been used to drive the gene of interest, as well as of any preferred plant

selectable marker cassette. This provides the opportunity to generate vector derivatives tailored for the particular requirements of various plant transformation systems, and for the ultimate elucidation of the function of any particular candidate DNA-sequence. The introduction of genes of interest in these generic vectors is greatly facilitated by the implementation of the GATEWAY™ recombinational cloning system. Transformation of immature barley embryos conducted with these vectors has reached efficiencies as high as 30-60% using the Hensel et al (2008) protocol, increasing barley transformation efficiency even further.

Experiments conducted to analyse the transformation and regeneration of adult plants (Section.4.2.5) showed satisfactory results (Table.4.5), obtaining an 11% of successfully regenerated transgenic plants. In addition, the protocol (Harwood et al., 2008) proved to be highly efficient in selecting the transformed samples as only 4 escapes were identified out of 68 independent plants (Table.4.5). These escapes were likely to have been caused by a close growing point within a callus, where several embryogenic callus regenerated shoots too close together, helping non-transformed shoots to grow (Harwood et al., 2008). Therefore, although the total plant regeneration was not very high, the majority of these plants were transformed, showing the high potential of this protocol. In addition, an improvement in the regeneration and isolation of independent plants was attempted in experiment 021211IET (Section.4.3.1). This included a triple separation protocol that allowed a better approach for analysis as well as a more accurate calculation of transformation efficiencies (Section.4.3.2; Fig.4.8). Different protocols achieve the separation of individual embryogenic callus in different ways depending on the species. Hiei et al (2008) reported that rice immature embryos co-cultured with *Agrobacterium* usually have multiple, independent transformation events in the scutellum. Therefore they cut up the embryo derived callus into 24 pieces after non-selective culture following co-cultivation so that as many independent events could be recovered as possible. Although, no such

division was performed in the experiments presented here, the triple division protocol showed a significant improvement in separation of independent plants separation (Fig.4.6), each of them considered an independent event of transformation originated from an independent embryogenic callus. These independent one shoot-plants were transferred to soil making sure that no other independent shoots were growing alongside and therefore, subsequent tillers that formed afterward were part of the same original independent plant.

Barley transformation was successfully carried out using three different constructs. However, results showed that the majority of the transgenic plants regenerated originated from a minimum number of embryo-derived calluses (Table.4.5). In comparison, non-inoculated embryo-derived callus showed a higher regeneration ratio (7 out of 12 callus regenerated adult plants; Table.4.4). This difference in regeneration success may be likely due to stress caused by the insertion of the transgene or the *Agrobacterium* contamination. *Agrobacterium* mediated transformation have been shown highly efficient in transforming barley immature embryos (Section.4.3.2) and several authors have remarked the difficulties of regenerating transgenic callus (Harwood et al., 2008, Kerry et al., 2001; Vogel et al., 2008). Vogel et al., (2008) reported that *Agrobacterium*-mediated transformation of *Brachypodium*, less than half of the confirmed transgenic callus regenerated adult plants. They reported that factors such as the promoter driving the selectable marker may affect the regeneration efficiency, therefore, other factors seems to limit the regeneration of transformed callus distinctive than the transformation efficiency (Kerry et al., 2001; Harwood et al., 2002).These factors, such as the starting material in barley, immature embryo, its age and manipulation, seems to be crucial for regeneration efficiency (Hawood et al., 2008; Kerry et al., 2001). In addition, donor plant health and growing conditions have also been reported essential (Harwood et al., 2008), having found that sprayed plants showed a poor transformation result. Therefore, standard growing conditions, an efficient method to manipulate and identify the right immature

embryo and the use of most the appropriated *Agrobacterium* strain, construct, selectable marker and media, are indispensable for the successful and highly efficient transformation/ regeneration of barley and other cereals.

CHAPTER 5.

5. Characterization of putative barley male sterile mutants.

5.1 Introduction

Controlling the process of pollen development and release is critical for selective breeding, the release of genetically modified (GM) pollen, and the commercial development of hybrid lines. Hybrids frequently exhibit heterosis or hybrid vigour, which means that the plants are stronger, develop more rapidly, and are higher yielding. F1 hybrid rice has an average 15% to 20% yield advantage over inbred lines (Zhong et al., 2004; Cheng et al., 2007). In China, it is planted on approximately 16 million hectares—more than half of China's total rice area of 28 million hectares (Barclay, 2007). Other than China, Vietnam, India, and the Philippines have commercialized hybrid rice. Bangladesh, Indonesia, and Pakistan have also achieved recent success with hybrid rice. Hybrid rice is expected to help to ameliorate the problem of hunger and malnutrition in Asia, Africa, and Latin America, where rice is a staple food for the poor.

The efficient production of hybrid seeds depends on an effective pollination control system that prevents unwanted self-pollination. A frequently used system for hybrid generation in self-fertilizing crop species, such as maize, rice and cotton is Cytoplasmic Male Sterility (CMS) lines. CMS has been spontaneously identified in many plants species due to disturbed nuclear-mitochondrial interactions, both as a consequence of cross-hybridization strategies, or rising naturally in wild populations (Hanso and Bentolila, 2004; Pelletier and Budar, 2007). One example of CMS hybrid barley was the world's first hybrid variety, Colossus, which was introduced in the United Kingdom in 2003 (Syngenta, July 2003). This barley hybrid has been specially

bred for improved performance and demonstrates "hybrid vigor", which translates into hardier crops and better yields (over 10%).

Alternative systems have relied upon the suppression and restoration of the transcription of key genes associated with pollen development. Transgenic nuclear male sterility has been developed using various transgenes, although few have been adapted for hybrid seed production (Mariani *et al.*, 1990; Perez-Prat and Van Lookeren Campagne, 2002). The commercial application of these transgenes is limited by the difficulties in propagating male sterile plants and the lack of suitable restorers (Perez- Prat and van Lookeren Campagne, 2002). The male sterility systems developed so far usually affect tapetum and pollen development, but many also interfere with plant growth (Kriete *et al.*, 1996; Hernould *et al.*, 1998; Napoli *et al.*, 1999; Goetz *et al.*, 2001; Yui *et al.*, 2003; Zheng *et al.*, 2003). Controlling the activity of a transcription factor essential for male fertility, but whose up- or down-regulation does not affect either plant development or productivity, would provide a means of addressing these difficulties in crops.

A collection of barley mutant seed stocks are held by the James Hutton Research Institute. These mutants were induced in the cultivar Optic using ethyl methane sulphonate (EMS) treatment of grain from which a structured mutation grid was developed for forward and reverse genetics. A total of 21,000 M2 or M3 families were phenotyped by visual observation. This database provides an account of phenotypes and includes: descriptions, candidate genes (only some mutants), photographs and DNA sequence variation.

Mutant seeds (M3), reported as having phenotypes associated with male sterility, were ordered from SCRI (Table5.1). Phenotyping of lines was conducted to characterise lines showing defects in pollen development. Pollen-less plants were selected and out-crossed with wild type and then a more detailed study was carried out on the subsequent generations. No gene identification has been reported for any of these lines.

Group	SCRI Phenotype
1	Spike appearance. Male sterile
2	Spike appearance. Male sterile florets
3	Spike appearance. Partial sterile
4	Spike appearance Infertile terminal florets

Table.5.1. Barley mutant groups selected for phenotype screening. These seeds were provided by SCRI and were generated by EMS.

5.2 Materials and methods.

5.2.1 Plant growing conditions.

Double rowed spring barley (Optic variety) EMS M3 generation (Table.5.2) supplied by the SCRI was grown in a growth room under controlled conditions (Section.2.1). These lines were selected based upon initial phenotyping conducted by SCRI (Table.5.1).

Manual crossing was carried out on lines presenting male sterility. Crossing was conducted first by localizing pollen donors at anthesis stage. Spikes from these pollen donors were collected and, carefully, using a scissors, awns were cut off, slightly uncovering the anthers by cutting the upper part of the florets. Three to four of these spikes donors were placed in a transparent plastic bag (15x5 cm) and once closed, the bag was hit against the full open hand to release as much pollen at possible. The result was the formation of a cloud of released pollen inside the plastic bag. The bag was open then and the anthers were collected from the inside and used to fertilise sterile florets also at anthesis stage (These sterile florets had also the awns cut off as well as the upper part of the florets, this facilitated the introduction of fertile anthers). Finally the sterile spike, was covered with the bag

containing the cloud of pollen as well as the donor spikes to enhance the pollination of these sterile lines. This operation was repeated as many times as sterile spikes were observed.

Seed Reference	Date	Expected Phenotype (Table.5.1)
233/53	08/05/09	2
91/84	08/05/09	2
146/18	08/05/09	2
93/53	08/05/09	2
232/39	08/05/09	2
75/91	08/05/09	2
12/17	22/07/09	1
257/74	22/07/09	4
18/06	22/07/09	3
08/27	22/07/09	1
07/34	22/07/09	1
07/93	22/07/09	1

Table.5.2. Barley male sterile mutant lines (SCRI). Two groups were sown on different dates. The numbers showed in the third column corresponds to the preliminary phenotype described by SCRI (Table.5.1).

5.2.2 Fertility characterization

Plants were left to grow until fertilization stages in order to observe self-pollination. Fertility evaluation was based on the percentage of completely fertile plants out of the total plants grown. Plants were classified as male sterile if the self-fertility rate was less than 5% and as male fertile if the fertility rate was greater than or equal to 5%. A Chi-square test was performed to determine the segregation pattern of the fertility.

5.3 Results.

From the 12 M3 generation lines phenotyped as male sterile (Table.5.3), only 2 lines showed male sterility phenotype, 233/53 and 08/27 (Table.5.3). These two lines were studied more in detail.

Seed reference	Expected Phenotype (Table.5.1)	Phenotype Observed
233/53	2	This line showed abnormal vegetative development (Fig.5.1). In addition, these plants were male sterile.
91/84	2	These lines were completely normal and fully fertile.
146/18	2	
93/53	2	
232/39	2	
75/91	2	
08/27	1	Sterile phenotype observed. Vegetative development was normal (Fig.5.3).
12/17	1	These lines were completely normal and fully fertile.
257/74	4	
18/06	3	
07/34	1	
07/93	1	

Table.5.3 Results for the phenotyping of the putative male sterile barley plants supplied by the SCRI (Table.5.2). Only two lines showed a sterile phenotype, 08/27 and 233/53. The remaining lines showed normal development and fertility.

5.3.1 Line 233/53

Line 233/53 (M3 generation) showed 3 out of 16 plants with abnormal development when compared to wt (Table.5.4). First of all, these three plants developed only one main shoot and no tillers were formed (Fig.5.1; 5.2). Moreover, these shoots grew much faster than the rest of the apparently normal plants, reaching Zadok stages 31-32 when the wt was still at stage before 30. In addition, shoots were split open and spikes observed at Zadok stage 31-32. At this stage, the spike was 1-2 cm long. This spike was clearly abnormal (Fig.5.1), no florets were observed at the bottom of the spikelet and when present, this florets were deformed (Fig.5.1.a-d). Furthermore, anthers showed an extra lobule (Fig.5.1.f). Neither of these two abnormal plants were grown till seeds formation. The remaining 13 plants showed normal development and were totally fertile, therefore were left to self fertilise. Seeds were harvested for further experiments (M4 generation).

Sixteen M4 generation seeds, collected from fertile plants obtained after self-pollination of generation M3, were sown (Section.5.2.1). Two plants presented similar growth pattern observed in the previous generation. Both of them were grown until heading (Head was completely out) at which point, the wt was still at early pseudostem elongation stages (31 to 34), and therefore still 2 weeks from heading. The first abnormal feature observed was the lack of tillers as only the main shoot was developed (Fig.5.2.a). Spikes were completely deformed (Fig.5.2.b) and several branches with numerous disorganized florets attached were observed alongside the spike. At the base, florets were absent as observed in the previous generation, or presented severe deformation (Fig.5.2.d). Two ovaries were found inside some of these deformed basal florets, whereas other florets contained two small and aberrant florets. (Fig.5.2.e). The Anthers which were observed showed no pollen inside, therefore, these two plants were completely sterile.

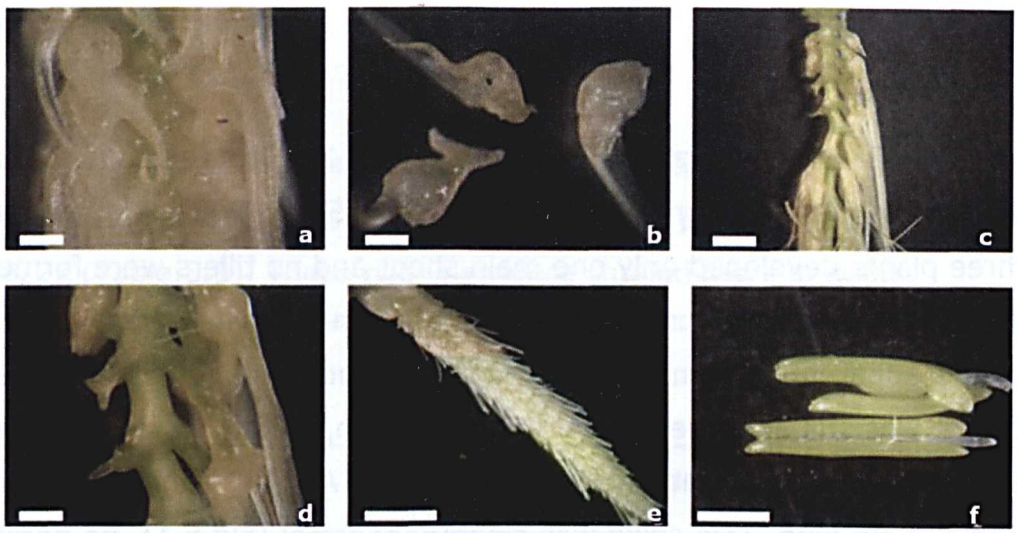

Fig.5.1 Phenotypic analysis of the putatively male sterile EMS mutant line 233/53. Three out of sixteen plants showed an abnormal and faster development (M3 generation). Figures a, c, d and f show the abnormal spikes observed in this mutant lines. a-b) Abnormal florets attached to the bottom of the spike. c) Bottom part of abnormal spike, florets within this parte were missing or deformed (b). d) Close look to bottom part of the spike. No florets were observed in some spikelets. e) Wild type spike. f) Anther observed within the abnormal florets. These anthers showed an extra lobule. e) Wild type spike. Bars: a, b and d= 0.5 mm; e and c= 0.4 cm; f= 0.5 cm.

Thirty two seeds from the M4 generation were sown in order to determine whether this mutation shows Mendelian segregation (Table.5.4). From the 32 plants, 5 showed the characteristic abnormal phenotype (~1/4). The remaining 27 plants were completely normal, and did not show any intermediate effects. Cross-pollination with wild type pollen failed; therefore no heterozygous line was regenerated.

Chi-square test showed that the fertility segregation fitted a ratio of 3:1 in all the M3 and M4 populations. The sterility was thus governed by a single recessive gene (Table.5.4).

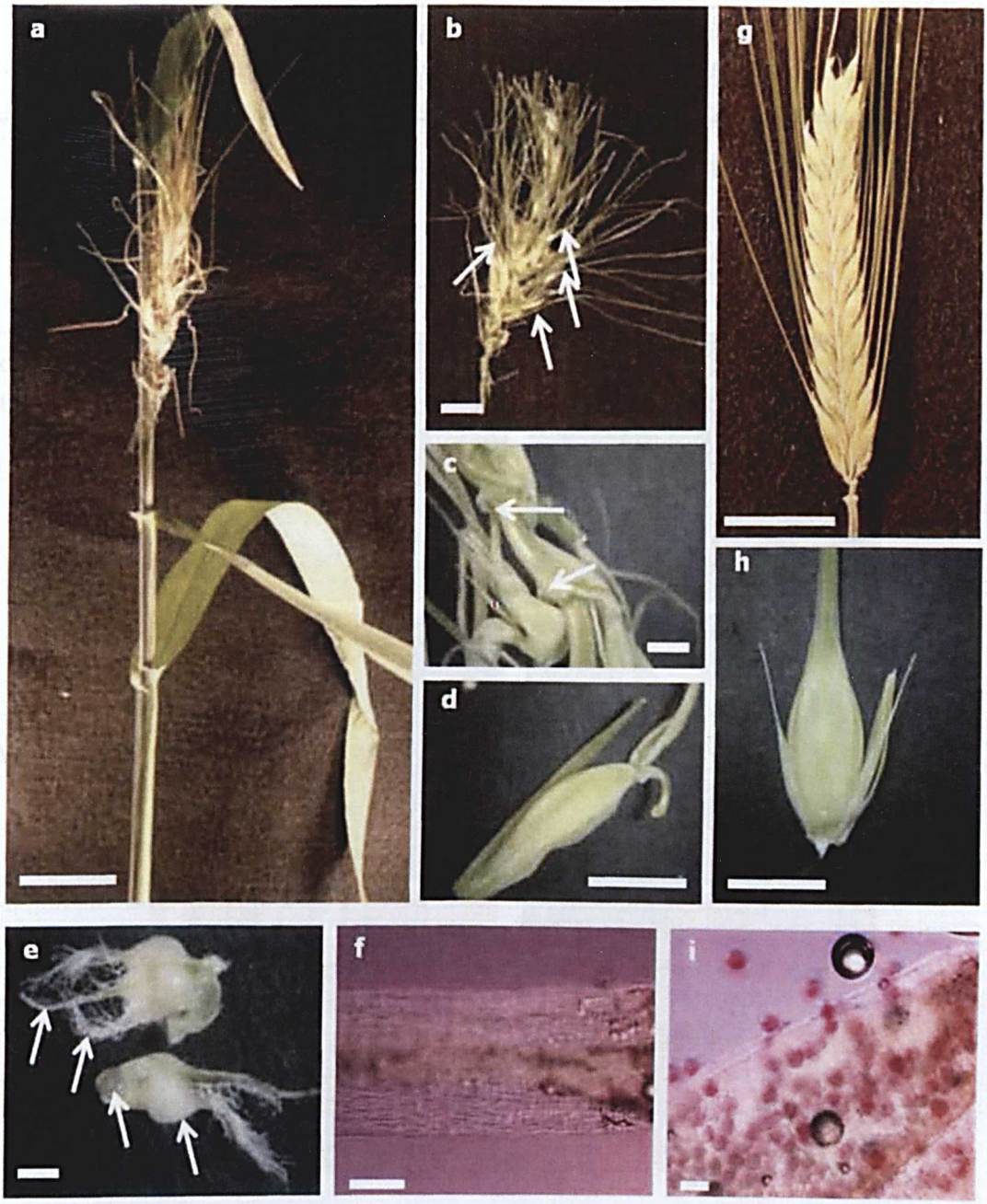

Fig.5.2 Comparison between wt and 233/53 mutant phenotype. a, b, c, d, e and f) 233/53 mutant line. g, h and i) wild type. Aberrant spikes were observed in line 233/53 (a and b). These spikes were formed by deformed florets (c and d). Inside this deformed florets, deformed ovaries were found (arrows)(e) and no pollen was observed in the mutant anthers (f) (Alexander stain) as compared to the viable pollen of the wild type (i (Alexander stain) g-h) Wild type spike and floret. Bars: a, b and g= 3 cm; d and h= 0.5 cm; c= 0.25 cm; e= 1 mm; f and i= 0.1 mm.

233/53	Total plants	Sterile plants	Fertile plants	$\chi 2$ (p 3:1)	P_{value}
M3(16)	16	3	13	0.33	0.5
M4(16)	16	2	14	1.33	0.3
M4(32)	32	5	27	1.49	0.2

Table.5.4 Chi square of the distribution of normal/sterile plants observed for two different generations of line 233/53. χ 2- (p 3 : 1), Chi-square test for the ratio of 3 fertile : 1 sterile; P, probability.

5.3.2 Line 08/27

From the first 16 M3 seeds sown (Table.5.5), 4 plants were completely sterile. The remaining 12 plants were fertile.

08/27	Total plants	Sterile plants	Fertile plants	$\chi 2$ (p 3:1)	P_{value}
M3 (16)	16	4	12	0	0.99
M4 (16)	16	2	14	1.33	0.3
F2 (50)	50	13	37	0.026	0.9

Table.5. Chi square of the distribution of normal/sterile plants observed for three different generations of line 08/27. χ 2- (p 3 : 1), Chi-square test for the ratio of 3 fertile : 1 sterile; P, probability.

Sixteen M4 generation seeds, produced by fertile M3 parents, were sown. Fully fertile (14) and sterile plants (2) were observed again. Comparison between wt and sterile florets at stages close to anthesis

(Fig.5.3) showed that the sterile florets had an open and globular appearance (Fig.5.3.a) at stages where these florets were expected to be closed and grain filling taking place (Fig.5.3.b). In addition, anthers were undeveloped (Fig.5.3.c and d), and pollen was totally absent (Fig.5.3.e and f).

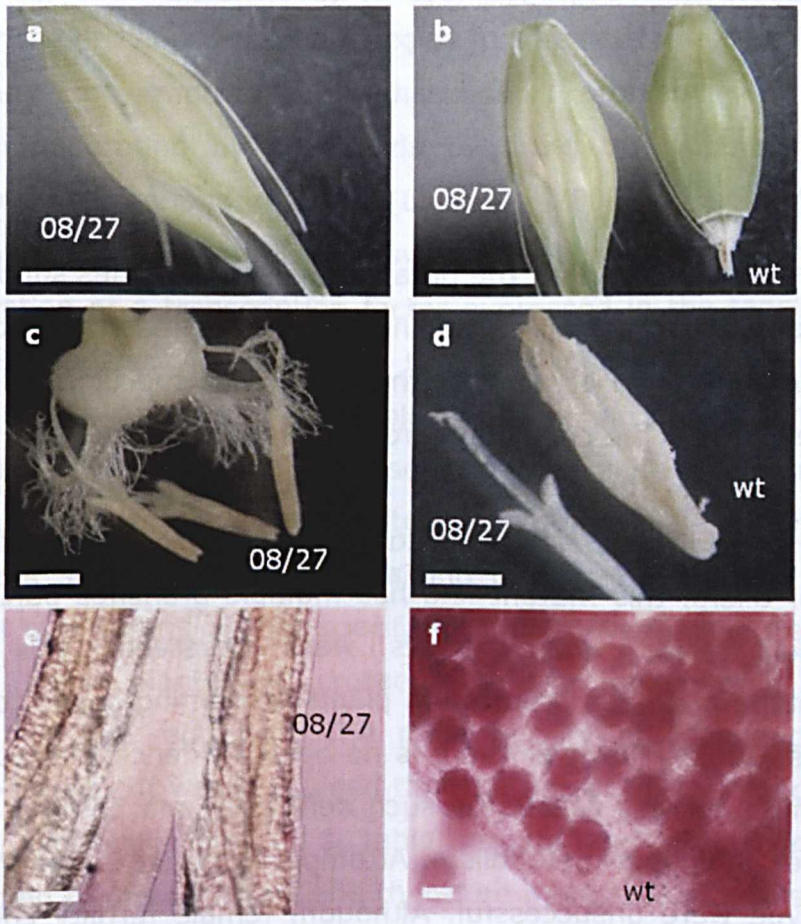

Fig.5.3 Comparison between reproductive development in sterile line 08/27 and wild type. Floret formation was different for the sterile line compared to wt (a and b). In addition, no pollen was observed within the immature 08/27 anthers (c, d and e). f) wt anthers were full of viable pollen. Bars: a and b= 0.5 cm; c and d= 0.75 mm; e and f= 0.1 mm. e and f were Alexander stained.

M4 sterile plants were crossed with wt pollen (Section.5.2.1) confirming that the sterility was restricted to the male organ formation as F1 seeds were formed. Sixteen F1 seeds were then sown and left to self (all of the 16 plants were completely fertile). Complete spikes

were harvested (F2) and 50 seeds were selected from different F1 spikes and sown. Thirteen plants were completely sterility (~1/4), the rest, 37, were fully fertile. In addition, Chi-square test showed that the fertility segregation fitted a ratio of 3:1 in M3, M4 and F2 generations. Therefore, the sterility of these plants is likely to be caused by a single recesive gene as F1 generation complete fertility and F2 Mendelian segregation (3:1) have shown.

5.4 Discussion

The results observed for the putative male sterile lines supplied by the SCRI showed that most of the lines, phenotyped as male sterile, were completely normal or at least the phenotype specified for them was not seen under the conditions grown. In addition, from the two sterile lines, only one (08/27) showed a normal vegetative phenotype. The other sterile line, 233/53, was completely aberrant. In addition to the lack of tillers, this mutant line has multiple branches parting from a common rachis where florets were observed. This particular phenotype has been reported in plants presenting copper deficiencies (Evans, 2001). However there is no other evidence that suggest that this mutation was caused by such deficiency and possibly by a gene involved in copper metabolism. Attempts to outcross this mutant with wild type were unsuccessful. Although, female fertility could not be confirmed, the failure in out-crossing the plant was more likely due to the decay of the female organs at the time of the pollination attempt. The distribution observed for this line, confirmed by the Chi square (Table.5.4), was 3:1, suggesting a recessive Mendelian inherited mutation.

Mutant line 08/27 also showed a Mendelian distribution. Sterile plants pollinated with wt pollen were fully fertile (F1), however, when F1s were left to cross and F2 seeds plants grew, the fertile/sterile distribution was 3:1 (Table.5.5). This also suggests that mutation has been caused by a single recessive allele. The sterile phenotype

observed in the 08/27 mutant, indicates that this line exhibited some of the traits of use in hybrid seed production, such as the normal vegetative development and the normal seed formation when heterozygous (Li et al., 2007). However, insufficient information is currently known about the causes of the mutation, and the nature of the defect. Gene mapping analysis and characterization is required for the potential future application of this gene. This information is also needed for the development of strategies for the restoration of fertility for seed and crop production. This has been a problem for previous attempt in generating hybrids seeds by using the suppression or restoration of transcription factors (Li et al., 2007). Li et al (2007) reported a hybrid seed production system that involved suppression and restoration of a transcription factor expressed in the tapetum of *Arabidopsis thaliana*, *AtMYB103*. In their study, the function of the *AtMYB103* gene was blocked by employing either an insertion mutant or an *AtMYB103EAR* chimeric repressor construct under the control of the *AtMYB103* promoter, which resulted in complete male sterility and failure to set seed. A restorer containing the *AtMYB103* gene under the control of a strong anther-specific promoter was introduced into the pollen donor plants and crossed into the male sterile plants transgenic for the repressor. The male fertility of F1 plants was restored. However, it was concluded that the use of this approach was limited by the availability of suitable targets and the incomplete understanding of this pathway, and therefore more research was to be done in order to improve this approach. Another example of transgenic sterility system was the floral tissue selective expressions of cytotoxic proteins or antisense genes that block essential metabolic processes (Williams, 1995; Neill et al., 1996). This approach was used satisfactory in canola (Bayer CropScience's (RTP, NC) InVigorTM). As male sterility is dominant, sterile lines are maintained by crossing with the identical non-transgenic genotype to produce a segregating population. A herbicide is used to remove non-transgenic, fertile plants in this population prior to hybrid production as the transgene that provides sterility also carries a gene for herbicide resistance. However, the application of herbicide to eliminate fertile plants

increased the costs, making this method difficult to apply in wheat (Edwards, 2001).

Work is also currently in progress to utilize chemically induced sterility. Conditional sterility by the application of a single dose of a chemical hybridizing agent (CHA) is simple and practical option (Edwards, 2001) that can be used for a range of cereals, although CHA effective products are the major limitation to this hybrid seed production method. More recently, Syngenta has presented a new protocol (Hawkes et al., 2011) that consists of using a nonphytotoxic enantiomero component (D-glufosinate) of commercial herbicide glufosinate (e.g sold by Bayer as LibertyTM, IgniteTM or BastaTM). This D-glufosinate is foliar applied prior to sporogenesis in transgenic plants that carriy the enzyme, DMRtDAAO (D-amino acid oxidase (DAAO) from *Rhodosporidium toruloides* (Rt)) under the control of an anther specific promoter (TAP1, tapetum specific promoter from *Antirrhinum majus*). This enzyme is expressesed in the anther and oxidises the D-glufosinate to its phytotoxic version, L-glufosinate, which causes damages within the anther tissues and male sterility. This method has a great potential as its extension to different crops depend on the availability of tapetum specific promoters than control the expression of the DMRtDAAO enzyme. Therefore, research of the anther and pollen development and the genes involved in their regulation is essential to design system that contributes to a improved hybrid seed production.

08/27 sterile lines may also be used for different purposes. For instance, a pollenless plant with a completely fertile female organs and a completely normal vegetative development can be used as an easy platform to outcross important transformed or mutant lines. Manual emasculation is tedious and time consuming, in addition, emasculation and fertilization must be conducted at a very precise moment in order to generate seeds successfully using pollen from a donor plant before the pollen decays (Pickett, 1998) and to avoid self-crossing that will compromise the cleanness of the out-crossing. In addition, the stability of transgenic lines is be better guaranteed by

out-crossing (McGinnis et al., 2007). Therefore, a complete male sterile line could be the perfect host for any desired genotypic background, such as experiments that do not involve studying sterility, but other plant characteristics, such as abiotic or biotic stress, could be clear examples. Therefore, by using the male sterile line, out-crossing is facilitated and secured by the total absence of pollen in the host plant avoiding unwanted contamination. This is also reinforced by the fact that the sterile host plant does not show any other defects beyond the pollen absence, and therefore, will not contribute in any negative way to the experiment design.

CHAPTER 6.

6. *HvMS1* characterization.

6.1 Introduction.

The characterization of important genes in cereal species has been facilitated by the sequencing and release of a number of grass genomes. To date, the complete genome of four grass species have been analysed (*Oriza sativa, Sorghum bicolor, Brachypodium distachyon and Zea mais* B73), and although grass genomes vary greatly in size, partly due to expansion of retroelement repeats, there is an underlying conserved gene order (Wicker et al., 2007; Moore et al., 1995). This conserved order can help in the identification of equivalent genes that are unknown in other species. Genes that have evolved from the same ancestral gene are generally called *homologues*. These can be classified into two categories, *orthologues* and *paralogues*, where orthologues refer to genes that have evolved from the same ancestral gene via speciation and have maintained the same biological function, while paralogues refer to genes that have evolved from the same ancestral gene via speciation and duplication, and perform similar but distinct biological functions (Eisen et al., 2002; Wu et al., 2007).

Arabidopsis MALE STERILITY1 (*MS1*) is a transcription factor that is expressed in the tapetum, which is critical for pollen development and viability (Section.1.2.3). *MS1* encodes a protein (672 amino acids), containing a putative Leucine Zipper and a Plant Homeodomain (PHD) finger motif which are essential for its function. There are a number of related genes in *Arabidopsis* (*MMD1, At1g33420 and A1g66170*), but also several putative orthologues in other species, such as *poplar* (Fig.6.1.), where six homologues have been detected (Shinozaki et al., 2007). Moreover, the rice *OsPTC1* gene has recently been

identified as the putative orthologue of *AtMS1* (Li et al, 2011); this contains a highly conserved PHD domain in the C-terminal region and appears to have a similar function to *AtMS1*. The barley genome has not been entirely sequenced and to date, no related gene has been found in barley. *AtMS1* shows very specific tapetal expression during microspore development and has therefore not been identified in any of the EST libraries. It is therefore not unexpected that no BLAST matches have been found using *AtMS1* or *OsPTC1* against the barley database.

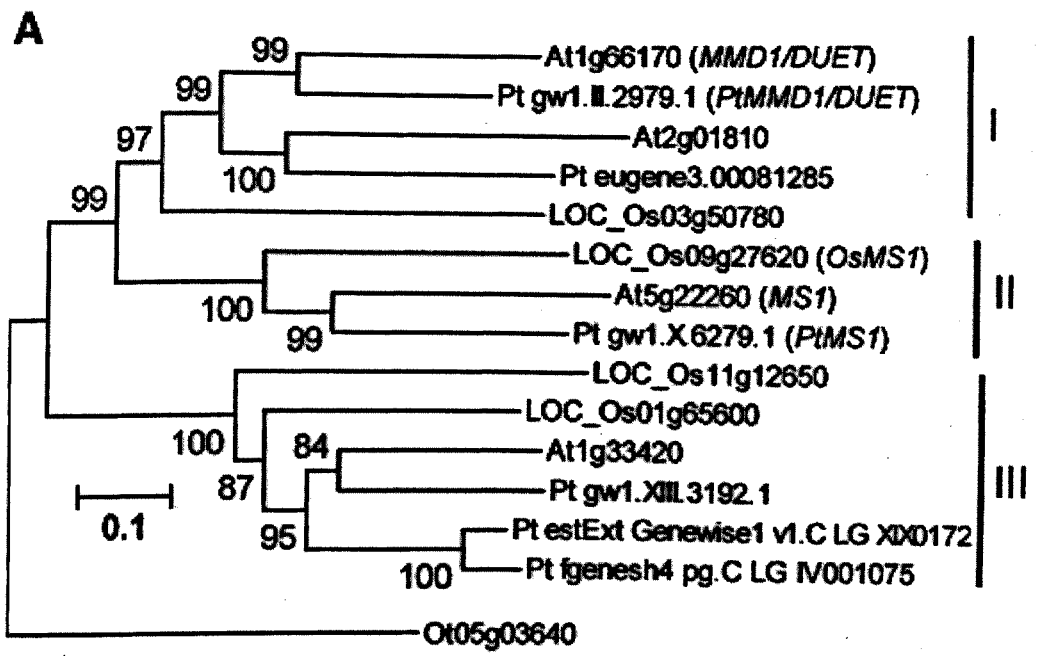

Fig.6.1. A rooted neighbour-joining tree of *Arabidopsis*, rice, poplar, and *Ostreococcus MS1* homologs. Gene identifier numbers starting with At indicate genes from *Arabidopsis*; names of genes with functional information are given after the identifier numbers. LOC_Os indicates genes from rice (*O. sativa*), with names given according to gene identifier from TIGR. Pt indicates genes from poplar (*P. trichocarpa*), with temporary names given according to gene identifier from the Floral Genome Project. Ot indicates a gene from *O. tauri*. Os *MS1*, Pt *MS1*, and Pt *MMD1/DUET* after the identifier numbers are names of genes with deduced functional information. Bootstrap values are shown near the relevant nodes (Shinozaki et al., 2007).

The release of the *Brachypodium distachyon* genome (Section.1.3) has lead to new opportunities to find orthologues sequences in barley.

The close relationship between *Brachypodium* and barley (Doonan et al., 2008) means that this genome provides a valuable link for the identification of conserved genes in temperate cereals. The *Brachypodium* genome alongside genes that have already been shown to be involved in pollen development in rice, should allow the design of primers to regions showing conservation between rice and *Brachypodium* to amplify equivalent sequences in barley.

The available sequence information from rice and *Brachypodium* was therefore used to identify the *MS1* orthologue in barley and functionally characterize its role in pollen development.

6.2 Materials and methods.

6.2.1 Bioinformatics analysis.

Bioinformatics tools were used in order to identify the orthologue gene to *MS1*. Databases such as Gramene and TAIR (www.gramene.org and www.*Arabidopsis*.org) were used to obtain the *Arabidopsis* and rice DNA and protein sequences corresponding to *MS1* and *OsPTC1* respectively. In addition, Gramene offers a gene orthologue/paralogue analysis where *Brachypodium*, sorghum or poplar genes can be found using corresponding *Arabidopsis* or rice genes.

Basic Local Alignment Search Tool (BLAST) (Altschul et al., 1990) analysis was carried out, using cDNA, to identify or confirm orthologues genes to those previously identified as involved in anther and pollen development. NCBI (National Center for Biotechnology Information; www.ncbi.nlm.nih.gov/guide) and *Brachypodium*.org (www.*Brachypodium*.org) BLAST analysis was extensively used for rice, *Arabidopsis* and *Brachypodium* orthologue gene analysis. BLAST was used for orthologue recognition and also, and more importantly, to compare new barley sequences against the rice database in order

to confirm levels of similarity to the *AtMS1* orthologue, *OsPTC1*. In addition, new barley sequences were BLASTed against the DFCI barley database (DFCI Barley Gene Index; http://compbio.dfci.harvard.edu/tgi/plant.html).

Alignment between *AtMS1*, *OsPTC1* and the *Brachypodium* genes was performed using the Needleman-Wunsch Global Sequence Alignment Tool (Needleman and Wunsch, 1970) available in the NCBI. This global alignment was only used on sequences that were expected to share significant similarity over most of their length. These alignments were used to recognise conserved regions between the different genes for primer design. In addition, all the barley amplified sequences were aligned to the above genes in order to compare sequences and establish the region where these they matched to.

MacVector (MacVector, Inc, PMB 150; 1939 High House Road, Cary, North Carolina 27519, USA) was used for sequence editing, primer design and checking, protein analysis and multiple sequence alignment. Primers design was conducted using Primer3 (http://frodo.wi.mit.edu/primer3/) and subsequently checked using MacVector.

6.2.2 PCR analysis.

PCR was performed using different polymerase enzymes as explained in section.2.3. cDNA, synthesised from RNA extracted from flowers at tetrad to early microspores release (Section.2.10; 2.11), was used as a template. Different sets of primers were designed based upon either rice *OsPTC1* or *OsPTC1/Bradi4g31760* (Fig.6.2). These two sequences were aligned using NCBI alignment software and the most similar regions selected for primer design. Regions containing conserved family domains were excluded to avoid non-specific amplification of gene family members. These primers were then used to amplify the equivalent sequences in barley.

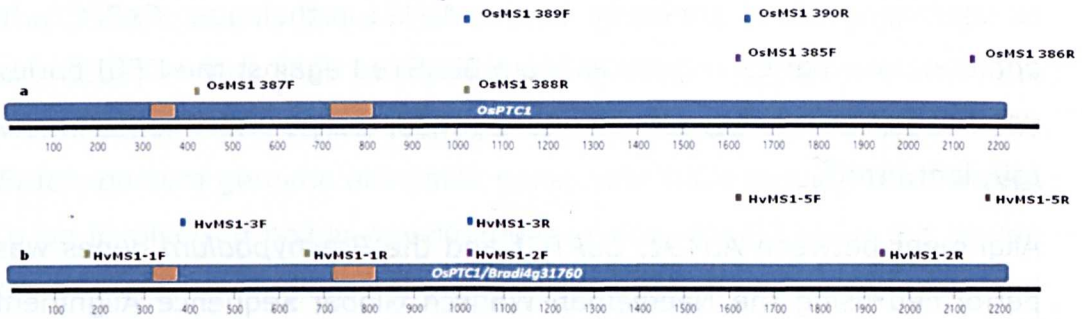

Fig.6.2 Primers designed using rice *OsPTC1* gene as template (a) and primer designed using conserved nucleotide regions between Rice-*Brachypodium*, *OsPTC1/Bradi4g31760* (b) as templates (Appendix.8). Blue bars represent the exons, and the orange boxes the intron. Scale bar: bp.

Primer combination was mainly used as shown in Table.6.1. However, different combinations were tested in order to find the clearest PCR product. Phusion enzyme proved to be more efficient than Taq for most of the reactions, and therefore, was predominantly used. Conditions were adapted specifically to each pair of primers, however, in order to optimize primers conditions, gradient PCR was used (Tm = 55ºC to 65ºC in 1.5ºC intervals using Phusion enzyme, section.2.3). PCR products were purified (Section.2.8) or extracted from gel (Section.2.6), cloned and sequenced (Section.2.4 and 2.9).

Primer	Forward/Reverse (5'...3')	Tm °C	Expected Size of product (bp)
OsPTC1 385-386	TGGACATCAAGCACTTCGTCAAA/ TAACAGTTGAAGGACGGGAACGA	60	587
HvMS1-1	AGACCAAGTGCTGGTCGTTC/ GTGCAAGGCTGAGCAAATG	63	502
HvMS1-3	AGGCATCTGATATGCAGCAA/ CTGATGGCCTGGTACTTGGT	65	642
HvMS1-16	TCACCAAGTACCAGGCCATCA/ ACATGTCCCTGAACAGCCTCT	64	800

Table.6.1. Primers designed using *OsPTC1* (*AtMS1* orthologue) as a template (OsPTC1385-386 to 389-390; Fig.6.2a). Moreover, additional primers were designed using the most conserved areas, between *OsPTC1-Bradi4g31760* (HvMS1-1 to HvMS1-16; Fig.6.2b). Other primers combinations were also combined in order to amplify a clear PCR product.

6.2.3 RACE-PCR.

RACE-PCR was conducted to obtain the full length sequence of *HvMS1* (Fig6.3). Total RNA was isolated from barley ears (3.5-4.5 cm long) as previously described (final tetrad stage to early microspore release, section.3.3.3). 5′ and 3′ RACE-PCR were conducted using the GeneRacerTM kit (Invitrogen) according to the manufacturer instructions.

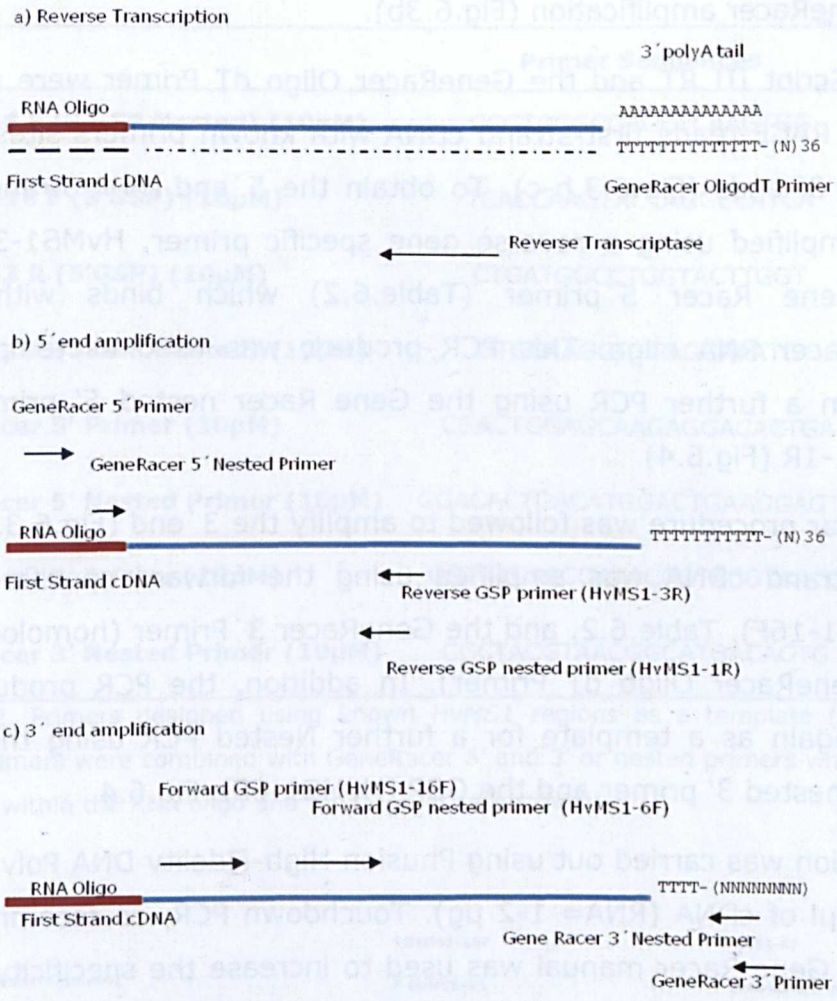

Fig.6.3 RACE-PCR reaction. a) Reverse transcription using an Oligo dT primer which included a PCR primer site. b) 5´end amplification. GeneRacer 5´primer and Reverse Gene Specific Primers were used for 5´amplification. c) 3´ end amplification. GeneRacer 3´Primer and Forward Gene Specific primers were used for the 3´amplification.

The mRNA was reverse-transcribed using the GeneRacer TM oligoTM primer (Invitrogen) (Fig.6.3a). Total RNA was first treated with calf intestinal phosphatase (CIP, 10u/µl) for 1 hour (50°C) to remove the 5′ phosphates and eliminate truncated mRNA and non-mRNA from the subsequent ligation with the GeneRacer RNA oligo. This dephosphorylated RNA was then treated with tobacco acid pyrophosphatase for 1 hour at 37°C (TAP, 0.5u/µl) to remove the 5′ cap structure from intact, full length mRNA. Finally the GeneRacer RNA Oligo was ligated to the 5′ end of the mRNA using T4 RNA ligase. The GeneRacer RNA Oligo was used to provide a known priming site for GeneRacer amplification (Fig.6.3b).

SuperScript III RT and the GeneRacer Oligo dT Primer were used to create RACE-ready first-strand cDNA with known primers sites at the 5′ and 3′ ends (Fig.6.3.b-c). To obtain the 5´end, first-strand cDNA was amplified using a reverse gene specific primer, HvMS1-3R, and the Gene Racer 5´primer (Table.6.2) which binds within the GeneRacer RNA oligo. This PCR product, was used as template to perform a further PCR using the Gene Racer nested 5′ primer and HvMS1-1R (Fig.6.4)

A similar procedure was followed to amplify the 3´end (Fig.6.3.c). The first strand cDNA was amplified using the forward specific primer (HvMS1-16F), Table.6.2, and the GeneRacer 3´Primer (homologous to the GeneRacer Oligo dT Primer). In addition, the PCR product was used again as a template for a further Nested PCR using the Gene Racer nested 3′ primer and the GSP (HvMS1-6F), Fig.6.4.

Extension was carried out using Phusion High-Fidelity DNA Polymerase and 1 µl of cDNA (RNA= 1-2 µg). Touchdown PCR, as recommended by the Gene Racer manual was used to increase the specificity of the amplification (98°C 30 sec; 5 cycles of 98°C 20 sec, 72°C 2 min; 5 cycles of 98°C 15 sec, 72°C 2 min; 30 cycles 98°C 15 sec, *°C 25 sec, 72°C 2 min; 1 cycle of 72°C 10 min; hold 4°C). * Tm used depended on the primer set used (Table.6.2). Gradient PCR was also used to improve the results.

Nested PCR was performed to increase the specificity and sensitivity of both 5′ and 3′ RACE-PCR products. The nested PCR was performed using 1 µl of the touchdown reaction and the GeneRacerTM nested primers and Gene-specific nested, HvMS1-1R for 5′ and HvMS1-6F for 3′ (Table.6.2; Fig.6.4). Amplification was conducted using Phusion polymerase enzyme and the reaction consisted on one cycle of 98ºC 2 min; 30 cycles of 98ºC 30 sec, 65ºC 30 sec, 68ºC 2 min; and one cycle of 68ºC 10 min.

Primer	Primer Sequences	Tm°C
HvMS1-6 F (3′GSP Nested) (10µM)	CCGTCGGCGAGCTCAAGTGG	70.7
HvMA1-16 F (3′GSP) (10µM)	TCACCAAGTACCAGGCCATCA	64
HvMS1-3 R (5′GSP) (10µM)	CTGATGGCCTGGTACTTGGT	65
HvMS1-1 R (5′GSP Nested) (10µM)	GTGCAAGGCTGAGCAAATG	63
GeneRacer 5′ Primer (10µM)	CGACTGGAGCAAGAGGACACTGA	74
GeneRacer 5′ Nested Primer (10µM)	GGACACTGACATGGACTGAAGGAGTA	78
GeneRacer 3′ Primer (10µM)	GCTGTCAACGATACGCTACGTAACG	76
GeneRacer 3′ Nested Primer (10µM)	CGCTACGTAACGGCATGACAGTG	72

Table.6.2. Primers designed using known *HvMS1* regions as a template (Fig.6.4). These primers were combined with GeneRacer 5′ and 3′ or nested primers which were included within the RNA oligo and the Oligo dt respectively.

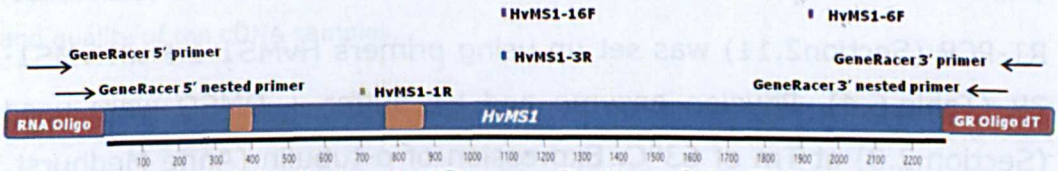

Fig.6.4 Structure of the barley *HvMS1* gene. Position of the RNA oligo, oligo dt (red boxes) and primers used for the amplification of the 5 and 3′ ends are shown (Table.6.2; Fig.6.3). Blue bars indicate exons and orange represent the introns. Scale bar: bp.

6.2.4 RT-PCR analysis.

6.2.4.1 Material collection.

Barley (*Hordeum vulgare*, Optic) was grown in a growth room at 12/15ºC with a 16 hours photoperiod (Section.2.1). Samples were classified from A to H depending on the spike size, going from 0-0.5 cm to >6 cm (Table.6.3). Pseudostems were split open and spikes measured following the spike size prediction model developed in Chapter 3. Spikes <1 cm were used entirely for RNA extraction, however, individual florets were collected from spikes bigger than 1 cm. Florets were collected only from the middle of the spike, and different florets collected from different spikes within the established sample sizes were mixed (Table.6.3). Samples were immediately frozen in liquid nitrogen and finally stored at -80ºC. In addition, samples representative of each group (A to H, Table.6.3) were used for transverse sectioning as described in section.3.2.3.

6.2.4.2 RT-PCR.

Total RNA was extracted from barley tissues using the RNeasy Qiagen kit (Section.2.10). Floral RNA was extracted from the entire ear and individual florets at different developmental stages (Section 6.2.4.1, Table.6.3). RNA was quantified and used for cDNA preparation (Section.2.10-11).

RT-PCR (Section2.11) was set up using primers HvMS1-1 F x HvMS1-3R (Table.6.4). Phusion enzyme and HF buffer + DMSO were used (Section.2.3) at Tm of 63ºC. Expression of α-tubulin (Anne Medhurst, Plant and Crop Science Division) was used to check the integrity and quality of the cDNA samples (Table.6.4), using a standard Taq polymerase reaction (Section.2.3; Tm= 61.3ºC).

	Sample characteristic	Expected Pollen development stage
1(A)	Ear 0-0.5 cm	Archesporial to primary sporogenous cells
2(B)	Ear 0.5-1 cm	Sporogenous Cells
3(C)	Florets ears 1-2 cm	Pollen Mother Cells
4(D)	Florets ears 2-3 cm	Pollen Mother Cells. Meiosis
5(E)	Florets ears 3-4 cm	Tetrad
6(F)	Florets ears 4-5 cm	Microspore release from Tetrad
7(G)	Florets ears 5-6 cm	Early vacuolated microspores
8(H)	Florets ears 6 cm	Vacuolated miscrospores

Table.6.3 Barley floret samples collected based upon ear size criteria (<0.5 cm to >6cm long). As explained in Chapter 3, a relationship was observed between the ear size and anther and pollen development stages.

Primers	**Forward/ Reverse**	**Size (bp)**	**Tm(°C)**
HvMS1-1F/1-3R	AGACCAAGTGCTGGTCGTTC/ CTGATGGCCTGGTACTTGGT	850	63
Alpha-Tubulin	AGTGTCCTGTCCACCCACTC/ AGCATGAAGTGGATCCTTGG	300	61.3

Table.6.4. Primers designed for RT-PCR. PCR was performed using Phusion enzyme (Section.2.3) at Tm of 63°. Expression of α-tubulin was used to check the integrity and quality of the cDNA samples.

6.2.5 *In situ* hybridisation of *HvMS1* in Optic wild type florets.

a) Tissue preparation for microscopy

Individual flowers were collected from optic wt ears at different ear sizes from 1.5 to 6 cm (Table.6.3). Florets were collected from the middle regions of the ears and fixed as follow.

Florets were incubated in fixative, 4% (v/v) paraformaldehyde in PBS (Appendix.1) overnight at 4°C and then washed twice with PBS (pH7.2) at room temperature. Fixed tissues were dehydrated in an ethanol series (30%, 50%, 70%, 90% and twice with 100% (v/v)) for at least 1 hour in each. After the last dehydratation step (100% ethanol) the tissue was cleared by dipping into 2:1, 1:1 and 1:2 (v/v) ethanol/histoclear (Cell-Path) for 1 hour each, and then 3 x 100% Histoclear for 3 min each at room temperature. Tissue was then transferred to a new tube containing 2:1 Histoclear/paraffin (Paramat extra pastille, BDH Laboratoty, Pool, England) at room temperature for 1h, to a 1:1 mixture for 2 h and to 1:2 mixture for 3 h. Finally, the mixture of Histoclear/paraffin was replaced with pure paraffin pellets (previously melted at 60°C) and the tubes containing the tissues were left on a oven at 60°C. The paraffin was replaced after 1 h and these changes were repeated after a further 2-3 hours. Tissue was left in the oven infiltrating, in fresh paraffin overnight. Warm paraffin was poured into plastic boats, placing the samples within the melted paraffin. Wax blocks were cooled in iced water and kept at 4°C until further use. Nine 9 µm sections were cut using a Microtome HM315.

b) RNA probes:

The plasmid pCR Blunt 4-topo (Appendix.2), containing the barley HvMS1-3F/R 500bp cDNA PCR product fragment, was used to synthesise riboprobes of 500 bp length. The sense and antisense digoxygenin-labelled riboprobes were generated by PCR (M13F/R:

Phusion enzyme, section 2.3, Tm=55°C) to obtain the desired fragment for subsequent use as a template by T3 and T7 RNA polymerase (Table.6.5). After synthesis, the probe was re-suspended in 50 µl of DEPC treated water. Probe concentration was checked by a dot-blot hybridisation. A 0.1 µl aliquot of the probe (0.2%) was spotted on to a nylon membrane (N+hybond, GE Healthcare, UK) and the dioxigenin signal (colour) developed according to the manufacturer's instruction (Sigma Fast BCIP/NBT). The colour reactions were monitored and stopped by washing the membrane with TE (10mM Tris-HCL pH 8.0, 1mM EDTA) after 3-12 h. A dark blue non-diffused dot was considered as evidence of a good quality probe.

c) Pre-hybridisation treatments

Slides carrying the sections were dried overnight at 37°C. Wax was removed by immersion in Histoclear (Cell-Path) twice for 15 min and slides were hydrated in an ethanol series (2x100%, 95%, 85%, 70%, 60%, 50%, 30% (v/v) for 1 min in each). Sections were then rinsed with PBS buffer (1.3mM NaCl, 0.03M Na2HPO4, 0.03M NaH2PO4) and proteins were partially removed by incubating in pronase E (Sigma) (0.125mg/l in 50mM Tris-HCl pH 7.5, 5 mM EDTA) for 10 min at room temperature. The deproteinisation solution was removed and the reaction was stopped by adding 0.2% (v/v) glycine. The slides were then washed with PBS and re-fixed with 4% (w/v) paraformaldehyde in PBS for 10 min. Acetylation reduces background by placing acetylation positive charges on the sections and the slides. Following this, they were rinsed with PBS and dehydrated through an ethanol series (30, 50%, 70%, 85%, 95%, 2x 100% (v/v), for 30 sec each). Prior to hybridisation slides were dried in a desiccator at room temperature.

Probe Labelling Reaction	
Template DNA	250-350 ng
Transcription buffer 5x P118B (Promega)	5 µl
DTT 100mM (Promega)	2.5 µl
5mM NTP mix (Promega)	2.5 µl
1mM-Dig-11-UTP 10mM (Roche)	2.5 µl
DEPC water	For a total of 25 µl
RNase inhibitor 40u/µl (Invitrogen)	1 µl
RNA polymerase T3/T7 50u/µl (Stratagene)	1 µl

Table.6.5 Probe labelling reaction.

d) Hybridisation

Once the slides were completely dry they were hybridised using the dioxigenin (DIG)-labelled RNA probes. Denatured probe was added to the hybridisation solution (5ml formamide, 1 ml of 20 x SSPE, 500µl of 100 x Denhardt's solution, 2 ml of 50% (w/v) dextran sulphate, 100µl of 10mg/ml tRNA, 500µl 10% (w/v) SDS, 840µl DEPC water) and 120µl of the resulting hybridisation mixture was applied to each slide. Sections were covered with cover slips, which had been previously baked at 240°C for 3h, placed in a humidified box and hydrolised overnight at 50°C.

e) Post-hybridisation washes

Coverslips were removed by placing slides in a box containing 0.2% x SSC (diluted from 20x SSC: 3M NaCl, 0.3M Na_3citrate) for 5 min. Slides were washed twice with 0.2 x SSC for 1 h at 55°C, washed with NTE (0.5M NaCl, 10mM Tris-HCl pH 7.5, 1mM EDTA), incubated at 37°C in 20µg/ml RNase A (Sigma) in pre-warmed NTE and rinsed

twice in NTE. Finally the slides were incubated for 1 h in 0.2 x SSC at 55°C, 2 min in 2 x SSC at room temperature and washed in PBS. Although slides could be kept in PBS at 4°C for a few hours it was found to be preferable to proceed immediately with detection.

f) Probe detection

Slides were washed in buffer 1 (100mM Tris-HCl, 150mM NaCl pH 7.5) for 5 min, incubated in blocking buffer 2 (buffer 1 containing 0.5% (w/v) blocking reagent (Boehringer Mannheim) for 1 h and then in buffer 3 (buffer 1 containing 1% (w/v) BSA, 0.3% (v/v) TritonX-100) for 30 min. Anti-digoxigenin-alkaline-phosphatase conjugate (Roche) was diluted 1:3000 in buffer 3 and left with the slides for 90 min. Following incubation with the antibody, slides were passed through 3 washes of buffer 3 for 20 min each, rinsed with buffer 1 and equilibrated for 5 min in buffer 4 (100mM Tris-HCl, 100mM NaCl pH 9.5). Hybridisation signal was detected by incubating the slide in fresh buffer 4 containing 50 µl/ml of nitro blue tetrazolium (NBT) (Roche) and 75 µl/ml of 5-bromo-4-chloro-3-indoyl phosphate (BCIP) (Roche). When the colour reaction was completed, they were washed with TE (10mM Tris-HCl pH 8.0, 1mM EDTA) for 5 min and examined under the microscope directly or air-dried and stained using 0.1% (w/v) calcofluor (Sigma). Slides were then examined using bright or dark field simultaneously with UV light after mounting with Entellan (Merck) according to the manufacturer's instructions.

6.3 Results.

6.3.1 *HvMS1* amplification.

6.3.1.1 BLAST analysis.

OsPTC1 (Os09g27620) is thought to be the orthologue gene to *Arabidopsis AtMS1* (Li et al., 2011). Similar putative orthologues have also been observed in other higher plant species (Fig.6.1). Therefore, this transcription factor is also likely to be conserved in temperate crop plants such as barley. BLAST analysis comparing *OsPTC1* against barley EST databases did not identify any equivalent *MS1* (At5g22260) sequence possibly due to the lack of a complete barley genome sequence and also the low expression level expected for the barley orthologue given the absence of *AtMS1* in *Arabidopsis* EST libraries.

Initially, due to the close relationship between rice and barley, and the completion of the rice genome sequencing, rice was thought to be the best template to design primers to amplify similar regions in barley (Fig.6.2.a). However the recent release of the *Brachypodium distachyon* genome, a grass which is closer to barley than rice, proved to be a useful tool to characterize barley genes (Opanowicz et al., 2008).

Comparing *OsPTC1* genomic sequence against the *Brachypodium* database (BLASTN, Appendix.8), a clear match was found (Table.6.6), *Bradi4g31760*. This sequence, 2082bp long, comprised of three exons and two introns, coding a protein of 693 amino acids (Appendix.7).

Nucleotide alignment between *OsPTC1* and *Bradi4g31760* showed similarities greater than 85% (90, 85 and 82% respectively, for the three exons (Fig.6.5; Appendix.8); this equates to 78% similarity at the protein level. Therefore, *Bradi4g31760* was likely to be the putative *OsPTC1* orthologue in *Brachypodium*. However, as before, no

similar barley sequence was found when *Bradi4g31760* cDNA was compared against the DFCI barley data base.

Gene	Amino acids	*AtMS1*	*OsPTC1*	*Bradi4g31760*	*HvMS1*
AtMS1	662	-	53.3%	54%	-
OsPTC1	679	53.3%	-	85%	-
Bradi4g31760	693	54%	85%	-	-

Table.6.6 BLASTn analysis between *AtMS1/OsPTC1* and the *Brachypodium* and barley databases. Similarities between *AtMS1* and *OsPTC1* were 53%. A putative orthologue was found in Brachypodium, *Bradi4g31760*, which showed 54% and 85% similarity to *AtMS1* and *OsPTC1* respectively. No equivalent sequence was found in barley. Protein length of the AtMS1 and the putative othologues in rice and *Brachypodium*, OsPTC1 and Bradi4g31760, are represented in the second column.

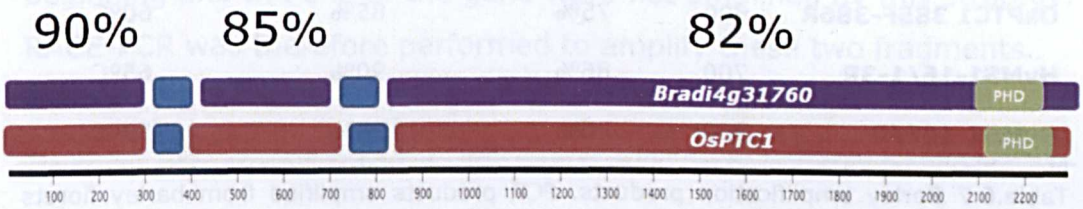

Fig.6.5 Alignment between *OsPTC1* and *Bradi4g31760* genomic sequences. Nucleotide alignment showed high similarities for the three exons (90, 85 and 82% respectively). Purple and red bars represent the exons. Light Blue boxes represent the introns. A PHD domain was also detected at the end of the third exon (green boxes). Scale bar: bp.

6.3.1.2 *HvMS1* amplification.

The failure to obtain any candidate from BLAST analysis of barley sequences using *OsPTC1* and *Bradi4g31760* indicated that a different approach was required to identify the orthologue sequence in barley.

Primers, designed using *OsPTC1* and the conserved regions between *OsPTC1/Bradi4g31760* as a template (Fig.6.2a,b; Table.6.1), were used to perform a series of PCR reactions using barley cDNA (Section.6.2.2). Reactions were set up using Phusion polymerase enzyme (Section.2.3; Table.6.7). Three primer pairs were successful in amplifying barley sequences of the expected sizes (Fig.6.7). Sequence alignment to *OsPTC1* and *Bradi4g31760* showed high similarities (Table.6.7) to *OsPTC1* template and even higher to *Bradi4g31760*. Barley amplification products were aligned to *OsPTC1* and *Bradi4g31760* in order to see the regions where these barley sequences matched to (Figure.6.6). The BLASTN analysis between these barley sequences using NCBI, DFCI and PLexdB barley database (Affymetrix 22K Barley1 GeneChip) did not generate any targets of significant similarities.

Primers	bps	~OsPTC1	~Bradi4g31760	Tm
OsPTC1 385F-386R	600	75%	85%	60°C
HvMS1-1F/1-3R	700	86%	90%	65°C
HvMS1-16F/R	800	86%	90%	59°C

Table.6.7 Barley amplification products. PCR products amplified from barley florets (Spike 3.5-4.5 cm) cDNA showed high similarities to the templates used for primer design (OsPTC1/Bradi4g31760).

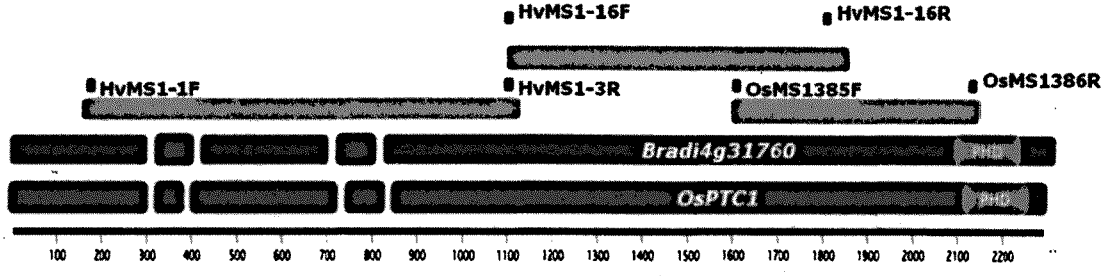

Fig.6.6 Alignment between *HvMS1* amplification products (Table.6.7) and its putative orthologues in rice and *Brachypodium* (*OsPTC1/Bradi4g31760*). The orange bars represent the barley PCR products amplified using the primers designed using *OsPTC1/Bradi4g31760* as templates (Table 6.7; Fig.6.2). Purple and red bars represent the *Bradi4g31760/OsPTC1* exons respectively. Light Blue boxes represent the introns. A PHD domain is also indicated for *OsPTC1/Bradi4g31760* at the end of the third exon (green boxes). Scale bar: bp.

Alignment between HvMS1-1Fx1-3R cDNA amplification product and *OsPTC1/Bradi4g31760* gDNA suggested that two regions were missing from the barley sequence. The alignment showed that the PCR product found the following similarities; 100 bps before the first exon, the whole second exon and 400 bps at the beginning of the third exon. The alignment was broken coinciding exactly where the first and second rice template introns were found. Barley gDNA amplification using the same set of primers generated a 200 bps bigger PCR product cDNA template (Fig.6.7b), which upon sequencing confirmed the presence of introns within the amplification region of these primers.

The full *HvMS1* gene sequence aligned using the derived PCR products. The results are showed below (Fig.6.8). Intron position within the barley sequence was based on the above previous alignment of the HvMS1-1Fx1-3R cDNA PCR product and the OsPTC1/Bradi4g31760 genomic DNA. Only two regions, at the beginning and the end of the gene were not amplified by this strategy. RACE-PCR was therefore performed to amplify these two fragments.

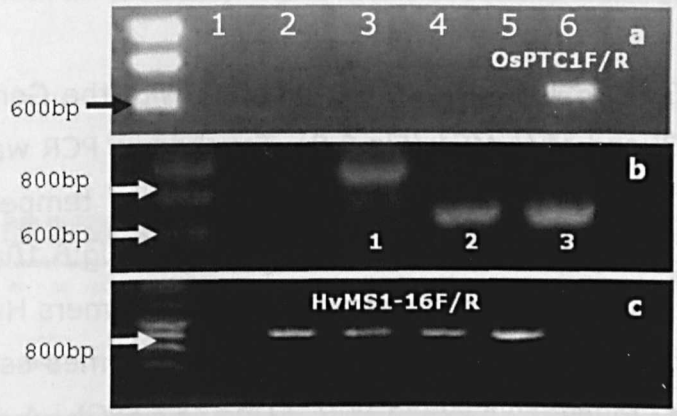

Fig.6.7. Barley PCR amplification products using primers from Table.6.1. a) Lane 6: OsPTC1.385F-386R primers amplified a 650bp fragment in barley. b) HvMS1-1FxHvMS1-3R barley amplification product. Lane 1 shows the amplification performed on barley gDNA, whereas lanes 2 and 3 were amplified using cDNA from flower buds. c) HvMS1-16F/R barley amplification product. These primers were designed using the sequences amplified by OsPTC1.385F-386R and HvMS1-1FxHvMS1-3R (a and b) (Fig.6.6).

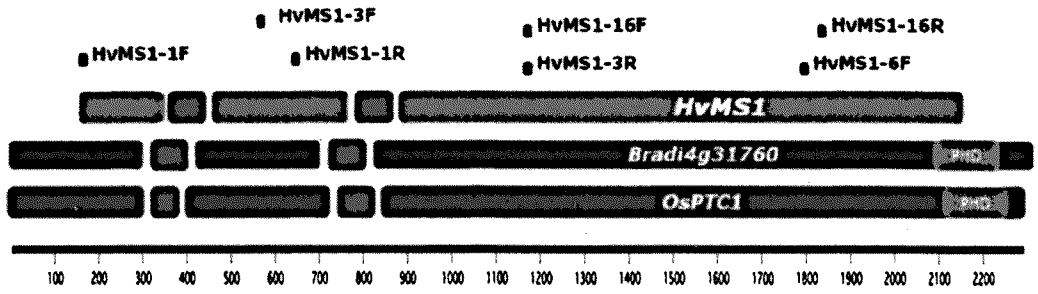

Fig.6.8 Alignment between the partially amplified *HvMS1* (orange bars, 5-3′ ends have not been amplified) and its putative orthologues *OsPTC1* and *Bradi4g31760* (purple and red bars represent the exons and light blue boxes represent the introns). Primers used for *HvMS1* amplification are shown. After the amplification of different regions of *HvMS1* (Fig.6.7), a continuous sequence was generated from the first to the third exon. Scale bar: bp.

Therefore, these results support the hypothesis that *AtMS1* might be conserved in higher plants such as rice, *Brachypodium* and also barley. Further experiments were conducted to complete the *HvMS1* sequence as well as expression analysis and characterization of this gene function in barley.

6.3.1.3 RACE-PCR

Primer HvMS1-16F was used in combination with the GeneRacer 3′ to amplify the 3′ end of *HvMS1* (Fig.6.9). Touchdown PCR was performed (Section.6.2.3) using 62.5ºC as the melting temperature. This reaction did not produce a clear PCR product (Fig.6.10a), however, was used as template for the nested PCR using primers HvMS1-6F and 3′ Nested primer (Fig.6.9). Nested PCR was performed using one µl of the previous touchdown Race-PCR (Tm= 62.5ºC). A specific PCR product was obtained from this amplification (Fig.6.10b). This was gel extracted, purified and used for cloning. Clones were PCR screened and positive colonies were cultured for plasmid extraction and sequencing. The sequence generated (Appendix.10) matched the 3′ end of *OsPTC1 and Bradi4g31760* (Table.6.8).

The 5′ end amplification followed a similar procedure. Touchdown PCR was performed combining the GeneRacer 5′ Primer included within the RNA added to the 5′ end (Section.6.2.3; Table.6.2) and HvMS1-3R (Fig.6.9; Tm= 65ºC). Similar non-specific results were obtained (Fig.6.10c). One µl of this PCR product was utilized for Nested PCR that combined the GeneRacer 5′Nested and HvMS1-1R primers (Fig.6.9). Gradient PCR was performed using 60, 61.4, 63.3, 64.4 and 65ºC as melting temperatures. A clear product was amplified at 60 and 61.4ºC (Fig.6.10d, lane 1 and 2N). After sequencing (Appendix.10), the result matched exactly with the 5′ end of *OsPTC1/Bradi4g31760* (Table.6.8).

	Size bp	Similarity to OsPTC1	Similarity to Brady4g31760
3´end	573	83%	92%
5´end	572	85%	90%

Table.6.8 BLAST analysis results performed between the 5′ and 3′ ends of *HvMS1* amplified using RACE-PCR against *OsPTC1* and *Bradi4g31760*. Results show clear similarities between the two barley fragments and its putative orthologues.

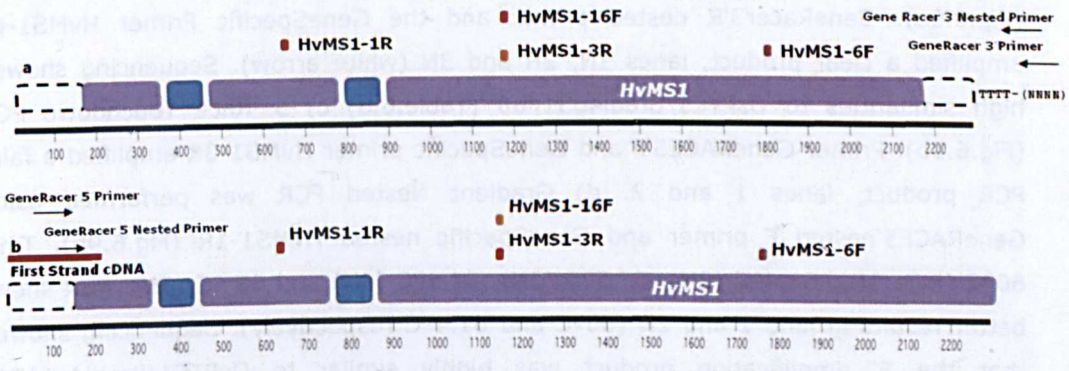

Fig.6.9 a) 3′ RACE-PCR of the *HvMS1* gene. Touchdown PCR was performed using the GeneRacer 3′ primer and HvMS1-16F. Nested GeneRacer 3′ primer was then combined with HvMS1-6F for nested PCR amplification. b) 5′ RACE-PCR. Touchdown PCR was performed using the GeneRacer 5′Primer and HvMS1-3R. Nested GeneRacer 5′ primer was then combined with HvMS1-1R for nested PCR amplification. Scale bar: bp.

The full length sequence of HvMS1 as identified from the RACE-PCR showed high similarities to the *OsPTC1/Bradi4g31760* sequences (Fig.6.11). The *HvMS1* cDNA was 2018 bps long and comprised of two introns and three exons (Fig.6.11). Translation of *HvMS1* (MacVector) indicated that HvMS1 protein, which showed very high similarities to its othologues in rice and *Brachypodium* (Fig.6.12), was 668 amino acids long and included a conserved PHD domain at the C terminal region (Fig.6.11). No sign of the Leuzine zipper, present in *AtMS1* (Section.1.2.3, Chapter 1), was found within the three grasses genes No other motifs were detected in the putative HvMS1 sequence.

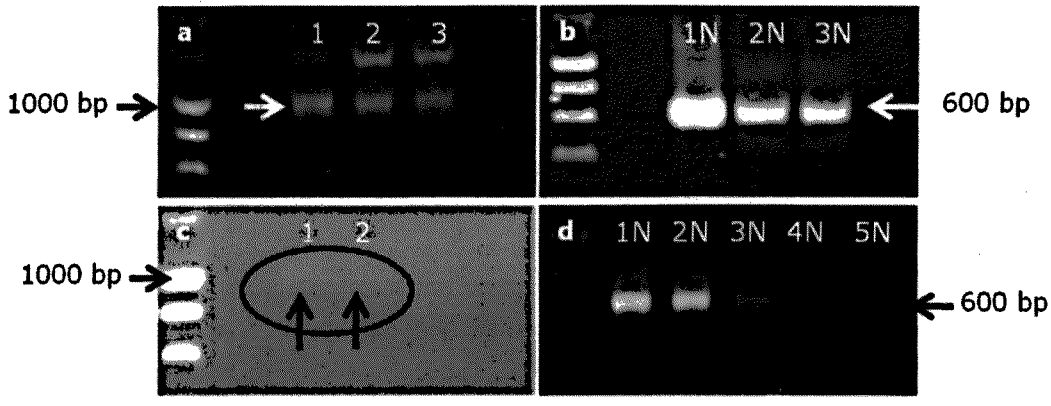

Fig.6.10. RACE-PCR reaction. a) Touchdown PCR reaction performed using HvMS1-16F and GeneRACE 3´primers (Fig.6.9a). Lane 1, 2 and 3 show a non-specific amplification. The white arrow marks the expected product size. b) 3' Nested PCR (Fig.6.9a). GeneRacer3'R nested primer and the GeneSpecific Primer HvMS1-6F amplified a clear product, lanes 1N, 2N and 3N (white arrow). Sequencing showed high similarities to OsPTC1/Bradi4g31760 (Table.6.8) c) 5'. Race Touchdown PCR (Fig.6.9b). Primer GeneRACE5'F and GeneSpecific primer HvMS1-3R amplified a faint PCR product, lanes 1 and 2. d) Gradient Nested PCR was performed using GeneRACE5'nested F primer and GeneSpecific nested HvMS1-1R (Fig.6.9b). Tm= 60°C (lane 1N), 61.4°C (2N), 63.3°C (3N), 64.4°C (4N) and 65 °C (5N). PCR shows better results in lane 1 and 2N (60°C and 61.4°C respectively). Sequencing showed that the 5' amplification product was highly similar to OsPTC1/Bradi4g31760 (Table.6.8).

a

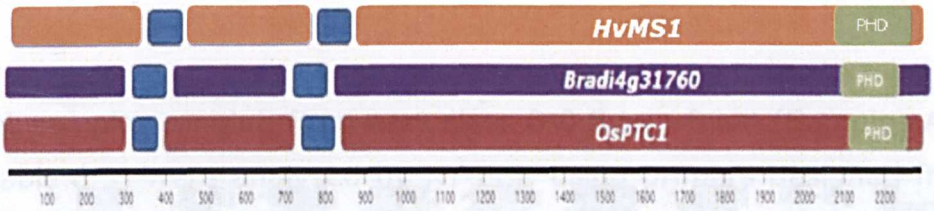

b

Gene	Gene bp	Exon 1	Exon 2	Exon 3	Protein length	Protein/ Protein
OsPTC1	2040bp	92%	83%	88%	679	83%
HvMS1	2007bp				668	

c

Gene	Gene bp	Exon 1	Exon 2	Exon 3	Protein length	Protein/ Protein
Bradi4g31760	2082bp	92%	92%	90%	693	83%
HvMS1	2007bp				668	

Fig.6.11 Gene and protein alignments of *AtMS1* putative orthologues. a) Alignment of *HvMS1/ Bradi4g31760/ OsPTC1* gDNA. *HvMS1* shows a similar gene structure to *OsPTC1* and *Bradi4g31760,* three exons (orange, purple and red bars respectively) and two introns (light blue boxes). BLASTn (exon/exon) and BLASTp between *OsPTC1/HvMS1* (b) and *Bradi4g31760/HvMS1* (c) analysis are represented. In addition, a conserved PHD domain was identified at the end of the third exon in all three genes (green boxes). Percentages of similarities between the three genes are very high both at the DNA and protein level (Figure.6.12; Appendix.9). Scale bar: bp.

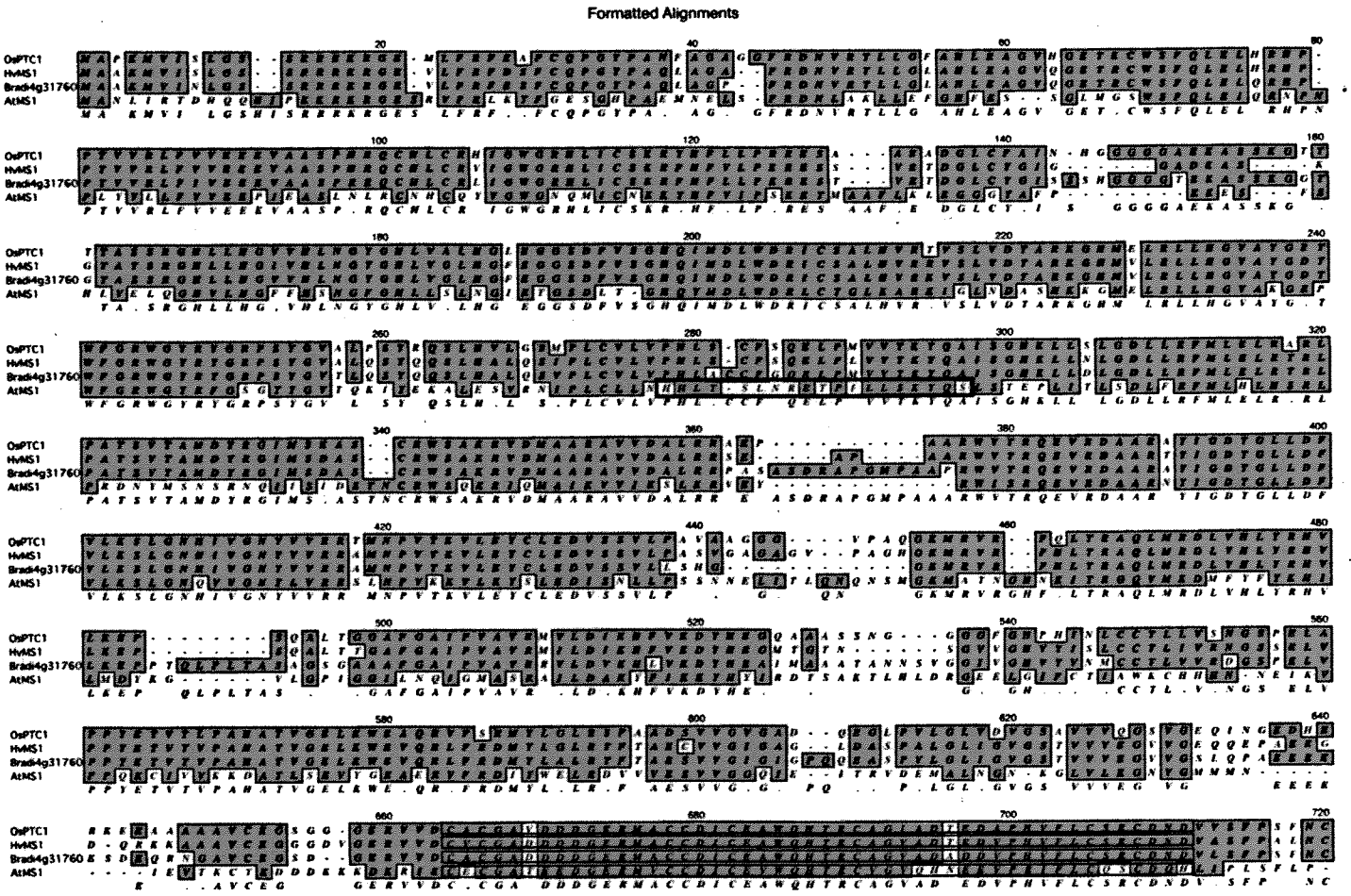

Fig.6.12 Alignment between AtMS1, OsPTC1, HvMS1 and Bradi4g31760 proteins. The Leucine zipper present within AtMS1 sequence is underlined (Blue). In addition, PHD finger domain was labelled in red for the four proteins.

6.3.2 Expression analysis.

Floret samples ranging from ears sizes 0-0.5 to >6 cm (Samples A to H, Table.6.3) were analysed by RT-PCR using primers designed from the barley sequence and OsPTC1/Bradi4g31760 conserved regions (Table.6.1).

To confirm the stages of the material collected for RT-PCR, anther transverse sections were analysed for representative samples from stages C to H (Fig.6.13c). Samples A and B were not represented due to the size of the sample. In sample C, sporogenous cells up to early PMC were observed, whereas PMCs undergoing meiosis were seen in sample D. Sample E showed late tetrad stage, while in F early microspores release from tetrad was observed. In samples G and H, late microspores and vacuolated microspores were seen respectively (Figure.6.13c).

HvMS1-1F/HvMS1-3R primers (Table.6.1) gave a highly specific RT-PCR product. Fig.6.13a shows the RT-PCR reaction performed using the samples from A to H (Table.6.3). No amplification was obtained for the first five samples, A (ear 0-0.5 cm) to E1 (ear 3-4 cm), (Fig.6.13a). Amplification products were seen in samples E2 (Ear 3-4 cm,), F (Ear 4-5 cm) and G (Ear 5-6 cm), but no expression was seen in sample H (Ear >6 cm). These results indicate that the *HvMS1* gene is expressed between microspore release from the tetrad and early microspore maturation. Samples were normalized using the α-tubulin gene (Fig.6.13b; Section.6.2.4.2). Genomic DNA was used as a PCR control and generated a larger fragment than the cDNA samples due to the presence of the first intron in the genomic amplification region (Fig.6.13a white arrow).

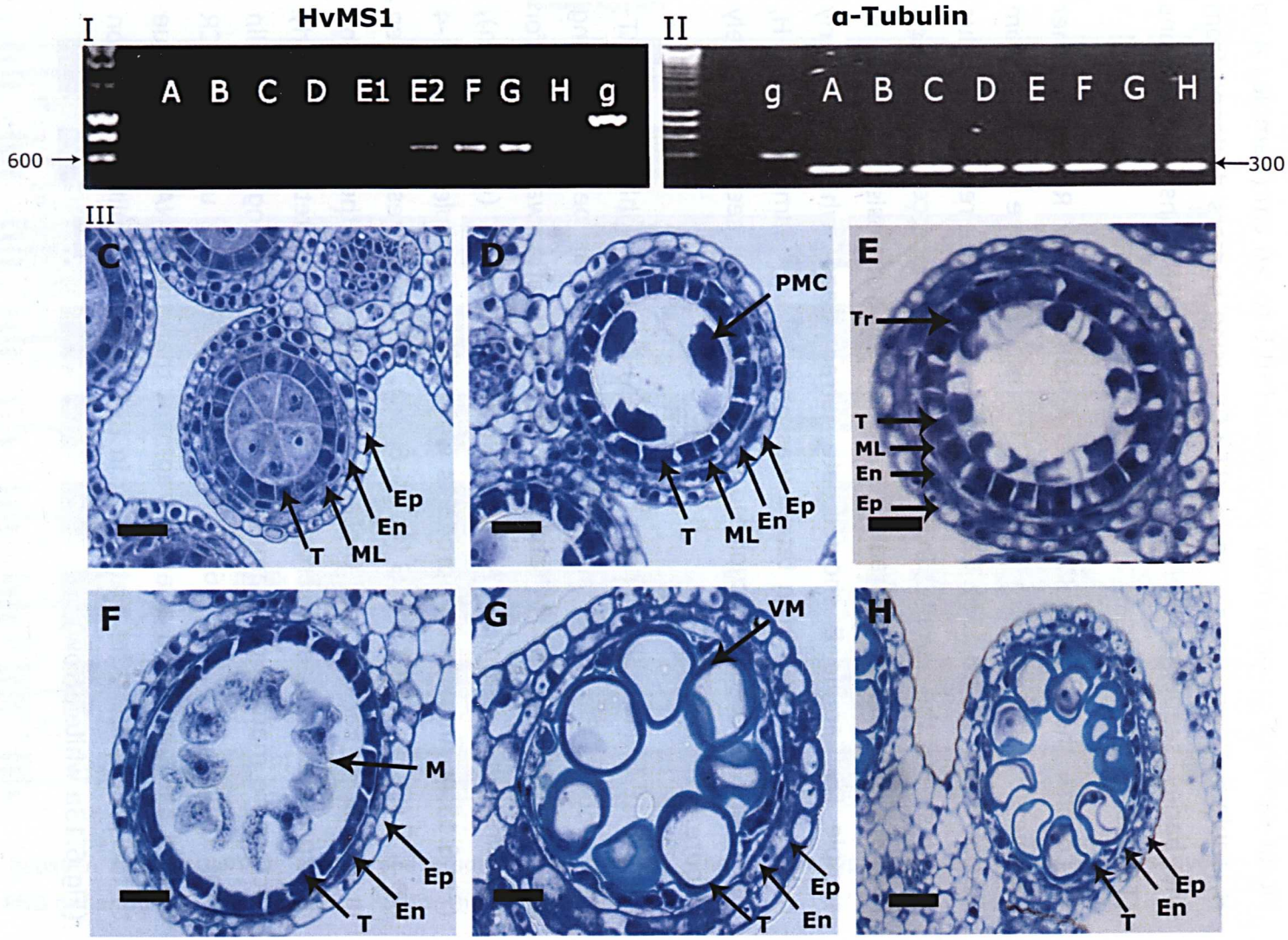
I
HvMS1
A B C D E1 E2 F G H g
600
II
α-Tubulin
g A B C D E F G H
300
III
C
Ep
En
T
ML
D
PMC
T
ML
En
Ep
E
Tr
T
ML
En
Ep
F
M
Ep
En
T
G
VM
Ep
T
En
H
Ep
En
T

Fig.6.13 *HvMS1* expression analysis. I) HvMS1-1F x HvMS1-3R RT-PCR reaction. Different cDNA samples going from stages before PMC to vacuolated microspore were analysed. Samples A to H were collected following the predictions of buds size (Table.6.3). Only samples E2, F and G generated and amplification product. II) A to H samples were normalized using the Alpha tubulin gene RT-PCR (Section.6.2.4.2). III) Anther and pollen development stages in barley. These transverse sections (Toluidin blue staining, Section.3.2.3) represent examples of the staged samples used for RT-PCR. Sporogenous cells- early Pollen Mother Cells (C), PMC at meiosis (D), late tetrad stage immediately prior to microspore release (E), early microspore release (F), late microspore release (G) and vacuolated microsopore (H) are showed. Bars 30 µm. Ep: Epidermis; En: Endothecium; ML: Middle layer; T: Tapetum; PMC: Pollen Mother Cells; M: Microspores; VM: Vacuolated microspores.

6.3.3 *In situ* hybridisation.

In order to further investigate *HvMS1* expression and to determine more precisely its spatial and temporal expression pattern, RNA *in situ hybridisation* was performed using wild type (Optic variety) anther sections (Fig.6.14). Fig.6.14 shows *HvMS1* RNA *in situ* hybridisation of the sense (E-F; Spikes 2-3 and 4-5 cm respectively) and antisense (A-D; Spikes 2-3, 3-4, 4-5 and 5-6 cm) probes to transverse sections of florets. Results showed that *HvMS1* expression was restricted to the tapetum (Fig.6.14B) within the spike size range of 3-4 cm (Fig.6.14B).

6.3.4 Further gene characterization.

Several *Arabidopsis* genes, involved in anther and pollen development (Fig.1.9), such as *EXS/EMS1, DYT1* or *AMS,* have been identified and characterized in rice (*MSP1, UTD1* and *TDR* respectively) (Nonomura et al. 2003; Zhang et al., 2006; Sorensen et al., 2003; Xu et al., 2010). BLASTn analysis using these rice sequences against the *Brachypodium* genome showed several significantly similar results (Table.6.9; Fig.6.15). Furthermore, other genes, among them a putative target of *MS1* (Yang et al., 2007), *MYB99*, showed a highly similar sequence in *Brachypodium*. However, no similar sequences to these found in *Brachypodium* were found in barley (Fig.6.9), except for *AtMS2*, a gene thought to be involved in sporopollenin biosynthesis (Aarts et al., 1997), which showed three significantly similar sequences in barley.

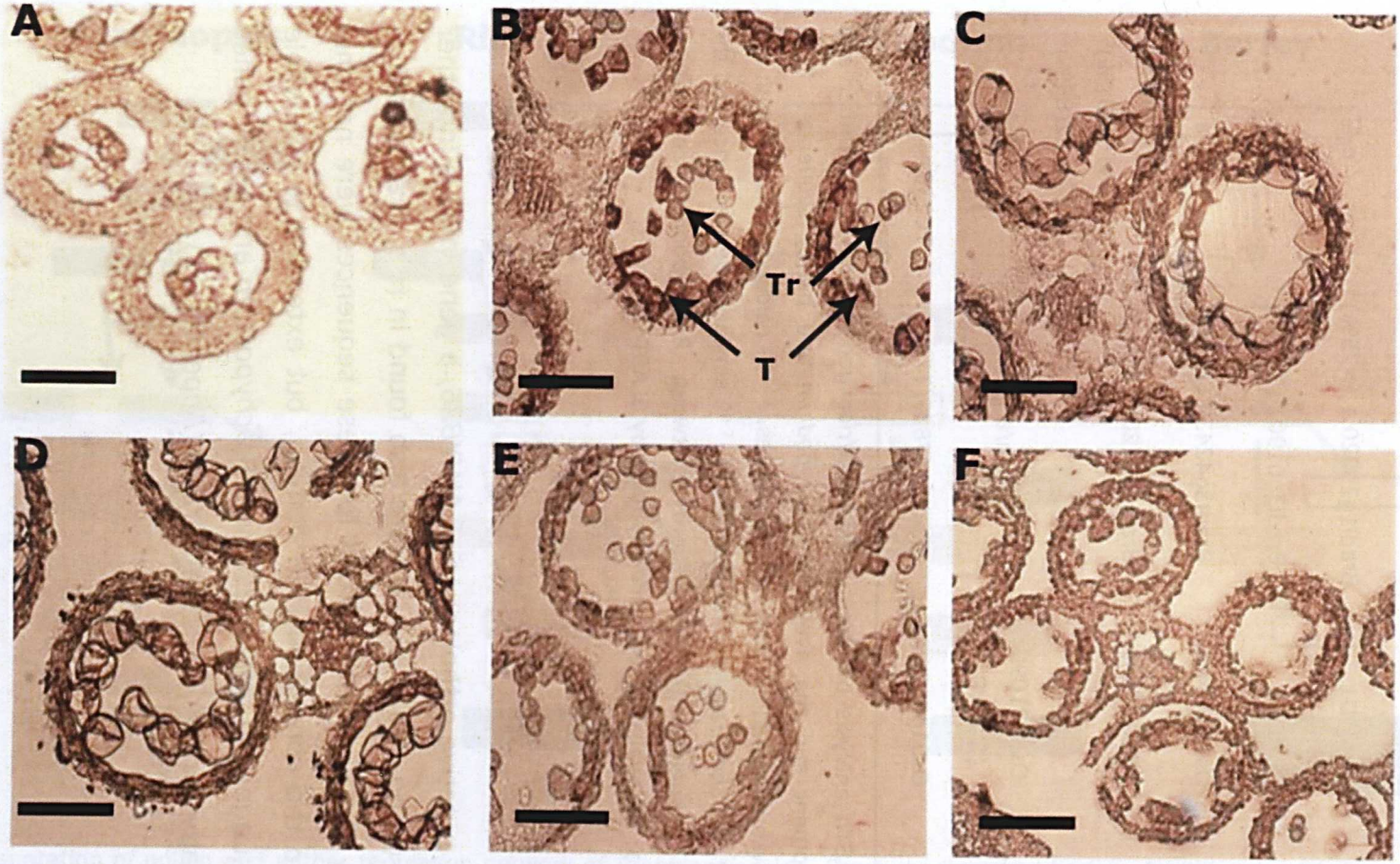

Fig.6.14 *HvMS1* RNA *in situ* hybridisation to transverse anther sections of barley. A) Antisense probe, samples 2-3 cm. B) Antisense probe, sample 3-4 cm. Hybridisation signal (arrows) was observed exclusively in the tapetal cells surrounding the tetrad. C) Antisense probe, samples 4-5 cm. No signal detected. D) Antisense probe, samples 5-6 cm. No signal detected. E) Sense control probe, sample 3-4 cm. No signal was detected. F) Sense probe, samples 4-5 cm. No signal was detected. Bars 50 μm. T: Tapetum; Tr: Tetrad.

Arabidopsis	Rice	Brachypodium	Barley
EXS/EMS1	MSP1	Bradi3g06980 (82%) [b]	n/a
DYT1	UTD1	Bradi1g25320.1 (>75%) [b]	n/a
AMS	TDR	Bradi3g01901 (70%) [b]	n/a
MYB99	Os08g43450	Bradi3g42430 (76%)[b]	n/a
MS2	OsMS2 (70%)[a]	Bradi4g01200 (91%)[b]	TC278678(92%)[c] TC259156(91%)[c] TC272182(89%)[c]
MYB33/MYB65	Os6g31090 (GAMYB)	n/a	n/a
MYB26	Os01g51260	Bradi2g47887(77%)[b]	TC236140 (82%) [c]

Table.6.9 BLASTn analysis between *Arabidopsis*/rice genes involved in anther and pollen development and the available *Brachypodium* and barley sequences. [a] % similarity between *Arabidopsis* and rice sequences. [b] % calculated based upon the comparison of rice and *Brachypodium* sequences. [c] % similarity between rice and the *Brachypodium* sequences. [c] % similarity between *Brachypodium* and barley sequences. n/a: NO available sequence identified by BLASTn analysis.

In addition, putative orthologues of *AtMYB26*, a gene involve in anther dehiscence (Yang et al., 2007), were also found in rice, *Brachypodium* and barley. The similarities found for these sequences were not only restricted to the conserved MYB domain, but extended to the whole sequence, suggesting that these rice, *Brachypodium* and barley genes are the putative orthologues of *AtMYB26* (Appendix.11).

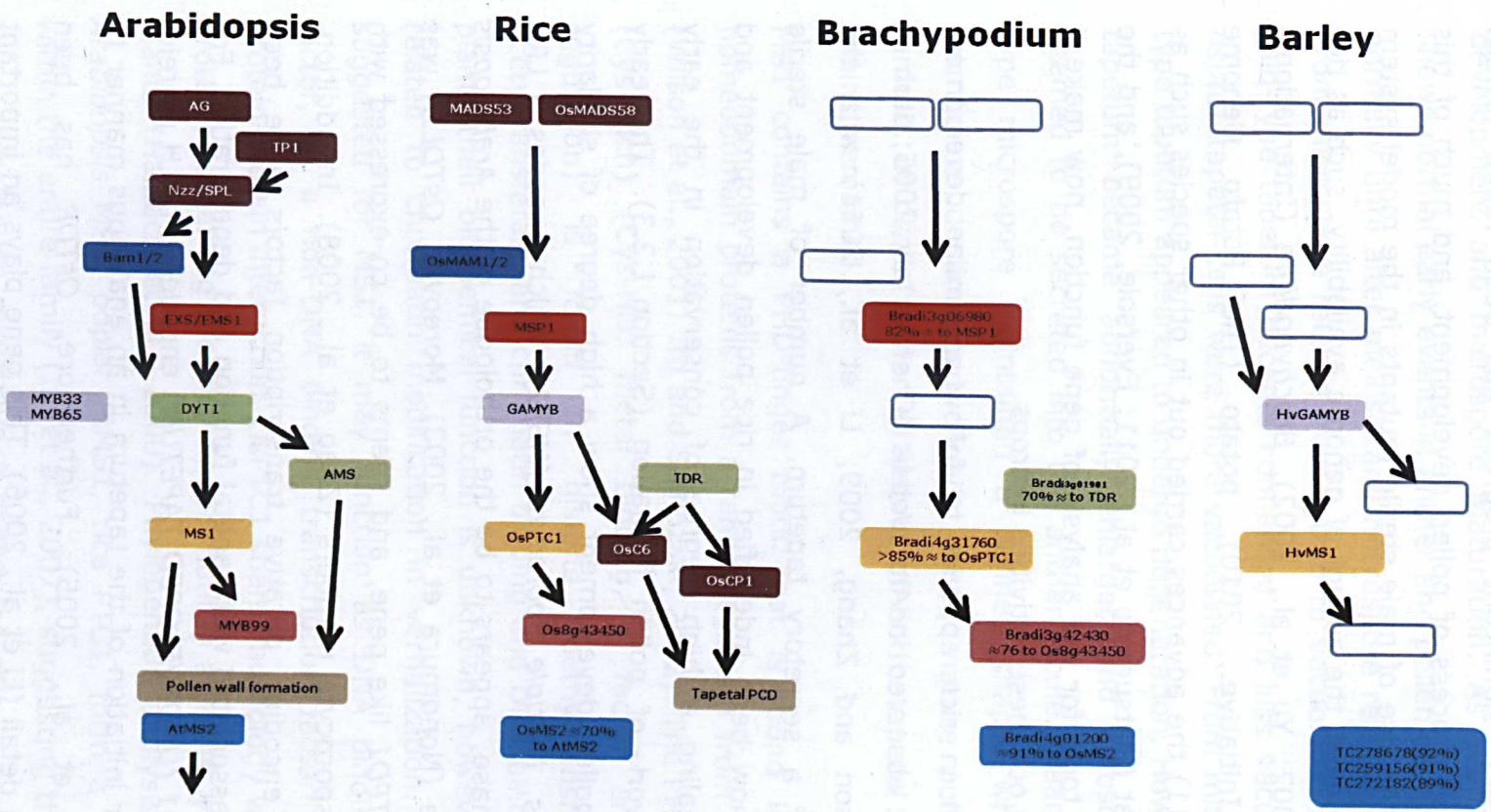

Fig.6.15 Representation of pollen and anther regulation network of *Arabidopsis*, rice, *Brachypodium* and barley. *Arabidopsis* and rice gene regulation networks were taken from Wilson and Zhang, 2009. *Brachypodium* genes were the result of BLASTn analysis between the rice genes and the *Brachypodium* genome, whilst barley sequences were obtained after BLASTn between *Brachypodium* sequences and barley databases available (Section.6.2.1).

6.4 Discussion.

Over recent years, significant progress has been made toward understanding the process of pollen development, and much of this has come from the use of male sterile mutants in the model system *Arabidopsis*. However, the advent of genome availability, such as rice (Goff et al., 2002; Yu et al., 2002), *Brachypodium* (International *Brachypodium* Initiative., 2010), potato (The Potato Genome Consortium, 2011) the advances carried out in other species such as barley and wheat (Matsumoto et al., 2011; Eversole, 2009), and the development of tools for the analysis of gene function, now make it possible to carry out these activities in crops.

Pollen formation in rice appears to follow a similar development pathway to that observed in *Arabidopsis* (Chen et al., 2005; Itoh et al., 2005; Wilson and Zhang, 2009; Li et al., 2011) with the development of a secretory tapetum. A number of male sterile mutants have now been indentified in rice pollen development and these are revealing a high degree of conservation in the early regulatory network of pollen formation (Section.1.2.3). The early stages of rice pollen development show a high degree of similarity with *Arabidopsis*. *Multiple Sporocyte (MSP1),* which encodes a LRR receptor-like kinase, appears to be the orthologue of the *Arabidopsis EMS1/EXS* gene (Nonomura et al., 2003). Moreover, *OsTDL1A* was reported as a *TPD1* like gene, and seems to be co-expressed with *MSP1* to limit sporocyte numbers (Zhao et al., 2008). In addition, several genes encoding putative transcription factors have been reported to be associated with tapetal function and degeneration. For instance *OsUTD1 (UNDEVELOPED TAPETUM)* encodes a bHLH protein, which acts after initiation of the tapetum in an analogous manner to *AtDYT1* (Jung et al., 2005). Furthermore, *OsTDR* has been characterized in detail (Li et al., 2006). This gene plays an important role during rice tapetal development and pollen formation in rice. Phylogenetic analysis suggests that *OsTDR* is an orthologue of the *Arabidopsis ABORTED MICROSPORES* (AMS).

It has also been reported that *OsPTC1*, an essential gene for pollen formation in the monocot crop rice, is the orthologue of the *Arabidopsis MS1* gene (Li et al., 2011). *MS1* is required for tapetal development and microspore maturation. As seen in *ms1*, *osptc1* shows normal early events in anther and pollen development progress normally until after meiosis and microspore release (Li et al., 2011). From microspore release from tetrad to vacuolated microspores, the wild-type tapetum became condensed and less vacuolated, whereas *osptc1* tapetal cells were more vacuolated. From mitosis I, the wild-type tapetum appeared to undergo degeneration. However, the *osptc1* tapetum became abnormally enlarged and cytosolic constituents seemed to be secreted into the anther locule. Meanwhile, the wild-type microspore maintained a defined shape, whilst the *osptc1* microspore degenerated. Finally, when mature pollen grains were formed, in *osptc1* only cell debris of both, tapetal cells and pollen grains, remained.

MS1 contains a PHD-finger motif that is found in a number of homeodomain proteins from a range organism from human to yeast (Wilson et al., 2001; Ito and Shinozaki, 2002). The PHD finger domain (Cys rich) (Cys-His, metal binding, T factor and transcription regulation) is found in histone methyltransferase, histone acetyltransferase and chromatin binding and DNA binding proteins. In plants their biochemical function is unknown, however, it has been related to chromatin modification in vernalization. Two roles are suggested for MS1, it may function as DNA binding transcription factor, or a non-DNA binding transcription factor which acts via protein-protein interaction. OsPTC1 shares homology with a number of proteins containing the PHD-finger motif in animals, yeast and higher plants (Halbach et al., 2000). Phylogenetic analysis indicates that *Arabidopsis* MS1, poplar PtMS1, rice PTC1, form a separate group within the entire family (Ito et al., 2007), suggesting that PTC1 and its close homologues may have a conserved role in plant reproductive development. Consistent with this hypothesis, *PTC1* driven by *MS1* promoter is able to rescue pollen wall development and pollen fertility

of the homozygous *ms1* mutant, suggesting a conserved role regulating programmed anther development in monocot and dicot species (Li et al., 2011).

Extension of this knowledge to other monocot crops such as barley has encountered certain difficulties derived from the lack of a completely sequenced genome. In addition to this, the expected low expression level of the *MS1* orthologue in barley, based on the expression levels observed in *MS1* and *OsPTC1* (Wilson et al., 2001; Li et al., 2011), made the isolation of this orthologue gene within the barley EST sequences available very challenging in the absence of full genome sequence.

Successful amplification of the *MS1* orthologue in barley, *HvMS1*, were facilitated by the conservation of *MS1* orthologues within higher plants. This conservation was extended to *Brachypodium*, a model grass for which the genome has recently been released. For instance, gene order or synteny is largely conserved between *Brachypodium* and the small grain cereals (Aragon-Alcaide et al., 1995; Foote et al., 2004; Moore et al., 1993), which has been instrumental for the characterization of the wheat gene *Ph1* (Griffiths et al., 2006) and the barley gene *Ppd-H1* (Turner et al., 2005). After BLAST analysis between *MS1* and *OsPTC1* against the *Brachypodium* database (Bd21 8x release, www.*Brachypodium*.org), it was clear that *Bradi4g31760* was the putative orthologue of *MS1* in *Brachypodium* (Appendix.8), and therefore, due to the close relation between *Brachypodium* and barley (Opanowicz et al., 2008), suggested a high likelihood of finding an orthologue in barley. This was confirmed when a barley gene, *HvMS1*, was amplified using primers designed based upon the conserved regions of the *OsPTC1/Bradi4g31760* alignment. The high similarities of the *HvMS1* nucleotide and protein sequences to the rice and *Brachypodium* orthologues (Appendix.9; Fig.6.12), make this gene a candidate otholog of *AtMs1* in barley. In addition, the HvMS1 protein includes also a PHD finger domain within its sequence. This PHD finger domain, as in OsPTC1 (Li et al., 2011), comprises about 50-80 amino acids and contain conserved Cys4-His-Cys3 motif,

indicating that HvMS1 may play a similar role in anther development. In addition, the HvMS1 protein as its orthologues in rice and *Brachypodium*, does not include the Leucine zipper (LZ), which is present within the AtMS1 protein. The LZ has been reported in dimeric complexes formation (Liu et al., 1999). However, *Atms1* allelic mutants all show a similar phenotype of male sterility regardless of the presence of the LZ motif (Wilson et al., 2001), implying that this region may be of secondary importance compared to the PHD-finger motif. Therefore, the lack of this domain within the three grasses mentioned might be due to conserved evolution, which does not alter the gene's primary function.

Expression analysis reinforced the hypothesis that *HvMS1* is the likely putative orthologue of *MS1* in barley. *HvMS1* gene showed a highly localized temporal and spatial expression pattern as seen in *MS1* (Wilson et al., 2001), around the stage of late tetrad to early microspore release (Fig.6.13a, samples E to G). No expression is seen in early stages such as sporogenous cells, pollen mother cells, or in latest stages such as vacuolated microspores (Fig.6.13a, samples C, D and H). Differences in *HvMS1* expression in samples E1 and E2 (Fig.6.13a) may be explained by the temporally regulated expression of this gene. Although samples E1 and E2 were collected from the same ear size samples 3-4 cm, the RNA was extracted from different florets collected from different spikes, which may show slightly different stages in terms of pollen development. This may therefore cause the apparent differences in expression level in the samples. In addition, a more detailed expression analysis using *in situ* hybridization showed that *HvMs1* is specifically expressed in the tapetum at the late tetrad stage (Fig.6.14B). This localised expression coincided with the tissue specificity expression of *MS1* and *OsPTC1* observed in *Arabidopsis* and Rice respectively (Yang et al., 2007; Li et al., 2011). Therefore, *HVMS1* shows similarities to *AtMS1* and *OsPTC1*, not only in sequence, but also in expression pattern. The observed tissue specificity indicates that *HvMS1* may play a role during for pollen development in barley. In order to clarify the role of HvMS1,

RNAi silencing was conducted (Chapter 7). Silenced plants were expected to present a similar sterile phenotype to that observed in *Arabidopsis* and rice *ms1* and *osptc1* mutants (Wilson et al., 2001; Li et al., 2011) with special deficiency in the tapetum. In addition, the HvMS1 sequence was tested for its ability to complement the *Arabidopsis ms1* mutant. This, as observed for OsPTC1 (Li et al., 2011), will reveal whether HvMS1 function is conserved by rescuing fertility in the *ms1* mutant.

HvMS1 characterization has been conducted using intermediate putative orthologue genes from *Brachypodium*. However, the release of new barley sequences (Matsumoto et al., 2011) has facilitated the identification of other barley putative orthologues genes that are possibly involved in anther and pollen development. BLASTn analysis using rice sequences against the *Brachypodium* database showed similarities to *TDR* (*AMS* orthologue in rice) and *AtMYB26* (an *Arabidopsis* gene essential for anther dehiscence) among other genes (Table.6.9). Although no orthologue have been identified to *AMS* in barley, a very similar barley sequence (82% similar nucleotide/nucleotide) to the *AtMYB26* putative orthologues in rice and *Brachypodium* has been identified (Table.6.9). Other putative orthologues genes that have been identified in rice as involved in pollen regulation genes, such as *MSP1 (EXS/EMS1), UTD1 (DYT1),* were not identified in barley, although some *Brachypodium* sequences were found to be highly similar (Table.6.9; Fig.6.15). It therefore seems likely that these genes are present in the barley genome. However they are currently not represented in the available sequence database. Therefore, as for *HvMS1*, primers designed using the putative orthologues sequences may be required to characterize these genes in barley.

CHAPTER 7.

7. *HvMS1* functional characterization.

7.1 Introduction.

Transgenic technologies are fundamental to state-of-the-art plant molecular genetics and GM crop improvement. The ability to engineer and transfer foreign DNA into the plant nuclear genome has been instrumental in the discovery and isolation of novel genes, for the analysis of gene function and regulation, and for manipulation to introduce new traits and characteristics.

HvMS1, as the putative otholog of *MS1* in barley, is expected to play an important role in pollen development, however, the silencing of this gene is critical to test for any changes in pollen formation and viability and confirm functionality. RNA silencing in plants is a rapid and facile approach for assignment of gene function and virus resistance (Matzke et al., 1998; Lindbo et al., 1993). It allows selective RNA degradation through a mechanism that is given specificity by short interfering RNAs. The RNA silencer sequences are normally delivered as transgenes or as part of virus-vectors. RNAi silencing will be used to reduce the *HvMS1* expression and characterize the gene function. As observed for *OsPTC1* (Li et al., 2011) in rice, *HvMS1* silencing is expected to produce sterile plants, affecting tapetum development and microspores maturation, leading to a non-viable pollen formation and therefore, male sterility.

RNAi is an evolutionary conserved mechanism for gene regulation that is critical for many examples of growth or development. RNA-induced gene silencing (RNAi) was originally observed as an unusual expression pattern of a transgene designed to induce over expression of chalcone synthase in petunia plants (Napoli et al., 1990). Similar results were reported in a range of organisms (Pandit et al., 1992;

Romano et al., 1992; Fire et al., 1991). In the years following these observations, experiments in many model systems contributed to rapid advancement in understanding the underlying mechanism, and RNA-mediated gene silencing processes came to be collectively known as RNA interference (RNAi).

Silencing requires production of small interfering RNA (siRNA), Fig.7.1, corresponding to the target gene. This can be achieved by constructing stable transgenic plants in which the transgene construct generates double stranded (ds) RNA or hpRNA. These are processed to siRNA (20-25 base pairs) in vivo by the endogenous enzyme Dicer (Fire et al., 1998; Hamilton et al., 1999; Zamore et al., 2000; Grishok et al., 2001). One of the two strands of each fragment, known as the guide strand, is then incorporated into the RNA-induced silencing complex (RISC) and pairs with complementary sequences. The most well-studied outcome of this recognition event is post-transcriptional gene silencing. This occurs when the guide strand specifically pairs with a mRNA molecule and induces the degradation by Argonaute, the catalytic component of the RISC complex (Fig.7.1). Another outcome is epigenetic changes to a gene – histone modification and DNA methylation – which affect the levels of gene transcription.

The possibility of using transgenes to generate dsRNAs that would trigger silencing of endogenous genes in a homology dependant fashion was first described in the late 1990s (Waterhouse et al., 1998). It was demonstrated that transgenes that include a segment of gene in an inverted repeat orientation around a spacer region will generate a dsRNA when expressed in plants. This method has been used to silence many endogenous target genes, resulting in a metabolically engineered plant with improved capacity, virus resistance, oil content, and health benefits (Mansoor et al, 2006). In addition, although dsRNAs are efficient at producing siRNAs, the comparative simplicity of hpRNA transgenes has led to the latter being more widely used. The hpRNA transgene is simply composed of a plant promoter and terminator between which an inversely repeated sequence of the target gene is inserted (with a spacer region between

the repeats). The RNA transcribed from such a transgene hybridises with itself to form a hairpin structure. This comprises a single-stranded loop region, encoded by the spacer region, and a base-paired stem encoded by the inverted repeats. The whole length of the stem appears to be used as a substrate for the generation of siRNAs, but few or none are generated from the loop. Since a spacer region is needed for the stability of the transgene construct, but is not involved in siRNA production, an intron sequence is often used in this position, especially as it appears to enhance the efficacy of silencing (Watson et al., 2005; Smith et al., 2000; Wesley et al., 2001).

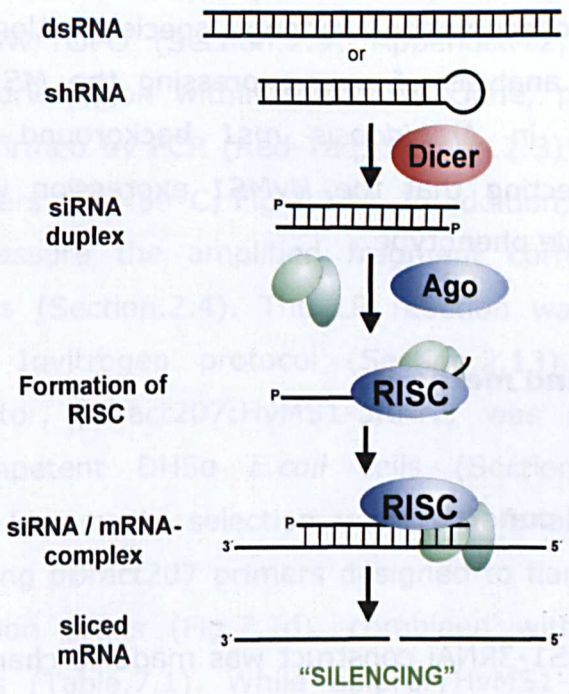

Fig.7.1. A simplified model for the RNAi pathway. This is based on two steps, each involving ribonuclease enzyme. In the first step, the trigger RNA (either dsRNA or miRNA primary transcript) is processed into a short, interfering RNA (siRNA) by the RNase II enzymes Dicer and Drosha. In the second step, siRNAs are loaded into the effector complex RNA-induced silencing complex (RISC). The siRNA is unwound during RISC assembly and the single-stranded RNA hybridizes with mRNA target. Gene silencing is a result of nucleolytic degradation of the targeted mRNA by the RNase H enzyme Argonaute (Slicer). http://www.uni-konstanz.de/FuF/chemie/jhartig/.

MS1 gene over-expression using the CaMV35S promoter in *Arabidopsis* plants, caused a variety of phenotypes. Plants were stunted, often forming flowering stems with only a minimal rosette (Yang et al., 2007). Moreover, depending on the severity of the phenotype, plants showed slower development, densely packed rosettes and short flowering stems. In addition, in some cases, the flowers were semi or completely sterile, however, this sterility broke down as the plant aged. Over-expressing *HvMS1* in barley is expected to show similar phenotypes to those described for *Arabidopsis MS1* over-expression. A similar phenotype for over-expression and a pollen related phenotype for the RNAi analysis would reinforce the hypothesis that *HvMS1* is the putative orthologue of *MS1* in barley and confirm the function conservation among species. Alongside this, a complementary analysis of over-expressing the *MS1* orthologue in barley, *HvMS1*, in *Arabidopsis ms1* background plants will be conducted, expecting that the *HvMS1* expression will recover the *Arabidopsis* sterile phenotype.

7.2 Materials and methods.

7.2.1 Silencing construct.

pBract207::HvMS1-3RNAi construct was made to characterize *HvMS1* function by silencing this gene. pBRACT vectors were chosen due to their suitability for barley transformation (Harwood et al., 2008). The gateway vector pBract207RNAi consists of two Gateway cassettes cloned in opposing directions (Appendix.13). This vector contains the *Ubi1* promoter to drive the RNAi cassette and Hygromycin selection regulated by the CaMV35S promoter. A negative selection gene (*ccdB*) flanked by the gateway recombination sites and controlled by the maize *Ubi1* promoter is included. pBract207 is based on pGreen technology, which is a small, versatile vector designed for easy manipulation in *E.coli* with a high copy number. To allow pGreen to be

of a small size, the pSa origin of replication, required for the replication in *Agrobacterium,* is separated into its two distinct functions. The replication origin (ori) is present on pGreen, and the trans-acting replication gene (RepA) is present on an additional vector, named pSoup. Both vectors are required in *Agrobacterium* for pGreen to replicate.

The silencing construct was made by inserting two opposed *HvMS1* inserts (500bp) amplified by HvMS1-3F/R primers (Table.6.1) into the pBract207 destination vector. This fragment was amplified using Phusion enzyme (Tm=65 °C; Section.2.3). The PCR product was gel extracted and precipitated (Section.2.6). Overhanging reaction (Section.2.16) was conducted previous to cloning into the donor vector, pCR8/GW/TOPO (Section.2.9; Appendix.12; Fig.7.2a). The insert and its orientation within the entry clone, pCR8GW:HvMS1-3F/R, were confirmed by PCR (Red-Taq, Section.2.3) using M13F and HvMS1-3R primers (Tm=59°C; Fig.7.2.b). In addition, sequencing was conducted to assure the amplified fragment corresponds to the expected inserts (Section.2.4). The LR reaction was performed as shown in the Invitrogen protocol (Section.2.13). The resultant expression vector, pBract207:HvMS1-3RNAi, was transferred into chemically competent DH5α *E.coli* cells (Section.2.9). Colonies growing under kanamycin selection were PCR analysed (Red-Taq; Section.2.3) using pBract207 primers designed to flank either side of the two insertion areas (Fig.7.2d), combined with HvMS1-3 F/R specific primers (Table.7.1). While ubiproF/HvMS1-3R allowed the confirmation of the sense insert, its expected size and orientation, iv2intronF/HvMS13F confirmed the antisense insert (Fig.7.2d). Positive colonies for the two inserts were plated onto LB + Spectonomycin (100 µg/ml) for negative screening in order to reject any colony growing on these plates; these colonies are likely to carry the entry and expression vector. The expression vector, pBract207:HvMS1-3 silencing, was extracted from the selected colonies and electroporated alongside pSoup into the *Agrobacterium* strain AGL1 identify (Section.2.15) *Agrobacterium* colonies were PCR analysed to localise

colonies carrying the expected construct plus the insert using the double primer combination mentioned above (Fig.7.2d). Positive colonies for the construct and carrying the inserts in the expected orientation were used for cryo stock (Section.2.18).

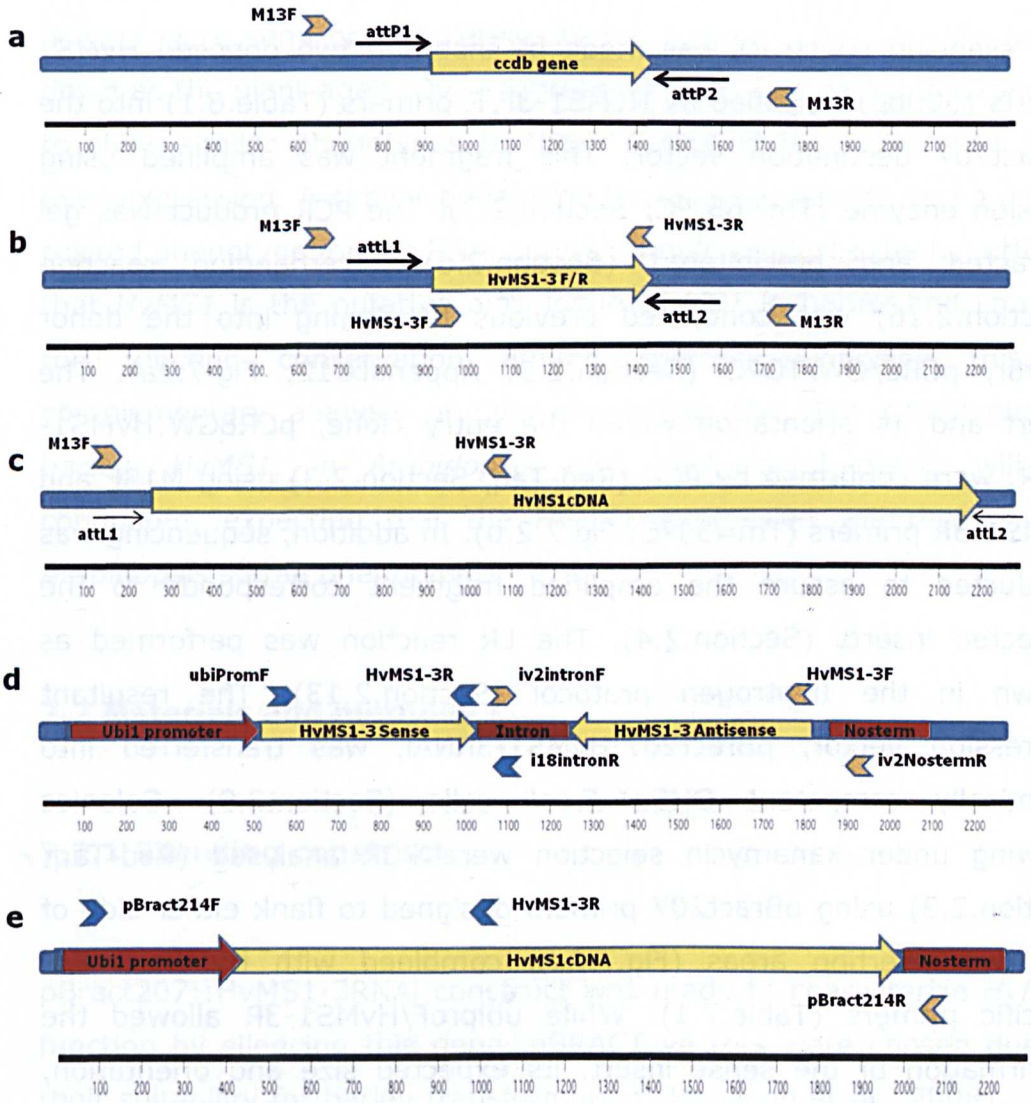

Fig.7.2 Design of RNAi and Over-expression casettes. a) pCR8GW donor vector (Section.2.9). b-c) Entry vectors, pCR8GW::HvMS1-3RNAi (b) and pCR8GW: :HvMS1cDNA (c). M13F was combined with the gene specific primer, HvMS1-3R, to check the insert and its orientation. d) RNAi expression vector, pBract207::HvMS1-3. UbipromF x HvMS1-3R and iv2intronFx HvMS1-3F were combined to check the sense and the antisense insert and their orientation. e) Over-expression vector, pBract214::HvMS1cDNA. Primers pBract214F and the gene specific primer, HvMS1-3R were used to check the HvMS1cDNA insert and its orientation.

Primers	Forward/ Reverse	Tm °C
UbiproF/ i18intronR	ATGCTCACCCTGTTGTTT/ CATCGTTGTATGCCACTGGA	60.9
Iv2introF/ nostermR	CCAAAATTTGTTGATGTGCAG/ TGTTTGAACGATCCTGCTTG	59.2
UbiproF/HvMS1-3R	ATGCTCACCCTGTTGTTT/ CTGATGGCCTGGTACTTGGT	59
Iv2intronF/HvMS1-3F	CCAAAATTTGTTGATGTGCAG/ AGGCATCTGATATGCAGCAA	59
M13F/HvMS1-3R	GTTTTCCCAGTCACGACGTTGTA/ CTGATGGCCTGGTACTTGGT	59
HygromycinF/R	TACACAGCCATCGGTCCAGA/ TAGGAGGGCGTGGATATGT	61

Table.7.1 Primers designed to flank the insertion area within the donor vector, pCR8GW (M13F/R; Fig.7.2.a), and destination vector, pBract207 (Ubipro/i18intron and Iv2intron/nosterm; Fig.7.2.d). Gene specific primers, HvMS1-3F/R were used in combination with pCR8GW and pBract207 specific primers to check the inserts and their orientation (Fig.7.2). Hygromycin primers are also shown.

7.2.2 Over-expression construct.

HvMS1 over-expression construct was prepared using the same donor vector, pCR8GW (Fig.7.2a and c). A different pBract construct was used, pBract214 (Appendix.14). This construct possesses the *Ubi1* promoter that controls the over-expression cassette and the Hyg plant selection agent controlled by the 35S promoter. *HvMS1* cDNA was amplified by HvMS1cDNAF and HvMS1cDNAR primers (Table.7.2) using Phusion (Section.2.3). This amplified fragment did not include the native stop codon. This cDNA was inserted into the destination vector following the same procedure used for the silencing construct. The construct was checked using the primer combination pBract214F and HvMS1-3R (Table.7.2e) by Red-Taq PCR (Section.2.3). AGL1::pBract214:: HvMS1cDNA cryo stock was made (Section.2.18).

Primers	Forward/ Reverse	Tm °C
pBRact214F/R	TTTAGCCCTGCCTTCATA/ CGCGCAATTAACCCTCACTA	60
pBRact214F/ HvMS1-3R	TTTAGCCCTGCCTTCATA/ CTGATGGCCTGGTACTTGGT	59
HvMS1cDNAF/R	ATGGCTGCGAAGATGGTGAT/ GCAGTTCAAGGCCGGGAACG	59

Table.7.2 Primers designed flanking the insertion area within the destination vector, pBract214 (pBRact214F/R) (Fig7.2e) and the combination of pBract214F and HvMS1-3R to check the insert and its orientation. HvMS1cDNAF/R primers were used to amplify the full length of *HvMS1* cDNA not including the stop codon.

7.2.3 Barley Transformation.

The transformation protocol was conducted as explained in section.4.2.5. Several experiments were conducted for each construct, for *HvMS1* silencing and over-expression in barley (Table.7.3). 100-120 barley immature embryos were inoculated per experiment alongside 25-30 non inoculated embryos that were control for the transformation experiment. These control embryos underwent the same regeneration protocol as the inoculated embryos, part growing with antibiotic treatment and the rest without antibiotic. Immature embryo extraction, *Agrobacterium* inoculums preparation (section.4.2), inoculation procedure and plant regeneration were conducted as explained in section.4.2.5.2 and 4.2.4 respectively.

Experiment	HvMS1-3 silencing	HvMS1Ovexp	Hyg-	Hyg+
200410IET	100		10	20
070510IET	115		10	20
010710IET	120		10	20
170910IET	120		10	20
021210IET		120	10	20

Table.7.3 Silencing and over-expression of *HvMS1* in barley. Several experiments were conducted using around 100-120 embryos per experiment. In addition, non-inoculated embryos were regenerated alongside as negative and positive control (Hyg- and Hyg+). These non-inoculated embryos were divided in two groups, the first were grown without antibiotics, while the second was grown with antibiotic (Hyg, 50mg/ml, and Timentin, 160mg/ml).

7.2.4 Analysis of transformed plants.

PCR was carried out to confirm the presence of the *HPT* gene and the silencing and over-expression inserts. DNA was extracted from young leaves as described in section.2.2. UbipromF/HvMS1-3R (Red-Taq polymerase, section.2.3; Table.7.1) and iv2intronF/HvMS1-3F (Red-Taq conditions, section.2.3; Table.7.1) were used to amplify the two inserts from the RNAi cassettes, while the combination pBract214/HvMS1-3R (Table.7.2), were used to amplify the over-expression cassette (Red-Taq polymerase, section.2.3). Primers for the *HYG* gene were also used (Red-Taq polymerase, section.2.3; Table.7.1). Floret samples from individual transgenic plants were collected at anthesis stage to observe the pollen viability. Anthers were Alexander stained (Section.2.20) and observed by light microscopy.

7.2.5 *ms1* Complementation. pGWB5:HvMS1Overex Construct.

The complementation of the *Arabidopsis ms1* mutant was carried out using the pGWB5:HvMS1overex construct. pGWB5 is a gateway vector consisting in a unique cassette driven by the CaMV35S promoter and carries a kanamycin resistance gene as a selection marker. *HvMS1*cDNA insertion within the pGWB5 vector was conducted as described previously (Section.7.2.2). The orientation of the insert was checked before *Agrobacterium* electroporation using the primers pGW8F and HvMS1-3R (Table.7.4).

Primers	Forward/ Reverse	Tm °C
pGW8F/R HvMS1-3R	TGAACGATCGGGGAAATTCG/ CTGATGGCCTGGTACTTGGT	59
EGFP.F/R	ATGGTGAGCAAGGGCGAGGA/ CTTGTACAGCTGGTCCATGCC	58
LmRNAsp/RRT	CCATTGCCAATATGTTGGTTG/ CAGCCTCAACTCCATTCCTT	59

Table.7.4 Primers used to confirm the presence of the *HvMS1* insert within the expression vector. pGW8F/R are placed at either side of the insertion region and were combined with *HvMS1* gene specific primers.

The construct carrying the *HvMS1*cDNA was electroporated into the *Agrobacterium* strain C58 (Section.2.15). Heterozygous *ms1MS1ttgTTG Arabidopsis* plants were transformed using this construct (Section.2.17). Seeds were collected and screened on Murashige and Skoog medium (Appendix.1) containing 50µg/ml kanamycin. T0 seedlings were selected for the presence of the transgene, transferred to soil and allowed to self fertilize. T0 plants were screened for *HvMS1* (HvMS1-1FxHvMS1-3R, Table.6.1) and *GFP* (Table.7.4) expression. The presence of the linked ttg mutation meant

that screening at the seedling stage for hairless ttgttg lines could be conducted. These mutants should also linked carry the MS1MS1 mutation. In addition, due to the MS1 mutation in these plants associated with the splicing of the second intron, RT-PCT was conducted to confirm the T0 plants background (Wilson et al., 2001). Primers LmRNAsp and RRT (Table.7.4; Red Taq, section.2.3) were used. The expected product for the Ler wild type RT-PCR was 351 bp, whilst, the spliced mutants product is 506 bp.

7.3 Results.

7.3.1 *HvMS1* silencing and over-expression constructs.

The 500 bp insert for the silencing construct (Fig.7.3.a, HvMS1-3F/R) and the 2019 bp for the over-expression (Fig.7.3.b, HvMS1cDNAF/R) were purified and cloned into the donor vector pCR8GW and then transformed into *E. coli* DH5 alpha cells (Section.2.9). Colonies growing on Spectonomycin were PCR analysed using the primer combination M13F and HvMS1-3R (Table.7.1; Section.7.2.1; Fig.7.2b-c) for either entry clones, giving several positive colonies which contained the insert in the correct orientation (Fig.7.3.c and d). Three colonies containing the pCR8GW::HvMS1-3RNAi and the HvMS1cDNAoverex were selected and cultured separately for plasmid extraction (section.2.5). Two LR reactions were performed using the entry clones generated above and the destination vectors pBract207RNAi and pBract214Overex (Section.2.13). The products of these reactions were again transformed into DH5alpha cells. Colonies growing on LB+Kan (50mg/ml) were PCR screened using the primer combination specified for each construct (Fig.7.2d-e; Fig.7.3.e-f). Colonies found carrying both the sense and antisense inserts for the RNAi construct (Lanes 1s to 3s and 1a to 3a respectively; Fig.7.3.e) and the *HvMS1* over-expression insert (Lane 1 to 6; Fig.7.3.f) were

subsequently selected on LB + Spectonomycin. None of these colonies grew on this selection media, confirming that the *ccdb* gene had been lost. Colonies growing on kanamycin, and confirmed as containing the expected inserts, were cultured in LB (50mg/ml Kan) and the expression construct extracted (Section.2.5). RNAi and Over-expression constructs were electroporated into *Agrobacterium* AGL1 accompanied by the helper plasmid pSoup (Section.2.15). The result cells were cultivated on LB + Kan (50 mg/ml) + Rif (50 mg/ml) at 28ºC for 3-5 days. They were screened by PCR to detect the expression vectors using the same primer combination used in sections.7.2.1 and 7.2.2 (Fig.7.2d-e).

Positive colonies were then liquid cultured and standard inoculums were prepared for barley immature embryo inoculation (Section.4.2.5.2).

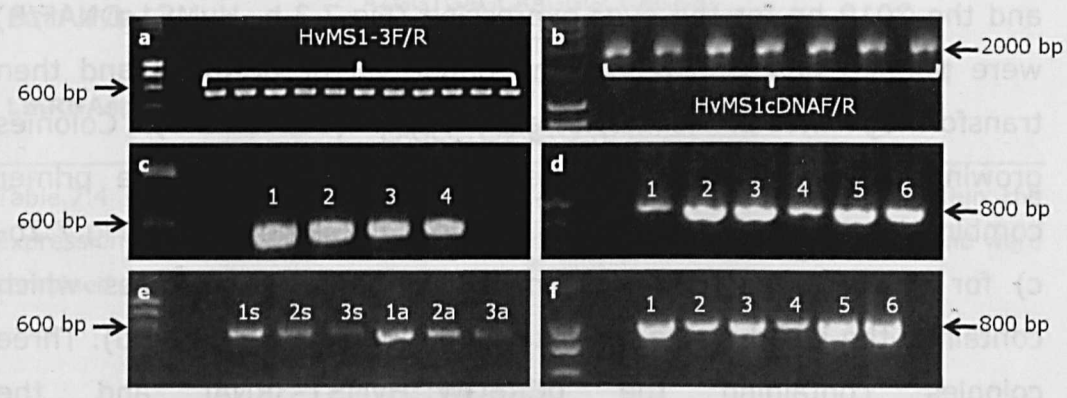

Fig.7.3 PCR reactions. a) RT-PCR using HvMS1-3F/R primers for RNAi construct. b) RT-PCR using HvMS1cDNAF/R primers for over-expression construct. c, d) PCR to confirm the entry clones contained the expected insert. Primers M13F x HvMS1- 3R were used for both entry clones, pCR8GW:HvMS1-3F/R (c, lanes 1 to 4) and pCR8GW:HvMS1cDNAF/R (d, lanes 1 to 6). Four and six colonies were found positive respectively for the inserts and the orientation was confirmed. e) Primers ubiF x HvMS1-3R (Sense) and iv2F x HvMS1-3F (Antisense) were used to confirm the sense and antisense of the RNAi construct after LR reaction. 3 samples 1s to 3s (Sense; s) and 1a to 3a (Antisense; a) were found positive for both inserts. f) pBract214F x HvMS1-3R were used to check the presence and the orientation of the *HvMS1*cDNA insert after the LR reaction. Six colonies were positive, lanes 1 to 6.

7.3.2 *HvMS1* silencing.

Table.5 shows the number of transgenic plants obtained from the different silencing experiments (Table.7.3). Experiment 200410IET generated two individual callus, 1 and 3, which regenerated several individual plants each, 17 and 6 respectively. Experiment 070510IET regenerated 7 individual plants from one single embryo. The other two experiments, 010710 and 170910IET, regenerated 3 and 1 plants respectively. Experiment 200410IET was selected to study the silencing effect on *HvMS1.*

Callus	Plants T0	Hyg +	Sense +	Antisense +
200410IET.1	17 (1-17)	16	8	8
200410IET.3	6 (18-23)	6	6	6
070510IET.1	7 (1-7)	7	7	7
010710IET	3	3	3	3
170910IET	1	1	1	1
Total	34	33	25	25

Table.7.5 Results obtained for the silencing experiments. 34 individual plants were regenerated. 33 were Hyg+, therefore, only 1 escape was observed. 25 out of 34 showed both, sense and antisense inserts. The numbers in bracket represents the identification given to each independent plant.

Individual T0 plants were PCR analysed using primers that covered the two insertion areas combined with the gene specific primer HvMS1-3F or Reverse (UbiproF/HvMS1-3R and iv2F/HvMS1-3F, Table.7.1; Fig.7.2d) and the Hygromycin gene (HygF/R, table.7.1.) (Fig.7.4). Thirty three plants were found positive for the *HYG* gene (Fig.7.4a and d), with only 1 plant showing negative results, which was probably an

escape. From the 33 Hyg positive, 8 plants did not carry the RNAi insert, the rest were positive for the sense and antisense inserts (Fig.7.4). No regeneration was seen for any of the control embryos, which were not inoculated and grown on antibiotic selection.

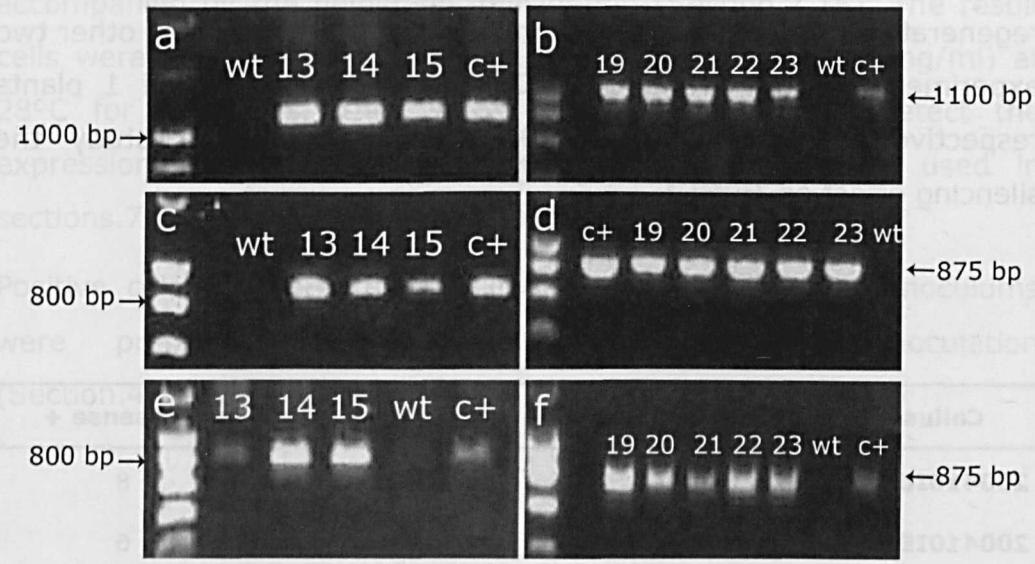

Fig.7.4 Genotyping of T0 transformed plants carrying the RNAi transgene. a-b) PCR using the HygF/R primers for lines 13, 14 and 15 (200510IET callus 1, T0) (a) and 19-23 (200410IET callus 3, T0) (b). All the lines showed positive result. c-d) PCR checking of sense insert (UbipromF x HvMS1-3R, Fig.7.2d). Same samples as a-b. e-f) PCR checking of antisense insert (iv2intronF x HvMS1-3F, Fig.7.2d). Same samples as a-b. Wild type control (wt) did not show amplification for any of the primers combination (a-f). Control (c+) was performed using the expression vector (pBract207::HvMS1-3RNAi) under the same genotyping conditions (Red-Taq, Section.2.3.).

Transgenic plants from experiment 200410IET callus 1 and 3 were phenotyped for signs of male sterility or any pollen defect. In comparison to wt, Alexander staining confirmed that transgenic lines, 200410IET callus 1, samples 13, 14, 15 and 20, and callus 3, samples 19.4, showed reduction in pollen viability (Fig.7.5). These lines were however fertile and seed set occurred. Positive lines, showing pollen

viability reduction, were sown to study the next generation (Table.7.6).

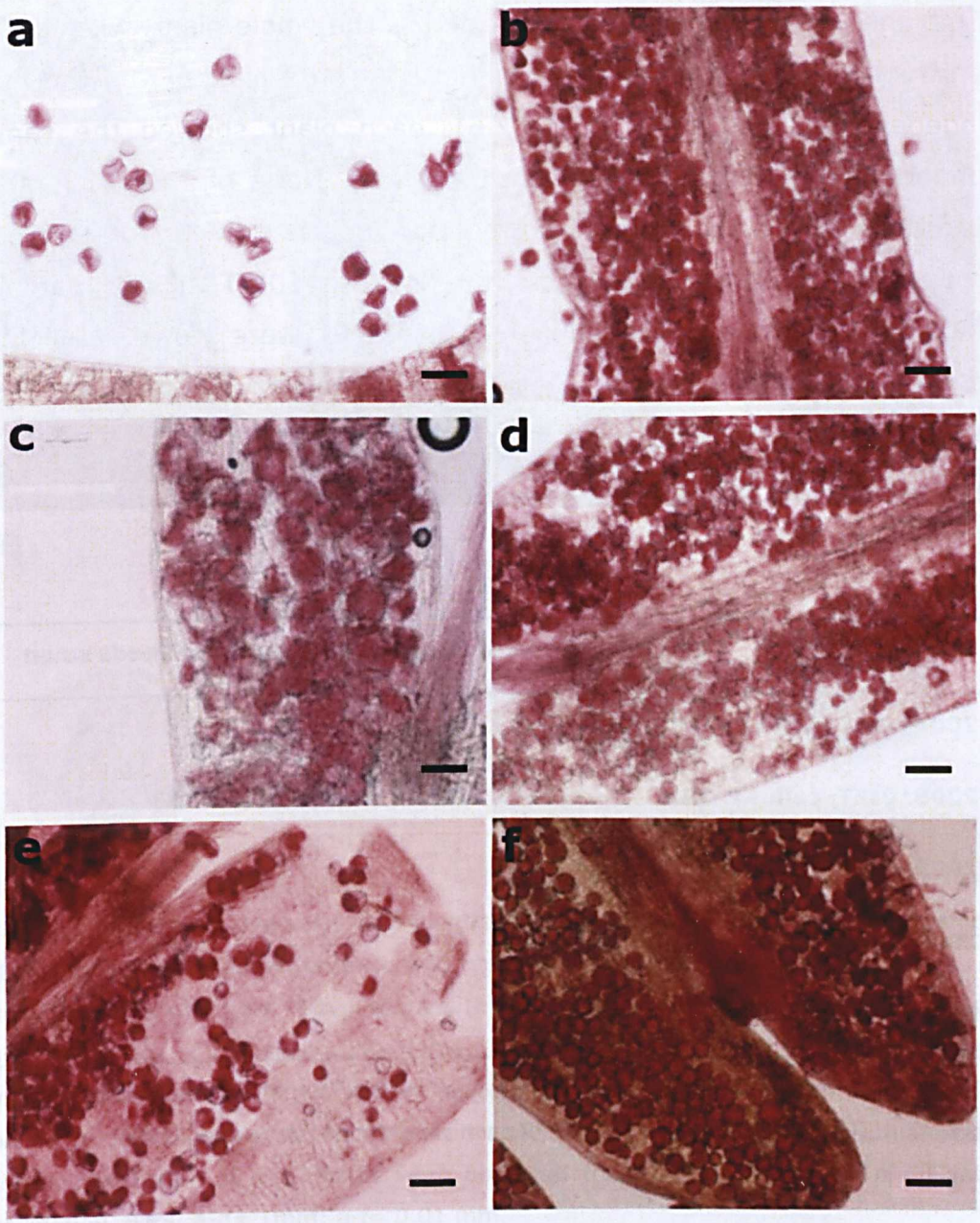

Fig.7.5 Anther samples from transgenic lines stained with Alexander Stain (Section.2.20). a) Sample 20 (200410IET callus 3). b) Sample 13e (200410IET callus 1). c) Sample 14c (200410IET callus 1). d) Sample 15a (200410iet callus 1). e) Sample19.4 (200410IET callus 3). f) wt. This wt control sample was also regenerated from immature embryo, although no antibiotic selection was used. Pollen viability reduction was observed in all the transgene lines. Bars= 0.1 mm.

The T1 generation was grown until anthesis. At heading, all the lines previously observed to have a reduction in pollen viability in the T0 generation, showed a clear sterile phenotype (Fig.7.6). Florets were observed to contain empty anthers or anther with non-viable pollen, with the ovary appearing normal (Fig.7.6a, c and e), but no seed set. This phenotype was not consistent across the whole plant, with fertile and non fertile tillers occurring within the same plant. From the five independent lines sown (Table.7.6), each plant showed the same phenotype, of fertile and non fertile tillers. None of the wt control plants (Fig.7.6b, d and f) showed any pollen defects, or viability reduction. Moreover, 3 T1 seeds from line 200410IET callus 1, sample 7c, which did not show any pollen defect in T0, were grown parallel to defective T1 plants. These plants did not show any defects in pollen viability, the three plants showing complete fertility.

Lines	Number of seeds sown
200510IET, Callus 1, 14.c	4
200510IET, callus1, 14a	4
200510IET, callus 3, 19.4	4
200510IET, callus 3, 20	4
200510IET, callus 1, 7c	3

Table.7.6 T1 transgenic lines sown from self-pollinated T0 that showed pollen viability reduction (Except transgenic sample 7c which did not show any defect in pollen viability in T0).

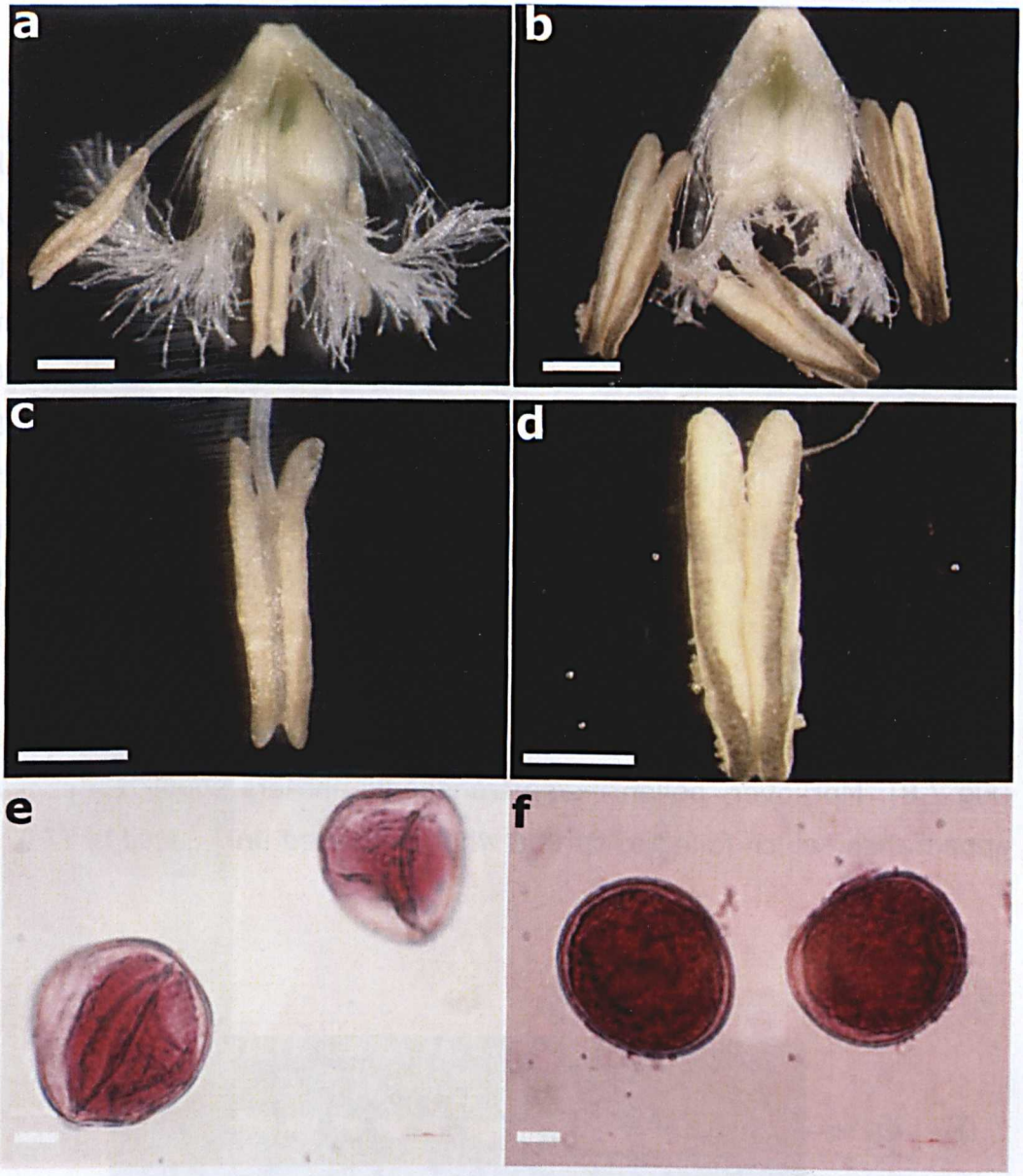

Fig.7.6 Comparison between representative T1 putative HvMS1RNAi transgenic/ silencing lines and Golden promise wild type. a, c and e show the silencing line. b, d and f show the wild type. Small anthers (a), which were not completely developed (c) and pollen less or containing non-viable pollen (e) were observed in the RNAi lines. Anthers dehiscence in the wt (b-d) was already ongoing and anthers contained viable pollen (f). Silencing lines show complete sterility through the whole spike with anthers showing reduction in size. Pistils were observed to be normal (a-b) and ready for pollination. Bars: a-d= 1mm; e-f= 0.01 mm.

7.3.3 *HvMS1* over-expression analysis.

Over-expression lines were generated by transformation of 120 immature embryos (Experiment 021210IET, Table.7.3). Twenty different individual plants were regenerated from this experiment using the individual shoot separation method explained in section.4.3.2 (Fig.4.6). Only 14 were transferred to soil. RT-PCR showed that these lines were expressing the transgene, *HvMS1* (Fig.7.7). At anthesis, florets were collected and anthers Alexander stained. Pollen showed no differences compared to the wt pollen (Fig.7.8), however no fertilization was observed in any of the 14 analysed plants, with all the tillers completely sterile. In addition, anther dehiscence did not occur in transgenic lines at any time. Therefore, although pollen was apparently viable, it was not release (Fig.7.8). Moreover, pollen inside transgenic anthers showed a sticky appearance, which failed to spread when dissected unlike wild type.

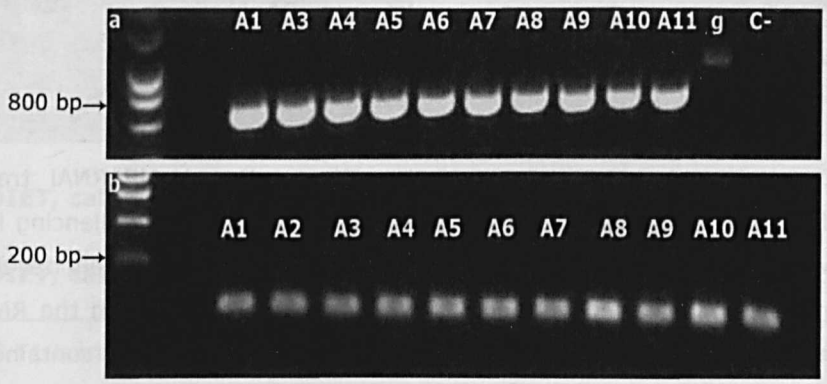

Fig.7.7. RT-PCR reaction of T0 *HvMS1* over-expression lines. a) Transgenic 021210IET plants, A1 to A11, showed *HvMS1* over-expression. g: Barley genomic DNA. A bigger PCR product was amplified due to the intron placed within the primers. c-: Wild type leaf sample. b) RT-PCR using α-tubulin for normalization (Table.6.4). Samples 12, 13 and 14 were also analysed (data not shown), and showed the same results.

Fig.7.8. Comparison between representative T0 transgenic/*HvMS1* overexpression line (A3) and wild type. a) Wild type spike during grain fill phase. b) T0 transgenic spike at grain filling stage. No grain was growing inside. c) Comparison between wt floret at grain filling stage and T0 transgenic floret beyond grain filling stage. No pollen was released and therefore, no grain was observed during the later stages. d) Wild type at anthesis. Anther break over the top and pollen grain were observed. e) T0 transgenic anther at anthesis stage. Anther dehiscence did not occur and no pollen was released. f and h) Wild type pollen grain. g and i) T0 transgenic pollen grains. Bars: a= 2 mm; b= 4mm; c=1 mm; d-e= 0.6 mm; f-g= 0.1 mm; h-i= 0.5 mm.

7.3.4 *ms1* complementation analysis.

A binary plasmid (pGWB5) carrying the CaMV35S promoter and the *HvMS1* coding region fused with the *GFP* (synthetic green fluorescent protein) was introduced into *MS1ms1* heterozygous *Arabidopsis* plants. The subsequent segregating generation were analysed for complementation of the *ms1ms1* mutation. Two lines (Lane 8 and 9), which showed a larger *MS1* RT- PCR product were identified (Fig.7.9). The increased size of the *MS1* RT-PCR band is due to the lack of splicing characteristic of the mutant transcript, indicating that they are homozygous *ms1/ms1* lines). These two lines, as seen in the rest of the T0 generation, expressed the *HvMS1* and *GFP* transgenes (Fig.7.9), however, in neither of the two *ms1ms1* homozygous lines was fertility rescued (Fig.7.10).

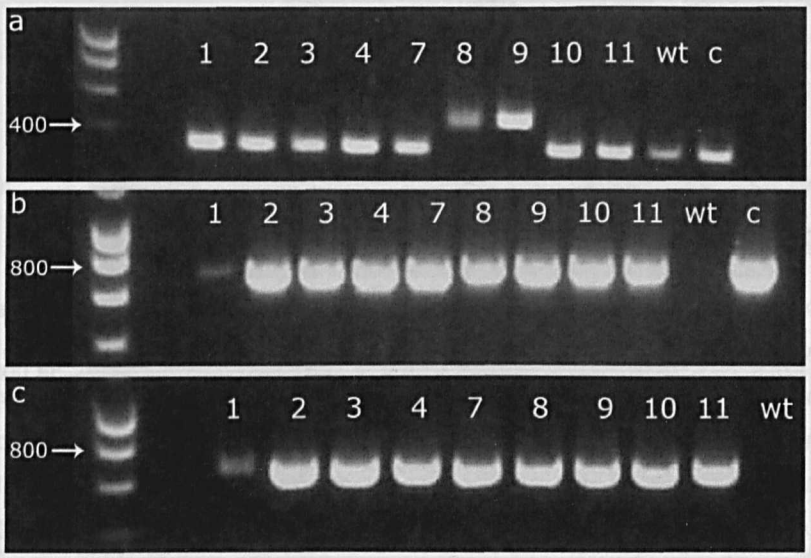

Fig.7.9 RT-PCR analysis of *Arabidopsis ms1ttg x Ler* F2 lines transformed with PGWB5*::HvMS1:GFP* over-expression (T0 generation). a) *MS1* RT-PCR of *ms1* splice mutant (*ms1ttg x Ler* F2) *HvMS1* over-expression lines (primers Table.7.4). A 400 bp mutant transcript was seen in lines 8 and 9, whilst the wt 300 bp band was seen in the other lines. b) *GFP* RT-PCR (Table.7.4); expression of *GFP* is seen in all putative transgenic lines. Lane c (control plasmid DNA). c) *HvMS1* RT-PCR (Primers HvMS1-1Fx HvMS1-3R, Table.6.4); expression of HvMS1 is seen in all putative transgenic lines.

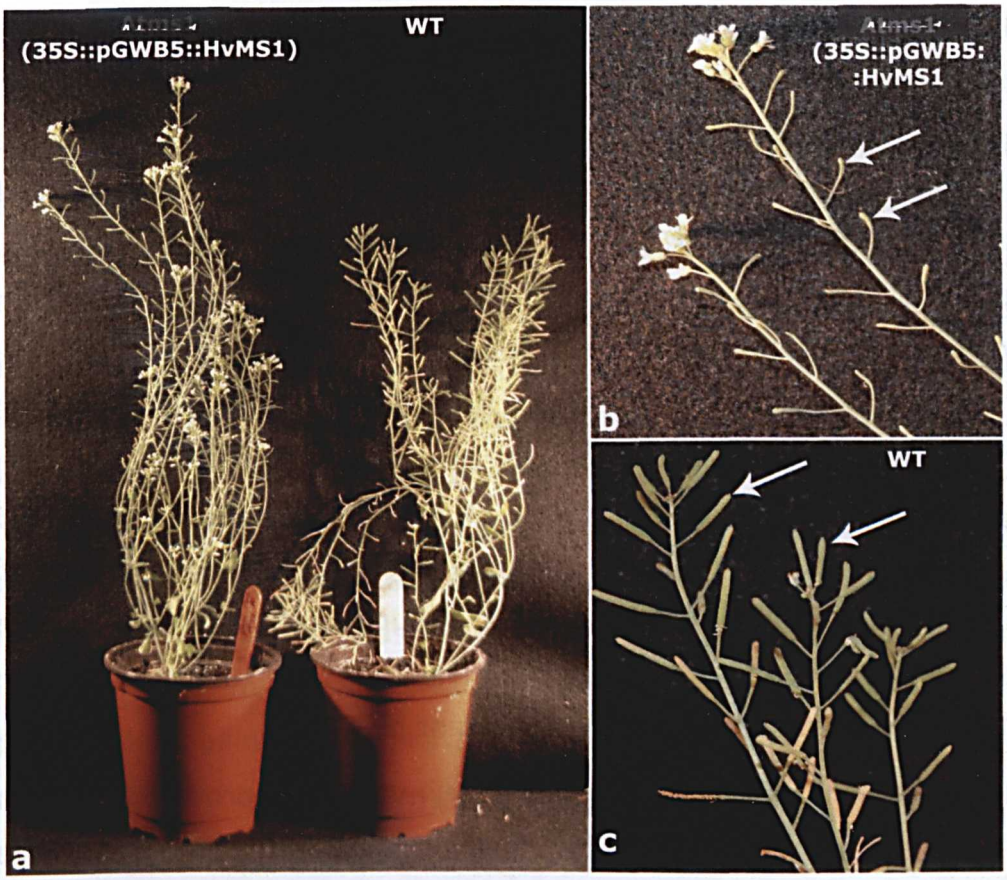

Fig.7.10 *Arabidopsis* homozygous *ms1/ms1* plants expressing the *HvMS*1 transgene compared to wild type fertile plants (Fig.7.9).

7.4 Discussion.

The characterization of *HvMS1* function is essential to confirm that this gene is the orthologue of the *Arabidopsis MS1* and rice *OsPTC1*genes (Wilson et al., 2001; Li et al., 2011). *HvMS1* has shown significant similarities to its putative orthologues in *Arabidopsis*, rice and *Brachypodium* (Appendix.9). In addition, several experiments carried out to investigate its expression pattern and tissue specificity have indicated that *HvMS1* is expressed in a similar pattern to *Arabidopsis MS1* gene (Fig.6.13a) and shows tapetal specific expression (Fig.6.14). However, none of these experiments have demonstrated the function of this gene.

In recent years, new tools have been developed that allow the characterization of gene function in crops. First, cereal transformation has been improved and efficient protocols for rice, wheat and barley are now available (Hiei et al., 2008; Harwood et al., 2008; He et al., 2010). In addition, for almost a decade, RNAi has been used as a research tool to discover or validate the functions of genes, and also as tools for commercially applications. The applications of RNAi cover a wide spectrum, from designer flower colours, to plant-produced medical therapeutics, falling all into two types of approach: protection of the plant against attack (Wang et al., 2000; Fusaro et al., 2006) and fine-tuning of metabolic pathways genes (Moritoh et al., 2005; Kapoor et al., 2002). RNAi therefore, has indeed been shown to be an effective mechanism for silencing many genes in many organisms, including several agriculturally significant plants.

Crucial in the barley transformation method improvement is the development of constructs specifically designed for barley transformation, pBract (www.pBract.org). pBract207RNAi silencing construct has two inverted repeat cassettes in the transcribed region, separated by an intron. This design facilitates the formation of dsRNA, essential for silencing (Waterhouse et al., 1998; Chuang and Meyerowitz, 2000) (Fig.7.1). In addition, the RNAi cassette is controlled by the Ubi1 promoter that has shown to be highly active in monocots in transient and stable transformation experiments (Schledzewski and Mendel, 1994; Li et al., 1997).

The *HVMS1* 500 bp fragments used for the RNAi construct was also carefully selected. Sense and antisense repeats ranging from 98 to 853 base pairs have been used for efficient silencing (Wesley et al., 2001), indicating that the length of the repeats sequence can be flexible. In the HvMS1 RNAi experiment, sequences derived from the ORF, 5'UTR and 3'UTR or highly conserved sequence were avoided as it has been reported that these sequences can knock down the target gene as well as its close homologues, with like region of 80% similarity (Yin et al., 2005). Therefore, the fragment selected for the *HvMS1* RNAi construct was located between the second and the

beginning of the third exon, far from the PHD finger domain found at the end of the third exon.

Silencing of *HvMS1* has encountered some difficulties in terms of regeneration of identifiable individual plants (Section.4.3.2). Immature derived embryos regenerated only a few regenerative callus that were significantly prolific in embryogenic callus production. Callus separation techniques carried out (Harwood et al., 2008) proved to not be sufficient to separate each independent embryogenic callus which was capable of regenerating numerous individual plants. Therefore, independent plants regenerated form the same callus were identified at the time of transfer to soil and labelled as independent lines. This identification was based on the observation that individual plants did not generate tillers when growing in the tube. Although, this identification allowed a more accurate analysis of independent transformation events, it was not very practical. Independent transgenic lines generated multiple tillers, therefore, if several independent plants were grown within the same pot, the number of tillers generated per plant was excessive and was a problem for tiller-plant identification. Therefore, many tillers were not analysed because their origin was not clear enough. Eventually, this callus derived plants separation problem was overcome by a triple separation protocol (Section.4.3.1) that allowed a more accurate isolation of independent plants, facilitating their analysis.

The majority of the 34 independent RNAi T0 transgenic lines analysed showed the presence of the two RNAi opposed inserts, along with the Hygromycin marker gene (Table.7.5). Only one escape was detected, this means that the Hygromycin selective marker is very efficient in the selection for transformed callus. This was also confirmed by the non-inoculated control callus growing on plates containing Hygromycin that were set up in parallel to every transformation experiment. None of these un-inoculated embryos regenerated a single green shoot, all became necrotic and died between the Transition to Regeneration stages. Eight plants, positive for the Hyg gene, did not contain the RNAi inserts. The absence of the sense and antisense inserts, while

the *HYG* gene was present did not agree with what was expected of the integration mechanism for the pBract vectors. pBract vectors have been specifically designed to carry the selectable marker (Hygromycin) at the left border and the gene of interest at the right (Harwood et al., 2009) so that the gene of interest is transferred first and the selectable marker second. This means that selected transformed plants have a greater chance of containing the gene of interest. However, these 8 plants only contained the Hyg resistance gene, with the transgene being lost by an unknown mechanism.

Vegetative growth of the HvMS1RNAi plants was normal. Partial silencing effects were observed in some of the T0 RNAi transgenic lines (Fig.7.5), however the presence of viable pollen was sufficient to make the plants fertile. This partial silencing effect may be because the transgene RNAi is present below a threshold level that is required for effective silencing (Lindbo et al., 1993). In addition, since RNAi lines are usually knock down rather than knock out the target gene expression (Yin et al., 2005), therefore, although the expression of the target gene mRNA is likely to be reduced, a small amount of transcript may remain which is sufficient to maintain wild type function. This incomplete silencing may explain the presence of normal pollen in some lines, the slight reduction in pollen viability in others and general fertility observed in different RNAi positive lines. There was no effect in the female organs, therefore, all the lines fertilised and produced seed.

A more severe silencing effect was observed in the next *HvMS1*RNAi generation (T1). Plants, which showed a reduction of viable pollen in the previous generation (Fig.7.6), showed a completely silenced phenotype where unviable pollen, or the complete absence of pollen was observed. However, this sterility was restricted to some tillers within the same plant, whilst the remaining were completely fertile. Another RNAi positive line, 7c, which did not show any reduction in pollen development in the T0, was completely fertile in T1. This observed increase in silencing may be explained by the increase of the number of copies of the transgene in the second generation after self-

pollination, increasing the silencing capacity beyond a required threshold level (Lindbo et al., 1993) to allow complete silencing of *HvMS1*. Morito et al (2005) reported that RNAi transformed rice plants showed a different percentage of fertility depending on the expression level of the native gene. However, the reason why the barley silencing is affecting different tillers within the same plant remains unknown, although it might be due to variation in expression levels and stability between independently transformed plants (Jones et al., 1985; Peach and Velten, 1991; Walters et al., 1992).

HvMS1 over-expression results showed similarities to the *Arabidopsis MS1* over-expressed lines reported by Yang et al (2007). Although no stunted plants, or any particular growth differences were seen between the vegetative development of the over-expressed lines and the wild type, male sterility was observed. Closer analysis of the anther and pollen development revealed mature pollen within the over-expressed anthers. The reason for the absence of anther dehiscence, and therefore pollen release and sterility in the OEx lines are unclear. However, anthers in *Arabidopsis MS1* over-expression lines showed increased indentation on the epidermal surfaces (Yang et al., 2007). In addition, the sticky appearance of the pollen observed in *Arabidopsis* OEx anthers indicated an abnormal conformation of the pollen wall. This was supported by microarray analysis that identified a number of genes with altered expression in the *ms1* mutant buds (Yang et al., 2007), three of which are associated with lipid biosynthesis and pollen wall development. These show reproducible down-regulation in *ms1* buds and increased expression in the *35S:MS1* over-expression lines, suggesting that expression of these floral-specific transcripts were activated by the ectopically expressed *MS1*. Pollen from the *MS1* over-expression lines was generally fertile but appeared to have increased deposition of `pollen coat material. This agrees with the increase in expression of wall components specifically oleosins observed in *MS1* over-expression lines (Yang et al., 2007). Further experiments therefore, need to be conducted to study in detail the effect of *HvMS1* over-expression on barley pollen

wall formation and the possible causes for the absence of anther dehiscence.

Over-expression of barley *HvMS1* in *Arabidopsis ms1ms1* homozygous background lines failed to restore fertility (Fig.7.10). This was most likely due to the promoter used for over-expression (*CaMV35S*), instead of using the *MS1* native promoter. A similar lack of complementation was observed for *ms1* (Ito et al., 2007) and *ptc1.* Neither mutant could be rescued using the equivalent wild type gene driven by the cauliflower mosaic virus 35S promoter. However, when the *MS1* native promoter was attached to the *MS1* orthologue in rice, *OsPTC1*, fertility was restored in *ms1ms1* homozygous lines (Li et al., 2011). Therefore, this suggests that the precise control of *MS1/PTC1* expression is critical for pollen development. Further complementation assays using *HvMS1* gene regulated by the native *Arabidopsis MS1* promoter could be conducted to confirm whether the barley putative orthologue can function in *Arabidopsis* and rescue the *ms1* mutation.

CHAPTER 8.

8. General conclusions.

The development of functional pollen that is released at the appropriate stage to maximize pollination is critical for plant reproduction and the creation of genetic diversity. Controlling the process of pollen release is important for selective breeding, the release of genetically modified (GM) pollen, and the commercial development of hybrids lines. Hybrids frequently exhibit heterosis or hybrid vigour, which means that the plants are stronger, develop more rapidly and are higher yielding.

MS1 is a transcription factor which shows a tightly regulated expression in the tapetum (Yang et al., 2007). *MS1* encodes a protein (672 amino acids), which contains a putative Leucine Zipper and a Plant Homeodomain (PHD) finger motif which are essential for the MS1 function. *MS1* expression commences as callose break down occurs, up to the free microspore stage. *ms1* mutants show pollen degeneration soon after microspore release from tetrads, the tapetum is abnormally vacuolated and the microspores tend to stick together, suggesting an unusual composition of pollen wall material. Preliminary exine (primexine) development occurs, however normal pollen wall development does not take place and pollen degeneration is initiated (Vizcay-Barrena and Wilson, 2006).

Over-expression of *MS1* was found to have a detrimental effect on plant development, suggesting that a tightly regulated system of expression is required to moderate the effects of missexpression of *MS1* (Yang et al., 2007). *Arabidopsis* over-expressed lines showed a range of severity of phenotypes linked to the level of *MS1* expression. Phenotypes from slow development, showing small densely packed rosettes and short flowering stems, to an increase in branching and longer flowering periods than wild type, were observed. In addition, in some cases, flowers were semi-or completely sterile, due to the

degeneration of mature pollen rather than early degeneration of microspores as seen in *ms1* (Yang et al., 2007).

Homologous genes to *MS1* identified in other species such as rice, poplar and the unicellular green alga *O. tauri* (Ito et al., 2007) suggest that the MS1 function may be conserved across species. Moreover, Kapoor et al (2002) reported that the Tapetum-Specific Zinc Finger Gene (*TAZ1)* in petunia showed a very similar expression pattern and mutant phenotype to *MS1,* suggesting that they could be involved in the same regulatory mechanism that controls tapetum development. In addition, the recent characterization of the *MS1* orthologue in rice has confirmed that *MS1* function is conserved in higher plants. The *PERSISTENT TAPETAL CELL 1 (PTC1)* shares homology with a number of proteins containing the PHD-finger motif in animals, yeast and higher plants (Halbach et al., 2000). Phylogenetic analysis indicates that *Arabidopsis AtMS1*, poplar *PtMS1*, RICE *PTC1*, form a separate group within the entire family (Ito et al., 2007), suggesting that *PTC1* and its close homologous may have a conserved role in plant reproductive development. Moreover, *ptc1* has a similar phenotype to *ms1* and *PTC1* driven by the *MS1* promoter has been able to restore pollen fertility in the *Arabidopsis* homozygous *ms1* mutant. This suggests a conserved role regulating programmed anther development in monocot and dicot species.

The extension of this conservation to other species, such as barley, has encountered problems because of a lack of a completely sequenced genome. The low level and specific expression of MS1 means that it is unlikely that any homologous sequence will be present in EST libraries. Therefore, in order to characterize the *MS1* orthologue in barley, this gene had to be amplified and sequenced using putative orthologues as templates for primer design, gene amplification and RACE-PCR. This approach has successfully amplified a putative orthologue to *AtMS1* in barley, *HvMS1. HvMS1* has shown a similar expression pattern to its putative orthologues in *Arabidopsis* and rice. In addition, silencing and over-expression of *HvMS1* in barley

generated equivalent phenotypes to these observed in *ms1* and *osptc1.*

8.1 *HvMS1* characterization.

8.1.1 Staging of barley anther and pollen development.

One of the principal problems when trying to characterize a gene that is expressed in a very narrow window of development is to find the right stage to collect samples. This difficulty is further compounded in cereals such as barley, since the floret development occurs enclosed within the pseudostem, making it impossible to observe its development without dissecting the plant.

Developmental staging methods have been suggested based upon plants external and internal growth characteristics (Zadoks et al, 1974; Haun et al., 1973; Waddington et al., 1986). Cereal development has been also characterised in terms of thermal time. This staging method allows the establishment of the duration of the different developmental stages depending on temperature, photoperiod and vernalization. Moreover, comparisons between this thermal time and reproductive organ development have been established (Kirby, 1988). However, none of these studies have related the plant external development to the events occurring within the anther.

Investigation of anther and pollen development, and spike size, indicated a relationship between these two factors that allowed a prediction of developmental stage based upon spike size. As described by Reynolds et al (2009), the spike follows a parallel development to the pseudostem elongation (Fig.3.20). Therefore, under controlled conditions, a relationship between barley external stages and the spike size was found (Section.3.3.2). This relationship was determined using an easy staging system that partially followed the traditional

decimal Zadok's staging (Section.3.3.2), but including additional intermediate stages and a later system based upon last flag extension (LFE). A clear relationship was observed between the spike size and new stages utilizing last flag extension (Last flag extension stages). These stages describe the final stages of barley growth prior to anthesis (LFE1-4; Section.3.3.1), and the corresponding events occurring within the anther. This relationship allows the prediction of these events through the external stages, allowing very accurate material collection for genetic and molecular analysis.

8.1.2 *HvMS1* amplification and characterization.

BLAST analysis performed using *Arabidopsis MS1* and the rice orthologue *PTC1* against barley sequence database failed to identify homologous sequences. Approaches to clone the barley *MS1* orthologue using primers designed using the *PTC1* gene as a template proved to be difficult, with amplification only occurring from a small region of the barley sequence. The release of the *Brachypodium* genome contributed greatly to the amplification of the *MS1* orthologue in barley due to its close relation to barley (Opanowicz et al., 2008). BLAST analysis between *PTC1* and the *Brachypodium* genome (www.brachypodium.org) succeeded in finding a highly similar sequence, *Bradi4g31760*, with homology to *PTC1* of greater than 85% (Fig.6.5). Primers designed using the most conserved regions between *OsPTC1-Bradi4g31760* amplified a highly similar sequence in barley, *HvMS1* (Fig.6.11), that was completely amplified by RACE-PCR. *HvMS1* encoded a predicted protein of 668 aa long, including, as in PTC1 (Li et al., 2011), a conserved Cys4-His-Cys3 PHD motif. The HvMS1 protein and its orthologues in rice and *Brachypodium*, do not contain a Leucine zipper motif (LZ), which is present within the AtMS1 protein. However this region may have a secondary importance as PTC1 similar function is carried out without this motif.

Therefore, this new-gene amplification approach which utilizes bridging genomes, in this case the Rice/*Brachypodium* genomes, may be used for the identification of other barley genes, which can not be found by BLAST analysis. This approach is applicable to other species where full genome sequences are not available.

8.1.3 *HvMS1* shows a similar expression pattern than *AtMS1*.

Experiments performed to study *HvMS1* expression using RT-PCR showed that this gene has a similar expression pattern to its putative orthologues genes in *Arabidopsis* and rice (Fig.6.13) (Li et al., 2011). cDNA samples used as template were synthesised from RNA extracted from florets collected from different spike sizes as explained at section.6.2.4.1. *HvMS1* expression was restricted to stages where microspores were about to be released from tetrad to early miscrospore (Fig.6.13). As in *Arabidopsis* and rice, *HvMS1* expression was observed from late tetrad stage to microspore release from tetrad (Fig.6.13). In addition, spatial and temporal expression was determined more specifically by *in situ* RNA hybridization. Results indicated that *HvMS1* is expressed specifically in the tapetum, providing additional confirmation that *HvMS1* is the putative orthologue of *AtMS1* and *OsPTC1*.

8.1.4 Barley tissue culture and transformation.

8.1.4.1 Barley plant regeneration from immature embryos.

Barley transformation was conducted to characterize the *HvMS1* gene function. An *Agrobacterium*-mediated barley transformation protocol based upon the protocol of Harwood et al (2008) was followed. First of all, tissue culture experiments were carried out to confirm the efficiency of plant regeneration from barley immature embryos

(Golden Promise). Plant regeneration proved to be highly efficient, yielding several individual plants per callus derived immature embryo. In addition, the duration of the plant regeneration from immature embryo to adult plants producing seeds was studied. Although regeneration showed some variability, possibly due to different immature embryo size or age (Kerry et al., 2000), in general, it took around 24-26 weeks (Fig.4.4). Furthermore, the efficiency of hygromycin as a selective agent was tested and showed that at 50µg/ml it was highly efficient in preventing regeneration of non-trangenic immature embryos.

Tissue culture and the regeneration of adult plants have been always limited by the responses of different genotypes to the regeneration treatments. In addition, starting material has a significant impact in successful plant regeneration. From all the tissues tested in barley, rice, or rye, immature embryos have shown to be the most responsive; however, the supply of immature embryos is costly and requires considerable efforts. Therefore, cheaper alternatives are being tested, for instance using mature embryos. Experiment using mature embryos in barley showed high success in regenerating adult plants from this tissue, however, this regeneration was very genotype dependent (Sharma et al., 2005). Firstly, the response to callus induction was seen to be different depending of the genotype. Moreover, the formation of embryogenic callus and the later plant regeneration was much more reduced and also highly genotype dependent. Similar phenotype dependency to tissue culture and response to callus generation was observed in rice (Hiei et al., 2008). In rice, immature embryos have shown high regeneration efficiencies; therefore, it has been the most commonly used starting material for transformation experiments. However, as in barley, mature embryos are being tested. The main problem in using this tissue is the low response to callus induction observed in some varieties, and therefore the impossibility of carrying on a subsequent successful transformation protocol. Hiei et al (2008) studied a range of rice varieties and designed different transformation protocols adapted to

most varieties. They observed that a good culture medium for one genotype does not work well for other; therefore, efforts were required on a genotype-by-genotype basis.

In the current study, problems were encountered relating to the separation of individual barley regeneration events. This was solved by using a triple separation protocol, consisting of: 1) Callus partition in smaller pieces between Selection 3 and Transition; 2) Plantlet separation at regeneration stage; 3) Shoots separation when plantlets are growing within the tube (Fig.4.4). An example of this was successfully tested on two plantlets that produced 5 and 6 individual plants respectively (Fig.4.3.1). Other protocols, such as those from Hiei et al (2008), recommend the separation of the regenerated callus into smaller pieces (up to 24) at different stages of the regeneration protocol. This attempts to separate individual embryogeic callus, which have the potential to regenerate adult plants. Although this technique (Hiei et al., 2008) does not guarantee the complete separation of each individual embryogenic callus, it allows an increase in individual plant regeneration per callus. The Harwood et al (2008) protocol for barley transformation separates these embryogenic callus, by utilizing callus partition between Selection 3 stage and Transition (Fig.4.4). However, the identification of individual embryogenic callus at this stage was complicated due to the proximity of the different embryogenic callus being generated. Therefore, the separation of individual regenerated plants from immature embryos can be achieved by a number of approaches.

Although regeneration protocols are progressing in almost every grass species, efforts have to be focused in improving media conditions, starting explants material and also in increasing the regeneration capacity of recalcitrant genotypes. Altogether the improvement of plant regeneration from tissues used for transformation purposes is essential in order to increase the overall efficiency of transformation protocols.

8.1.4.2 Barley *Agrobacterium*-mediated transformation efficiency.

Transformation of barley immature embryo and further regeneration of adult plants was tested (Section.4.3.2). *Agrobacterium* proved to be very effective in transforming immature embryos. Experiment carried out using *GUS* expression indicated that, as previous authors have claimed (Harwood et al., 2002), 50% of the inoculated callus were effectively transformed and expressed the *GUS* gene (Fig.4.6). However, whilst transformation of immature embryos showed high efficiency, the regeneration of these transgenic callus was, in appearance, the limiting factor (Section.4.3.2). This lack of regeneration had been previously cited as a limiting factor of the high frequency transformation in barley (Harwood et al., 2002).

From the total number of adult barley plants regenerated after inoculation, 94% were shown to carry the Hygromycin gene, and therefore, were transgenic plants, with only 4 escapes out of 68 plants. However, although the regeneration of inoculated embryos into adult plants was successfully conducted, a lower efficiency than that claimed by Harwood's protocol (Harwoods et al., 2008) was obtained (only 68 independent plants out of 675 immature embryos inoculated; Table.4.5). In addition, these 68 plants were all produced from only 9 immature embryo derived callus, indicating the high plant regeneration capacity of some embryo-derived callus, but also the lack of response from most of the embryos to the regeneration protocol. Various authors have shown that the state of the initial material is essential for a successful plant regeneration protocol, and therefore for transformation (Kerry et al., 2001; Harwood et al., 2008; Hiei et al., 2008). The regeneration of inoculated embryos is highly dependent on the immature embryo age and size. Immature embryos that are too old are less responsive to embryogenic callus formation, reducing the transformation protocol efficiency (Kerry et al., 2001). In addition, immature embryo disinfection has to be carried out carefully, since breaking the grain coat is thought to cause damage to the

immature embryo (Harwood et al., 2008). Moreover, the process of removing the immature embryo axis is highly sensitive, as any damage to the scutellum or the remaining immature embryo may reduce its regeneration capabilities. The number of totipotent cells ready to be transformed in the scutellum area is also thought to be crucial for high transformation efficiency (Cho et al., 1998). Therefore, the immature embryo collection is a key stage that may be the limiting factor for an efficient barley transformation protocol.

Other factors, such as medium composition, *Agrobacterium* strain, or inoculation procedure have been identified as important in order to obtain efficient transformation. However, they have been more standardized and do not show the same degree of variation as immature embryo extraction. Moreover, the stress suffered by the inoculated embryos growing on plates containing the *Agrobacterium,* as well as the selectable marker and also the antibiotic used to control the *Agrobacterium* overgrowth, are also key factors determining regeneration frequency. The introduction of transition stages has shown great success in regenerating plants from recalcitrant barley genotypes inoculated callus (Cho et al., 1998). Therefore, most of the transformation protocols are including transition stages in order to facilitate the transition from callus induction to regeneration, increasing the number of embryogenic callus that have the potential to regenerate new plants (Harwood et al., 1998; Cho et al., 1998).

8.1.5 Barley *HvMS1* silencing and over-expression.

8.1.5.1 *HvMS1* RNAi silencing.

HvMS1 silencing showed that this gene is involved in anther and pollen development in a similar way to its orthologues in *Arabidopsis* and rice. However, the partial reduction in pollen viability observed in T0 and T1 RNAi plants indicates that the silencing was not complete. The effect of gene silencing was however increased in the T1

generation, probably due to increased copy number of the RNAi transgene. In the T0 plants, plants showed a significant reduction in pollen viability but full seed set was still observed. However, this was increased in specific tillers in the T1 plants with five different lines showing completely sterility, although other tillers did not show any alteration in fertility.

Gene silencing is frequently associated with knocking down gene expression rather than knocking it out (Yin et al., 2005). Therefore, although the expression of the target mRNA is likely to be reduced, a small amount of transcript may remain, which may be sufficient to maintain wild type function. In addition, *HvMS1* expression is characterized for being very low and temporally localized; therefore, only a very low level of *HvMS1* expression may be required for functional pollen development.

However, it is unclear why the T1 sterility affects only certain tillers and not all of them. Transgene expression in plants remains largely unpredictable, and there is a considerable variation in expression levels and stability between independently transformed plants (Jones et al., 1985; Peach and Velten, 1991; Walters et al., 1992). Different integration sites, copy number and transgenic locus configuration, as well as epigenetic silencing mechanism, can all contribute to this variability (Finnegan and McElroy, 1994; Meyer, 1995; Matzke and Matzke, 1998; Iyer et al., 2000).

Vain et al (2002) showed that in a population of transgenic rice plants over two generation, only a small proportion of the plant lines exhibited Mendelian inheritance and stable expression of the transgene. Transgene inactivation occurred in primary transgenic plants in 41% of the lines. In addition, the same study revealed that, in the next generation (T1), loss of transgene expression was mostly due to plant sterility, non-transmission of intact transgenes and transgene silencing. In addition, transgene silencing has been reported to be one of the biggest obstacles in genetic engineering of crops (Anand et al., 2003). Silencing of a foreign gene after integration into the genome within a few generations illustrates the

inherent defence mechanisms of plants against foreign DNA invasion and expression (Demeke *et al*1999; Kumpatla *et al* 1997; Matzke *et al* 1996). In addition, unstable gene expression is often related to the integration of multiple copies of the transgene in the plant genome (Muller et al., 1996), position effect (Weiler and Wakimoto, 1995) and to the extent of methylation in the transgene loci (Srivastava et al., 1996). This could explain the phenotype observed in the first barley RNAi transgenic generation. These plants, regenerated directly from inoculated immature embryos, may have suffered different transgene silencing processes that, in combination to the *HvMS1* low level expression needed for its function, made the complete silencing of this gene unlikely and therefore, these plants showed complete fertility, although overall pollen viability was reduced.

The stability of transgene expression during vegetative propagation has been studied by Bettany et al (1998). In this study carried out on tall fescue plants (*Festuca arundinacea* Schreb.), they found that gene expression was particularly unstable during early generation of tillering, but more stable in the fourth of or fifth generation. Experiments conducted to find out the causes of this transgene expression instability discounted any deletion, gross rearrangement or hypermethylation, however, none of them were completely ruled out (Bettany et al., 1998). Moreover, this author claimed that for agricultural purposes, transgene stability must be observed not only during the meiotic processes of flowering, but also during the mitotic processes of vegetative propagation (Tillering). Therefore the tiller dependent sterile phenotype observed in barley RNAi T1 plants may be due to genetic mechanisms that affect trangene stability, or to the low level of *HvMS1* expression that make complete silencing very difficult.

Therefore, overall, although *HvMS1* silencing was not complete, the partial reduction in pollen viability (T0) and the sterility observed in the T1 generation indicate that this gene might be involved in pollen development. In addition, the observed phenotypes agree with those phenotype observed in rice *osptc1* mutant. However, further

confirmation of the role of *HvMS1* could be obtained using stable mutant lines obtained for example by tilling (Caldwell et al., 2004).

8.1.5.2 *HvMS1* over-expression.

Golden Promise *HvMS1* over-expression lines showed a completely sterile phenotype that affected the whole plant. This sterile phenotype was also observed in some *Arabidopsis MS1* over-expression lines (Yang et al., 2007). Vegetative development was normal, including spikes and florets formation (Fig.7.8.a-c). Anther appearance looked normal, however, after a closer analysis it was seen that anthers failed to dehisce (Fig.7.8.g-e). Old florets confirmed that dehiscence was not delayed but failed to occur at any stage. Inside the anthers, pollen was abundant and appeared fully viable (Fig.7.8.f-i). Anther dissection at dehiscence stage showed that in over-expression line the pollen stuck together, whilst wild type pollen was easily released from the anther. This characteristic may be due to some malformation in the pollen wall synthesis. A similar observation was seen in *Arabidopsis MS1* over-expression lines with an increase deposition of pollen coat material. Further work is needed to fully characterize these over-expression lines. Scanning electron microscope (SEM) may help to observe differences in pollen wall formation and explain why the pollen grains stick together. In addition, sectioning and light microscopy may also help to elucidate any changes contribute to study the anther elucidate any changes associated with pollen development and anther dehiscence.

Over-expression of *HvMS1* in *Arabidopsis ms1ms1* homozygous sterile lines failed to restore the fertility of these plants. This was most likely due to a lack of precise control of *MS1* expression in the tapetum since complementation of the *ms1* and *ptc1* mutants was also not possible when the native genes were regulated using the CaMV35S promoter (Ito et al., 2007; Li et al., 2011). Further complementation analyses are therefore needed using the *HvMS1* gene controlled by the native

MS1 promoter to confirm whether the barley *MS1* gene is functional in *Arabidopsis*.

Barley *HvMS1* silencing and over-expression studies, have contributed significantly to characterising this gene's function. However, due to inconclusive silencing results, tilling may be necessary to fully confirm involvement of *HvMS1* in anther and pollen development. In addition, although barley transformation has been conducted successfully, it has proved to be time consuming and excessively long (23-26 weeks for adult plants) in terms of flower development studies. Therefore, other methods, such as Virus Induces Gene Silencing (VIGs) may provide mechanism to rapidly test gene function (Velasquez et al., 2009). This approach although not guaranteeing complete silencing, can provide an efficient way to test gene function on growing plants without the need for callus development or regeneration, in a relatively high-through put manner. This can therefore be used as an additional tool for functional gene analysis prior to, or alongside, the development of stable mutant and transgenic lines.

8.1.6 Conservation of pollen regulation pathway in higher plants.

The conservation of genes involved in anther and pollen development has been observed between species. Orthologues genes to those observed in *Arabidopsis,* which are involved in this fundamental process of plant reproduction, have been localised and some of them well characterized in rice. Genes such as *DYT1, MS1* or *AMS* have been found to have an equivalent in this crop, maintaining similar function to their *Arabidopsis* orthologues (Wilson and Zhang, 2009). This conservation in regulation is allowing the researcher to go further in finding similar genes in different less characterised species.

Barley is an economically important crop, essential for animal feeding, human consumption and industry. Understanding anther and pollen regulation is essential to improve barley yield. Nowadays, population

increases are causing increased demand for better and more adaptable crops, producing more food in less space. Therefore, in order to improve barley productivity, as in rice (Barclay, 2007), hybrid seed production is becoming a necessity. For instance, transgenic nuclear male sterility has been developed using various transgenes, although only a few have been adapted for hybrid seed production (Mariani *et al.*, 1990; Perez-Prat and Van Lookeren Campagne, 2002). However, the commercial application of these transgenes is limited by the difficulties in propagating male sterile plants and the lack of suitable restorers (Perez- Prat and van Lookeren Campagne, 2002). Also because although the male sterility systems developed so far usually affect tapetum and pollen development, many also interfere with overall plant growth (Kriete *et al.*, 1996; Hernould *et al.*, 1998; Napoli *et al.*, 1999; Goetz *et al.*, 2001; Yui *et al.*, 2003; Zheng *et al.*, 2003). Therefore, controlling the activity of a transcription factor essential for male sterility, but whose up- or down-regulation does not affect either plant development or productivity, would provide a means of addressing these difficulties in crops.

The anther and pollen regulation pathway is unknown in barley. The comparative analysis between rice genes involved in anther and pollen development has currently failed due to the lack of a completely sequenced barley genome. However, the release of the *Brachypodium distachyon* genome and its closer relationship to barley allowed a more accurate comparative analysis that included rice, *Brachypodium* and barley, using *Brachypodium* an intermediate step between rice and barley. Using this approach, and thanks to a new release of barley sequences (Matsumoto et al., 2011), sequences similar to *AtMS2* and *AtMYB26* (Table.6.9; Appendix.6.6) have been found in rice, *Brachypodium* and barley (Table.6.9) This indicates that the release of the full barley genome will further facilitate the identification of orthologues genes to those involved in anther and pollen development in *Arabidopsis*. BLAST analysis conducted between *DYT1, EMS/EXS, AMS* orthologues in rice, *UTD1, MSP1* and *TDR* respectively, and the *Brachypodium* database indicated that these genes are probably

conserved in this grass (Table.6.9). However, BLAST analysis of these *Brachypodium* genes against barley EST databases showed no positive results, probably due to their localized and temporal expression that make these genes unlikely present in EST collection or simply because the barley equivalent sequence has not been released. However, similarities between rice and *Brachypodium* were significantly high to allow a similar approach to be conducted as used to identify the *OsPTC1* orthologue in barley (Section.8.1.2).

Comparative analysis has been an useful tool to characterize unknown genes in barley. In addition, as more and more barley and other species sequences are released, this approach will allow a more global analysis, identification and further characterization of novel genes and developmental networks. BLAST analysis alone normally gives hundred of similar results, most of them based upon short sequences or conserved domain (i.e. MYB domain in *AtMYB26*). Therefore, BLAST analysis needs to be complemented by the introduction of additional criteria that contribute to a more accurate identification. Conserved synteny (the maintenance of gene content and order in certain chromosomal regions of related species) provides valuable information for the analysis of families of homologous genes (Lehman et al., 2008). In addition, comparative genomic studies based on restriction fragment length polymorphism (RFLP) markers indicate that the linear order of markers remained largely conserved between grasses species over 50-70 million years of divergent evolution (Salse and Feuillet, 2007). Therefore, this conserved order may facilitate the identification of genes just by the proximity to these markers, differentiating it from other genes located within a different region of the genome. Also, due to the conservation of the exon structure in cereals (Salse and Feuillet, 2011), defining intron/exon conformation can provide higher accuracy while selecting BLAST results. In addition, gene expression patterns may be the final criterion that contributes to the selection of the most similar sequence to the target gene. However, to fully confirm the identity of related sequences a combination of these approaches is required.

REFERENCES

Aarts, M.G., Hodge, R., Kalantidis, K., Florack, D., Wilson, Z.A., Mulligan, M.J., Stiekema, W.J., Scott, R., Pereira, A. (1997) The Arabidopsis MALE STERILITY 2 protein shares similarity with reductases in elongation/condensation complexes. The Plant Journal, 12, 6115-623.

Aasland, R., Gibson, T.J., Stewart, A.F. (1995) The PHD finger: implications for chromatin-mediated transcriptional regulation. Trends Biochemestry Science, 20, 56–59.

Abiko, M., Akibayashi, K., Sakata, T., Kimura, K., Kihara, M., Itoh, K., Asamizu, E., Sato, S., Takahashi, H., Higashitani, A. (2005) High-temperature induction of male sterility during barley (*Hordeum vulgare* L.) anther development is mediated by transcriptional inhibition. Sex Plant Reproduction, 18, 91–100.

Albrecht, C., Russinova, E., Hecht, V., Baaijens, E., de Vries, S. (2005) The Arabidopsis thaliana SOMATIC EMBRYOGENESIS RECEPTORLIKE KINASES1 and 2 control male sporogenesis. The Plant Cell, 17, 3337–3349.

Altschul, S.F., Gish, W., Miller, W., Myers, E.W., Lipman, D.J. (1990) Basic local alignment search tool. Journal of Molecular Biology, 215, 3, 403-10.

Alves-Ferreira, M., Wellmer, F., Banhara, A., Kumar, V., Riechmann, J.L., Meyerowitz, E.M. (2007) Global expression profiling applied to the analysis of Arabidopsis stamen development. Plant Physiology, 145, 747–762.

Anand, A., Harold, N., Bikram, T., Gill, S., Muthukrishnan, S. (2003) Stable transgene expression and random gene silencing in wheat. Plant Biotechnology Journal, 241–251.

Anderson, P.M., Oelke, E.A., Simmons, S.R. (2002) Growth and development guide for spring barley. Regents of the University of Minnesota.

Aragon-Alcaide, L. (1995) A cereal centromeric sequence. Chromosoma, 105, 206–268.

Arduini, I., Ercoli, L., Mariotti, M., Masoni, A. (2010) Coordination between plant and apex development in *Hordeum vulgare* ssp. *Distichum.* Comptes Rendus Biologies, **333**, 5: 454-460.

Ariizumi, T., Hatakeyama, K., Hinata, K., Sato, S., Kato, T., Tabata, S., Toriyama, K. (2003) A novel male-sterile mutant of Arabidopsis thaliana, faceless pollen-1, produces pollen with a smooth surface and an acetolysis-sensitive exine. Plant Molecular Biology, 53, 1-2, 107-16.

Ariizumi, T., Hatakeyama, K., Hinata, K., Sato, S., Kato, T., Tabata, S., Toriyama, K. (2005) The HKM gene, which is identical to the MS1 gene of *Arabidopsis thaliana*, is essential for primexine formation and exine pattern formation. Sexual Plant Reproduction. 18, 1–7.

Arisnabarreta, S., Miralles, D.J. (2008) Radiation effects on potential number of grains per spike and biomass partitioning in two and six-rowed near isogenic barley lines. Field Crop Research, 107, 203-210.

Aya, K., Ueguchi-Tanaka, M., Kondo, M., Hamada, K., Yano, K., Nishimura, M., Matsuoka, M. (2009) Gibberellin modulates anther

development in rice via the transcriptional regulation of *GAMYB*. Plant Cell, 21, 1453-1472.

Baillie, A.M.R, Rossnagel, B.G., Kartha, K.K. (1993b) Evaluation of 10 canadian barley (*Hordeum vulgare* L.) cultivars for tissue culture response. Canadian Journal Plant Science, 73, 171-174.

Baker. C.K., Gallagher, J.N. (1983) The development of winter wheat in the field.1. Relation between apical development and plant morphology within and between seasons. The Journal of Agricultural Science, 101, 327-335.

Balk, J., Leaver, C.J. (2001) The PET1-CMS mitochondrial mutation in sunflower is associated with premature programmed cell death and cytochrome c release. The Plant Cell, 13, 1803-1818.

Barclay, A. (2007) A hybrid history. Rice Today, 6, 4, 22-25.

Bartlett, J.G., Alves, S.C., Smedly, M., Snape, J.W., Harwood, W. (2008) High-Throughput *Agrobacterium* mediated barley transformation. Plant Methods, 4, 22.

Bebeli, P.J., Kaltsikes, P.J., Karp, A. (1988) Plant regeneration and somaclonal variation from immature cultured embryos of sister lines of rye and triticale differing in their content of heterochromatin. 1. Morphological response. *Theoretical Applied Genetic*, 75, 929-936.

Bedinger, P. (1992) The remarkable biology of pollen, Plant Cell, 4, 879–887.

Bhaskaran, S., Smith, R.H. (1990) Regeneration in cereal tissue culture: a review. Crop Science. 30, 1328-1336.

BirdLife International (2008b). *Agricultural expansion is a major threat to birds, and appears to be increasing in importance*. BirdLife State of the World's Birds website. Available online at: http:// www.biodiversityinfo.org/sowb/casestudy.php?r=pressure&id=112.

Blaydes, D.F. (1966) Interaction of kinetin and various inhibitors in the growth of soybean tissue. Physiologia Plantarum, 19, 748-753.

Bonnet, O.T. (1966). Inflorescence of maize, wheat, rye, barley and oats: their initiation and development. Agricultural Experiment Station (College of Agriculture, University of Illinois), 721.

Bowman, J.L., Drews, G.N., Meyerowitz, E.M. (1991) Expression of the Arabidopsis Floral Homeotic Gene *AGAMOUS* 1s Restricted to-Specific Cell Types Late in Flower Development. The Plant Cell, 3, 749-758.

Bregitzer, P. (1992) Plant regeneration and callus type in barley: effects of genotype and culture medium. Crop Science. 32, 1108-1112.

Bregitzer, R., Dahleen, L.S., Campbell, R.D. (1998) Enhancement of plant regeneration from embryogenic callus of commercial barley cultivars. Plant Cell Reports, 17, 941-945.

Buitink, J., Leprince, O., Hemminga, M.A., Hoekstra, F.A. (2000) The effects of moisture and temperature on the ageing kinetics of pollen: Interpretation based on cytoplasmic mobility. Plant Cell Environ. 23, 967–974.

Caldwell, D.G., McCallum, N., Shaw, P., Muehlbauer, G.J., Marshal, D.F., Waugh, R. (2004) A structured mutant population for forward and reverse genetics in barley (Hordeum vulgare L.). The Plant Journal, 40, 143-150.

Canales, C., Bhatt, A.M., Scott, R.J., Dickinson, H.G. (2002) *EXTRA SPOROGENOUS CELLS* (*EXS*), a putative LRR receptor kinase, regulates male germline cell number and tapetal identity, and promotes seed development in *Arabidopsis*. Current Biology. 12, 1718–1727.

Castillo, A.M., Egana, B., Sanz, J.M., Cistue, L. (1998) Somatic embryogenesis and plant regeneration from barley cultivars grown in Spain. Plant Cell Reports, 17, 902-906.

Chan, M.T., Chang, H.H., Ho, S.L., Tong, W.F., Yu, S.M. (1993) *Agrobacterium*-mediated production of transgenic rice plants expressing a chimeric alpha-amykase promoter/Beta-glucoronidase gene. Plant Molecular Biology, 22, 491-506.

Chasan, R. (1992) Breaching the callose wall. Plant Cell, 4, 745–746.

Chaudhury, A. (1993) Nuclear genes controlling male fertility. Plant Cell, 5, 1277–1283.

Chen, C.B., Xu, Y.Y., Ma, H., Chong, K. (2005) Cell biological characterization of male meiosis and pollen development in rice. Journal of Integrative Plant Biology, 47, 734-744.

Cheng, M., Fry, J.E., Pang, S., Zhou, H., Hironaka, C.M., Duncan, D.R., Conner, T.W., Wan, Y. (1997) Genetic transformation of wheat mediated by *Agrobacterium tumefaciens*. Plant Physiology, 115,971-980.

Cheng, S.H., Zhuang, J.Y., Fan, Y.Y., Du, J.H., Cao, L.Y. (2007) Progress in research and development on hybrid rice: a super-domesticate in China. Annals of Botany,100, 959–966.

Cho, M.C., Jiang, W., Lemaux, P.G. (1998) Transformation of recalcitrant barley cultivars through improvement of regenerability and decreased albinism. Plant Science, 138, 2, 229-244

Christensen, A.H., Sharrock, R.A., Quail, P.H. (1992) Maize polyubiquitin genes—structure, thermal perturbation of expression and transcript splicing, and promoter activity following transfer to protoplasts by electroporation. Plant Molecular Biology, 18, 675–689.

Chu, C.C., Wang, C.C., Sun, C.S., Hsu, C., Yin, K.C., Bi, C.V. (1975) Establishment of an efficient medium for anther culture of rice through comparative experiments on the nitrogen source. Sci. Sinica, 18, 659-668.

Chuang, C.H., Meyerowitz, E.M. (2000) Specific and heritable genetic interference by double-stranded RNA in Arabidopsis thaliana. Proc Natl Acad Sci USA, 97, 4985–4990.

Clark, G.B., Turnwald, S., Tirlapur, U.K., Haas, C.J., von der Mark, K., Roux, S.J., Scheuerlein, R. (1995) Polar distributions of annexin-like proteins during phytochrome-mediated initiation and growth of rhizoids in the ferns Dryopteris and Anemia. Planta, 197, 376–384.

Colcombet, J., Boisson-Dernier, A., Ros-Palau, R., Vera, C.E., Schroeder, J.I. (2005) Arabidopsis SOMATIC EMBRYOGENESIS RECEPTOR KINASES1 and 2 are essential for tapetum development and microspore maturation. The Plant Cell, 17, 3350–33561.

Coronado, M.J., Hensel, G., Broeders, S., Otto, I., Kumlehn, J. (2005) Immature pollen-derived doubled haploid formation in barley cv. Golden Promise as a tool for transgene recombination. Acta Physiologiae Plantarum, 27, 591–599.

Dahleen, L.S. (1995) Improved plant regeneration from barley callus cultures by increased copper levels. Plant Cell Tissue and Organ Culture, 43, 267–269.

Dahleen, L.S., Bregitzer, P. (2002) An improved media system for high regeneration rates from barley immature embryo-derived callus. Crop Science, 42, 934-938.

Dearnaley, J.D.W., and Daggard, G.A. (2001) Expression of a polygalacturonase enzyme in germinating pollen of Brassica napus. Sex. Plant Reprod. 13, 265–271.

Demeke, T., Hucl, P., Baga, M., Caswell, K., Leung, N., Chibbar, R.N. (1999) Transgene inheritance and silencing in hexaploid spring wheat. Theoretical and Applied Genetic, 99, 947–953.

De Lucia, F., Crevillen, P., Jones, A.M., Greb, T., Dean, C. (2008) A PHD-polycomb repressive complex 2 triggers the epigenetic silencing of FLC during vernalization. Proc Natl Acad Sci USA, 105, 16831–16836.

Department for Environment Food and Rural Affairs (2011) Crop areas, yields and production, and livestock populations: 2011 UK – Provisional results.

Dickinson, H. (1995) Dry stigmas, water and self-incompatibility in Brassica. Sex. Plant Reprod. 8, 1–10.

Dickinson, H.G., Elleman, C.J., and Doughty, J. (2000) Pollen coatings: Chimaeric genetics and new functions. Sex. Plant Reprod, 12, 302–309.

Dixit, R., Rizzo, C., Nasrallah, M., and Nasrallah, J. (2001) The Brassica MIP-MOD gene encodes a functional water channel that is expressed in the stigma epidermis. Plant Mol. Biol, 45, 51–62.

Dong, X., Hong, Z., Sivaramakrishnan, M., Mahfouz, M., Verma, D.P. (2005) Callose synthase (CalS5) is required for exine formation during microgametogenesis and for pollen viability in Arabidopsis. Plant Journal, 42, 315–328.

Doughty, J., Hedderson, F., McCubbin, A., Dickinson, H. (1993) Interaction between a coating-borne peptide of the Brassica pollen grain and stigmatic S (self-incompatibility)-locus-specific glycoproteins. Proc. Natl. Acad. Sci. USA 90, 467–471.

Draper, J., Mur, L.A.J., Jenkins, G., Ghosh-Biswas, G.C., Bablak, P., Hasterok, R., Routledge, A.P.M. (2011) Brchypodium distachyon. A new model system for functional genomic in grasses. Plant Phisiology, 127, 1539-1555.

Edlund, A.F., Swanson, R., Preuss, D. (2004) Pollen and Stigma Structure and Function: The Role of Diversity in Pollination. The Plant Cell, 16, S84-S97.

Edwards, I.B. (2001) Hybrid Wheat. In The World Wheat Book (Bonjean, A.P. and Angus, W.J., eds), Paris: Lavoisier Publishing. 103–125.

Eisen, J.A., Wu, M. (2002) Phylogenetic Analysis and Gene function predictions: Phylogenomics in action. Theorical Population Biology, 61, 481-487.

Elleman, C.J., and Dickinson, H.G. (1986) Pollen-stigma interactions in Brassica. IV. Structural reorganization in the pollen grains during hydration. J. Cell Sci, 80, 141–157.

Elleman, C.J., Franklin-Tong, V., Dickinson, H.G. (1992) Pollination in species with dry stigmas: The nature of the early stigmatic response and the pathway taken by pollen tubes. New Phytol, 121, 413–424.

Evans, L.R. (2001) Agricultural and Rural development. Government of Alberta, Canada.Eversole, K., Graner, A., Stein, N. **(2009) Wheat and Barley Genome Sequencing . Plant Genetics and Genomics, Crops and Models, 7, 4, 713-742.**

FAOSTAT (2009) Food and agricultural commodities production. Available online at: http://faostat.fao.org/ site/339/default.aspx.

Feijo, J.A., Malho, R., Obermeyer, G. (1995) Ion dynamics and its possible role during in-vitro pollen germination and tube growth. Protoplasma 187, 155–167.

Fiebig, A., Kimport, R., Preuss, D. (2004) Comparisons of pollen coat genes across Brassicaceae species reveal rapid evolution by repeat expansion and diversification. Proc. Natl. Acad. Sci. USA 101, 3286–3291.

Finnegan, J., McElroy, D. (1994) Transgene inactivation: plants fight back. BioTechnology, 12, 883–888.

Fire, A., Albertson, D., Harrison, S., Moerman, D. (1991) Production of antisense RNA leads to effective and specific inhibition of gene expression in *C. elegans* muscle. Development, 113, 503–514.

Fire, A., Xu S.Q., Montgomery, M.K., Kostas, S.A., Driver, S.E., Mello, C.C. (1998) Potent and specific genetic interference by double-stranded RNA in Caenorhabditis elegans. Nature, 391, 806–811.

Fischer, R.A. (1984). Wheat. In: Smith, W.H., Banta, S.J. (Eds.), Symposium on Potential Productivity of Field Crops under Different Environments. IRRI, Los Baños, pp. 129–153.

Foote, T., Griffiths, S., Allouis, S., Moore, G. (2004) Construction and analysis of a BAC library in the grass Brachypodium sylvaticum: its use as a tool to bridge the gap between rice and wheat in elucidating gene content. Functional and Integrative Genomics, 4, 26–33.

Frank, A.B. (1996) Evaluating grass development for grazing management. Rangelands, 18, 106–109.

Fusaro, A.F., Matthew, L., Smith, N.A., Curtin, S.J., Dedic-Hagan, J., Ellacott, G.A., Watson, J.M., Wang, M.B., Brosnan, C., Carroll, B.J. (2006) RNA interference-inducing hairpin RNAs in plants act through the viral defense pathway. EMBO, 7, 1168–1175.

Gamborg, O.L., Wetter, L.R. (1975) Plant tissue culture methods. Saskatoon, Saskatchewan, Canada. National Research Council of Canada, Prairie Regional Laboratory.

Ghana, J.A., Sharma, G.C., Zipf, A., Saha, S., Roberts, J., Wesemberg, D.M. (1995) Genotype effects on plant regeneration in callus and suspension cultures of Avena. Plant Cell Tissue Organ Culture, 40, 217-224.

Gherardini, G.L., Healey, P.L. (1969) Dissolution of outer wall of pollen grain during pollination. Nature 224, 718–719. Dickinson, H.G., and Lewis, D. (1974). Changes in the pollen grain wall of Linum grandiflorum following compatible and incompatible intraspecific pollinations. Ann. Bot. 38, 23–29.

Göbel, U., Maas, R., Clad, A. (1987) Quantitative electroelution of oligonucleotides and large DNA fragments from gels and purification by electrodialysis. Journal Biochem Biophys Methods, 14, 5, 245-60.

Goetz, M., Godt, D.E., Guivarc'h, A., Kahmann, U., Chriqui, D., Roitsch, T. (2001) Induction of male sterility in plants by metabolic engineering of the carbohydrate supply. PNAS, 98, 11, 6522–6527.

Goff, S.A., Ricke, D., Lan, T.H., Presting, G., Wang, R., Dunn, M., Glazebrook, J., Sessions, A., Oeller, P., Varmab, H. (2002) A draft sequence of the rice genome (*Oryza sativa L. ssp. japonica*). Science, 296, 92–100.

Goldberg, R.B., Beals, T.P., Sanders, P.M. (1993) Anther development: Basic principles and practical applications. Plant Cell 5, 1217–1229.

Goldman, M.H., Goldberg, R.B., Mariani, C. (1994) Female sterile tobacco plants are produced by stigma-specific cell ablation. EMBO J. 13, 2976–2984.

Green, J.R. (1894) On the germination of the pollen grain and the nutrition of the pollen tube. Ann. Bot. 8, 225–228.

Griffiths, S., Sharp, R., Foote, T.N., Bertin, I., Wanous, M., Reader, S., Colas, I., Moore, G. (2006) Molecular characterization of Ph1 as a major chromosome pairing locus in polyploid wheat. Nature, 439, 749–752.

Grishok, A., Pasquinelli, A.E., Conte, D. (2001) Genes and mechanisms related to RNA interference regulate expression of the small temporal RNAs that control C. Elegans developmental timing. Cell, 106, 1, 23–34.

Gu, Y.Q., Vernoud, V., Fu, Y., Yang, Z. (2003) ROP GTPase regulation of pollen tube growth through the dynamics of tip-localized F-actin. J. Exp. Bot. 54, 93–101.

Gustavsson, A.M. (2011) A developmental scale for perennial forage grasses based on the decimal code framework. Grass and Forage Science, 66, 93–108.

Halbach, T., Scheer, N., Werr, W. (2000) Transcriptional activation by the PHD finger is inhibited through an adjacent leucine zipper that binds 14-3-3proteins. Nucleic Acids Research, 28, 3542–3550.

Hamilton, A.J., Baulcombe, D.C. (1999) A species of small antisense RNA in posttranscriptional gene silencing in plants. Science, 286, 950–952

Hanson, M.R., Bentolila, S. (2004) Interactions of mitochondrial and nuclear genes that affect male gametophyte development. The Plant Cell, 16, S154–S169.

Hanzel, J.J., Miller, J.P., Brinkman, M.A., Fendos, E. (1985) Genotype and media effects on callus formation and regeneration in barley. Crop Science, 25, 27-31.

Harwood, W., Bartlett, J.G., Laves, S.C., Perry, M., Smedly, M., Leyland, N., Snape, J.W. (2008) Barley Transformation Using *Agrobacterium* Mediated Transformation. Methods in Molecular Biology. Transgenic Wheat, Barley and Oats, 478.

Harwood, W.A., Ross, S.M., Cilento, P., Snape, J.W. (2000) The effect of DNA/gold particles preparation technique and particle bombardment device, on the transformation of barley (*Hordeum Vulgare*). Euphytica, 111, 67-76.

Harwood, W.A., Ross, S.M., Travella, S., Busc, B., Harden, J., Snape, J.W. (2002) Use of the firefly luciferase gene in a barley (*Hordeum vulgare*) transformation system. Plant Cell Reports, 21, 320-326.

Haun, J.R. (1973) Visual quantification of wheat development. Agronomy Journal, 65, 116-119.

Hawkes, T., Pline-Srnic, W., Dale, R., Friend, E., Hollinshead, T., Howe, P., Thompson, P., Viner, R., Greenland, A. (2011) D-glufosinate as a male sterility agent for hybrid seed production. Plant Biotechnology Journal, 9, 301–314.

Hay, R.K.H. (1986) Sowing date and the relationships between plant and apex development in winter cereals. *Field Crops Research*, **14**:321-337.

Hay, R.K.H., Kirby, E.J.M. (1991) Convergence and synchrony- A review of the coordination of development in wheat. Australian Journal of Agricultural Research, 42, 661-700.

He, Y., Jones, H.D., Chen, S., Chen, X.M., Wang, D.W., Li, K.X., Wang D.S., Xia, L.Q. (2010) *Agrobacterium*-mediated transformation of durum wheat (*Triticum turgidum* L. var. durum cv Stewart) with improved efficiency. Journal Experimental Botany, 61, 6, 1567-1581.

Heizmann, P., Luu, D.T., and Dumas, C. (2000) The clues to species specificity of pollination among Brassicaceae. Sex. Plant Reprod, 13, 157–161.

Hellens, R.P., Edwards, E.A., Leyland, N.R., Beans, S., Mullineaux, P.M. (2000) pGreen: a versatile and flexible binary Ti vector from *Agrobacterium* mediated plant transformation. Plan Molecular Biology, 42, 819-832.

Hensel, G., Valkov, V., Middlefell-Williams, J., Kumlehn, J. (2008) Efficient generation of transgenic barley: The way forward to modulate plant-microbe interaction. Journal Plant Physiology, 165, 71-82.

Hernould, M., Zabaleta, E., Carde, J.P., Litvak, S., Araya, A., Mouras, A. (1998) Impairment of tapetum and mitochondria in engineered male-sterile tobacco plants. Plant Molecular Biology, 36, 499–508.

Heslop-Harrison, J. (1979b) Aspects of the structure, cytochemistry and germination of the pollen of rye. Ann. Bot. 44, 1–47.

Heslop-Harrison, J. (1979b) Aspects of the structure, cytochemistry and germination of the pollen of rye. Ann. Bot. 44, 1–47.

Heslop-Harrison, J. (1979a) An interpretation of the hydrodynamic of pollen. Am. J. Bot, 66, 737–743.

Heslop-Harrison, Y. (1977) The pollen-stigma interaction: Pollen tube penetration in crocus. Ann. Bot. 41, 913–922.

Heslop-Harrison, J., Heslop-Harrison, Y. (1985) Germination of stress-tolerant Eucalyptus pollen. J. Cell Sci. 73, 135–157.

Heslop-Harrison, Y., Heslop-Harrison, J. (1992) Germination of monocolpate angiosperm pollen evolution of the actin cytoskeleton and wall during hydration activation and tube emergence. Ann. Bot. 69, 385–394.

Heslop-Harrison, Y., Shivanna, K.R. (1977) The receptive surface of the angiosperm stigma. Ann. Bot. 41, 1233–1258.

Heslop-Harrison, Y., Heslop-Harrison, J.S., Heslop-Harrison, J. (1986b) Germination of Corylus avellana L. (Hazel) pollen: Hydration and the function of the oncus. Acta Bot. Neerl. 35, 265–284.

Hibberd, J.M., Sheehy, J.E., Langdale, J.A. (2008) Using C-4 photosynthesis to increase the yield of rice—rationale and feasibility. Current Opinions in Plant Biology, 11, 228–231.

Hiei, Y., Komati, T. (2008) *Agrobacterium* mediated transformation of rice using immature embryos or calli induced from mature seed. Nature protocols, 3, 5, 824-834.

Hiei, Y., Ohta, S., Komari, T., Kumashiro, T. (1994) Efficient transformation of Rice (Oryza Sativa L.) mediated by Agribacterium and sequence analysis to the boundaries of the T-DNA. Plant Journal, 6, 271-282.

Higashiyama, T., Yabe, S., Sasaki, N., (2002) Pollen tube attraction by the synergid cell. Science, 293, 1480–1483

Higashiyama, T., Kuroiwa, H., Kawano, S., Kuroiwa, T. (1998) Guidance in vitro of the pollen tube to the naked embryo sac of *Torenia fournieri*. Plant Cell, 10, 2019–2031

Himmelbach, A., Zierold, D., Hensel, G., Riechen, J., Douchkov, D., Schweizer, P., Kumlehn, J. (2007) A Set of Modular Binary Vectors for Transformation of Cereal. Plant Physiology, 145, 1192-1200.

Hiscock, S.J., Dewey, F.M., Coleman, J.O.D., Dickinson, H.G. (1994). Identification and localization of an active cutinase in the pollen of Brassica napus L. Planta 193, 377–384.

Hiscock, S.J., Bown, D., Gurr, S.J., and Dickinson, H.G. (2002a) Serine esterases are required for pollen tube penetration of the stigma in Brassica. Sex. Plant Reprod. 15, 65–74.

Hiscock, S.J., Hoedemaekers, K., Friedman, W.E., and Dickinson, H.G. (2002b) The stigma surface and pollen-stigma interactions in Senecio squalidus L. (Asteraceae) following cross (compatible) and self (incompatible) pollinations. Int. J. Plant Sci. 163, 1–16.

Hoeberichts, F.A., Woltering, E.J. (2003) Multiple mediators of plant programmed cell death: Interplay of conserved cell death mechanisms and plant-specific regulators. Bioessays, 25, 47–57.

Hockett, E.A. (2000) Barley, Handbook of cereal science and technology,81-125.

Holme, B.I., Brinch-Pedersen, H., Lange, M., Holm, P.B. (2006) Transformation of barley (*Hordeum vulgare* L.) by *Agrobacterium tumefaciens* infection of in vitro cultured ovules. *Plant Cell Rep.* 25, 12, 1325–1335.

Honma, T., Goto, K. (2001). Complexes of MADS-box proteins are sufficient to convert leaves into floral organs. Nature, **409,** 525–529.

Hord, C.L., Chen, C., Deyoung, B.J., Clark, S.E., Ma, H. (2006) The BAM1/BAM2 receptor-like kinases are important regulators of Arabidopsis early anther development. The Plant Cell, 18, 1667–1680.

Hord, C.L., Sun, Y.J., Pillitterie, L., Toriie, K.U., Wang, H., Zhang, S., Ma, H. (2008) Regulation of Arabidopsis early anther development by the mitogen-activated protein kinases, MPK3 and MPK6, and the ERECTA and related receptor-like kinases. Molecular Plant, 1, 645–658.

Hulskamp, M., Kopczak, S.D., Horejsi, T.F., Kihl, B.K., Pruitt, R.E. (1995) Identification of genes required for pollen-stigma recognition in Arabidopsis thaliana. Plant J. 8, 703–714.

Hulskamp, M., Kopczak, S.D., Horejsi, T.F., Kihl, B.K., Pruitt, R.E. (1995) Identification of genes required for pollen-stigma recognition in Arabidopsis thaliana. Plant J. 8, 703–714.

International Brachypodium Initiative. Genome sequencing and analysis of the model grass Brachypodium distachyon. Nature, 463, 763-768.

Ishid, Y., Sito, S., Hiei, Y., Komari, T and Kumashiro, T. (1996) High efficiency transformation of maize (*Zea mays* L.) mediated by *Agrobacterium tumesfaciens*. Nature Biotechnology, 14, 745-750.

Ito T., Ng, K.H., Lim, T.S., Yu, H., Meyerowitz, E.M. (2007b) The homeotic protein AGAMOUS controls late stamen development by regulating a jasmonate biosynthetic gene in Arabidopsis. The Plant Cell, 19, 3516–3529.

Ito, T., Nagata, N., Yoshiba, Y., Ohme-Takagi, M., Ma, H., Shinozaki, K. (2007) *Arabidopsis MALE STERILITY1* Encodes a PHD-Type Transcription Factor and Regulates Pollen and Tapetum Development. Plant Cell, 19, 11, 3549–3562.

Ito, T., Shinozaki, K. (2002) The MALE STERILITY1 gene of Arabidopsis, encoding a nuclear protein with a PHD-finger motif, is

expressed in tapetal cells and is required for pollen maturation. Plant Cell Physiology, 43, 1285–1292.

Itoh, J., Nonomura, K., Ikeda, K., Yamaki, S., Inukai, Y., Yamagishi, H., Kitano, H., Nagato, Y. (2005) Rice plant development: from zygote to spikelet. Plant and Cell Physiology, 46, 23-47.

Iyer, L.M., Kumpatla, S.P., Chandrasekharan, M.B., Hall, T.C. (2000) Transgene silencing in monocots. Plant Molecular Biology, 43, 323–346.

Jefferson, R.A., Kavanaugh, T.A., Bevan, M.W. (1987) GUS fusions: β-glucuronidase as a sensitive and versatile gene fusion marker for higher plants. EMBO J, 6, 3901-3907.

Jia, G., Liu, X., Owen, H.A., Zhao, D. (2008) Signaling of cell fate determination by the TPD1 small protein and EMS1 receptor kinase. PNAS, 105, 6, 2220–2225.

Jones, J.D.G., Dunsmuir, D., Bedbrook, J. (1985) High level expression of introduced chimearic genes in regenerated transformed plants. EMBO Journal, 10, 2411–2418.

Johnson, S.A., McCormick, S. (2001) Pollen germinates precociously in the anthers of raring-to-go, an Arabidopsis gametophytic mutant. Plant Physiol, 126, 685–695.

Johnson, M.A., Preuss, D. (2002) Plotting a course: Multiple signals guide pollen tubes to their targets. Dev. Cell 2, 273–281.

Joshi, A., Kothari, S.L. (2007) High cooper levels in the medium improves shoot bud differentiation and elongation from cultured

cotyledons of *Caypsicum annuum* L. Plant Cell Tissue and Organ Culture, 88, 127-133.

Jung, K.H., Han, M.J., Lee, Y.S., Kim, Y.W., Hwang, I., Kim, M.J., Kim, Y.K., Nahm, B.H., An, G. (2005) Rice Undeveloped Tapetum1 is a major regulator of early tapetum development. The Plant Cell, 17, 2705-2722.

Kandasamy, M.K., Thorsness, M.K., Rundle, S.J., Goldberg, M.L., Nasrallah, J.B., and Nasrallah, M.E. (1993) Ablation of papillar cell function in Brassica flowers results in the loss of stigma receptivity to pollination. Plant Cell 5, 263–275.

Kao, K.N. (1977) Chromosomal behaviour in somatic hybrids of soybean *Nicotiana glauca*. Molecular General Genetic, 150, 225-230.

Kapoor, S., Kobayashi, A., Takatsuji, H. (2002) Silencing of the tapetum-specific zinc finger gene TAZ1 causes premature degeneration of tapetum and pollen abortion in petunia. Plant Cell, 14, 2353–2367.

Khanna, H.K., Daggard, G.E. (2003) Agrobacterium tumefacien mediated transformation of wheat using a superbinary vector and a polyamine-supplemented regeneration medium. Plant Cell Reports, 21, 429-436.

King, S.P., Kasha, K.J. (1994) Optimizing somatic embryogenesis and particle bombardment of barley (*Hordeum vulgare* L.) immature embryos. In Vitro Cellular Development Biology. Plant, 30, 117-123.

Kim, H.U., Chung, T.Y., and Kang, S.K. (1996) Characterization of anther-specific genes encoding a putative pectin esterase of Chinese cabbage. Mol. Cells 6, 334–340.

Kirby, E.J.M. (1993) Effect of sowing depth on seedling emergence, growth and development in barley and wheat. Field Crops Research, **35**, 2: 101-111.

Kirby, E.J.M. and Appleyard, M. (1984a) Cereal Development Guide. In: (2nd Edn. ed.). *Arable Unit, National Agricultural Centre, Coventry*: 95.

Kirby, E.J.M. and Appleyard, M. (1984b) Cereal plant development assessment and use. In: *The Nitrogen Requirements of Cereals Reference Book 385*, Ministry of Agriculture, Fisheries and Food, H.M.S.O., pp. 21–38.

Kirby, E.J.M., Appleyard, M. (1986) Cereal Development Guide (2nd edition). National Agricultural Centre Arable, Stoneleigh, Warwickshire, Great Britain, p. 95.

Kirby, E.J.M., (1988) Analysis of leaf, stem and ear growth in wheat from terminal spikelet stage to anthesis. Field Crops Reserach, 18, 127-140.

Kirby, E.J.M., Appleyard, M. (1987) Cereal development guide. NAC Cereal Unit, Stoneleigh, UK, 95 pp.

Kitchen, B.M., Rasmusson, D.C. (1983) Duration and inheritance of leaf initiation, spike initiation, and spike growth in barley. Crop Science, 23, 939-942.

Knox, R.B., Heslop-Harrison, J. (1970). Pollen-wall proteins: Localization and enzymic activity. J. Cell Sci. 6, 1–27.

Kost, B., Lemichez, E., Spielhofer, P., Hong, Y., Tolias, K., Carpenter,vC., Chua, N.H. (1999) Rac homologues and compartmentalized phosphatidylinositol 4,5-bisphosphate act in a

common pathway to regulate polar pollen tube growth. J. Cell Biol. 145, 317–330.

Kriete, G., Niehaus, K., Perlick, A.M., Pühler, A., Broer, I. (1996) Male sterility in transgenic tobacco plants induced by tapetum-specific deacetylation of the externally applied non-toxic compound N-acetyl-L -Phosphinothricin. The Plant Journal. 9, 6, 809-818.

Krizek, B.A., Fletcher, J.C. (2005) Molecular mechanism of flower development: an armchair guide. Nature Review Genetic, 6, 688-698.

Kumlehn, J., Serazetdinova, L., Hensel, G., Becker, D., Loerz, H. (2006) Genetic transformation of barley (*Hordeum vulgare* L.) via infection of androgenetic pollen cultures with *Agrobacterium tumefaciens*. Plant Biotechnology Journal, 4, 251-261.

Kumpatla, S.P., Teng, W., Buchholz, W.G., Hall, T.C. (1997) Epigenetic transcriptional silencing and 5-azacytidine-mediated reactivation of a complex transgene in rice. Plant Physiology, 115, 361–373.

Lalanne, E., Twell, D. (2002) Genetic control of male germ unit organization in Arabidopsis. Plant Physiol. 129, 865–875.

Lalonde, B.A., Nasrallah, M.E., Dwyer, K.G., Chen, C.H., Barlow, B., and Nasrallah, J.B. (1989) A highly conserved Brassica gene with Pollen and Stigma Structure and Function S95 homology to the S-locus-specific glycoprotein structural gene. Plant Cell, 1, 249–258.

Lam, E., del Pozo, O. (2000) Caspase-like protease involvement in the control of plant cell death. Plant Molecular Biology, 44, 417–428.

Lancashire, P.D., Bleiholder, H., Van Den Boom, T. Langeluddeke, P., Stauss, R., Weber, E., Witzenberger, A. (1991) A uniform decimal code for growth stages of crops and weeds. Annals of Applied Biology, 119, 561–601.

Landes, A., Porter, J.R. (1989) Comparison of scales used for categorizing the development of wheat, barley, rye and oats. Annals of Applied Biology, 115, 343–360.

Lange M., Vincze, E., Wieser, H., Schjørring, J.K., Holm, P.B. (2007) Effect of an antisense C-hordein gene on the storage protein composition in the barley seed. Journal of Agricultural and Food Chemistry, 55, 6074-6081.

Large, E.G. (1954) Growth stages in cereals: Illustration of the Feeke's scale. Plant Pathology, 3, 4, 128–129.

Lehman, J., Stadler, P.F., Prohaska, S.J. (2008) SynBlast: Assisting the analysis of conserved synteny information. BMC Bioinformatics, 9, 351.

Lewis, D., Crowe, L.K. (1958) Unilateral interspecific incompatibility in flowering plants. Heredity 12, 233–256.

Li, H., Li., Yuan Z., Vizcay-Barrena, G., Yang, C., Liang, W., Zong, J., Wilson, Z.A., Zhang, D. (2011) PERSISTENT TAPETAL CELL1 encodes a PHD-finger protein that is required for tapetal cell death and pollen development in rice. Plant Physiology, 156, 2, 615-30.

Li, N., Zhang, D.S., Liu, H.S., Yin, C.H., Li, X.X., Liang, W.Q., Yuan, Z., Xu, B., Chu, H.W., Wang, J., Wen, T.Q., Huang, H., Luo, D., Ma, H., Zhang, D.B. (2006) The Rice Tapetum Degeneration Retardation Gene Is Required for Tapetum Degradation and Anther Development. The Plant Cell, 18, 2999-3014.

Li, S.F., Iacuone, S., Parish, R.W. (2007) Suppression and restoration of male fertility using a transcription factor. Plant Biotechnology Journal, 5,297–312.

Li, H., Lin, Y., Heath, R.M., Zhu, M.X., Yang, Z. (1999) Control of pollen tube tip growth by a Rop GTPase-dependent pathway that leads to tip-localized calcium influx. Plant Cell 11, 1731–1742.

Li, Z., Upadhayaya, N.M., Meena, S., Gibbs, A.L., Waterhouse, P.M. (1997) Comparison of promoters and selectable markers gene of use in Indica rice transformation. Molecular Breeding, 3, 1-14.

Linacero, T., Vazquez, A.M. (1986) Somatic embryogenesis and plant regeneration from leaf tissues of rye (*Secale cereale* L.). Plant Science, 44, 219-222.

Lindbo, J.A., Silva-Rosales, L., Proebsting, W.M., Dougherty, W.G. (1993). Induction of a highly specific antiviral state in transgenic plants: Implications for regulations of gene expression and virus resistance. Plant Cell, 5, 1749-1759.

Liu, L.S., White, M.J., MacRae, T.H. (1999) Transcription factors and their genes in higher plants functional domains, evolution and regulation. European Journal of Biochemestry, 262, 247-257.

Lolle, S.J., Berlyn, G.P., Engstrom, E.M., Krolikowski, K.A., Reiter, W.D., and Pruitt, R.E. (1997) Developmental regulation of cell interactions in the Arabidopsis fiddlehead-1 mutant: A role for the epidermal cell wall and cuticle. Dev. Biol, 189, 311–321.

Lolle, S.J., Cheung, A.Y. (1993) Promiscuous germination and growth of wildtype pollen from Arabidopsis and related species on the shoot of the Arabidopsis mutant, fiddlehead. Dev. Biol. 155, 250–258.

Lolle, S.J., Hsu, W., and Pruitt, R.E. (1998) Genetic analysis of organ fusion in Arabidopsis thaliana. Genetics, 149, 607–619.

Lord, E.M, Rusell, S.D. (2002) The Mechanism of Pollination and Fertilization in Plants. Ann. Rev. Cell. Dev. Biol, 18, 81-105.

Luehrs, R., Loerz, H. (1987) Plant regeneration in vitro from embryogenic cultures of spring- and winter-type barley (*Hordeum vulgare* L.) varieties. Theoretical and Applied Genetic, 75,16-25.

Luu, D.T., Heizmann, P., and Dumas, C. (1997a) Pollen-stigma adhesion in kale is not dependent on the self-(in)compatibility genotype. Plant Physiol, 115, 1221–1230.

Luu, D.T., Heizmann, P., Dumas, C., Trick, M., and Cappadocia, M. (1997b) Involvement of SLR1 genes in pollen adhesion to the stigmatic surface in Brassicaceae. Sex. Plant Reprod, 10, 227–235.

Luu, D.T., Marty-Mazars, D., Trick, M., Dumas, C., and Heizmann, P. (1999) Pollen-stigma adhesion in Brassica spp involves SLG and SLR1 glycoproteins. Plant Cell, 11, 251–262.

Lush, W.M., Grieser, F., Wolters-Arts, M. (1998) Directional guidance of Nicotiana alata pollen tubes in vitro and on the stigma. Plant Physiol. 118, 733–741.

Lynn, S., Dahleen, Bregitzer, P. (2002) An Improved Media System for High Regeneration Rates from Barley Immature Embryo-Derived Callus Cultures of Commercial Cultivars. Crop Science. 42, 934–938.

Ma, H. (2005) Molecular genetic analyses of microsporogenesis and microgametogenesis in flowering plants. Plant Biology, 56, 393-434.

Machii, H., Mizuno, H., Hirabayashi, T., Li, H., Hagio, T. (1998) Screening Wheat Genotypes for High Callus Induction and Regeneration Capability from Anther and Immature Embryo Cultures. Plant Cell, Tissue Organ Cult. 53, 67–74.

Mansoor, S., Amin, I., Hussain, M. (2006). Engineering novel traits in plants through RNA interference. Trends Plant Science, 11, 11, 559–65.

Mariani, C., Beuckeleer, M., Truettner, J., Leemans, J., Goldberg, R.B. (1990) Induction of male sterilityin plants by a chimeric ribonuclease gene. Nature, 347, 737–741.

Matsumoto, T., Tanaka, T., Sakai, H., Amano, N., Kanamori, H., Kurita, K., Kikuta, A., Kamiya, K., Yamamoto, M., Ikawa, H., Fujii, N., Hori, K., Itoh, T, Sato, K. (2011) Comprehensive Sequence Analysis of 24,783 Barley Full-Length cDNAs. Journal of Plant Physiology, 156, 1, 20-28.

Matthews, P.R., Wang, M.B., Waterhouse, P.M., Thornton, S., Fieg, S.J., Gubbler, F., Jacobsen, J.V. (2001) Marker gene elimination from transgenic barley using co-transformation with adjacent twin T-DNA on a standard *Agrobcterium* transformation vector. Molecular Breeding, 172, 281-290.

Matzke, A.J.M., Matzke, M.A. (1998) Position effect and epigenetic silencing of plant transgenes. Current Opinion Plant Biology, 1, 142–148.

Matzke, M.A., Matzke, A.J.M. (1998) Epigenetic silencing of plant transgenes as a consequence of diverse cellular defense responses. Cell Molecular Life Science, 54, 94–103.

Matzke, M.A., Matzke, J.M., Eggleston, W.B. (1996) Paramutation and transgene silencing: a common response to invasive DNA? Trends Plant Science, 1, 382–388.

Mayfield, J.A., Fiebig, A., Johnstone, S.E., Preuss, D. (2001) Gene families form the Arabidopsis thaliana pollen coat proteome. Science 292, 2482–2485.

Mayfield, J.A., Preuss, D. (2000) Rapid initiation of Arabidopsis pollination requires the oleosin-domain protein GRP17. Nat. Cell Biol. 2, 128–130.

Mazina, S., Matveeva, N., Ermakov, I. (2002) Determination of a position of a functional pore. Tsitologiya 44, 33–39.

McGinnis, K., Murphy, N., Carlson, A.R., Akula, A., Akula, C., Basinger, H., Carlson, M., Hermanson, P., Kovacevic, N., McGill, M.A., Seshadri, V., Yoyokie, J., Cone, K., Kaeppler, H.F., Kaeppler, S.W., Springer, N.H. (2007) Assessing the Efficiency of RNA Interference for Maize Functional Genomics1. Plant Physiology, 143, 1441–1451.

Meshi, T., Iwabuchi, M. (1995) Plant transcription factors. Plant Cell Physiology. 36, 1405–1420.

Meuter-Gerhards, A., Riegart, S., Wiermann, R. (1999) Studies on sporopollenin biosynthesis in Curcurbita maxima (DUCH)-II: the involvement of aliphatic metabolism. Journal of Plant Physiology, 154, 431–436.

Meyer, P. (1995) Understanding and controlling transgene expression. Trends Biotechnology, 13, 332–337.

Millar, A.A., Gubler, F. (2005) The Arabidopsis GAMYB-Like genes, MYB33 and MYB65, are microRNA-regulated genes that redundantlyfacilitate anther development. The Plant Cell, 17, 705–721.

Miralles, D.J., Richards, R.A., Slafer, S.A. (2000) Duration of the stem elongation period influences the number of fertile florets in wheat and barley. Aust. J. Plant Physiol, 27, 931-940.

Miralles, D.J., Slafer, G.A. (1999) Wheat development. In: Satorre, E.H., Slafer, G.A. (Eds.), Wheat: Ecology and Physiology of Yield Determination. Haworth Press Inc., New York, pp. 13–43.

Mollet, J.C., Park, S.Y., Nothnagel, E.A., Lord, E.M. (2000) A lily stylar pectin is necessary for pollen tube adhesion to an in vitro stylar matrix. Plant Cell, 12, 1737–1749.

Moore, G. (1993) Molecular analysis of small grain cereals. Nature Biotechnology, 11, 584–589.

Moore, G., Devos, K.M., Wang, Z., Gale, M.D. (1995) Cereal genome evolution. Grasses, line up and form a circle. Current Biology, 5, 737-739.

Moritoh, S., Miki, D., Akiyama, M., Kawahara, M., Izawa, T., Mak,i H., Shimamoto, K. (2005) RNAi-mediated silencing of OsGEN-L (OsGEN-like), a new member of the RAD2/XPG nuclease family, causes male sterility by defect of microspore development in rice. Plant Cell Physiology, 46, 699–715.

Muller, E., Lorz, H., Lutticke, S. (1996) Variability of transgene expression in clonal cell lines of wheat. Plant Science, 114, 71–82.

Murashige, T., Skoog, F. (1962) A revised medium for rapid growth and bioassays with tobacco tissue culture. Physiol Plantarum, 15, 473-497.

Murray, F., Brettell, R., Mattews, P., Bishop, D., Jacobsen, J. (2004) Comparison of Agrobacterium mediated transformation of four barley culivars using GFP and GUS reporter gene. Plant Cell Reports. 22, 397-402.

Murray, F., Kalla, R., Jacobsen, J.V., Gubler, F. (2003) A role for HvGAMYB in anther development. Plant Journal, 33, 481–491.

Muschietti, J., Eyal, Y., and McCormick, S. (1998) Pollen tube localization implies a role in pollen-pistil interactions for the tomato receptor-like protein kinases LePRK1 and LePRK2. Plant Cell 10, 319–330.

Napoli, C., Lemieux, C. Jorgensen, R. (1990) Introduction of chimeric chalcone synthase gene into petunia results in reversible co-suppression of homologous gene in trans. Plant Cell, 2, 279–289.

Napoli, C.A., Fahy, D., Wang, H.Y., Taylor, L.P. (1999) White anther: a *Petunia* mutant that abolishes pollen flavonol accumulation, induces male sterility, and is complemented by a chalcone synthase transgene. Plant Physiology, 120, 615–622.

Needleman, S.B., Wunsch, C.D. (1970) A general method applicable to the search for similarities in the amino acid sequence of two proteins. *Journal of Molecular Biology,* 48, 3, 443–53.

Neill, J., Pierce, D.A., Cigan, A.M. (1996) Methods and compositions for controlling plant development. U.S. Patent, 5583210.

Ninkovic, V., Ahman, I.M. (2009) Aphid acceptance of *Hordeum* genotypes is affected by plant volatile exposure and is correlated with aphid growth. *Euphytica*, **109**.

Nonomura, K., Miyoshi, K., Eiguchi, M., Suzuki, T., Miyao, A., Hirochika, H., Kurata, N. (2003) The MSP1 gene is necessary to restrict the number of cells entering into male and female sporogenesis and to initiate anther wall formation in rice. The Plant Cell, 15, 1728-1739.

Norstog, K. (1973) New synthetic medium for the culture of premature embryos. In Vitro, 8, 307-308.

Oldach, K.H., Becker, D., Lörz, H. (2001) Heterologous expression of genes mediating enhanced fungal resistance in transgenic wheat. Molecular Plant Microbe Interaction, 14, 832–838.

Opanowicz, M., Vain, P., Draper, J., Parker, D., Doohan, J.H. (2008) Brachypodium dustachyon: Making a hay with a wild grass. Trends in plant science, 13, 4, 172-177.

Owen, H.A., Makaroff, C.A. (1995) Ultrastructure of microsporogenesis and microgametogenesis in *Arabidopsis thaliana* (L.) Heynh. ecotype Wassilewskija (Brassicaceae). Protoplasma, 185, 7–21.

Pacini, E., Franchi, G., and Hesse, M (1985) The tapetum: Its form, function, and possible phylogeny in embryophyta. Plant Systematic and Evolution, 149, 155–185.

Pandit, N.N., Russo, V.E. (1992) Reversible inactivation of a foreign gene, hph, during the asexual cycle in Neurospora crassa transformants. Molecular General Genetic, 234, 3, 412–22.

Park, S.Y., Jauh, G.Y, Mollet, J.C., Eckard, K.J., Nothnagel, E.A. (2000) A lipid transferlike protein is necessary for lily pollen tube adhesion to an in vitro stylar matrix. Plant Cell, 12, 151–163.

Parish, R.W., Li, S.F. (2010) Death of a tapetum: a programme of developmental altruism. Plant Science, 178, 73–89.

Peach, C., Velten, J. (1991) Transgene expression variability (position effect) of CAT and GUS reporter genes driven by linked divergent T-DNA promoters. Plant Molecular Biology, 17, 49–60.

Pelaz, S., Ditta, G.S., Baumann, E., Wisman, E., Yanofsky, M.F. (2000) B and C floral organ identity functions require *SEPALLATA* MADS-box genes. Nature, 405, 200–203.

Pelletier, G., Budar, F. (2007) The molecular biology of cytoplasmically inherited male sterility and prospects for its engineering. Current Opinion in Biotechnology, 18, 121–125.

Pena, P.V., Davrazou, F., Shi, X., Walter, K.L., Verkhusha, V.V., Gozani, O., Zhao, R., and Kutateladze, T.G. (2006) Molecular mechanism of histone H3K4me3 recognition by plant homeodomain of ING2. Nature, 442, 100–103.

Perez-Prat, E., Van Lookeren-Campagne, M.M. (2002) Hybrid seed production and the challenge of propagating male sterile plants. Trends in Plant Science,7, 5.

Pickett, A.A. (1998): Wheat. In: Banga, S. S., Banga, S. K. (eds.), *Hybrid Cultiva Development:* Narosa Publishing House, New Delhi, India. 257–281.

Piffanelli, P., Ross, J.H.E., Murphy, D.J. (1998) Biogenesis and function of the lipidic structures of pollen grains. Sexual Plant Reproduction, 11, 65–80.

Potrykus, I. (1990) Gene transfer to cereals: an assessment. BioTechnology, 8, 533-542.

Potrykus, I., Harms, C.T., Loerz, H. (1979) Callus formation from cell culture protoplasts of corn (*Zea mays* L.) Theoretical and Applied Genetic, 54,209-214.

Preuss, D., Lemieux, B., Yen, G., Davis, R.W. (1993) A conditional sterile mutation eliminates surface components from Arabidopsis pollen and disrupts cell signaling during fertilization. Genes Dev. 7, 974–985.

Procissi, A., de Laissardiere, S., Ferault, M., Vezon, D., Pelletier, G., Bonhomme, S. (2001) Five gametophytic mutations affecting pollen development and pollen tube growth in Arabidopsis thaliana. Genetics 158, 1773–1783.

Pruitt, R.E., Vielle-Calzada, J.P., Ploense, S.E., Grossniklaus, U., and Lolle, S.J. (2000) FIDDLEHEAD, a gene required to suppress epidermal cell interactions in Arabidopsis, encodes a putative lipid biosynthetic enzyme. Proc. Natl. Acad. Sci. USA, 97, 1311–1316.

Rebetzke, G.J., Richards, R.A., Sirault, X.R.R, Morrison, A.D. (2004) Genetic analysis of coleoptile length and diameter in wheat. Australian Journal of Agricultural Research, 55(7), 733–743.

Regan, S.M., Moffatt, B.A. (1990). Cytochemical analysis of pollen development in wild-type Arabidopsis and a male-sterile mutant. Plant Cell, 2, 877-889.

Reynolds, M., Foulkes, J., Slafer, G.A., Berry, P., Parry, M.A.J., Snape, J.W., Angus, W.J. (2009) Raising yield potential in wheat. Journal of Experimental Botany, 60, 7, 1899–1918.

Romano, N., Macino, G. (1992) Quelling: transient inactivation of gene expression in Neurospora crassa by transformation with homologous sequences. Molecular Microbiology, 6, 22, 3343–53.

Salse, J., Feuillet, C. (2007) Comparative genomics of cereals. Genomics-assisted crop improvement, 177-205.

Salse, J., Feuillet, C. (2011) Palaeogenomics in cerelas: Modeling of ancestors for modern species improvement. Comptes Rendus Biologies, 334, 205-211.

Sanders, P.M., Bui, A.Q., Weterings, K., McIntire, K.N., Hsu, Y.C., Lee, P.Y., Truong, M.T., Beals, T.P., Goldberg, R.B (1999) Anther developmental defects in Arabidopsos thaliana male-strile mutants. Sex Plant Reproduction, 11, 297–322.

Schiefthaler, U., Balasubramanian, S., Sieber, P., Chevalier, D., Wisman, E., Schneitz, K. (1999) Molecular analysis of NOZZLE, a gene involved in pattern formation and early sporogenesis during sex organ development in *Arabidopsis* thaliana. PNAS, 96, 11664–11669.

Schledzewski, K., Mendel, R.R. (1994) Quantitative transient gene expression: comparison of the promoters for maize polyubiquitin1, rice actin1, maize-derived *Emu* and CaMV *35S* in cells of barley, maize and tobacco. Transgenic Research, 3, 4, 249–255.

Scott, R.J., Spielman, M., Dickinson, H.G. (2004) Stamen Structure and function. The Plant Cell, 16, S46-S60.

Sears, R.G., Deckard, E.L. (1982) Tissue culture variability in wheat: callus induction and plant regeneration. Crop Science, 22, 546-550.

Sharma, G.C., Bello, L.L., Sapra, V.T. (1980) Genotypic differences in organogenesis from callus of ten triticale lines. Euphytica, 29,751-754.

Sharma, V.K., Hansch, R., Mendel, R.R., Cshulze, J. (2005) Mature embryo axis-based high frequency somatic embryogenesis and plant regeneration from multiple cultivars of barley (*Hordeum vulgare* L.). Journal of Experimental Botany, 56, 417, 1913-1922.

Sharma, V.K., Hansch, R., Mendel, R.R., Schulz, J. (2004) A highly efficient plant regeneration system through multiple shoot differentiation from commercial cultivars of barley (*Horedum vugare* L.) using meristematic shoot segments excised from germinated mature embryos. Plant Cell Reports, 23, 9-16.

Sarker, R.H., Elleman, C.J., Dickinson, H.G. (1988) Control of pollen hydration in Brassica requires continued protein-synthesis, and glycosylation is necessary for intraspecific incompatibility. Proc. Natl. Acad. Sci. USA 85, 4340–4344.

Shenk, R.V., Hildebrandt, A.C. (1972) Medium and techniques for induction and growth of monocotyledonous and dicotyledonous plant cell cultures. Canadian Journal Botany, 50, 199-204.

Sheridan, W. F., Avalkina, N. A., Shamrov, I. I., Batygina, T. B., Golubovskaya, I.N. (1996) The *mac1* gene: controlling the commitment to the meiotic pathway in maize. Genetics, 142, 1009–1020.

Shi, X., Hong, T., Walter, K.L., Ewalt, M., Michishita, E., Hung, T., Carney, D., Peña, P., Lan, F., Kaadige, M.R., Lacoste, N., Cayrou, C., Davrazou, F., Saha, A., Cairns, B.R., Ayer, D.E., Kutateladze, T.G., Shi, Y., Côté, J., Chua, K.F., Gozani. O. (2006)

ING2 PH domain links histone H3 lysine 4 methylation to active gene repression. Nature, 442, 96–99.

Shinozaki, K., Ito, T. (2002) The MALE STERILITY1 Gene of Arabidopsis, Encoding a Nuclear Protein with a PHD-finger Motif, is Expressed in Tapetal Cells and is Required for Pollen Maturation. Plant Cell Physioogy,. 43, 11, 1285–1292.

Shrawat, A.K., Becker, D., Lorz. H. (2007) *Agrobacterium Tumesfaciens*-mediated genetic transformation of barley (*Hordeum Vulgare* L.). Plant Science, 172, 281-290.

Shrawat, A.K.,, Lorz, H. (2006) *Agrobacterium*-mediated transformation of cereals: a promising approach crossing barriers. Plant Biotechnology Journal, A, 575-603.

Simmons, A.T., Nicol, H.I., Gurr, G.M. (2006) Resistance of wild *Lycopersicon* species to the potato moth, *Phthorimaea operculella* (Zeller) (Lepidoptera: Gelechiidae). *Australian Journal of Entomology*, **45**, 81–86.

Slafer, G.A. (2002) Barley science: recent advances from molecular biology to agronomy of yield and quality. Routledge.

Smith, N.A., Singh, S.P., Wang, M-B., Stoutjesdijk, P., Green, A. and Waterhouse, P.M. (2000) Total silencing by intron-spliced hairpin RNAs. Nature, 407, 319–320.

Smyth, D.R., Bowman, J.L., Meyerowitz, E.M. (1990) Early flower development in Arabidopsis. Plant Cell, 2, 755-767.

Solomon, M., Belenghi, B., Delledonne, M., Menachem, E., Levine, A. (1999) The involvement of cysteine proteases and protease inhibitor genes in the regulation of programmed cell death in plants. Plant Cell, 11, 431–444.

Sorensen, A.M., Krober, S., Unte, U.S., Huijser, P., Dekker, K., Saedler, H. (2003) The Arabidopsis ABORTED MICROSPORES (AMS) gene encodes a MYC class transcription factor. The Plant Journal, 33, 413–423.

Srivastava, V., Vasil, V., Vasil, I.K. (1996) Molecular characterization of the fate of transgenes in transformed wheat (*Triticum aestivum* L.). Theoetical Applied Genetic, 92, 1031–1037.

Stelglitz, H. (1977) Role of B-1,3-glucanase in postmeiotic microspore release. Developmental Biology, 57, 87-97.

Sutherland, W.J. (2004) A blueprint for the countryside. Ibis 146, Suppl 1, 120–124.

Takayama, S., Shiba, H., Iwano, M., Asano, K., Hara, M., Che, F.S., Watanabe, M., Hinata, K., and Isogai, A. (2000) Isolation and characterization of pollen coat proteins of Brassica campestris that interact with S locus-related glycoprotein 1 involved in pollen-stigma adhesion. Proc. Natl. Acad. Sci. USA, 97, 3765–3770.

Tang, W., Ezcura, I., Muschietti, J., and McCormick, S. (2002) A cysteine-rich extracellular protein, LAT52, interacts with the extracellular domain of the pollen receptor kinase LePRK2. Plant Cell 14, 2277–2287.

The potato sequencing consortium (2011) Genome sequence and analysis of the tuber crop potato. Nature Volume, 475, 189–1950.

The Royal society (2009) Ripening the benefits: Science and substantial intensification of global agriculture.

Thorsness, M.K., Kandasamy, M.K., Nasrallah, M.E., and Nasrallah, J.B. (1993) Genetic ablation of floral cells in Arabidopsis. Plant Cell 5, 253–261.

Thorstensen, T., Grini, P.E., Mercy, I.S., Alm, V., Erdal, S., Aasland, R., Aalen, R.B. (2008) The Arabidopsis SET-domain protein ASHR3 is involved in stamen development and interacts with the bHLH transcription factor ABORTED MICROSPORES (AMS). Plant and Molecular Biology, 66, 47–59.

Tingay, S., McElroy, D., Kalla, R., Fieg, S., Wang, M., Thornon, S., Brettell, R. (1997) *Agrobacterium tumesfaciens*-mediated barley transformation. The Plant Journal, 11, 6, 1369-1376.

Tottman, D.R. (1987) The decimal code for growth stages of cereals, with illustration. Annals of Applied Biology, 110, 441-454.

Trevaskis B., Hemming M.N., Dennis E.S., Peacock W.J. (2007). The molecular basis of vernalization-induced flowering in cereals. Trends in Plant Science, 12,352-357.

Turner, A., Beales, J., Faure, S., Dunford, R.P., Laurie, D.A. (2005) The pseudo-response regulator Ppd-H1 provides adaptation to photoperiod in barley. Science 310, 1031–1034.

Twell, D., Park, S.K., Lalanne, E. (1998) Asymmetric division and cell-fate determination in developing pollen. Trends Plant Sci. 3, 305–310.

Tyson, H. (2009) Future direction in research relating to food security. The Biotechnology and Biological Sciences Research Council.

Vain, P., James, V.A., Worland, B., Snape, J.W. (2002) Transgene behaviour across two generations in a large random population of transgenic rice plants produced by particle bombardment. Theoretical and Applied Genetic, 105, 878–889.

Velásquez, A.C., Chakravarthy, S., Martin, G.B. (2009) Virus-induced Gene Silencing (VIGS) in Nicotiana benthamiana and Tomato. Journal of Visualized Experiments, 28 1292.

Vizcay-Barrena, G., Wilson, Z.A. (2006) Altered tapetal PCD and pollen wall development in the *Arabidopsis ms1* mutant. Journal of Experimental Botany, 57, 2709–2717.

Vogel, J., Hill, T. (2008) High-efficiency *Agrobacterium*-mediated transformation of *Brachypodium distachyon* inbred line Bd21-3. Plant Cell Reproduction, 27, 471-478.

Waddington, S.R., Cartwright, P.M. (1983) A quantitative scale of spike initial and pistil development in barley and wheat. Annals of botany Company, 51, 119-130.

Walmsley, A.M., Henry, R.J., Birch, R.G. (1995) Optimization of tissue culture conditions for transformation studies using immature embryos of Australian barley cultivars. Australian Journal of Botany, 43, 499-504.

Walters, D.A., Vetsch, C.S., Potts, D.E., Lundquist, R.C. (1992) Transformation and inheritance of a *hygromycin phosphotransferase* gene in maize plants. Plant Molecular Biology, 18, 189–200.

Wan, Y., Lemaux, P.G. (1994) Generation of large numbers of independently transformed fertile barley plants. Plant Physiology, 104, 37-48.

Wang, Z., Morris, J.C., Drew, M.E., Englund, P.T. (2000) Inhibition of *Trypanosoma brucei* gene expression by RNA interference using an integratable vector with opposing T7 promoters. Journal Biological Chemistry, 275, 40174–40179.

Waterhouse, P.M, Graham, M.W., Wang, M.B. (1998). Virus resistance and gene silencing in plants can be induced by simultaneous expression of sense and antisense RNA. Proc. Natl. Acad. Sci. U.S.A, 95, 13959-13964.

Watson, J.M., Fusaro, A.F., Wang, M., Waterhouse, P.M. (2005) RNA silencing platforms in plants. *FEBS Letters*, 579, 26, 5982-5987.

Weiler, K.S., Wakimoto, B.T. (1995) Heterochromatin and gene expression in Drosophila. Annual Review Genetic. 29, 577–605.

Wesley, S.V., Helliwell, C., Smith, N.A., Wang, M.B., Rouse, D., Liu, Q., Gooding, P., Singh, S., Abbott, D., Stoutjesdijk, P., Robinson, S., Gleave, A., Green, A., Waterhouse, P.M. (2001) Constructs for efficient, effective and high throughput gene silencing in plants. Plant Journal, 27, 581–590.

Wheeler, M.J., Franklin-Tong, V.E., and Franklin, F.C.H. (2001) The molecular and genetic basis of pollen-pistil interactions. New Phytol, 151, 565–584

Wicker T., Keller, B. (2007) Genome-wide comparative analysis of copia retrotransposons in Triticeae, rice, and Arabidopsis reveals conserved ancient evolutionary lineages and distinct dynamics of individual copia families. Genome Res 2007, 17:1072-1081.

Williams, M.E. (1995) Genetic engineering for pollination control. Trends Biotechnology, 13, 344–349.

Wilson, Z.A., Morroll, S.M., Dawson, J., Swarup, R., Tighe, P.J. (2001) The *Arabidopsis MALE STERILITY1* (*MS1*) gene is a transcriptional regulator of male gametogenesis, with homology to the PHD-finger family of transcription factors. Plant Journal, 28, 27–39.

Wilson, Z.A., Song, J., Taylor, B., Yang, C. (2011) The final split: the regulation of anther dehiscence. Journal of Experimental Botany, 62, 5, 1633–1649.

Wilson, Z.A., Yang,C. (2004) Plant gametogenesis: conservation and contrast in development. Reproduction, 128, 5, 483-92.

Wilson, Z.A., Zhang, D.B. (2009) From *Arabidopsis* to rice: pathways in pollen development. Journal of Experimental Botany, 60, 5, 1479-1492.

Wolters-Arts, M., Lush, W.M., Mariani, C. (1998) Lipids are required for directional pollen-tube growth. Nature 392, 818–821.

Wolters-Arts, M., Van Der Weerd, L., Van Aelst, A.C., Van As, H., Mariani, C. (2002) Water-conducting properties of lipids during pollen hydration. Plant Cell Environ. 25, 513–519.

Worrall, D., Hird, D.L., Hodge, R., Paul, W., Draper, J., and Scott, R. (1992) Premature dissolution of the microsporocyte callose wall causes male sterility in transgenic tobacco. Plant Cell, 4, 759–771.

Wu, G.S., Lewis, D.R., Spalding, E.P. (2007) Mutations in Arabidopsis multidrug resistance-like ABC transporters separate the roles of acropetal and basipetal auxin transport in lateral root development. Plant Cell, 19, 1826–1837.

Wu, G., Gu, Y., Li, S., and Yang, Z. (2001) A genome-wide analysis of Arabidopsis Rop-interactive CRIB motif–containing proteins that act as Rop GTPase targets. Plant Cell 13, 2841–2856.

Wu, Y.Z., Qiu, X., Du, S., and Erickson, L. (1996) PO149, a new member of pollen pectate lyase-like gene family from alfalfa. Plant Mol. Biol. 32, 1037–1042.

Wysocka, J., Swigut, T., Xiao, H., Milne, T.A., Kwon, S.Y., Landry, J., Kauer, M., Tackett, A.J., Chait, B.T., Badenhorst, P., Wu, C., Allis, C.D. (2006) A PHD finger of NURF couples histone H3 lysine 4 trimethylation with chromatin remodeling. Nature, 442, 86–90.

Xu, J., Yang, C., Yuan, Z., Zhang, D., Gondwe, M.Y., Ding, Z., Liang, W., Zhang, D., Wilson, Z.A. (2010) The ABORTED MICROSPORES regulatory network is required for postmeiotic male reproductive development in Arabidopsis thaliana. The Plant Cell, 22, 1, 91-107.

Yamaguchi, T., Lee, D.Y., Miyao, A., Hirochika, H., An, G., Hirano, H.Y. (2006) Functional diversification of the two C-class MADS box genes OSMADS3 and OSMADS58 in Oryza sativa. The Plant Cell, 18, 15–28.

Yang, C., Vizcay-Barrena, G., Conner, K., Wilson, Z.A. (2007) MALE STERILITY1 is required for tapetal development and pollen wall biosynthesis. *The Plant Cell,* 19:3530-3548.

Yang, C., Xu, Z., Song, J., Conner, K., Vizcay Barrena, G., Wilson, Z.A. (2007) Arabidopsis MYB26/MALE STERILE35 Regulates Secondary Thickening in the Endothecium and Is Essential for Anther Dehiscence. *The Plant Cel,l* 19, 534-548.

Yang, S.L., Jiang, L., Puah, C.S., Xie, L.F., Zhang, X.Q., Chen, L.Q., Yang, W.C., Ye, D. (2005) Overexpression of *TAPETUM DETERMINANT1* alters the cell fates in the Arabidopsis carpel and tapetum via genetic interaction with *EXCESS MICROSPOROCYTES1/ EXTRA SPOROGENOUS CELLS.* Plant Physiology, 139, 186–191.

Yang, S.L., Xie, L.F., Mao, H.Z., Puah, C.S., Yang, W.C., Jiang, L., Sundaresan, V., Ye, D. (2003a) TAPETUM DETERMINANT1 is required for cell specialization in the Arabidopsis anther. Plant Cell, 15, 2792–2804.

Yang, W.C., Sundaresan, V. (2000) Genetics of gametophytic biogenesis in Arabidopsis. Curr. Opin. Plant Biol, 3, 53–57.

Yang, W.C., Ye, D., Xu, J., Sundaresan, V. (1999) The SPOROCYTELESS gene of Arabidopsis is required for initiation of sporogenesis and encodes a novel nuclear protein. Genes Dev, 13, 2108–2117.

Yin, Y., Vafeados, D., Tao, Y., Yokoda, T., Asami, T., Chory, J. (2005) A new class of transcription factors mediates brassinosteroid-regulated gene expression in Arabidopsis. Cell, 120, 249-259.

Yin, Y., Chory, J., Baulcombe, D. (2005) RNAi in Transgenic Plants. Current Protocols in Molecular Biology.

Yu, J., Hu, S., Wang, J., Wong, G.K., Li, S., Liu, B., Deng, Y., Da,i L. Zhou, Y., Zhang, X. (2002) A draft sequence of the rice genome (*Oryza sativa L. ssp. indica*). Science, 296, 79–92.

Yui, R., Iketani, S., Mikami, T., Kubo, T. (2003) Antisense inhibition of mitochondrial pyruvate dehydrogenase E1α subunit in anther tapetum causes male sterility. Plant Journal, 34, 57–66.

Zadoks, J.C., Chang, T.T., Konzak, C.F. (1974) A decimal code for the growth stages of cereals. Weed Research, 14, 6, 415–421.

Zamore, P.D., Tuschl, T., Sharp, P.A., Bartel, D.P. (2000) RNAi: double-stranded RNA directs the ATP-dependent cleavage of mRNA at 21 to 23 nucleotide intervals. Cell, 101, 25–33.

Zhang, D.S., Liang, W.Q., Yuan, Z., Li, N., Shi, J., Wang, J., Liu, Y.M., Yu, W.J., Zhang, D.B. (2008) Tapetum degeneration retardation is critical for aliphatic metabolism and gene regulation during rice pollen development. Molecular Plant, 1, 599–610.

Zhang, W., Sun, Y., Timofejeva, L., Chen, C., Grossniklaus, U., Ma, H. (2006) Regulation of Arabidopsis tapetum development and function by DYSFUNCTIONAL TAPETUM1 (DYT1) encoding a putative bHLH transcription factor. Development, 133, 3085–3095.

Zhang, W., Sun, Y.L., Timofejeva, L., Chen, C., Grossniklaus, U., Ma, H. (2006) Regulation of Arabidopsis tapetum development and function by DYSFUNCTIONAL TAPETUM (DYT1) encoding a putative bHLH transcription factor. Development, 133, 3085–3095.

Zhao, D.Z., Wang, G.F., Speal, B., Ma, H. (2002) The EXCESS MICROSPOROCYTES1 gene encodes a putative leucine-rich repeat receptor protein kinase that controls somatic and reproductive cell fates in the Arabidopsis anther. Genes and Development , 16, 2021–2031.

Zhao, X., de Palma, J., Oane, R., Gamuyao, R., Luo, M., Chaudhury, A., Herve, P., Xue, Q., Bennett, J. (2008) OsTDL1A binds to the LRR domain of rice receptor kinase MSP1, and is required to limit sporocyte numbers. The Plant Journal, 54, 375-387.

Zheng, Z., Xia, Q., Dauk, M., Shen, W., Selvaraj, G., Zou, J. (2003). Arabidopsis AtGPAT1, a member of the membrane-bound

glycerol-3-phosphate acyltransferase gene family, is essential for tapetum differentiation and male fertility. Plant Cell, 15, 1872-1887.

Zhong, X., Peng, S., Wang, F., Huang, N. (2004) Using heterosis and hybrid rice to increase yield potential in China. Proceedings of the world rice research conference. Tokyo and Tsukuba, Japan. International Rice Research Institute.

Zinkl, G.M., Zwiebel, B.I., Grier, D.G., and Preuss, D. (1999) Pollen-stigma adhesion in Arabidopsis: A species-specific interaction mediated by lipophilic molecules in the pollen exine. Development 126, 5431–5440.

Appendix

1. Chemical and Reagents.

10 x TBE buffer	
NaCL	0.89 M
Tris-HCl (pH 7.5)	10 mM
Na2-EDTA	1 mM
Dilute to 0.5x to use in electrophoresis	

Lauria-Bertani (LB) medium	
Bacto-Tryptone	20 g
Bacto-yeast extract	10 g
NaCl	10 g
Agar (if for solid medium)	15 g
ddH2O	Add up to 1 L
Total Volume	1 L
Adjust pH to 7.0 and autoclave to sterilize; antibiotics added when sterilized medium cool to approx 50°C.	

Murashine and Skoog Basal (MS) medium	
MS powder	2.15 g
Sucrose (optional)	10 g
Agar	9 g
ddH2O	Add up to 1 L
Total volume	1 L

Adjust pH to 7.0 and autoclave to sterilize; antibiotics added when sterilized medium cool to approx 50°C.

MG/L	
Tryptone	5 g
Mannitol	5 g
Yeast Extract	2.5 g
L-Glutamic acid	1 g
KH2PO4	250 mg
NaCl	100 ml
MgSO4•7H2O	100 mg
Biotin	10µl (0.1 mg/l stock)
ddH2O	Add up to 1 L
Total Volume	1 L

Adjust pH to 7.0 and autoclave to sterilize; antibiotics added when sterilized medium cool to approx 50°C

10 x PBS	
1.3M NaCL	**74 g**
0.03M Na2HPO4	**9.94 g**
0.03M MH2PO4	**4.14 g**
Total Volume	**1 L**

Adjust pH to 7.2 and autoclave to sterilize. Store at RT. For In situ hybridization, 1 ml of DEPC water must be added to the water and leave it over night. Autoclave and add the buffer components. Autoclave again.

Paraformaldehyde 4%	
Paraformaldehyde (Sigma)	2 g
1xPBS	50 ml
Tween20	50 µl
Triton	50 µl

2. pCR4TOPO

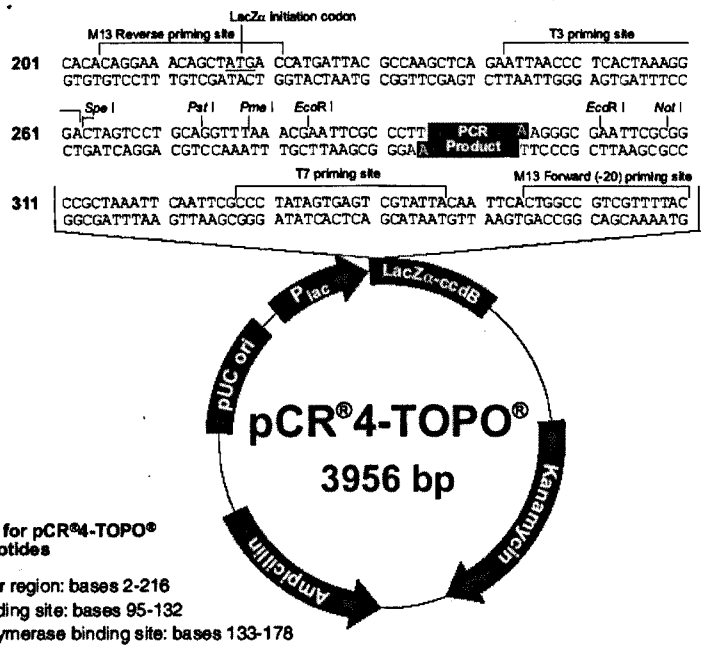

Comments for pCR®4-TOPO®
3956 nucleotides

lac promoter region: bases 2-216
  CAP binding site: bases 95-132
  RNA polymerase binding site: bases 133-178
  Lac repressor binding site: bases 179-199
Start of transcription: base 179
M13 Reverse priming site: bases 205-221
LacZα-*ccdB* gene fusion: bases 217-810
  LacZα portion of fusion: bases 217-497
  ccdB portion of fusion: bases 508-810
T3 priming site: bases 243-262
TOPO® Cloning site: bases 294-295
T7 priming site: bases 328-347
M13 Forward (-20) priming site: bases 355-370
Kanamycin promoter: bases 1021-1070
Kanamycin resistance gene: bases 1159-1953
Ampicillin (*bla*) resistance gene: bases 2203-3063 (c)
Ampicillin (*bla*) promoter: bases 3064-3160 (c)
pUC origin: bases 3161-3834
(c) = complementary strand

3. pCR-BluntII-TOPO

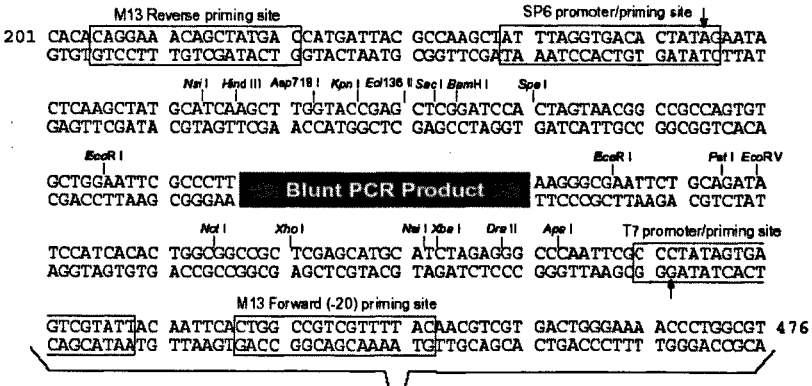

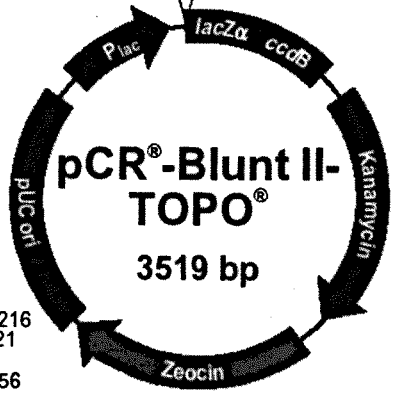

Comments for pCR®-Blunt II-TOPO®
3519 nucleotides

lac promoter/operator region: bases 95-216
M13 Reverse priming site: bases 205-221
LacZ-alpha ORF: bases 217-576
SP6 promoter priming site: bases 239-256
Multiple Cloning Site: bases 269-399
TOPO®-Cloning site: bases 336-337
T7 promoter priming site: bases 406-425
M13 (-20) Forward priming site: bases 433-448
Fusion joint: bases 577-585
ccdB lethal gene ORF: bases 586-888
kan gene: bases 1099-2031
kan promoter: bases 1099-1236
Kanamycin resistance gene ORF: bases 1237-2031
Zeocin resistance ORF: bases 2238-2612
pUC origin: bases 2724-3397

4. Zadok´s scales.

Stages	General Description
	Germination
00	Dry seed
01	Water uptake (imbibition) started
03	Imbibition complete
05	Radicle emerged from seed
07	Coleoptile emerged from seed
09	Leaf just at coleoptile tip
	Seedling developmet
10	First leaf emerged
11	First leaf unfolded
12	2 leaves unfolded
13	3 leaves unfolded
14	4 leaves unfolded
15	5 leaves unfolded
16	6 leaves unfolded
17	7 leaves unfolded
18	8 leaves unfolded
19	9 or more leaves unfolded
	Tillering
20	Main shoot only
21	Main shoot and 1 tiller
22	Main shoot and 2 tillers
23	Main shoot and 3 tillers
24	Main shoot and 4 tillers
25	Main shoot and 5 tillers
26	Main shoot and 6 tillers
27	Main shoot and 7 tillers
28	Main shoot and 8 tillers
29	Main shoot and 9 or more tillers
	Stem elongation or jointing
30	Pseudo stem erection
31	1st node detectable
32	2nd node detectable
33	3rd node detectable
34	4th node detectable
35	5th node detectable
36	6th node detectable
37	Flag leaf just visible
39	Flag leaf ligule/collar just visible

Stages	General Description
	Booting
40	Flag leaf sheath extending
45	Boot just swollen
47	Flag leaf sheath opening
49	First awns visible
	Heading
50	First spikelet of head visible
53	1/4 of head emerged
55	1/2 of head emerged
57	3/4 of head emerged
59	Emergence of head complete
	Flowering of Anthesis
60	Beginning of flowering
65	Flowering half complete
69	Flowering complete
	Milk
70	--
71	Kernel watery
73	Early milk
75	Medium milk
77	Late milk
	Dough
80	----
83	Early dough
85	Soft dough
87	Hard dough
	Ripening
90	----
91	Kernel hard (difficult to separate by fingernail)
92	Kernel hard
93	Kernel loosening in daytime
94	Overripe, straw dead and collapsing
95	Seed dormant
96	50% of viable seed germinates
97	Seed not dormant
98	Secondary dormancy
99	Secondary dormancy los

5. Embryo regeneration media.

1000 ml (1x)	C. Induction	Transition	Regeneration
***MS salts (M0221)**	4.3 g	_	_
***MS salts without Amonium nitrate (M0238)**	_	2.7 g	2.7 g
***Casein hydrolysate**	1 g	_	_
***Maltose**	30 g	20 g	20 g
****Myo-inosotol**	350 mg	100 mg	100 mg
***Glutamine**		750 mg	750 mg
****Proline**	690 mg	_	_
****Thiamine HCL**	1 mg	0.4 mg	0.4 mg
****CuSO4**	1.25 mg	1.25 mg	_
***NH4NO3**		165 mg	165 mg
****Dicamba(Sigma-Aldrich D5417)**	2.5 mg	_	_
****2,4-Dichlorophenoxy acetic acid**	_	2.5 mg	_
****6-benzylaminopurine (BAP)**	_	0.1 mg	_
*****Phytagel**	**3.5 g**	**3.5 g**	**3.5 g**

* Prepare 1 litre of callus induction media/Transition/Regeneration adding first these components and check the pH. Adjust the medium to 5.8 using NaOH. Then filter the media into an autoclaved bottle. Do not autoclave. Do not mix it at this stage with phytagel as the mix will solidify very quickly. It is important to prepare this media at double concentration, as later it will be mix with the same volume of phytagel, also at double concentration, bringing the final concentration to this represented in the table above.

** Prepare individual stocks of the following components. Filter using 0.22 µl filter:

- 69 g/l proline (water). Keep at 4°C
- 35 g/l myo-inositol (water). Keep at 4°C
- 100 mg/l Thiamine HCL (Water). Keep at 4°C
- 2.5 g/l 2,4-D (100% ethanol). Keep at -20°C

- 125 mg/100ml CuSO4 (water). Keep at 4°C
- 1 mg/l of BAP made up in water with a few drops of 1 M NaOH and store at -20°C
- 125 mg/100ml CuSO4 (water). Keep at 4°C
- 2.5 g/l Dicamba (water). Prepare individual aliquots and keep it at -20°C.

*** Prepare 1 litre of phytagel at double concentration. Try to dissolve the phytagel as much as possible before autoclaving. Once autoclaved, keep it at room temperature.

For one litre, pour 500 ml of autoclaved 2x phytagel into a 1 litre sterile bottle and another 500 ml of filtered sterilised 2x Callus Induction/Transition/Regeneration, into the 500 ml sterile bottle. Set up a water bath at 55°C and place the two bottles in it. Once the 60°C has been reached, take the callus induction/Transition/Regeneration bottle, and add the rest of the components (**). Place the bottle again into the incubator for 5 minutes. Pour the 500 ml of Callus Induction/Transition/Regeneration plus additives into the phytagel bottle and mix well. Pour the mix immediately into the Petri dishes. All these steps must be carried out in a flow cabinet under sterile conditions.

6. pBI121 construct.

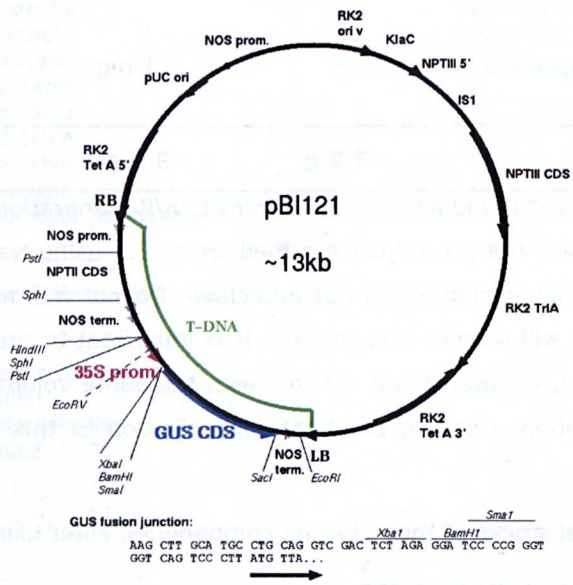

7. Bradi4g31760/OsPTC1/HvMS1 protein sequences.

Bradi4g31760 (BRADI4G31760.1).

MAAKMVINLGSSRRRKRGEVLFRFESFCQPGYPAQLAGPFRDNVRTLLGLAHLEAGVQGE
TRCWSFQLELQRHPPTVVRLFIVEEEVAASPRRQCHLCRLIGWGRHLICSKRFHFLLPKR
ESTVETDGLCYGISSSHGGGGTEKASSKGGTGTASSRGHLLHGVVHLNGYGHLVGLHGFE
GGSDFVSGHQIMDLWDRICSALHVRKVSLVDTARKGHMVLRLLHGVAYGDTWFGRWGYRY
GRPSYGVTLQSYQQSLHALQSVPLCVLVPHLACCFGQELPMVVTKYQAISGHKLLDLGDL
LRFMLELRTRLPATSVTAMDYRGIMSDASCRWSAKRVDMAARAVVDALRRPASASDRAPG
MPAAPRWVTRQEVRDAARAYIGDTGLLDFVLKSLGNHIVGNYVVRRAMNPVTKVLEYCLE
DVSSVLLSHGGKMRVRFHLTRAQLMRDLVHLYRHVLKEPPTQLPLTASAGSGAAAFGAIP
VAVRRVLDVKHLVKDYHEAIMAAATANNSVGGIVGHVYVNMCCTLVVRDGSPELVPPYET
VTVPAHATVGELKWEVQRLFRDMYLALRTFTAESVVGIGIGPQQEASPVLGLIGVGSTVV
VEGVVGSLQPAEEEEESDEQRNGAVCEGSDGERVVDCACGADDDDGERMACCDICEAWQH
TRCAGVADADDVPHVFLCSRCDNDVLSFPSFNC

OsPTC1 (NP_001063319.2).

MAPKMVISLGSSRRRKRGEMLFRFEAFCQPGYPANFAGAGGFRDNVRTLLGFAHLEAGVH
GETKCWSFQLELHRHPPTVVRLFVVEEEVAASPHRQCHLCRHIGWGRHLICSKRYHFLLP
RRESAAEADGLCFAINHGGGGGAEKASSKGTTTTASSRGHLLHGVVHLNGYGHLVALHGL
EGGSDFVSGHQIMDLWDRICSALHVRTVSLVDTARKGHMELRLLHGVAYGETWFGRWGYR
YGRPSYGVALPSYRQSLHVLGSMPLCVLVPHLSCFSQELPMVVTKYQAISGHKLLSLGDL
LRFMLELRARLPATSVTAMDYRGIMSEASCRWSAKRVDMAARAVVDALRRAEPAARWVTR
QEVRDAARAYIGDTGLLDFVLKSLGNHIVGNYVVRRTMNPVTKVLEYCLEDVSSVLPAVA
AGGGVPAQGKMRVRFQLTRAQLMRDLVHLYRHVLKEPSQALTGGAFGAIPVAVRMVLDIK
HFVKDYHEGQAAASSNGGGGFGHPHINLCCTLLVSNGSPELAPPYETVTLPAHATVGELK
WEAQRVFSEMYLGLRSFAADSVVGVGADQEGLPVLGLVDVGSAVVVQGSVGEQINGEDHE
RKEEAAAAAVCEGSGGGERVVDCACGAVDDDGERMACCDICEAWQHTRCAGIADTEDAPH
VFLCSRCDNDVVSFPSFNC

HvMS1 (BAK05033.1).

MAAKMVISLGSSRRRKRGEVLFRFDSFCQPGYPAQLAGAFRDNVRTLLGLAHLEAGVQGET
RCWSFQLELHRHPPTVVRLFVVEEEVAASPHRQCHLCRVIGWGRHLICSKRFHFVLPKRES
SVETDGLCYGIGGADKASKGTATSRGHLLHGIVHLNGYGHLVGLHGFEGGSDFVSGHQIMD
LWDRICSALHVRRVSLVDTARKGHMVLRLLHGVAYGDTWFGRWGYRYGRPSYGVALQSYQQ
SLHALQSIPLCVLVPHLSCFSQELPLVVTKYQAISGHKLLNLGDLLRFMLELRTRLPATSV
TAMDYRGIMSDASCRWSAKRVDMAARAVVDALRRSEAPAARWVTRQEVRDAARTYIGDTGL
LDFVLKSLGNHIVGNYVVRRAMNPVTKVLEYCLEDVSSVLPASVGAGAGVPAGHGKMRVRF
HLTRAQLMRDLVHLYRHVLKEPSQALTTGAFGAIPVAVRMILDIKHFVKDYHEGMTGTNSG
VVGHVYISLCCTLIVRNGSSELVPPYETVTVPAHATVGELKWEVQRLFRDMYLGLRTFTAE
CVVGIGAGLDASPALGLGVGSTVVVEGVVGEQQEPAEEGDQRKKAAAVCEGGGDVGERVVD
CVCGADDDDGERMACCDICEAWQHTRCAGVADTEDVPHVFLCSRCDNDVASFPALN

8. *Bradi4g31760* (BRADI4G31760) x *OsPTC1* (NM_001069854) cDNA sequence alignment.

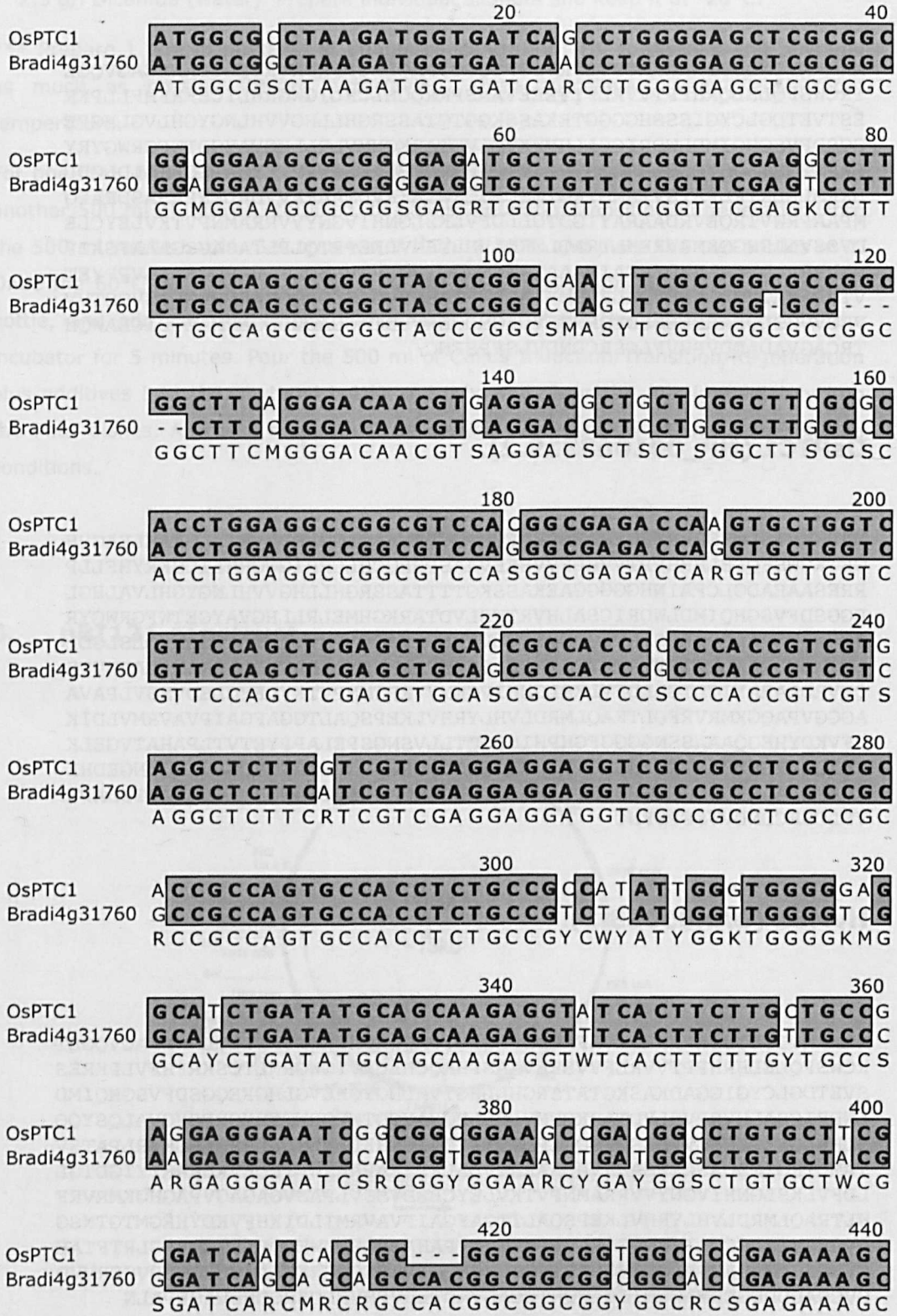

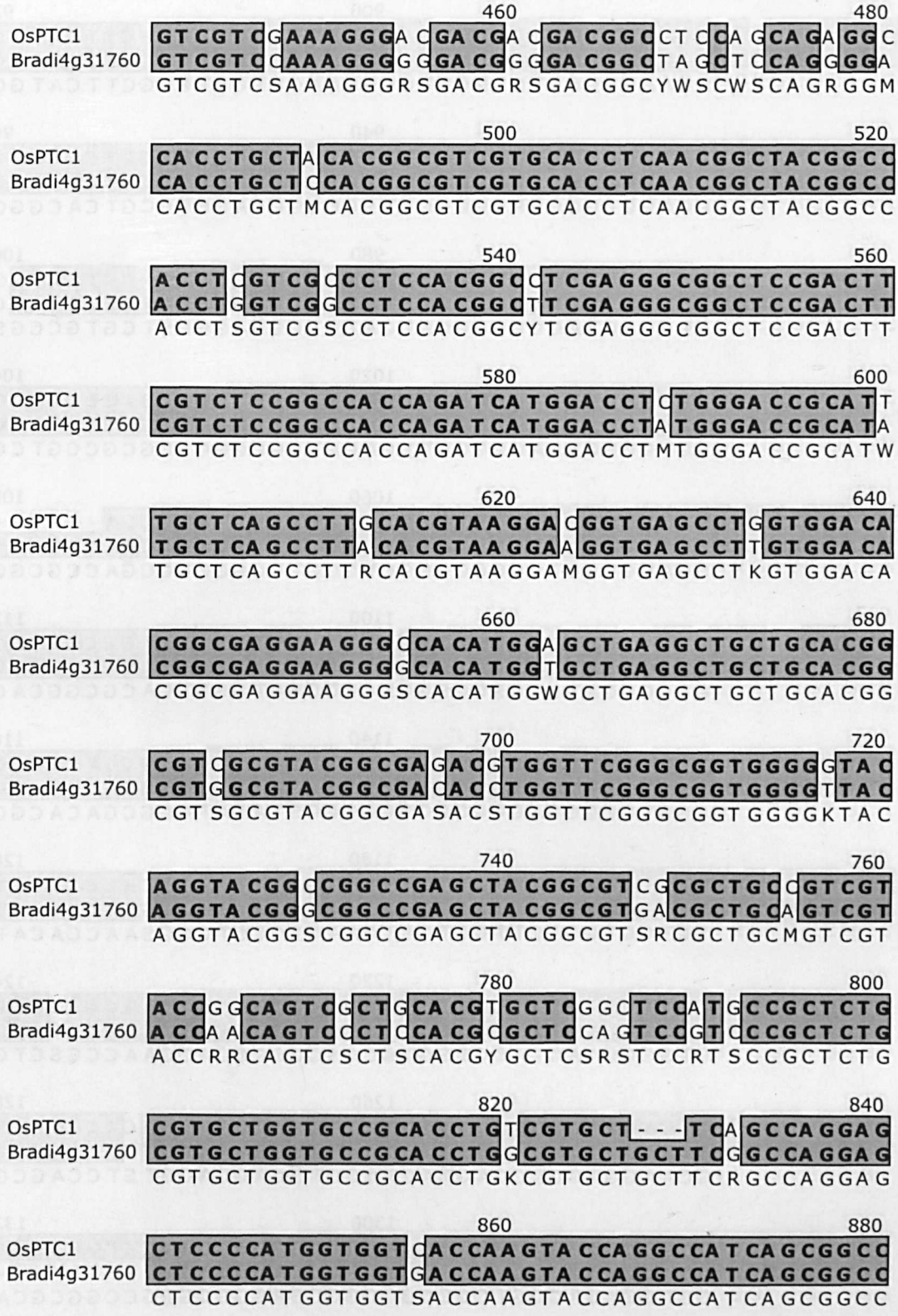
460
480
OsPTC1 GTCGTCGAAAGGGACGACGACGACGGCCTCCAGCAGAGGC
Bradi4g31760 GTCGTCCAAAGGGGGGACGGGGGACGGCTAGCTCAGGGGA
GTCGTCSAAAGGGRSGACGRSGACGGCYWSCWSCAGRGGM
500
520
OsPTC1 CACCTGCTACACGGCGTCGTGCACCTCAACGGCTACGGCC
Bradi4g31760 CACCTGCTCCACGGCGTCGTGCACCTCAACGGCTACGGCC
CACCTGCTMCACGGCGTCGTGCACCTCAACGGCTACGGCC
540
560
OsPTC1 ACCTCGTCGCCCTCCACGGCCTCGAGGGCGGCTCCGACTT
Bradi4g31760 ACCTGGTCGGCCTCCACGGCTTCGAGGGCGGCTCCGACTT
ACCTSGTCGSCCTCCACGGCYTCGAGGGCGGCTCCGACTT
580
600
OsPTC1 CGTCTCCGGCCACCAGATCATGGACCTCTGGGACCGCATT
Bradi4g31760 CGTCTCCGGCCACCAGATCATGGACCTATGGGACCGCATA
CGTCTCCGGCCACCAGATCATGGACCTMTGGGACCGCATW
620
640
OsPTC1 TGCTCAGCCTTGCACGTAAGGACGGTGAGCCTGGTGGACA
Bradi4g31760 TGCTCAGCCTTACACGTAAGGAAGGTGAGCCTTGTGGACA
TGCTCAGCCTTRCACGTAAGGAMGGTGAGCCTKGTGGACA
660
680
OsPTC1 CGGCGAGGAAGGGCCACATGGAGCTGAGGCTGCTGCACGG
Bradi4g31760 CGGCGAGGAAGGGGCACATGGTGCTGAGGCTGCTGCACGG
CGGCGAGGAAGGGSCACATGGWGCTGAGGCTGCTGCACGG
700
720
OsPTC1 CGTCGCGTACGGCGAGACGTGGTTCGGGCGGTGGGGGTACC
Bradi4g31760 CGTGGCGTACGGCGACACCTGGTTCGGGCGGTGGGGTTACC
CGTSGCGTACGGCGASACSTGGTTCGGGCGGTGGGGKTAC
740
760
OsPTC1 AGGTACGGCCGGCCGAGCTACGGCGTCGCGCTGCCGTCGT
Bradi4g31760 AGGTACGGGCGGCCGAGCTACGGCGTGACGCTGCAGTCGT
AGGTACGGSCGGCCGAGCTACGGCGTSRCGCTGCMGTCGT
780
800
OsPTC1 ACCGGCAGTCGCTGCACGTGCTCGGCTCCATGCCGCTCTG
Bradi4g31760 ACCAAACAGTCCCTCCACGCGCTCCAGTCCGTCCCGCTCTG
ACCRRCAGTCSCTSCACGYGCTCSRSTCCRTSCCGCTCTG
820
840
OsPTC1 CGTGCTGGTGCCGCACCTGTCGTGCT---TCAGCCAGGAG
Bradi4g31760 CGTGCTGGTGCCGCACCTGGCGTGCTGCTTCGGCCAGGAG
CGTGCTGGTGCCGCACCTGKCGTGCTGCTTCRGCCAGGAG
860
880
OsPTC1 CTCCCCATGGTGGTCACCAAGTACCAGGCCATCAGCGGCC
Bradi4g31760 CTCCCCATGGTGGTGACCAAGTACCAGGCCATCAGCGGCC
CTCCCCATGGTGGTSACCAAGTACCAGGCCATCAGCGGCC

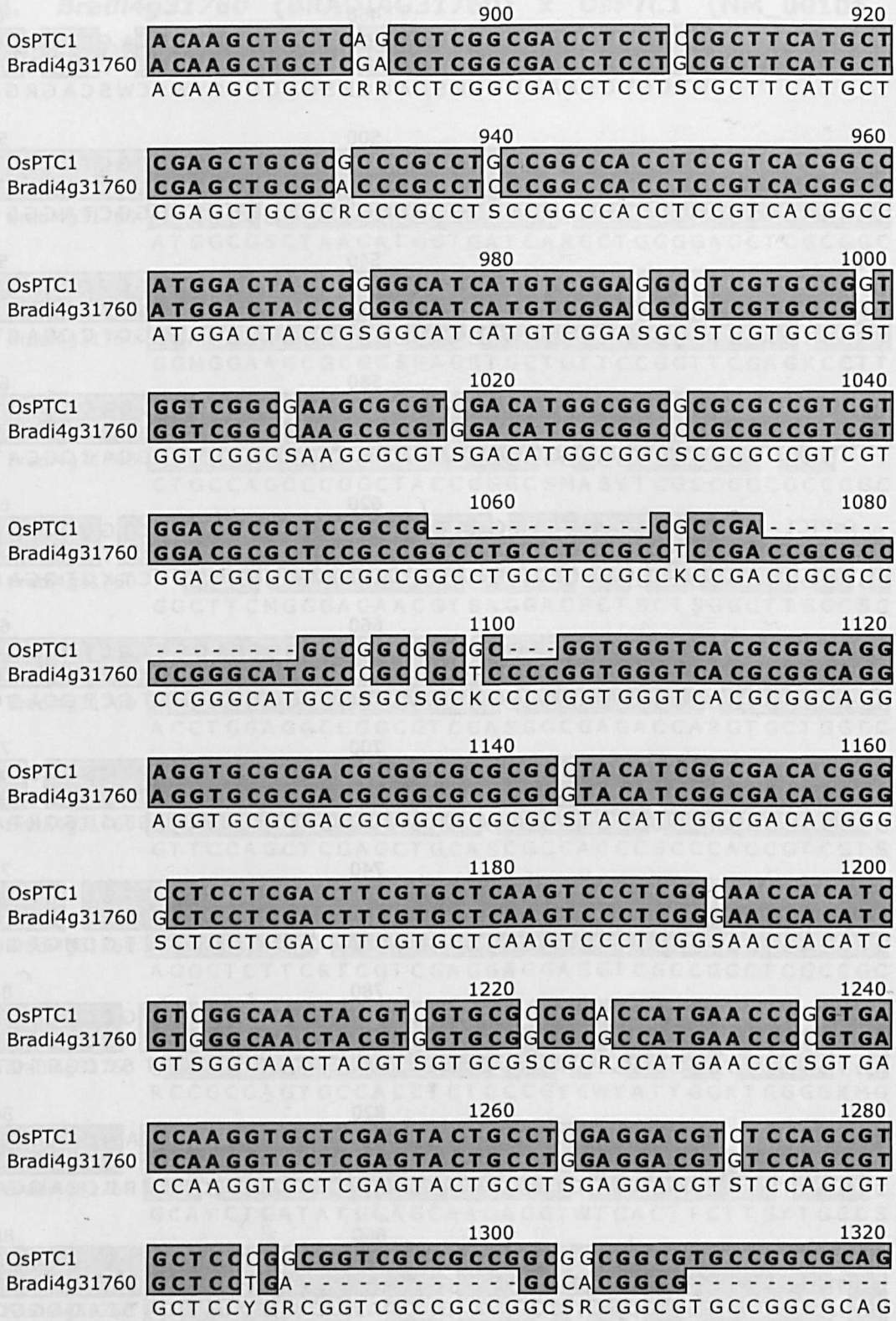
900
920
OsPTC1
Bradi4g31760
940
960
980
1000
1020
1040
1060
1080
1100
1120
1140
1160
1180
1200
1220
1240
1260
1280
1300
1320

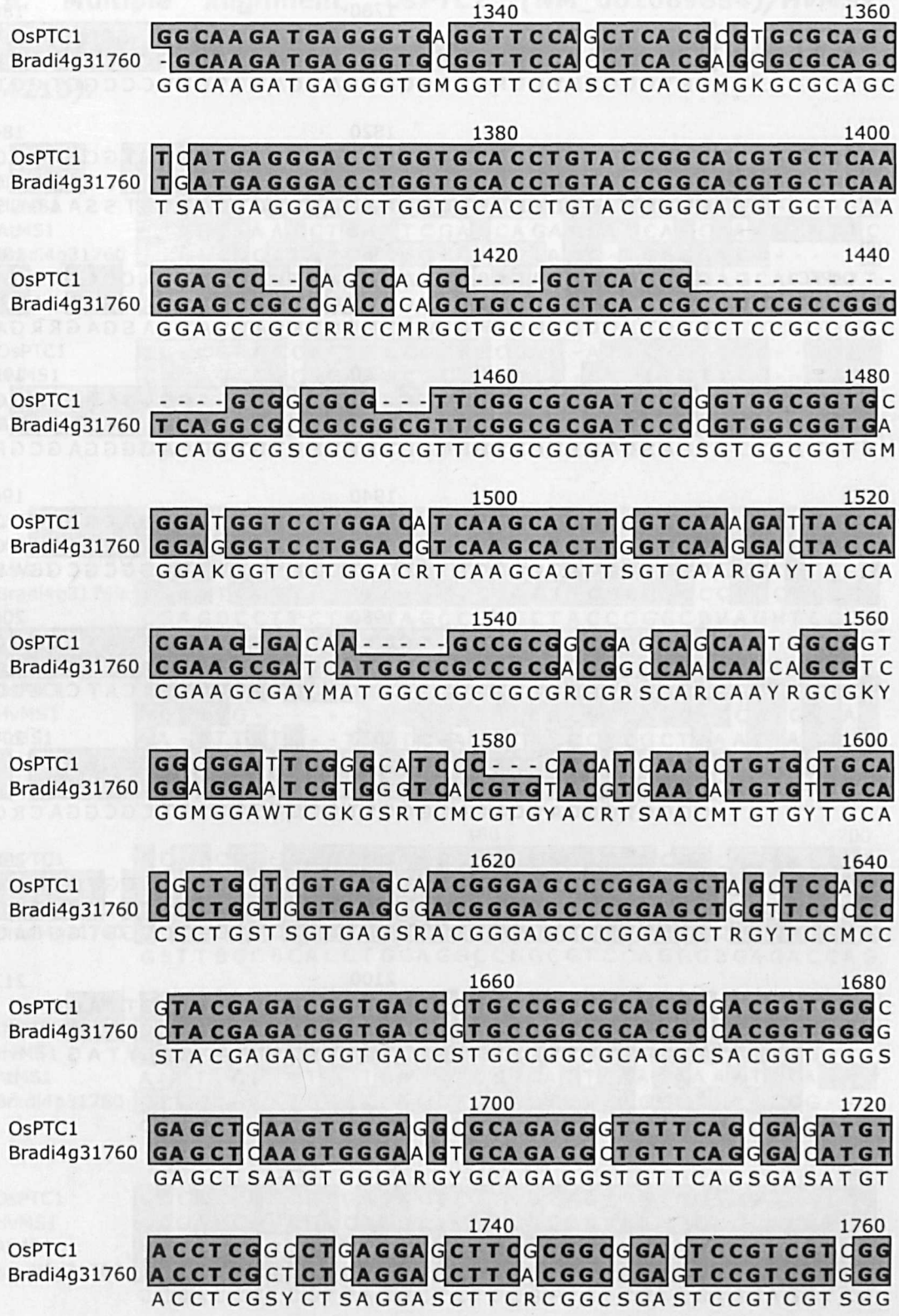
1340
1360
OsPTC1 GGCAAGATGAGGGTGAGGTTCCAGCTCACGCGTGCGCAGC
Bradi4g31760 -GCAAGATGAGGGTGCGGTTCCACCTCACGAGGGCGCAGC
GGCAAGATGAGGGTGMGGTTCCASCTCACGMGKGCGCAGC
1380
1400
OsPTC1 TCATGAGGGACCTGGTGCACCTGTACCGGCACGTGCTCAA
Bradi4g31760 TGATGAGGGACCTGGTGCACCTGTACCGGCACGTGCTCAA
TSATGAGGGACCTGGTGCACCTGTACCGGCACGTGCTCAA
1420
1440
OsPTC1 GGAGCC--CAGCCAGGC----GCTCACCG----------
Bradi4g31760 GGAGCCGCCGACCCAGCTGCCGCTCACCGCCTCCGCCGGC
GGAGCCGCCRRCCMRGCTGCCGCTCACCGCCTCCGCCGGC
1460
1480
OsPTC1 ----GCGGCGCG---TTCGGCGCGATCCCGGTGGCGGTGC
Bradi4g31760 TCAGGCGCCGCGGCGTTCGGCGCGATCCCCGTGGCGGTGA
TCAGGCGSCGCGGCGTTCGGCGCGATCCCSGTGGCGGTGM
1500
1520
OsPTC1 GGATGGTCCTGGACATCAAGCACTTCGTCAAAGATTACCA
Bradi4g31760 GGAGGGTCCTGGACGTCAAGCACTTGGTCAAGGACTACCA
GGAKGGTCCTGGACRTCAAGCACTTSGTCAARGAYTACCA
1540
1560
OsPTC1 CGAAG-GACAA-----GCCGCGGCGAGCAGCAATGGCGGT
Bradi4g31760 CGAAGCGATCATGGCCGCCGCGACGGCCAACAACAGCGTC
CGAAGCGAYMATGGCCGCCGCGRCGRSCARCAAYRGCGKY
1580
1600
OsPTC1 GGCGGATTCGGGCATCCC---CACATCAACCTGTGCTGCA
Bradi4g31760 GGAGGAATCGTGGGTCACGTGTACGTGAACATGTGTTGCA
GGMGGAWTCGKGSRTCMCGTGYACRTSAACMTGTGYTGCA
1620
1640
OsPTC1 CGCTGCTCGTGAGCACACGGGAGCCCGGAGCTAGCTCCACC
Bradi4g31760 CCCTGGTGGTGAGGGACGGGAGCCCGGAGCTGGTTCCCCC
CSCTGSTSGTGAGSRACGGGAGCCCGGAGCTRGYTCCMCC
1660
1680
OsPTC1 GTACGAGACGGTGACCCTGCCGGCGCACGCGACGGTGGGC
Bradi4g31760 CTACGAGACGGTGACCGTGCCGGCGCACGCCACGGTGGGG
STACGAGACGGTGACCSTGCCGGCGCACGCSACGGTGGGS
1700
1720
OsPTC1 GAGCTGAAGTGGGAGGCGCAGAGGGTGTTCAGCGAGATGT
Bradi4g31760 GAGCTCAAGTGGGAAGTGCAGAGGCTGTTCAGGGACATGT
GAGCTSAAGTGGGARGYGCAGAGGSTGTTCAGSGASATGT
1740
1760
OsPTC1 ACCTCGGCCTGAGGAGCTTCGCGGCGACTCCGTCGTCGG
Bradi4g31760 ACCTCGCTCTCAGGACCTTCACGGCCGAGTCCGTCGTGGG
ACCTCGSYCTSAGGASCTTCRCGGCSGASTCCGTCGTSGG

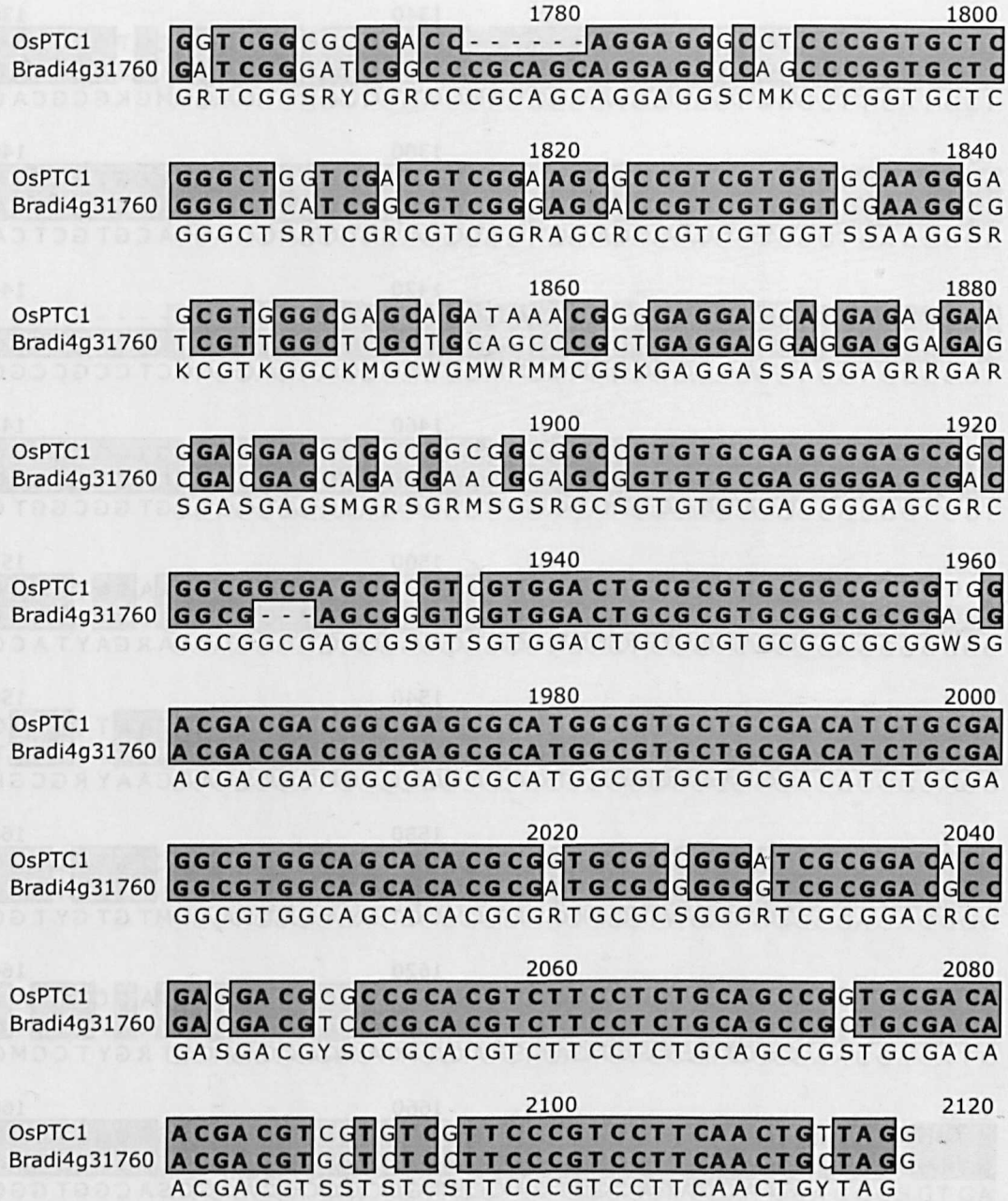
1780
1800
OsPTC1 GGTCGGCGCCGACC------AGGAGGGCCTCCCGGTGCTC
Bradi4g31760 GATCGGGATCGGCCCGCAGCAGGAGGCCAGCCCGGTGCTC
GRTCGGSRYCGRCCCGCAGCAGGAGGSCMKCCCGGTGCTC
1820
1840
OsPTC1 GGGCTGGTCGACGTCGGAAGCGCCGTCGTGGTGCAAGGGA
Bradi4g31760 GGGCTCATCGGCGTCGGGAGCACCGTCGTGGTCGAAGGCG
GGGCTSRTCGRCGTCGGRAGCRCCGTCGTGGTSSAAGGSR
1860
1880
OsPTC1 GCGTGGGCGAGCAGATAAACGGGGAGGACCACGAGAGGAA
Bradi4g31760 TCGTTGGCTCGCTGCAGCCCGCTGAGGAGGAGGAGGAG
KCGTKGGCKMGCWGMWRMMCGSKGAGGASSASGAGRRGAR
1900
1920
OsPTC1 GGAGGAGGCGGCGGCGGCGGCGTGTGCGAGGGGAGCGGC
Bradi4g31760 CGACGAGCAGAGGAACGGAGCGGTGTGCGAGGGGAGCGAC
SGASGAGSMGRSGRMSGSRGCSGTGTGCGAGGGGAGCGRC
1940
1960
OsPTC1 GGCGGCGAGCGCGTCGTGGACTGCGCGTGCGGCGCGGTGG
Bradi4g31760 GGCG---AGCGGGTGGTGGACTGCGCGTGCGGCGCGGACG
GGCGGCGAGCGSGTSGTGGACTGCGCGTGCGGCGCGGWSG
1980
2000
OsPTC1 ACGACGACGGCGAGCGCATGGCGTGCTGCGACATCTGCGA
Bradi4g31760 ACGACGACGGCGAGCGCATGGCGTGCTGCGACATCTGCGA
ACGACGACGGCGAGCGCATGGCGTGCTGCGACATCTGCGA
2020
2040
OsPTC1 GGCGTGGCAGCACACGCGGTGCGCCGGGATCGCGGACCACC
Bradi4g31760 GGCGTGGCAGCACACGCGATGCGCGGGGGTCGCGGACGCC
GGCGTGGCAGCACACGCGRTGCGCSGGGRTCGCGGACRCC
2060
2080
OsPTC1 GAGGACGCGCCGCACGTCTTCCTCTGCAGCCGGTGCGACA
Bradi4g31760 GACGACGTCCCGCACGTCTTCCTCTGCAGCCGCTGCGACA
GASGACGYSCCGCACGTCTTCCTCTGCAGCCGSTGCGACA
2100
2120
OsPTC1 ACGACGTCGTGTCGTTCCCGTCCTTCAACTGTTAGG
Bradi4g31760 ACGACGTGCTCTCTTCCCGTCCTTCAACTGCTAGG
ACGACGTSSTSTCSTTCCCGTCCTTCAACTGYTAG

9. Multiple alignment, *OsPTC1* (NM_001069854)/*HvMS1* (AK373836)/*Bradi4g31760* (BRADI4G31760) *AtMS1* (AJ344210).

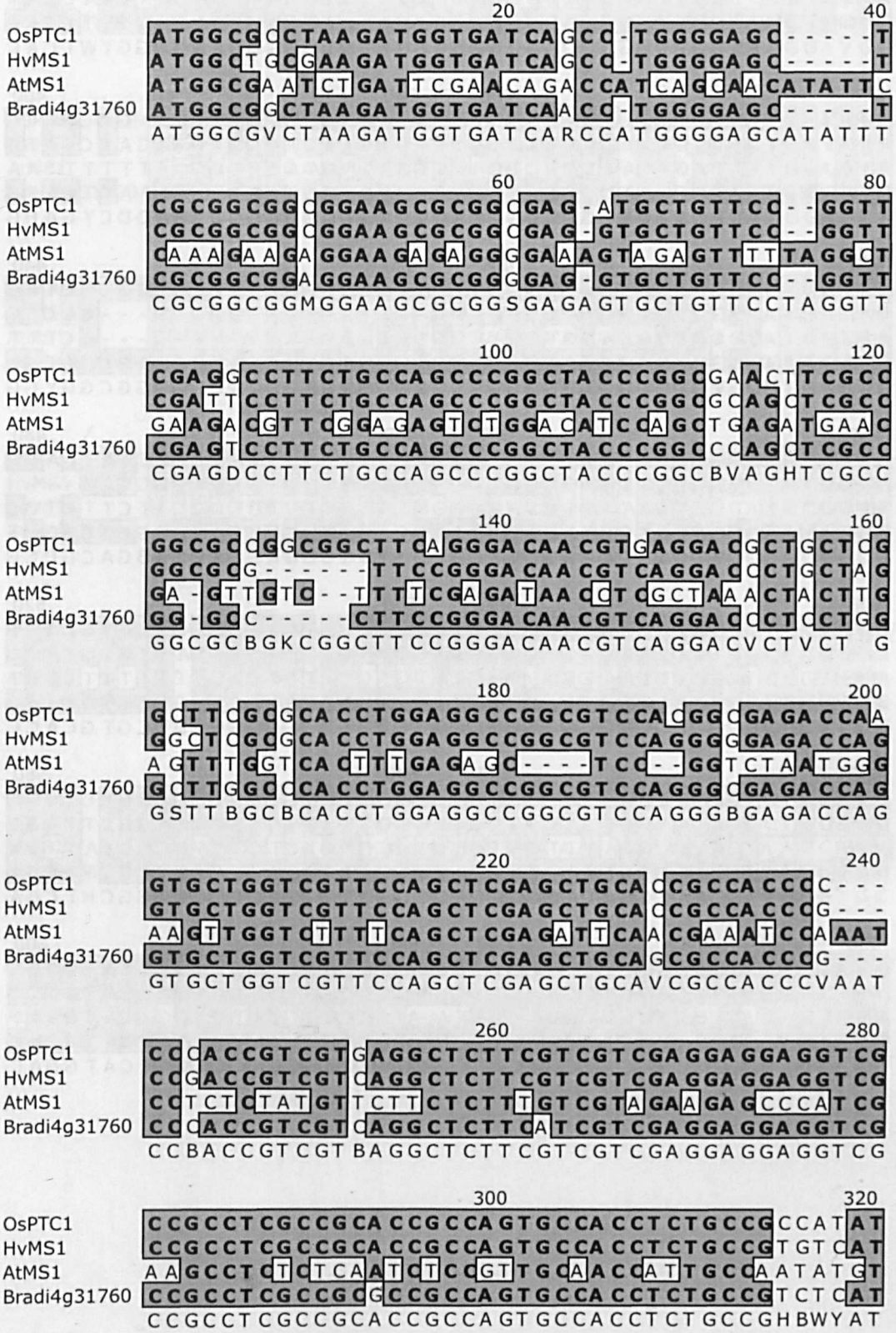

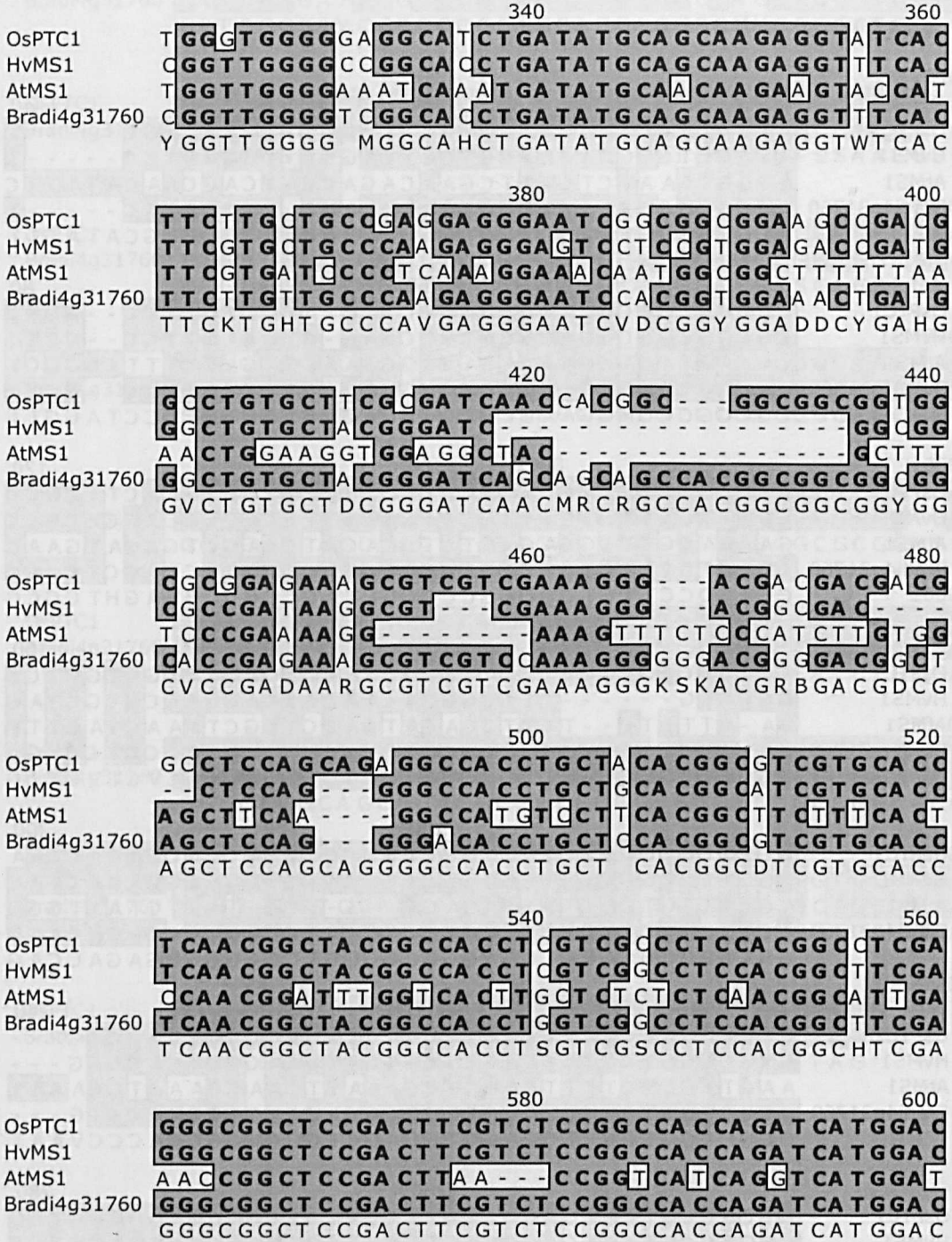
340
360
OsPTC1
HvMS1
AtMS1
Bradi4g31760
Y G G T T G G G G M G G C A H C T G A T A T G C A G C A A G A G G T W T C A C
380
400
OsPTC1
HvMS1
AtMS1
Bradi4g31760
T T C K T G H T G C C C A V G A G G G A A T C V D C G G Y G G A D D C Y G A H G
420
440
OsPTC1
HvMS1
AtMS1
Bradi4g31760
G V C T G T G C T D C G G G A T C A A C M R C R G C C A C G G C G G C G G Y G G
460
480
OsPTC1
HvMS1
AtMS1
Bradi4g31760
C V C C G A D A A R G C G T C G T C G A A A G G G G K S K A C G R B G A C G D C G
500
520
OsPTC1
HvMS1
AtMS1
Bradi4g31760
A G C T C C A G C A G G G G C C A C C T G C T C A C G G C D T C G T G C A C C
540
560
OsPTC1
HvMS1
AtMS1
Bradi4g31760
T C A A C G G C T A C G G C C A C C T S G T C G S C C T C C A C G G C H T C G A
580
600
OsPTC1
HvMS1
AtMS1
Bradi4g31760
G G G C G G C T C C G A C T T C G T C T C C G G C C A C C A G A T C A T G G A C

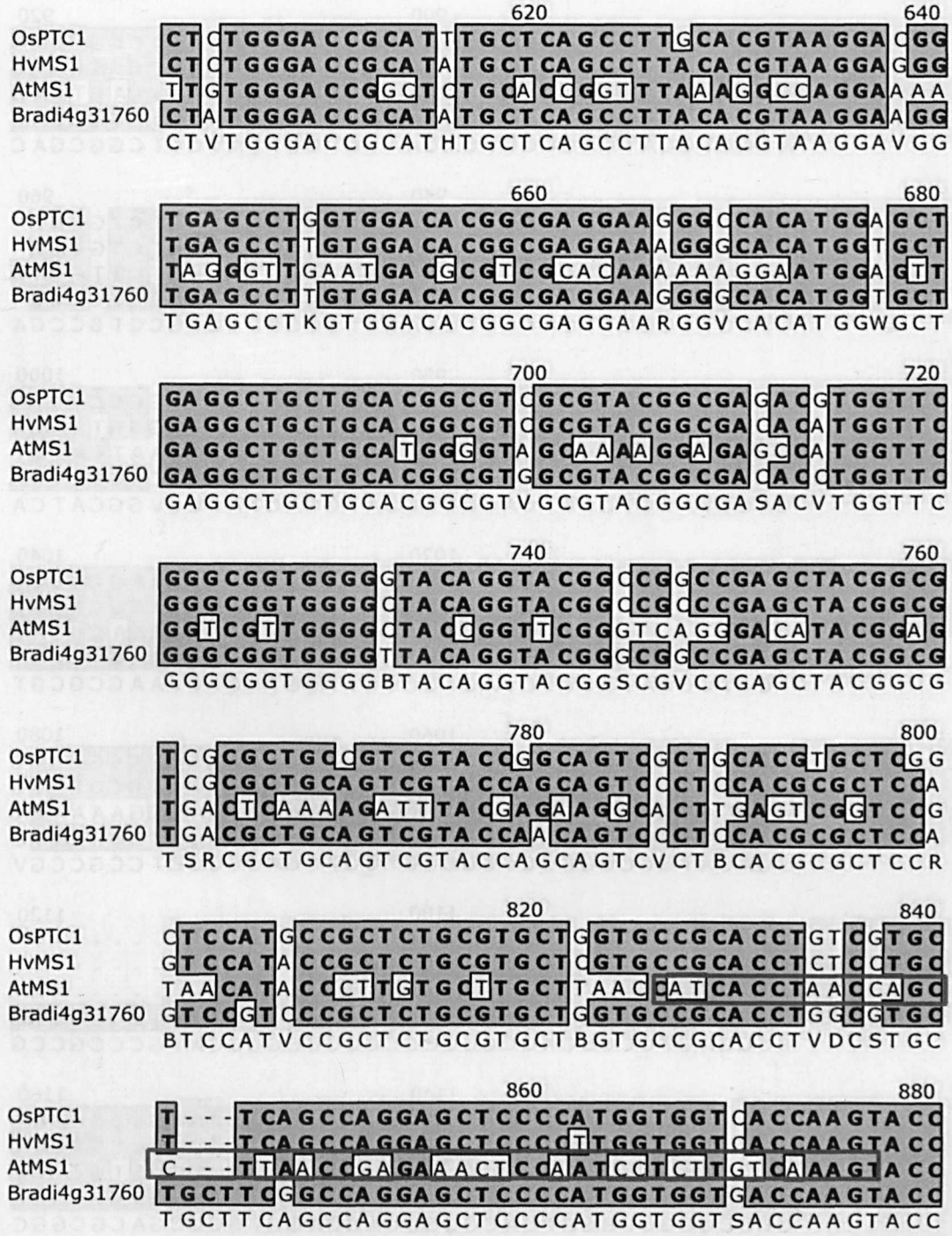
620
640
OsPTC1
HvMS1
AtMS1
Bradi4g31760
CTVTGGGACCGCATHTGCTCAGCCTTACACGTAAGGAVGG
660
680
TGAGCCTKGTGGACACGGCGAGGAARGGVCACATGGWGCT
700
720
GAGGCTGCTGCACGGCGTVGCGTACGGCGASACVTGGTTC
740
760
GGGCGGTGGGGBTACAGGTACGGSCGVCCGAGCTACGGCG
780
800
TSRCGCTGCAGTCGTACCAGCAGTCVCTBCACGCGCTCCR
820
840
BTCCATVCCGCTCTGCGTGCTBGTGCCGCACCTVDCSTGC
860
880
TGCTTCAGCCAGGAGCTCCCCATGGTGGTSACCAAGTACC

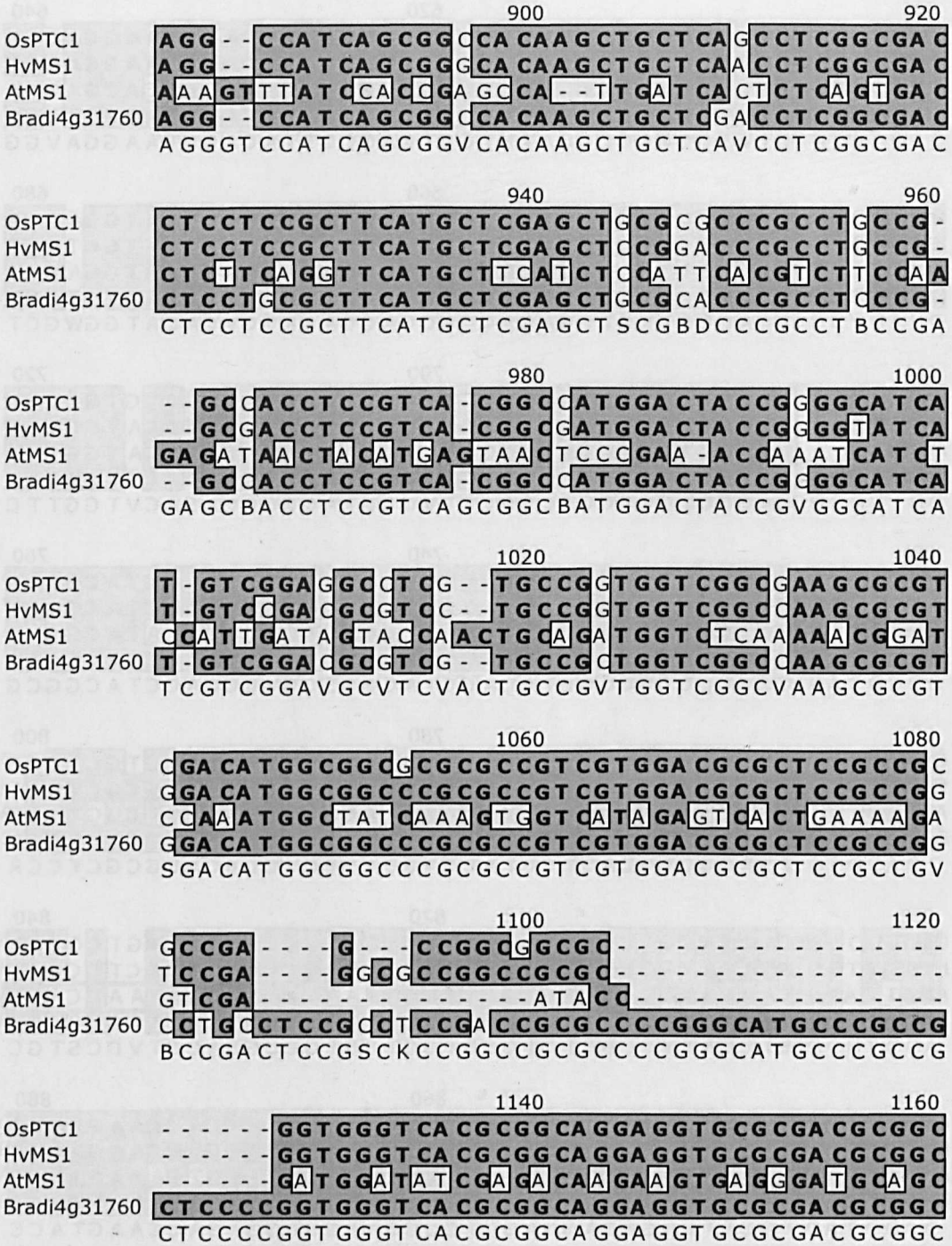
900
920
OsPTC1
HvMS1
AtMS1
Bradi4g31760
940
960
1000
1020
1040
1060
1080
1100
1120
1140
1160

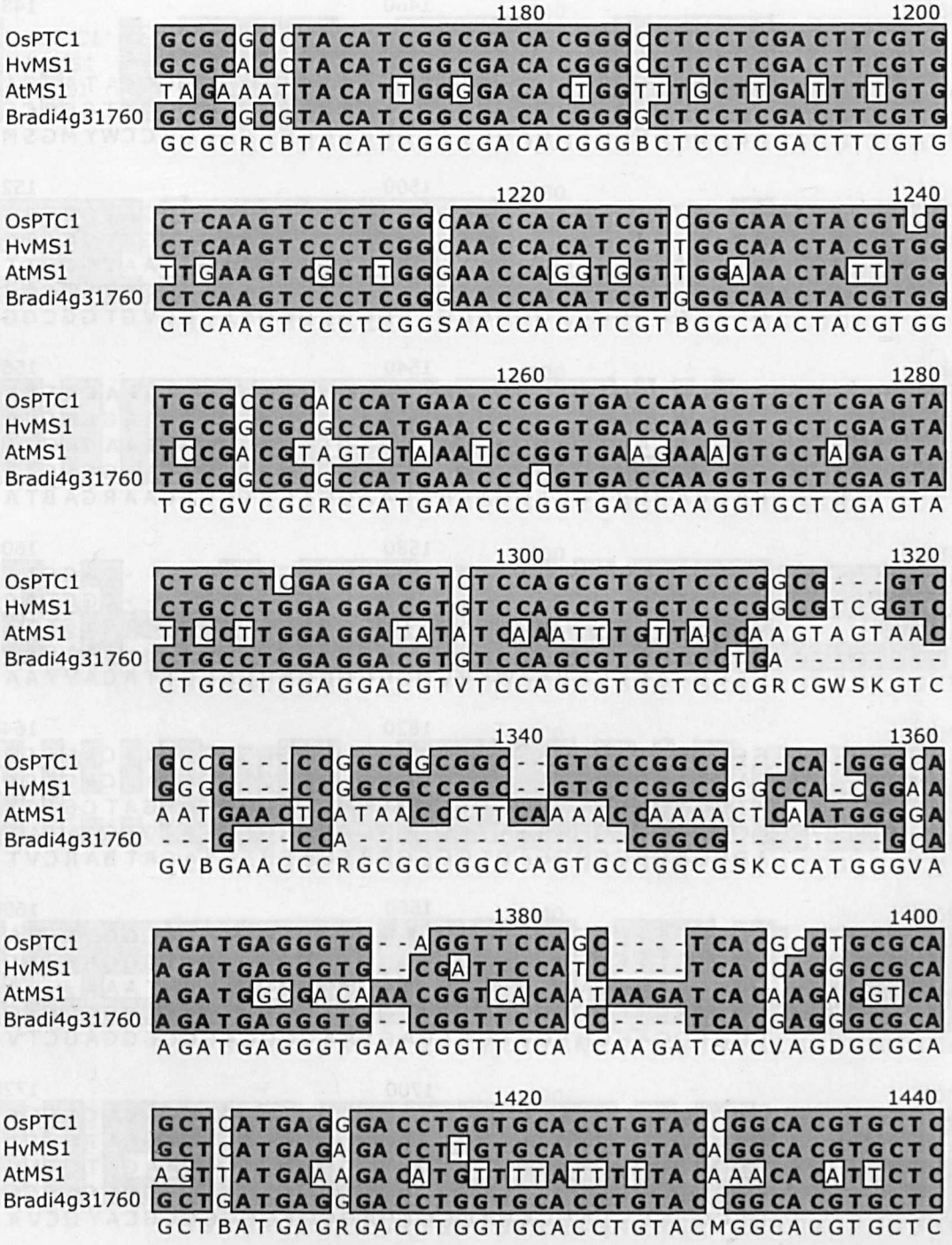
1180
1200
OsPTC1
HvMS1
AtMS1
Bradi4g31760
1220
1240
1260
1280
1300
1320
1340
1360
1380
1400
1420
1440

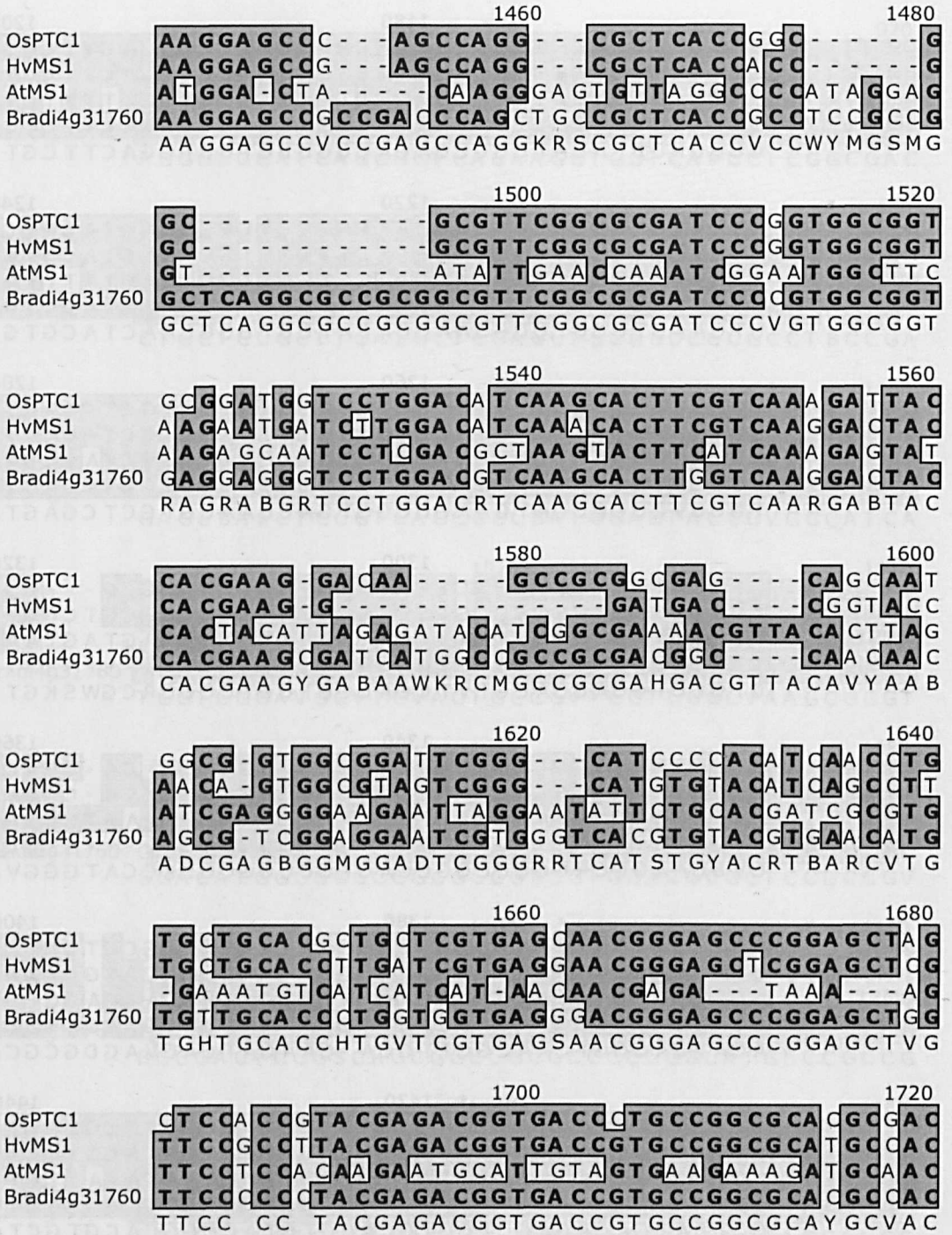
1460
1480
OsPTC1
HvMS1
AtMS1
Bradi4g31760
AAGGAGCCVCCGAGCCAGGKRSCGCTCACCVCCWYMGSMG
1500
1520
GCTCAGGCGCCGCGGCGTTCGGCGCGATCCCVGTGGCGGT
1540
1560
RAGRABGRTCCTGGACRTCAAGCACTTCGTCAARGABTAC
1580
1600
CACGAAGYGABAAWKRCMGCCGCGAHGACGTTACAVYAAB
1620
1640
ADCGAGBGGMGGADTCGGGRRTCATSTGYACRTBARCVTG
1660
1680
TGHTGCACCHTGVTCGTGAGSAACGGGAGCCCGGAGCTVG
1700
1720
TTCC CC TACGAGACGGTGACCGTGCCGGCGCAYGCVAC


1740
1760
OsPTC1
HvMS1
AtMS1
Bradi4g31760
1780
1800
1820
1840
1860
1880
1900
1920
1940
1960
1980
2000

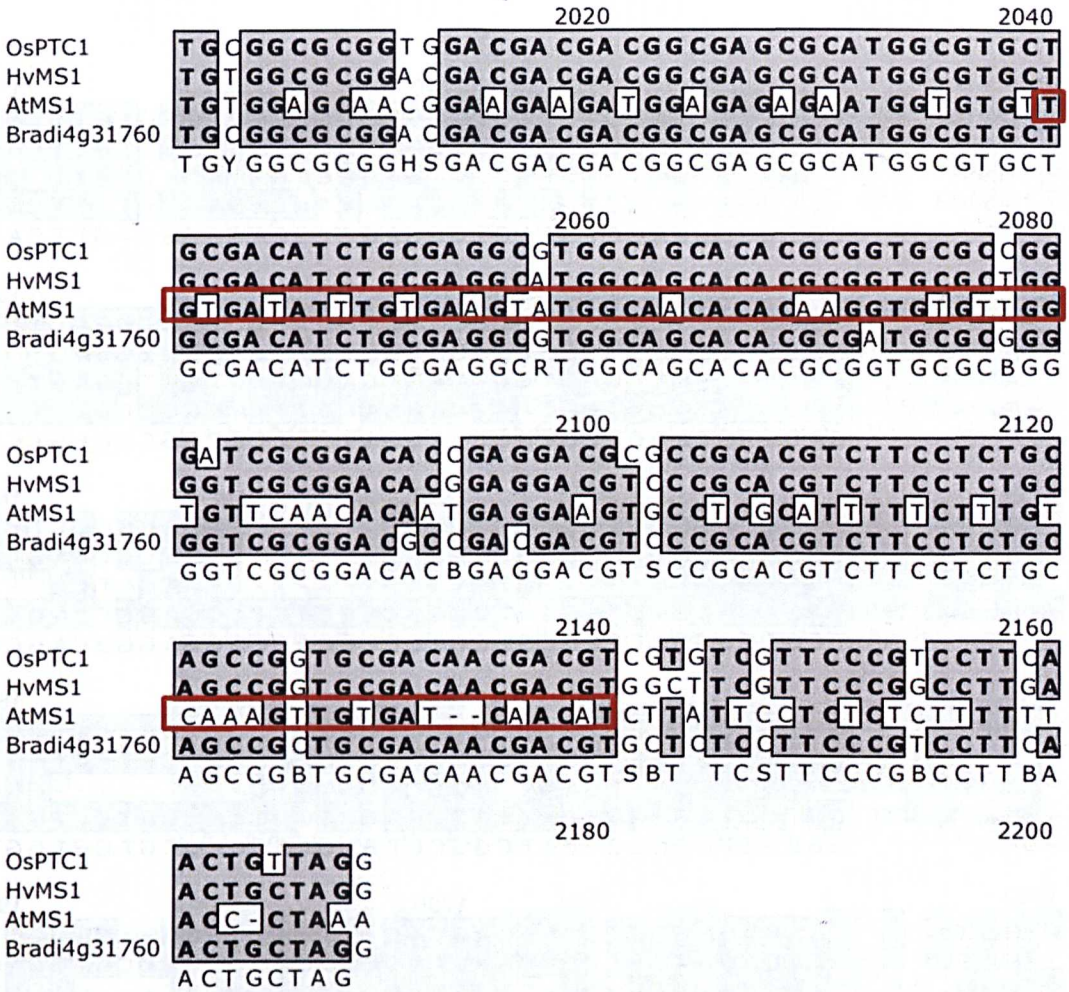
2020
2040
OsPTC1
HvMS1
AtMS1
Bradi4g31760
TGYGGCGCGGHSGACGACGACGGCGAGCGCATGGCGTGCT
2060
2080
GCGACATCTGCGAGGCRTGGCAGCACACGCGGTGCGCBGG
2100
2120
GGTCGCGGACACBGAGGACGTSCCGCACGTCTTCCTCTGC
2140
2160
AGCCGBTGCGACAACGACGTSBT TCSTTCCCGBCCTTBA
2180
2200
ACTGCTAG

10. RACE-PCR amplifications of *HvMS1*.

3′ RACE

GTCGGCGAGCTCAAGTGGGAGGTGCAGAGGCTGTTCAGGGACATGTACCTCGGCCTGAGGACCTT
CACGGCGGAGTGCGTCGTGGGGATCGGCGCCGGCCTGGACGCCAGCCCGGCGCTCGGGCTGATCG
GGGTGGGAAGCACCGTCGTGGTCGAAGGGGTGGTCGGCGAGCAGCAGGAACCGGCCGAGGAGGGC
GACCAGAGGAAGAAAGCGGCTGCCGTGTGCGAGGGGGGCGGCGACGTCGGAGAGAGGGTCGTAGA
CTGCGTATGTGGCGCGGACGACGACGACGGCGAGCGCATGGCGTGCTGCGACATCTGCGAGGCAT
GGCAGCACACGCGGTGCGCTGGGGTCGCGGACACGGAGGACGTCCCGCACGTCTTCCTCTGCAGC
CGGTGCGACAACGACGTGGCTTCGTTCCCGGCCTTGAACTGCTAGACTAGAAGCTGCCGCAGGCA
TGCTCGGTACGGCATAAACGTTGCTGCAAACAATCGCTGCTATATTAGTCTATCTATACATGTAC
TGTACTGTATAACCGAAGACTTCAACTGTTTAAAAAAAAAAAAAAAAAAAAA

5′RACE

ATGGCTGCGAAGATGGTGATCAGCCTGGGGAGCTCGCGGCGGCGGAAGCGCGGCGAGGTGCTGTT
CCGGTTCGATTCCTTCTGCCAGCCCGGCTACCCGGCGCAGCTCGCCGGCGCGTTCCGGGACAACG
TCAGGACCCTGCTAGGGCTCGCGCACCTGGAGGCCGGCGTCCAGGGGGAGACCAGGTGCTGGTCG
TTCCAGCTCGAGCTGCACCGCCACCCGCCGACCGTCGTCAGGCTCTTCGTCGTCGAGGAGGAGGT
CGCCGCCTCGCCGCACCGCCAGTGCCACCTCTGCCGTGTCATCGGTTGGGGCCGGCACCTGATAT
GCAGCAAGAGGTTTCACTTCGTGCTGCCCAAGAGGGAGTCCTCCGTGGAGACCGATGGGCTGTGC
TACGGGATCGGCGGCGCCGATAAGGCGTCGAAAGGGACGGCGACCTCCAGGGGCCACCTGCTGCA
CGGCATCGTGCACCTCAACGGCTACGGCCACCTCGTCGGCCTCCACGGCTTCGAGGGCGGCTCCG
ACTTCGTCTCCGGCCACCAGATCATGGACCTCTGGGACCGCATTTGCTCAGC

11. Alignment between *Brachypodium AtMYB26* equivalent (BRADI2G47887) and Barley putative ortholog, AK372926.

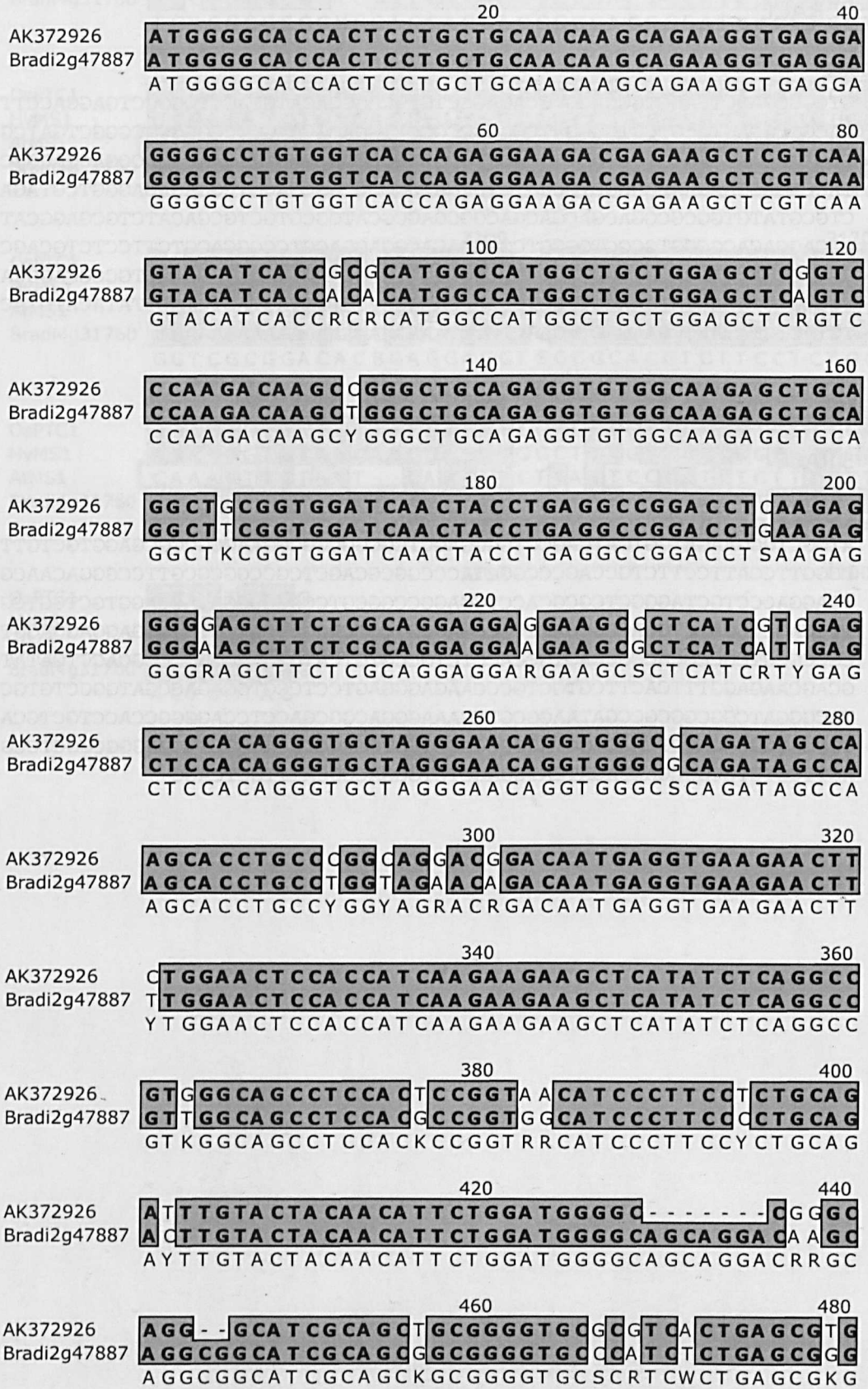

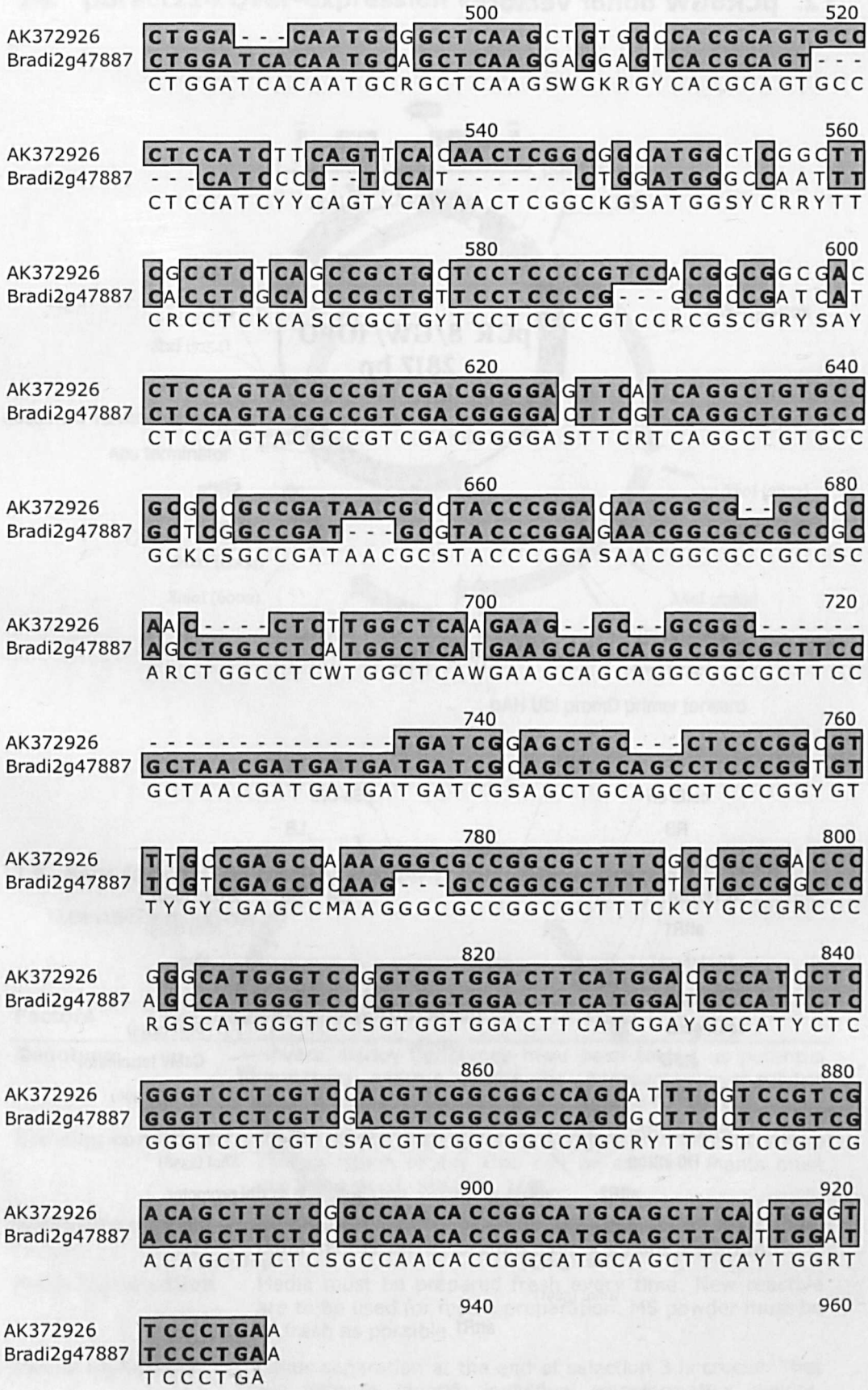
500
520
AK372926 CTGGA---CAATGCGGCTCAAGCTGTGGCCACGCAGTGCC
Bradi2g47887 CTGGATCACAATGCAGCTCAAGGAGGAGTCACGCAGT---
CTGGATCACAATGCRGCTCAAGSWGKRGYCACGCAGTGCC
540
560
AK372926 CTCCATCTTCAGTTCACAACTCGGCGGCATGGCTCGGCTT
Bradi2g47887 ---CATCCCC--TCCATGGATGGGCCAATTT
CTCCATCYYCAGTYCAYAACTCGGCKGSATGGSYCRRYTT
580
600
AK372926 CGCCTCTCAGCCGCTGCTCCTCCCCGTCCACGGCGGCGACC
Bradi2g47887 CACCTCGCACCCGCTGTTCCTCCCCG---GCGCCGATCAT
CRCCTCKCASCCGCTGYTCCTCCCCGTCCRCGSCGRYSAY
620
640
AK372926 CTCCAGTACGCCGTCGACGGGGAGTTCATCAGGCTGTGCC
Bradi2g47887 CTCCAGTACGCCGTCGACGGGGACTTCGTCAGGCTGTGCC
CTCCAGTACGCCGTCGACGGGGASTTCRTCAGGCTGTGCC
660
680
AK372926 GCGCCGCCGATAACGCCTACCCGGACAACGGCG--GCCCC
Bradi2g47887 GCTCGGCCGAT---GCGTACCCGGAGAACGGCGCCGCCGC
GCKCSGCCGATAACGCSTACCCGGASAACGGCGCCGCCSC
700
720
AK372926 AAC----CTCTTGGCTCAAGAAG--GC--GCGGC------
Bradi2g47887 AGCTGGCCTCATGGCTCATGAAGCAGCAGGCGGCGCTTCC
ARCTGGCCTCWTGGCTCAWGAAGCAGCAGGCGGCGCTTCC
740
760
AK372926 ----------------TGATCGGAGCTGC---CTCCCGGCGT
Bradi2g47887 GCTAACGATGATGATGATCGCAGCTGCAGCCTCCCGGTGT
GCTAACGATGATGATGATCGSAGCTGCAGCCTCCCGGYGT
780
800
AK372926 TTGCCGAGCCAAAGGGCGCCGGCGCTTTCGCCGCCGACCC
Bradi2g47887 TCGTCGAGCCCAAG---GCCGGCGCTTTCTCTGCCGGCCC
TYGYCGAGCCMAAGGGCGCCGGCGCTTTCKCYGCCGRCCC
820
840
AK372926 GGGCATGGGTCCGGTGGTGGACTTCATGGACGCCATCCTC
Bradi2g47887 AGCCATGGGTCCCGTGGTGGACTTCATGGATGCCATTCTC
RGSCATGGGTCCSGTGGTGGACTTCATGGAYGCCATYCTC
860
880
AK372926 GGGTCCTCGTCCACGTCGGCGGCCAGCATTCGTCCGTCG
Bradi2g47887 GGGTCCTCGTCGACGTCGGCGGCCAGCGCTTCCTCCGTCG
GGGTCCTCGTCSACGTCGGCGGCCAGCRYTTCSTCCGTCG
900
920
AK372926 ACAGCTTCTCGGCCAACACCGGCATGCAGCTTCACTGGGT
Bradi2g47887 ACAGCTTCTCCGCCAACACCGGCATGCAGCTTCATTGGAT
ACAGCTTCTCSGCCAACACCGGCATGCAGCTTCAYTGGRT
940
960
AK372926 TCCCTGAA
Bradi2g47887 TCCCTGAA
TCCCTGA

12. pCR8GW donor vector.

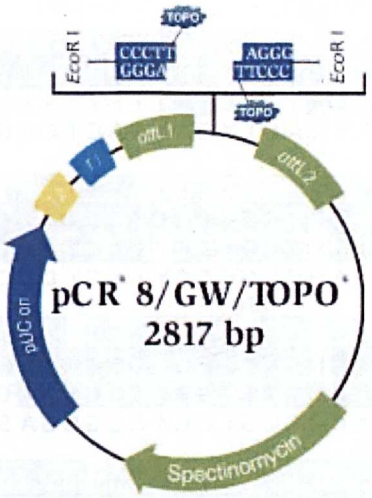

13. pBract207RNAi silencing vector.

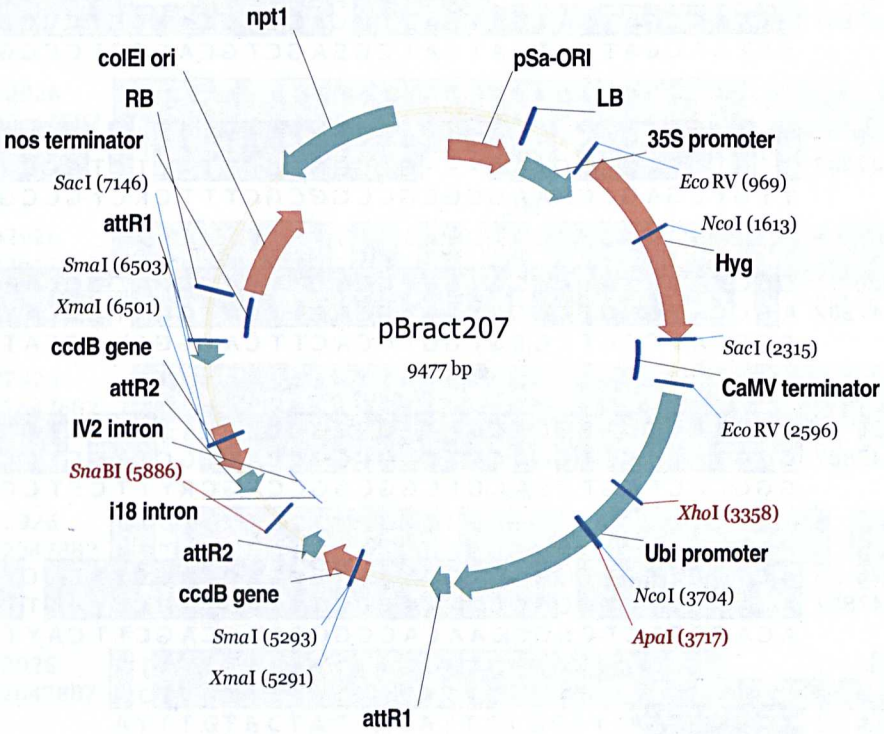

14. pBract214 Over-expression vector

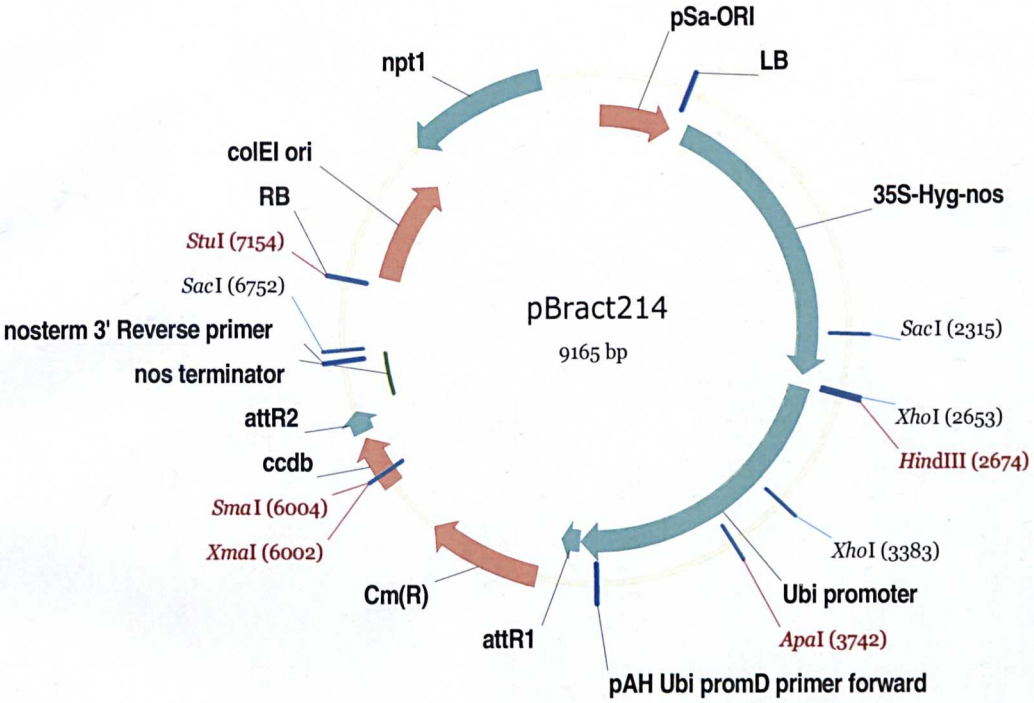

15. Key factors in barley *Agrobacterium*-mediated transformation.

Factors	Comments
Genotype	Several barley genotypes have been tested as potential immature embryo donor for *Agrobacterium*-mediated transformation. Golden Promise showed higher efficiency.
Growing conditions	Donor plants must grow in a clean environment where contamination of any kind can be avoided. Plants must not be sprayed. 15/12ºC 16H.
Immature embryo	Immature embryos must be collected at the right time. Embryos between 1.5-2mm diameters are preferred.
Media composition	Media must be prepared fresh every time. New reactive are to be used for media preparation. MS powder must be as fresh as possible.
Callus separation	Callus separation at the end of selection 3 is crucial. That will help to identify individual transformation events, therefore facilitating the analysis.